THE UNIVERSITY OF ADELAIDE

DOCTORAL THESIS

Cell wall biosynthesis in barley powdery mildew Blumeria graminis f. sp. hordei

---

Author:
Trang Anh PHAM

Supervisors:
Vincent BULONE
Alan LITTLE

A thesis submitted in fulfilment of the requirements
for the degree of Doctor of Philosophy

School of Agriculture, Food and Wine
Faculty of Sciences

University of Adelaide, Waite Campus
Glen Osmond, SA 5064
Australia

May, 2019

Declaration of Authorship

I certify that this work contains no material which has been accepted for the award of any other degree or diploma in my name, in any university or other tertiary institution and, to the best of my knowledge and belief, contains no material previously published or written by another person, except where due reference has been made in the text. In addition, I certify that no part of this work will, in the future, be used in a submission in my name, for any other degree or diploma in any university or other tertiary institution without the prior approval of the University of Adelaide and where applicable, any partner institution responsible for the joint-award of this degree.

I acknowledge that copyright of published works contained within this thesis resides with the copyright holder(s) of those works.

I also give permission for the digital version of my thesis to be made available on the web, via the University's digital research repository, the Library Search and also through web search engines, unless permission has been granted by the University to restrict access for a period of time.

I acknowledge the support I have received for my research through the provision of an Australian Government Research Training Program Scholarship.

Name: Trang Anh Pham

Date: November 2018

Signed:

THE UNIVERSITY OF ADELAIDE

Abstract

Faculty of Sciences

School of Agriculture, Food and Wine

Doctor of Philosophy

Cell wall biosynthesis in barley powdery mildew Blumeria graminis f. sp. hordei

by Trang Anh PHAM

Blumeria graminis f. sp. *hordei* (*Bgh*) is the causal agent of powdery mildew in *Hordeum vulgare* (barley). *Bgh* is an obligate biotrophic pathogen, meaning that it relies on the host for survival. The *Bgh* asexual life cycle initiates when airborne conidia land on the host surface and germinate. An appressorium develops and penetrates the host to form an intracellular feeding structure called a haustorium. Following successful host entry, epiphytic mycelia spread along the surface and conidiophores emerge to produce vast quantities of conidia.

As the fungal cell wall is essential for survival it is an obvious target for the design of novel antifungal agents for disease control. Depending on the pathogen species, the composition of the cell wall can vary significantly. In order to advance disease control practices, it is imperative to understand the composition of the cell wall and the genes involved in cell wall metabolism. This work focuses on characterising the *Bgh* fungal cell wall and examining the genes responsible for its synthesis during pre-penetrative events of pathogenesis. In addition, *in vitro* assays have been performed to investigate the biochemical activity for a number of key biosynthetic enzymes.

Permethylation glycosidic linkage analysis of the *Bgh* conidia cell wall has revealed their cell wall composition for the first time. The conidial cell wall of *Bgh* is predominantly made of glucose and has a greater proportion of galactose residues compared to other well characterised fungal cell walls. Trace amounts of xylose residues were also observed. Analysis of the Carbohydrate Active enZymes (CAZy) present within the *Bgh* genome was conducted to identify genes involved in cell wall metabolism, as previous CAZy annotations of the genome were incomplete. A greater number of CAZy genes were identified compared to previous studies.

Many of the biochemical activities of CAZy enzymes involved in cell wall synthesis are still unknown due to the technically challenging work required. In an attempt to understand cell wall synthesis in *Bgh*, several genes involved in chitin and β-1,3-glucan synthesis were heterologously expressed with the aim to confirm biochemical activity and perform *in vitro* enzyme kinetic assays. Following successful expression of four chitin synthases, only the class I chitin synthase was able to be expressed and purified in an active state.

To examine pre-penetrative events in *Bgh* without any contamination from the host plant it was essential to establish an *in vitro* system for germination of the *Bgh* conidia. A previously established *in vitro* assay using *n*-hexacosanal was adapted to generate *in vitro* fungal material for analysis. *n*-Hexacosanal is a known inducer of *Bgh* germination and appressorial development. Profiling of the transcriptome and proteome during the appressorial germ tube stage revealed that there was a notable shift towards energy and protein production during appressorial development. Linkage analysis of the appressorial cell wall showed a significant decrease in the galactose portion of the cell wall during the appressorial stage and the appearance of novel branched xylose linkages that have not been observed in fungal pathogens previously. The use of this cultivation method demonstrates that it is possible to analyse the pre-penetrative processes of *Bgh* development *in vitro*.

Acknowledgements

The completion of this thesis was made possible with the support of several people. Firstly, I would like to express my sincerest appreciation to my supervisors Prof. Vincent Bulone and Dr. Alan Little for their continuous guidance, patience, and support throughout my Ph.D studies.

I would like to thank the past and present members of the Plant Cell Walls group for providing a friendly and enjoyable working environment during my studies. I am especially grateful to the postdoctoral fellows Dr. Neil Shirely, Dr. Julian Schwerdt, and Dr. Bianca Kyriacou for their continued help throughout my project. Your assistance was absolutely invaluable.

I would also like to thank Prof. Vincent Bulone for providing me with the opportunity to visit his laboratory at the Royal Institute of Technology (KTH). There are a number of postdoctoral fellows at KTH to whom I am grateful for their help and direction, namely, Dr. Osei Ampomah, Dr. Vaibhav Srivastava, Dr. Xiaohui Xing, and Dr. Yves Hsieh, all from the Division of Glycoscience at the School of Engineering Sciences in Chemistry.

The support of my fiancé and family has been incredibly important to me during the pursuit of this project. Thank you for your kindness and patience throughout the years, it wouldn't have been possible without you all.

Finally, I must thank the University of Adelaide and Plant Cell Walls for providing me with a generous scholarship.

Contents

Declaration of Authorship iii

Abstract v

Acknowledgements vii

1 Introduction 1
- 1.1 Powdery mildew . . . 1
- 1.2 Asexual life cycle . . . 2
- 1.3 Recognition of the plant host . . . 2
- 1.4 Fungal cell walls . . . 7
- 1.5 Glucans . . . 12
- 1.6 Chitin . . . 15
- 1.7 Chitin synthase . . . 17
- 1.8 Chemical inhibitors of fungal cell wall synthesis . . . 21
- 1.9 Resources available for *Bgh* research . . . 24
- 1.10 Aims of this work . . . 26

2 Composition and biosynthetic machinery of the *Blumeria graminis* f. sp. *hordei* conidia cell wall 29
- 2.1 Abstract . . . 33
- 2.2 Introduction . . . 34
- 2.3 Materials and Methods . . . 36
  - 2.3.1 Fungal material . . . 36
  - 2.3.2 Preparation of cell walls . . . 36
  - 2.3.3 Permethylation glycosidic linkage analysis . . . 36
  - 2.3.4 RNA extraction and RNAseq library creation . . . 37
  - 2.3.5 Quantitative polymerase chain reaction validation . . . 37
  - 2.3.6 Transcriptome analysis and genome annotation . . . 37
- 2.4 Results . . . 39
  - 2.4.1 Glycosidic linkage analysis of *Bgh* conidia . . . 39
  - 2.4.2 Annotation of Carbohydrate Active enZymes (CAZy) in the *Bgh* genome . . . 39
  - 2.4.3 Transcriptome analysis of ungerminated *Bgh* conidia . . . 45
- 2.5 Discussion . . . 48

2.6 Supplementary Figures and Tables . . . 53

3 Establishment of an *in vitro* germination system for analysis of *Blumeria graminis* f. sp. *hordei* pre-penetrative events 79
3.1 Introduction . . . 79
3.2 Materials and Methods . . . 82
3.2.1 Fungal and plant material . . . 82
3.2.2 Synthesis of n-hexacosanal . . . 82
3.2.3 Preparation of artificial surfaces . . . 82
3.2.4 *Bgh* pre-penetrative process observations . . . 82
3.2.5 Light microscopy . . . 83
3.2.6 Large scale *Bgh* sample collection for downstream analysis . . . 83
3.2.7 RNA extraction . . . 83
3.3 Results . . . 85
3.3.1 *Bgh* germination and differentiation analysis on artificial surfaces 85
3.3.2 *n*-Hexacosanal dilution series . . . 87
3.3.3 RNA extraction and qPCR . . . 87
3.3.4 Cell wall chitin labelling . . . 88
3.4 Discussion . . . 94
3.5 Conclusion . . . 96

4 Analysis of cell wall synthesis and metabolism during early germination of *Blumeria graminis* f. sp. *hordei* 99
4.1 Link to previous chapters . . . 103
4.2 Abstract . . . 103
4.3 Introduction . . . 104
4.4 Materials and Methods . . . 107
4.4.1 Fungal material . . . 107
4.4.2 *In vitro* growth of *Bgh* . . . 107
4.4.3 Preparation of *Bgh* cell wall samples . . . 107
4.4.4 Permethylation glycosidic linkage analysis . . . 107
4.4.5 RNA extraction . . . 108
4.4.6 RNAseq library creation . . . 108
4.4.7 Quantitative polymerase chain reaction (qPCR) validation . . . 108
4.4.8 Transcriptome analysis . . . 109
4.4.9 Protein extraction and sample preparation for proteomics . . . 109
4.4.10 Nano-LC-MS/MS analysis of samples subjected to iTRAQ labelling . . . 110
4.4.11 Data processing and protein identification . . . 110
4.4.12 Light microscopy . . . 111
4.5 Results . . . 112
4.5.1 Transcriptomic and proteomic analysis . . . 112
4.5.2 Compositional analysis of *Bgh* cell wall . . . 118

4.5.3 *Bgh* cell wall labelling . . . 118
4.5.4 *Bgh* cell wall metabolism . . . 122
4.6 Discussion . . . 128
4.7 Supplementary Figures and Tables . . . 132

5 Biochemical characterisation of *Blumeria graminis* f. sp. *hordei* cell wall biosynthetic enzymes 137
5.1 Introduction . . . 137
5.2 Materials and Methods . . . 142
5.2.1 Fungal material . . . 142
5.2.2 Cloning of target *Bgh* genes and sequence validation . . . 142
5.2.3 Subcloning and expression of target *Bgh* proteins in *E. coli* . . . 142
5.2.4 Protein extraction and Western blot analysis . . . 145
5.2.5 Cloning and transformation of target *Bgh* proteins into *S. cerevisiae* . . . 146
5.2.6 Expression and screening of *Bgh* target proteins in *S. cerevisiae* . 146
5.2.7 In-gel proteolysis and mass spectrometry . . . 148
5.2.8 Preparation of solubilised membrane fractions for chitin synthase assays . . . 149
5.2.9 His-tagged protein purification . . . 149
5.2.10 Chitin synthase activity assay . . . 150
5.3 Results . . . 151
5.3.1 Expression of GEL proteins in *E. coli* . . . 151
5.3.2 Expression of chitin synthases and β-1,3-glucan synthase in *S. cerevisiae* . . . 151
5.3.3 Activity of solubilised membrane fractions in chitin synthase assays . . . 157
5.3.4 Purification of *Bgh* CHSI . . . 160
5.4 Discussion . . . 166
5.4.1 Heterologous expression of *Bgh* FKS1 and GEL proteins . . . 166
5.4.2 Heterologous expression of *Bgh* CHS proteins . . . 167
5.5 Primer Tables . . . 170

6 Conclusion 177

References 181

List of Abbreviations

AA	Auxiliary activity
ACN	Acetonitrile
agt	Appressorial germ tube
AIR	Alcohol insoluble residue
APP	Automated proteomics pipeline
Bgh	*Blumeria graminis* f. sp. *hordei*
CAZy	Carbohydrate Active enZyme
CBM	Carbohydrate binding modules
cDNA	Complementary DNA
CE	Carbohydrate esterase
CHAPS	3-[(3-Cholamidopropyl)dimethylammonio]-1-propanesulphonate
CHS	Chitin synthase
CWI	Cell wall integrity
DAPI	4′,6-Diamidino-2-phenylindole
DNA	Deoxyribonucleic acid
DTT	Dithiothreitol
EC	Enzyme Commission
EDTA	Ethylenediaminetetraacetic acid
EGTA	Ethylene glycol-bis(β-aminoethyl ether)-N,N,N′,N′-tetraacetic acid
FA	Formic acid
FID	Flame ionization detection
f. sp.	*Forma specialis*
g	Centrifugal force
Gal	Galactose
GFP	Green fluorescent protein
GH	Glycoside hydrolase
Glc	Glucose
GlcNAc	*N*-acetyl-D-glucosamine
GPI	Glycosylphosphatidylinositol
GT	Glycosyl transferase
h	Hours
HIGS	Host-induced gene silencing
IAA	indole-3-acetic acid
IPTG	Isopropyl β-D-1-thiogalactopyranoside
KEGG	Kyoto Encyclopedia of Genes and Genomes

LB	Luria broth
Man	Mannose
min	Minutes
MPa	Mega pascal
MS	Mass spectrometry
OD	Optical density
PCR	Polymerase chain reaction
PEG	Polyethylene glycol
PFAM	Protein families
pgt	Primary germ tube
PL	Polysaccharide lyase
PMAAs	Partially methylated alditol acetates
PMSF	Phenylmethane sulphonyl fluoride
PVP40	Polyvinylpyrrolidone 40
qPCR	Quantitative polymerase chain reaction
RNA	Ribonucleic acid
rpm	Revolutions per minute
s	Seconds
SDC	Sodium deoxycholate
SDS	Sodium dodecyl sulphate
SDS-PAGE	Sodium dodecyl sulphate–polyacrylamide gel electrophoresis
sgt	Secondary germ tube
TBS	Tris-buffered saline
TEAB	Tetraethylammonium bromide
TFA	Trifluoroacetic acid
UDP	Uridine diphosphate
WGA	Wheat germ agglutinin

Chapter 1

Introduction

1.1 Powdery mildew

Fungi are prominent threats to plants, causing severe yield and economic losses in a wide range of agricultural and ornamental plants (Dean et al., 2012). One of the most common fungal diseases encountered around the world is powdery mildew, caused by obligate biotrophic ascomycete pathogens. They have an extensive host range, infecting the leaves, stems, flowers, and fruits of nearly 10,000 angiosperm species (Glawe, 2008).

Individual fungal species can display a wide range of host specificities, ranging broadly from the polyphagy observed in *Golovinomyces orontii*, which has been associated with over 90 host species (Ing, 1990), to the highly specialised *Blumeria graminis* where the *forma specialis tritici* (*Bgt*) and *hordei* (*Bgh*) exclusively infect wheat and barley, respectively (Wyand and Brown, 2003). Powdery mildew of cereals is one of the most economically important diseases in agriculture. An outbreak of *Bgh* in the field can potentially lead to severe yield losses (Murray and Brennan, 2010). In Australia barley is the second most important crop after wheat, contributing almost 1/3 of the world's malting barley trade and approximately 20% of the world's feed trade. Foliar diseases such as powdery mildew over wide areas have caused estimated annual losses of $39 million to the Australian barley industry (Murray and Brennan, 2010) Reliable control of major diseases is an essential requirement in agriculture; however fungicides are extremely costly, an estimated $52 million is spent annual on controlling powdery mildew alone in Australia (Murray and Brennan, 2009).

Like all powdery mildew fungi, *Bgh* are strictly obligate biotrophic pathogens. They infect their host plant without causing any cell death and establish a long-term relationship, being completely dependent on the host for water and nutrients.

1.2 Asexual life cycle

Powdery mildew infestations are quite conspicuous, easily recognisable as white powdery pustules on the leaves, stems or fruits of infected host plants (Glawe, 2008) (Figure 1.1). Epidemics are instigated by the rapid succession of asexual cycles that commence when airborne conidia land on a host surface. The asexual conidia of *Bgh* germinate and develop synchronously, proceeding through an ordered sequence of morphogenesis on the surface of the host (Figure 1.2).

Following contact to the barley surface, the conidium germinates and produces a short primary germ tube (pgt) within minutes. The germ tube breaches the cuticular layer, but not the cell wall (Edwards, 2002; Yamaoka et al., 2006). It functions as a sensory appendage by perceiving host factors and facilitates the adhesion of the conidium to the host surface as well as water uptake. The recognition of host factors drives the emergence of a secondary germ tube (sgt). The sgt subsequently elongates and differentiates into an appressorial germ tube (agt). The apical part of the agt matures and becomes a septate, lobed appressorium. A penetration peg forms beneath the appressorium to penetrate through the cell wall. Through the combination of increased turgor pressure and enzymatic activities, the peg can progress through both the host cuticle and cell wall (Pryce-Jones et al., 1999).

Inside the epidermal cell, the peg establishes a multidigitate haustorium surrounded by a perihaustorial matrix and an intact host membrane (Micali et al., 2011). The haustorial complex operates as a nutrient acquisition centre dedicated to feeding further epiphytic growth of *Bgh* (Bushnell et al., 1987). The successful establishment of the haustorium is followed by the development of secondary hyphae on the leaf surface that establish secondary haustoria in other epidermal cells. Within 3 days post-infection, aerial conidiophores are erected from the mycelia on the leaf's surface and produce masses of conidia. The sheer quantity of conidia produced enables the rapid spread of disease over large areas when they become airborne (Brown and Hovmøller, 2002).

1.3 Recognition of the plant host

Plants are exposed to a multitude of abiotic and biotic stress factors. Plants are covered by a hydrophobic cuticle, providing protection against desiccation and environmental stresses (Yeats and Rose, 2013). The primary function of the cuticle is to prevent water loss by transpiration, with a secondary role in controlling the uptake of solutes, gases, and lipophilic organic compounds. As a point of contact between the plant and its environment, it acts as a barrier against herbivores and prevents invasion by pathogenic fungi and other microorganisms.

FIGURE 1.1: Barley leaves infected with *Blumeria graminis* f. sp. *hordei*

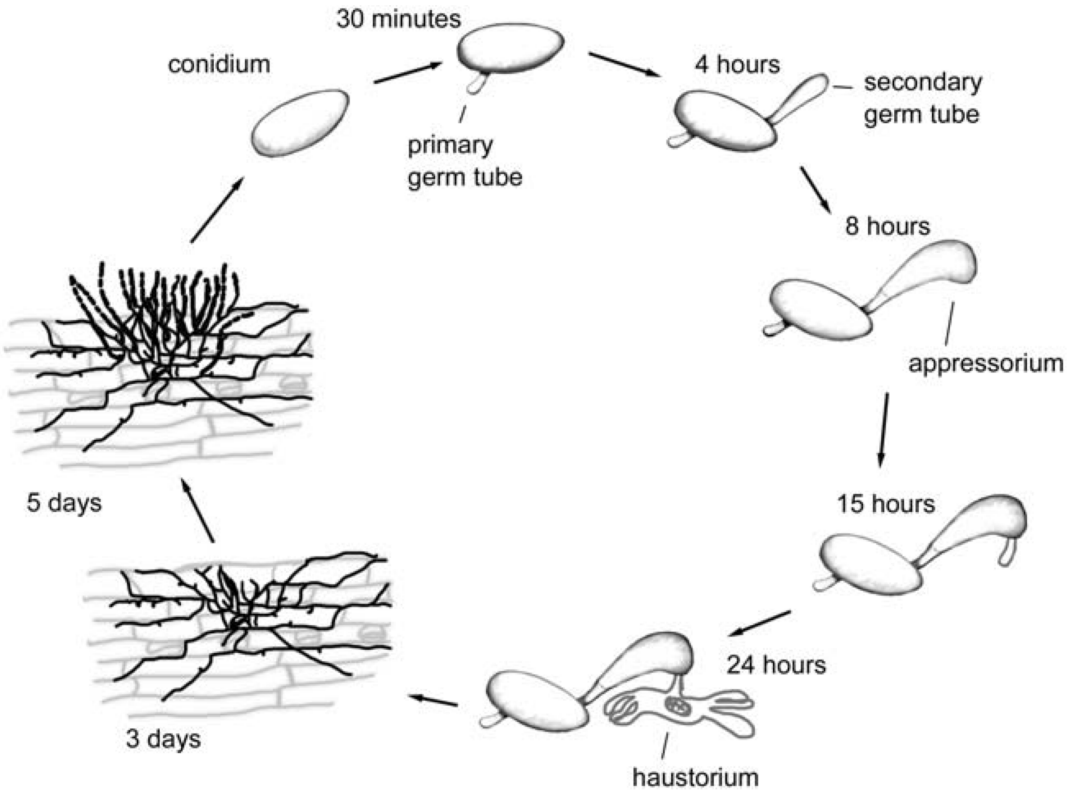

FIGURE 1.2: Asexual life cycle of *Blumeria graminis* f. sp *hordei* (*Bgh*). The complete pathogenic life cycle of *Bgh* from a single conidium landing on a barley leaf to forming conidiophores. The pre-penetrative stages are from the ungerminated conidium up until the development of the appressorium. The post-penetrative stages follow after the penetration peg forms and pierces through the host cell wall. Following this a haustorium develops, allowing the pathogen to siphon nutrients and water from the host cell. Epiphytic mycelia spread on the surface of the leaf, producing secondary haustoria, feeding the development of conidiophores which results in the release of more *Bgh* conidia. This figure was adapted from Both et al. (2005a).

The cuticle is the interface between the plant and microorganisms in which they converse, providing a multitude of physical and chemical cues that promote pathogenesis and invasion. Pathogens also release their own chemical and physical cues that the plant senses, allowing it to call upon its own defence systems against the invading pathogen (Raffaele et al., 2009). There have been several studies that corroborate the role of plant surface properties in triggering pathogenesis (Carver and Thomas, 1990; Tsuba et al., 2002; Gniwotta et al., 2005; Mendoza-Mendoza et al., 2009). More specifically, how the initial events of the infection process develop in response to cuticle derived constituents. The cuticle is comprised of cutin, a polymer matrix, and cuticular waxes, solvent-soluble lipids.

The cutin primarily consists of hydroxyl and epoxy C_{16} and C_{18} fatty acids while the cuticular waxes are comprised of a mixture of very-long-chain aliphatic compounds (primary and secondary alcohols, aldehydes, esters, ketones, alkanes), and cyclic compounds (triterpenoids and phenylpropanoids) (Jetter et al., 2000, 2007) (Figure 1.3).

The pre-penetrative processes during the early stages of pathogenesis are imperative to the fungal life cycle. Early studies utilised the barley wax mutant *eceriferum* (*cer*) and various artificial surface constructs to investigate how the surface features of the host affect th *Bgh* germination process (Yang and Ellingboe, 1972; Carver and Ingerson, 1987; Carver and Thomas, 1990). Tsuba et al. (2002) were able to identify *n*-hexacosanal (C_{26} aldehyde), a chemical component of the cuticular wax, to strongly stimulate appressorium formation in *Bgh*. Further support for *n*-hexacosanal as a *Bgh* germination trigger was given by Hansjakob et al. (2010), where an extensive analysis on the composition of the barley cuticle and the roles of individual constituents was performed, showing *n*-hexacosanal was the most effective at inducing germination and differentiation.

Throughout the process of pathogenesis *Bgh* is continuously synthesising new structures to aid the infection process: from the short primary germ tube that aids in adhesion to the host surface and sensing the environment, the penetration peg which invades the host by piercing through the plant cell wall, and the development of the haustorium that siphons nutrients and water from the host cell. During these processes, the *Bgh* must be able to adapt to the physiological stresses and changes that occur during pathogenesis. The fungal cell wall, a network of polysaccharides enveloping the fungal cell, is an important structure that assists the fungus in maintaining cellular integrity and an important factor to pathogenesis. The dynamic nature of the cell wall allows it to be rigid enough to endure fluctuating osmotic pressures, withstanding pressures of up to 2–4 MPa generated by the penetration peg during host penetration (Pryce-Jones et al., 1999). At the same time, the cell wall is elastic enough to facilitate the continuous cell growth and changes throughout the course of the fungal life cycle.

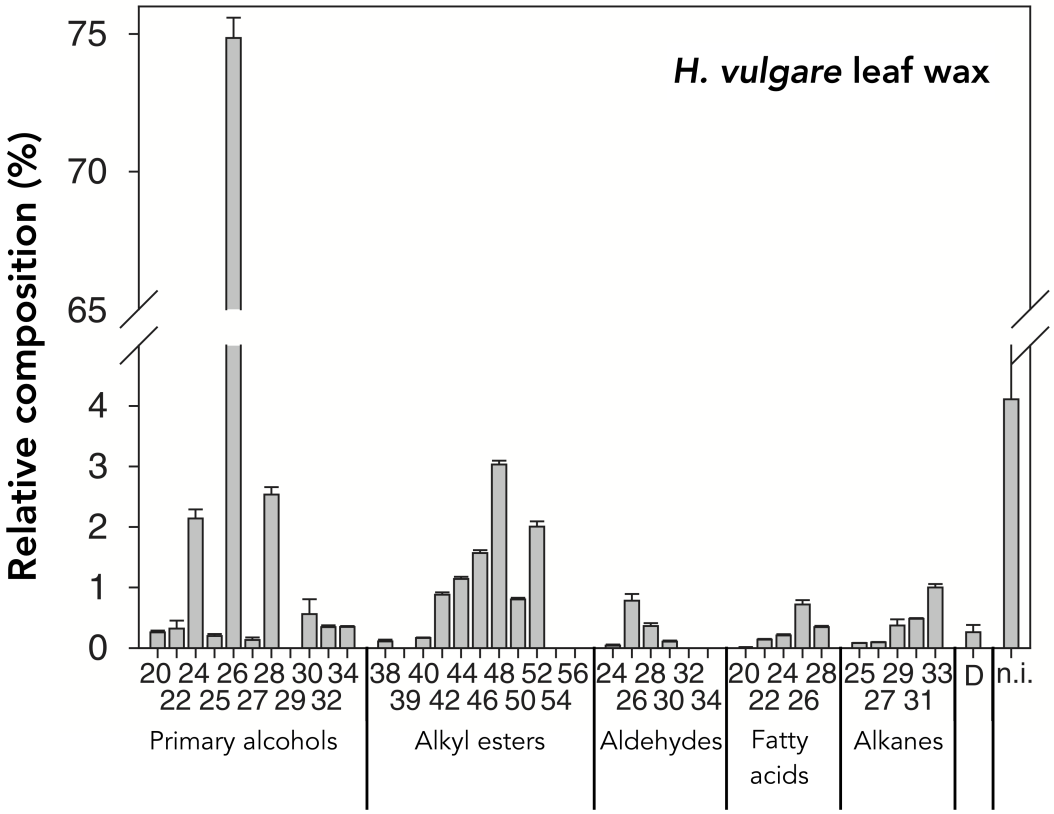

FIGURE 1.3: Relative composition (%) of total leaf wax extracts from *Hordeum vulgare* cv Bonus. Carbon chain lengths are indicated for each chemical compound class. n. i., nonidentified. D, *n*-hexacosane-1,3-diol. Data are given as means of five replications ± SD. Adapted from Hansjakob et al. (2010).

1.4 Fungal cell walls

The development of a protective shield against the elements is crucial to the growth, survival, and morphogenesis of the fungal cell in the diverse environments that they inhabit. The dynamic nature of the cell wall is integral to a multitude of cellular functions. As one of the first barriers to the environment, it is confronted with stresses such as extreme temperatures, desiccation, osmolarity, oxidative agents, and mechanical injuries. The cell wall holds a critical role in identifying hostile or favourable environments and provides the fungus with adaptive responses to environmental stresses. Fungi have developed many cell wall repair mechanisms that swiftly activate following damage. These environmental stimuli are perceived by the signal transduction cascade referred to as the cell wall integrity (CWI) pathway, which is well characterised in the model yeast *Saccharomyces cerevisiae* (Levin, 2011; Kock et al., 2015). This pathway transmits wall stress signals from the cell surface through a signal cascade to mobilise a variety of cell wall remodelling effectors.

In addition to preserving the cell shape and keeping it robust in the face of environmental stress, the cell wall also mediates interactions with the environment and modulates the selective uptake of nutrients. The internal cell wall layer acts as a scaffold to an external layer of glycoproteins, which collectively generate a shield that limits the permeability of the cell wall, defending the internal framework of polysaccharides from degradation. The functions of the cell wall proteins are diverse and largely uncharacterised. Genomic and proteomic approaches in Ascomycetous yeast reveal multiple different proteins incorporated into the cell wall (Yin et al., 2005).

The expansive repertoire of proteins embedded in the cell wall bestows a variety of essential functions. Adhesins and mucins mediate adhesive properties of the fungal cells and allow them to colonise virtually any surface. For pathogenic fungi, the cell wall is critical for virulence and pathogenicity, facilitating evasion and resistance to host defence responses. Given the complexity of the cell wall, its biogenesis requires a substantial number of cellular activities acting in concert to erect and mobilise the dynamic structural network.

The fungal cell wall represents a considerable metabolic investment as it accounts for 15–30% of the cellular biomass in some species (Klis et al., 2007; Orlean, 2012). It plays such a momentous role to survival and maintaining homeostasis that up to 20% of the genes in *S. cerevisiae* are associated with the cell wall (de Groot et al., 2001). Although a considerable variation in the cell wall composition occurs across different species a general scheme can be established for the Ascomycetes. The cell walls of known Ascomycetous yeast and mycelial species are bilayered. Transmission electron microscopy (TEM) reveals that the cell walls of *S. cerevisiae* and *Candida albicans* possess a fibrillar electron dense external layer stemming from

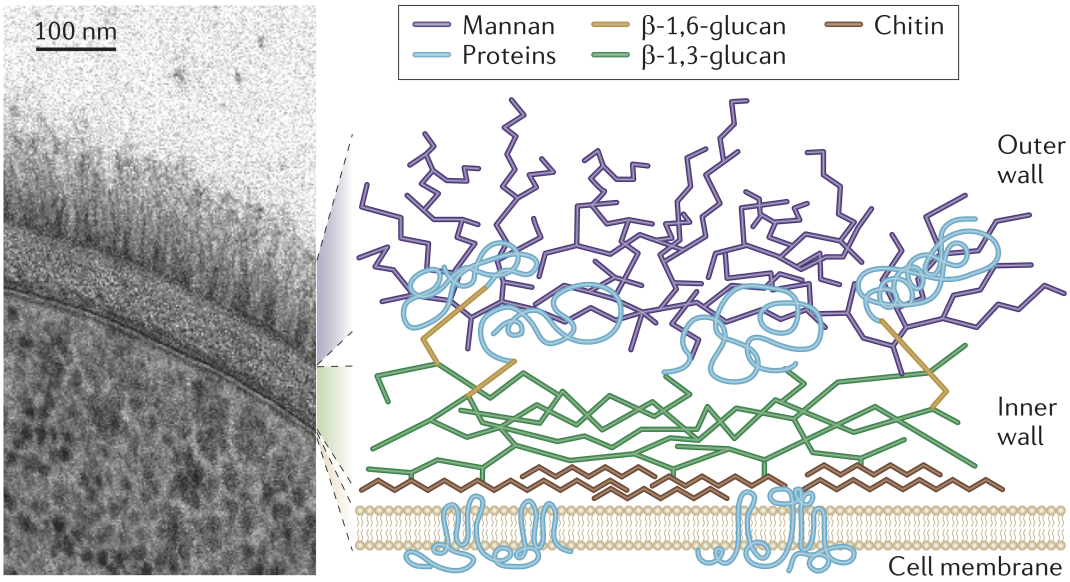

FIGURE 1.4: Basic fungal cell wall structure. On the left is an electron micrograph of the *C. albicans* cell wall while the image on the right depicts a generalised schematic of the fungal cell wall. Major cell wall components are chitin, glucans and glycoproteins. Most of the chitin is situated next to the plasma membrane while β-1,3-glucan extends throughout the cell wall. The chitin and glucan cross-link together to form the core matrix, which confers cell shape and strength. GPI-anchored glycoproteins and non-anchored glycoproteins are covalently attached to the cell wall. These proteins are extensively enriched with N- and O- oligosaccharides that have been modified with the addition of mannan or galactomannan. Adapted from Gow et al. (2011).

an underlying electron-transparent skeletal framework (Osumi, 1998; Ruiz-Herrera et al., 2006) (Figure 1.4). Additional TEM of Ascomycetous yeasts such as *Candida tropicalis*, *Schizosaccharomyces pombe*, *Kluyveromyces polysporus*, and *Exophila dermatitidis* and filamenetous fungi such as *Aspergillus nidulans*, *Aspergillus fumigatus*, *Fusarium oxysporum*, and *Neurospora crassa* also show similar bilayered walls (de Groot et al., 2005; Klis et al., 2007).

The electron dense outer layer can be removed by proteolysis and thereby consists mostly of proteins, while the transparent inner layer can be degraded with β-glucanases, indicating that its major components are glucan (Kopecká et al., 1974; Zlotnik et al., 1984). Collectively these data indicate that the cell walls of Ascomycete fungi consist of a dense external protein layer associated with a polysaccharide rich internal core.

Cell wall polysaccharides are typically separated between alkali-soluble and alkali-insoluble fractions for analysis. One of the best characterised cell walls are those of *C. albicans*. The alkali-insoluble fraction represents the fibrillar skeleton of β-1,3-glucan cross-linked to chitin embedded in an amorphous matrix of alkali-soluble polysaccharides, α-1,3-glucan and glycoprotein (Latgé, 2007) (Figure 1.4). The structural polysaccharides account for over 90% of the cell wall and are composed predominantly of glucan polymers and chitin (Cid et al., 1995; Chaffin et al., 1998). The central core is constructed primarily of β-1,3-glucan chains branched through β-1,6 linkages and anchored to chitin. The network of β-glucans and chitin serves as a major structural component in the cell wall and is largely responsible for the cell wall's mechanical strength and elasticity. The core structure of branched β-1,3-glucan covalently bound to chitin is a common feature in a majority of cell walls while the composition of the alkali-soluble component varies between fungi.

The complex of stress-bearing polysaccharides serves as a platform to an external lattice of glycoproteins. In contrast to polysaccharides, proteins are present in minuscule amounts. Nevertheless, proteins play a critical role in the cell wall structure, physiological activities, and organisation. Most cell wall proteins are glycoproteins that have travelled through the secretory pathway in transit to the cell wall. As they mature towards the cell wall they are modified extensively with N- and O-linked carbohydrates. The structures of the oligosaccharide chains attached to the glycoproteins vary between fungi. Both *S. cerevisiae* and *C. albicans* cell walls contain mannoproteins (Ruiz-Herrera et al., 2006; Orlean, 2012) whereas *N. crassa* and *A. fumigatus* contain galactomannan structures (Fontaine et al., 2000; Free, 2013).

In terms of their linkages, there are two classes of cell wall glycoproteins, linked by covalent or noncovalent bonds. In Ascomycota, which are the best studied examples, three categories of covalently bound proteins exist. The majority of covalently bound proteins are glycosylphosphatidylinositol(GPI)-anchored proteins, bound to β-1,6-glucan by a glycosidic linkage (Kollár et al., 1997;

de Groot et al., 2005). The β-1,6-glucan can be further linked to β-1,3-glucan or chitin, resulting in a strong covalent attachment of GPI-cell wall proteins to the cell wall. The other class of cell wall proteins are Pir-proteins (proteins with internal repeats) (Toh-e et al., 1993), linked to β-1,3-glucan through an unknown alkali labile bond, possibly an O-glycosidic linkage (Ecker et al., 2006). The last class of proteins is linked to other cell wall proteins through disulphide bonds (Moukadiri and Zueco, 2001).

The cell wall is a dynamic structure, both in form and composition. While the base constituents of the cell wall are the same there are striking differences in different developmental stages or growing under different conditions. Cell walls have adapted to a multitude of environments to survive and avoid detection by other organisms. There is a constant arms race between the development of the fungi and host systems. Host systems are able to mount an immune response against invading pathogens upon recognising pathogen-associated molecular patterns (PAMPs). The strongest fungal PAMPs identified to date are chitin or β-1,3-glucan based. In the yeast cells of *C. albicans* the inner core network of chitin and β-1,3-glucan is buried under a layer of mannans (Figure 1.5 (a)), however this can be exposed at the cell surface at the site of bud scars. Consequently, yeast cells are strong elicitors of β-1,3-glucan-induced phagocytosis in humans. On the other hand, the *C. albicans* hyphae, which do not have bud scars, do not trigger a response (Gantner et al., 2005).

There are several examples of outer fungal cell wall layer adaptions that prevent the recognition of the highly immunogenic inner cell wall layers. The spores of *A. fumigatus* cell walls consist of an immunologically inert outer hydrophobin rodlet layer and includes an inner melanin layer, whereas the hyphae of *A. fumigatus* have an outer cell wall layer of α-1,3-glucan, galactomannan and galactosaminoglycan (GAG). The GAG has been shown to be important to pathogenesis as it harbours immunosuppressive properties (Figure 1.5 (b)(c)) (Rappleye et al., 2007; Beauvais et al., 2014).

An outer layer of α-1,3-glucan also masks the highly immunogenic β-1,3-glucans of *Histoplasma capsulatum* (Rappleye et al., 2007) (Figure 1.5 (e)). Likewise, the yeast *Cryptococcus* is surrounded by a thick gelatinous capsule comprised of glucuronoxylomannan (GXM) and galactoxylomannan (GalXM). The capsule is able to impair phagocytosis by macrophages as well as mask the recognition of the underlying cell wall mannan and β-1,3-glucan (O'Meara and Alspaugh, 2012) (Figure 1.5 (d)). The unique adaptions of the cell wall structures play an important role in fungal survival and pathogenesis.

Plants are also able to evoke an innate immunity against microbial pathogens when PAMPs are recognised. Plant pathogens, such as *Puccinia graminis* f. sp. *tritici*, *Uromyces fabae*, and *Colletotrichum graminicola*, have been known to deacetylate chitin to chitosan on the surface of infection structures that are formed within host tissue

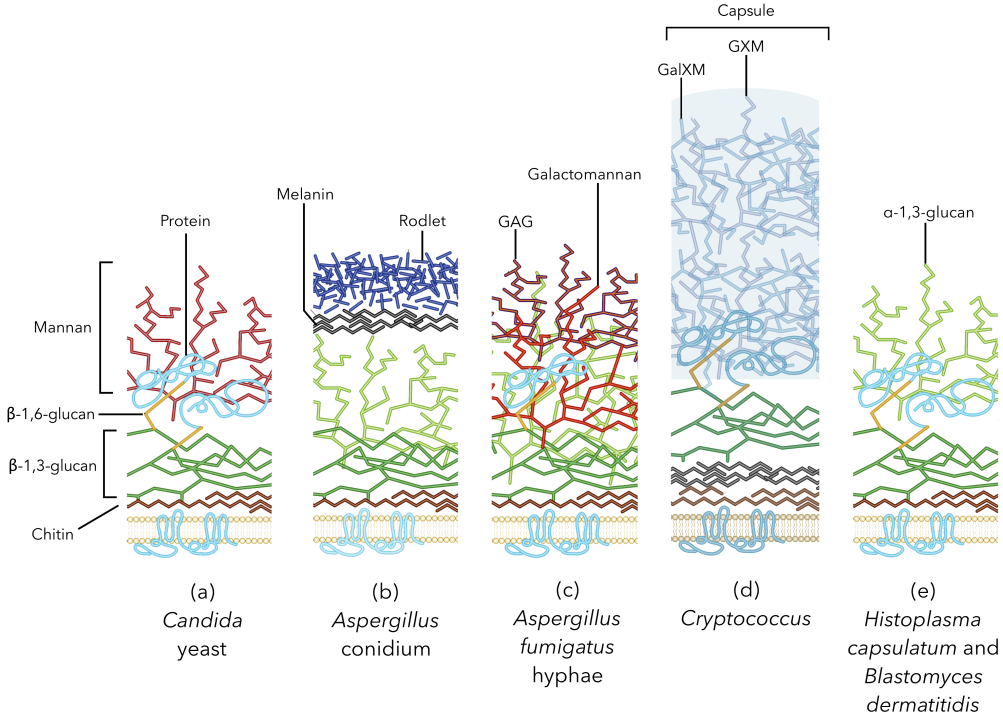

FIGURE 1.5: Fungal cell wall composition of various fungi. The inner layer of fungi typically consists of a polysaccharide core of chitin and β-1,3-glucans. **(a)** The *Candida* cell wall comprises of an outer layer of O-linked mannan, N-linked mannan and phosphorylated mannan. **(b,c)** The cell wall of *Aspergillus* conidia consists of an outer layer of hydrophobin rodlets and an inner layer of melanin. In contrast, the hyphal cell wall of *Aspergillus fumigatus* has α-1,3-glucan, galactomannan and galactosaminoglycan (GAG) in the outer layer. **(d)** The *Cryptococcus* cell wall is surrounded by a thick gelatinous capsule comprising of glucuronoxylomannan (GXM) and galactoxylomannan (GalXM) and has an inner layer of melanin. **(e)** The hyphal cell wall of dimporhic fungi, such as *Histoplasma capsulatum* and *Blastomyces dermatitidis*, possess an outer layer of α-1,3-glucan. This figure was adapted from Erwig and Gow (2016).

in order to evade detection by the host (El Gueddari et al., 2002). *C. graminicola* also rigorously down-regulates genes responsible for β-1,3- and β-1,6-glucan synthesis in its biotrophic infectious hyphae to attenuate the plant immune response (Oliveira-Garcia and Deising, 2013, 2016). Similar to the human pathogens *Magnaporthe oryzae, Cochliobolus miyabeanus* and *Rhizoctonia solani* also accumulate α-1,3-glucan on the surface of their infectious hyphae to conceal chitin from the host (Fujikawa et al., 2009, 2012).

In addition to modifying the cell wall to protect against the plant defences, plant pathogens are also thought to produce an array of effectors that can interfere with the plant defence response. *Cladosporium fulvum* produces several types of effectors that bind to chitin during pathogenesis. The virulence protein Avr4 binds to chitin oligomers in the cell wall to protect the chitin against hydrolysis by plant chitinases while the effector protein Ecp6 mediates virulence by sequestering chitin oligosaccharides that are released from the cell wall of invading hyphae to prevent detection (van den Burg et al., 2006; de Jonge et al., 2010).

1.5 Glucans

Glucana are major structural components of the fungal cell wall, constituting the majority of the cell wall mass. Glucans exist in a number of structural conformations, differing in the carbon units involved in the chemical linkages connecting the glucose monomers. The basic structure of glucans has been examined extensively (Kim et al., 2000; Lowman and Williams, 2001). The majority of the glucans in fungi are present as 1,3 and 1,6 β-glucans. Mixed (1,3;1,4)-β-glucan has also been observed in *A. fumigatus*, (Fontaine et al., 2000), *N. crassa*, (Maddi and Free, 2010) and *Rhynchosporium secalis* (Pettolino et al., 2009), however not much is known about the species distribution of this molecule and its role in the fungal cell wall (Samar et al., 2015). β-1,6-Glucan plays an important role in the formation of the cell wall matrix, cross-linking GPI-anchored cell wall proteins to β-1,3-glucan and chitin. Interestingly while β-1,6-glucans have been found in *S. cerevisiae* and *C. albicans* they are not present in *N. crassa* (Free, 2013) or *A. fumigatus* (Fontaine et al., 2000), indicating that in the absence of β-1,6-glucan an alternative mechanism of cross-linking or cell wall strengthening is employed.

β-1,3-Glucan is a major cell wall polymer found virtually in all fungi and serves as primary structural element that anchors the other cell wall components to the wall. Fungal linear β-1,3-glucan chains have a helical structure, existing as single helical strands or triple helices stabilised by extensive hydrogen bonding. The coiled spring-like structure of the glucan bestows the cell wall with a high degree of elasticity and tensile strength (Klis et al., 2002; Lesage and Bussey, 2006). Recent work on *C. albicans* hyphal cell walls showed that its β-glucan has a unique cyclic structure not found in yeast (Lowman et al., 2014). The glucan was composed of a

cyclic β-1,3-linked polymer backbone with long β-1,6-linked side chains stemming from the 6-position of 3,6 branches. Additionally, 2,3-linkages were also identified in the hyphal glucan. Despite containing the same polymers, the structures of the β-glucans in yeast and hyphal cell walls can differ vastly.

β-1,3-Glucans (FKS) are synthesised by plasma membrane bound glucan synthase complexes primarily located at sites of cell growth, budding, and branching. The glucan synthases are well conserved integral membrane complexes, consisting of a catalytic subunit with multiple transmembrane domains. Genome surveys have illustrated the β-1,3-glucan synthases are conserved across all fungal genera (Coronado et al., 2007; Muszewska et al., 2018). The enzyme accepts cytoplasmic UDP-glucose and transfers the glucose unit onto a growing β-1,3-glucan chain extruding into the extracellular space (Douglas, 2001). This manner of synthesis encourages the nascent glucan polymers to associate with the extracellular space and facilitates their integration into the cell wall (Figure 1.6).

Rho1p is a regulatory subunit that is associated with regulating FKS. In *S. cerevisiae* Rho1p is part of the signal transduction system that controls the MAP kinase signalling pathways that regulate fungal growth and CWI responses and is a key regulator in driving or arresting β-1,3-glucan synthesis (Drgonová et al., 1996). FKS1 is required to associate with Rho1p in order to be active. This allows the production of β-1,3-glucan during times of growth and cell wall stress as well as its restriction when it is not required. Rho1p and FKS1 are transported together as an inactive complex to the plasma membrane through a classical secretion pathway (Abe et al., 2003). Upon arriving at the membrane, Rho1p is activated by Rom2p, a GDP/GTP exchange factor. In its GTP-bound state Rho1p activates FKS1.

Most fungi have alternative FKS proteins that are differentially regulated. In *S. cerevisiae* there are three *Fks* genes. The two highly homologous FKS1 and FKS2 proteins act as the primary catalytic enzymes and encode two functionally redundant units. FKS1 is responsible for the majority of β-1,3-glucan synthesis during vegetative growth while FKS2 assumes this task under starvation conditions, sporulation, and when cells are exposed to mating pheromones (Mazur et al., 1995; Douglas, 2001; Lesage and Bussey, 2006). FKS3 is also required for normal spore wall formation (Ishihara et al., 2007).

In contrast to yeast, in which several *Fks* genes have been identified, all known filamentous Ascomycete genomes sequenced to date only have one *Fks* orthologue (Latgé and Calderone, 2006; Riquelme, 2013). Using the work from the yeast systems as a model, only one *Fks* homologue has been characterised in *A. fumigatus* (Firon et al., 2002), *A. nidulans* (Kelly et al., 1996), *Cryptococcus neoformans* (Thompson et al., 1999), *Paracoccidioides brasiliensis* (Pereira et al., 2000) and *N. crassa* (Sánchez-León et al., 2015).

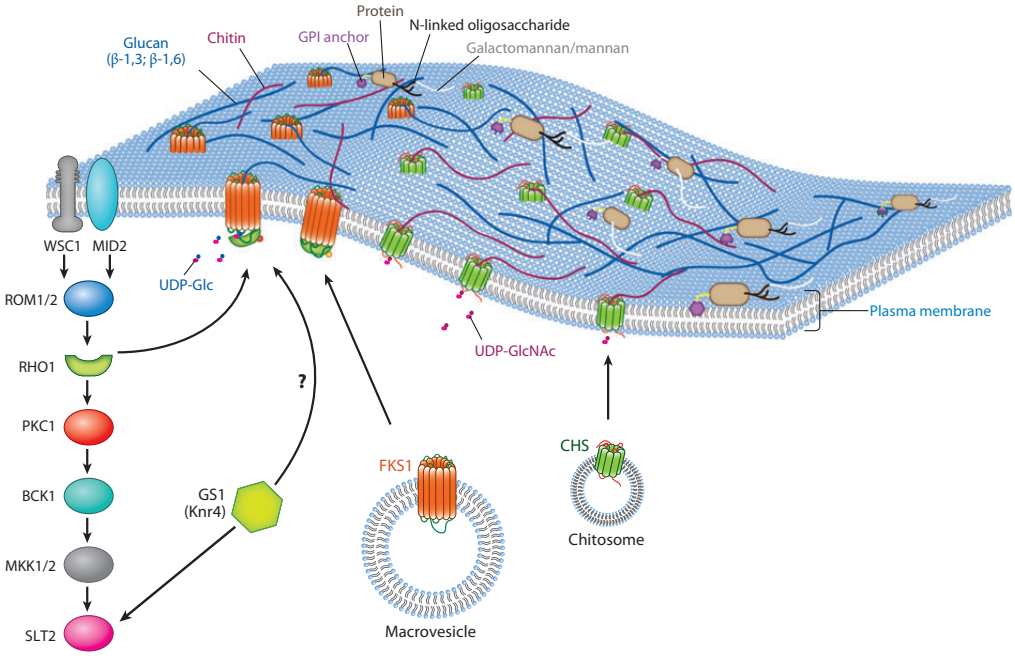

FIGURE 1.6: Schematic representation of fungal cell wall biosynthesis in *Neurospora crassa*. Chitin and glucan synthases are transported to the plasma membrane through different secretion pathways. The vesicles fuse with the plasmalemma into which the synthase complexes are inserted. Chitin and β-1,3-glucan microfibrils are synthesised vectorially into the extracellular space using their respective subunits. Adapted from Riquelme (2013).

1.6 Chitin

Chitin is a linear polysaccharide of β-1,4-linked *N*-acetylglucosamine units and is a structurally important element in the fungal cell wall. In yeast, chitin accounts for only 1–2% of the cell wall, in contrast filamentous fungi, such as Mucoromycotina, can have up to 40% of chitin in their cell walls (Mélida et al., 2015). Chitin is synthesised at the cell surface as microfibrils by organised membrane-bound chitin synthase proteins (CHS). CHS catalyses the polymerisation of *N*-acetylglucosamine (GlcNAc) from the cytoplasmic side of the membrane and transfers the reducing end of GlcNAc to the non-reducing end of the growing chain (Figure 1.6).

Chitin polymers are elongated by vectorial synthesis such that the nascent chains are extruded through the plasma membrane as they are made (Sietsma and Wessels, 2006). Three different forms of chitin exist in nature, differing in the arrangement of the chains in the microfibrils. The β-form exists as parallel chains, the α-form exists as antiparallel chains and the γ-form consists of two parallel chains adjacent to one antiparallel chain (Ruiz-Herrera, 1992). In nature, the α-form is the most abundant.

Chitin microfibrils possess high tensile strength and contribute significantly to the rigidity and integrity of the cell wall. The crystalline arrangement of chitin renders it as one of the most insoluble natural products. As the nascent chitin chains are released into the extracellular matrix, they are covalently attached to their partner load-bearing polysaccharide, β-1,3-glucan.

Chitin synthesis occurs primarily at active sites of growth or cell wall remodelling, where CHS proteins are transported by secretory vesicles called chitosomes (Bartnicki-García, 2006). Chitosomes are highly specialised secretory vesicles distinct from the classical secretory pathway. The microvesicles fuse with the plasma membrane at sites of active cell wall growth where the CHS mobilises and synthesises chitin. In yeast this occurs at the bud tip during polarised growth or at the septa during cytokinesis, while in filamentous fungi this also occurs at the septa and also at the hyphal apex (Riquelme, 2013).

The number of chitin synthase genes differs depending on the fungal species. Most have one or two *Chs* genes responsible for the majority of chitin synthesis during vegetative growth, while other *Chs* are activated temporally at specific stages of development (Free, 2013). One to three *Chs* have been found in yeasts (Cid et al., 1995; Orlean, 2012), whereas filamentous fungi typically have seven *Chs* (Borkovich et al., 2004; Latgé et al., 2005), with some species possessing more than 20 (Ruiz-Herrera and Ortiz-Castellanos, 2010). It has been suggested that the number of *Chs* genes roughly correlates to the chitin content within the cell wall. Yeast possess fewer *Chs* gene families in correspondence to the 1-2% of chitin in their cell wall. Likewise filamentous fungi, which have significantly higher levels of chitin, generally have a greater number of *Chs* genes.

The biosynthesis of chitin is understood best in *S. cerevisiae*. Chitin is a very minor component in the cell wall, generally found as part of the lateral walls and concentrated in the bud neck, bud scar and septa during cell division. The three genes responsible for chitin synthesis are *Chs1, Chs2* and *Chs3* (Cid et al., 1995). Gene disruption experiments suggest that each *Chs* governs a different function. *Chs3* is responsible for generating the majority of chitin in the cell wall, including the formation of the chitin ring during septation (Bulawa, 1992). Mutant *Chs3* lines present reduced growth and chitin levels by tenfold and exhibit cell wall integrity defects. *Chs2* has been observed to be involved in the formation of the septum, while *Chs1* acts as a repair enzyme by replenishing chitin lost during cytokinesis (Silverman et al., 1988).

In the case of the filamentous fungus *A. fumigatus*, which has seven *Chs* encoding genes designated as *ChsA-G* (Mellado et al., 1995), all the *Chs* genes have been cloned and disrupted, yet none of them have been observed as essential. Disruptions of *ChsA, ChsB, ChsC* and *ChsD* genes have not been accompanied by any apparent defect in phenotype (Mellado et al., 1996b,a; Rogg et al., 2011). The only genes whose disruption led to altered phenotypes were *ChsG* and *ChsE. ChsG* was suggested to function at hyphal tips as mutants exhibited reduced radial growth rates and highly branched hyphae (Mellado et al., 1996a). On the other hand, *ChsE* mutants resulted in extreme hyphal swelling and reduced conidiation. A double *ChsE/ChsG* mutant exhibited diminished levels of chitin synthesis, reduced colony radial growth, and aberrant features such as highly branched hyphae, hyphal swelling and a block in conidiation, yet it was still viable (Mellado et al., 2003).

The multiplicity of the CHS enzymes, particularly in filamentous fungi, suggests redundant roles in cell wall synthesis. Compensatory increases in transcription in response to disruption of *Chs* genes have been observed in both yeast and filamentous fungi. When any of the *Chs* genes are disrupted in *C. albicans, Chs1* transcription was increased (Munro et al., 2007). Similarly, in *Wangiella dermatitidis, Chs5* transcription was elevated when the other *Chs* genes were deleted (Wang et al., 2002). Analysis of chitin cell wall in *C. albicans* by shadow-cast transmission electron microscopy demonstrated two prominent forms of chitin microfibrils, one was the short crystalline chitin rodlets that composed the majority of chitin in the cell wall while the other was as a network of long intertwined fibrils located in bud scars and septa plates (Lenardon et al., 2007).

Virtually nothing is known about chitin synthases in *Bgh*. As a filamentous fungus, it is expected that the *Bgh* genome encodes several *Chs* genes. The first and only report of *Chs* gene isolation was of the two genes named *BgChs1* and *BgChs2* (Zhang et al., 2000). The genes were cloned using degenerate PCR primers designed to conserved regions of fungal *Chs* genes. RT-PCR analyses revealed the upregulation of *BgChs1* during stages of primary and secondary germ tube formation while *BgChs2* was only upregulated at the primary germ tube stage. Treatment with CHS inhibitors,

nikkomycin Z and polyoxin D, was reported to result in a reduction of appressorial germ tube formation and caused the tip of the tubes to swell abnormally and eventually lyse.

1.7 Chitin synthase

The exact mechanism in which chitin is assembled and cross linked with other components of the cell wall is poorly understood. Due to difficulty in isolating CHS proteins most of the knowledge is based on bioinformatic analysis of their sequences. CHS are proteins with four to seven predicted transmembrane domains. Three conserved motifs are common to all forms of CHS, from both yeast and filamentous fungi (QXXEY, EDRXL, and QXRRW) (Choquer et al., 2004; Mandel et al., 2006). The region containing these conserved motifs is called the Conserved Region 1 (CON1) and is part of the Chitin synthase 2 domain CS2 (Nagahashi et al., 1995) (Chitin_synth_2, PF03142).

CHS are classified into multiple divisions and classes according to protein similarities in their catalytic domain. There are seven classes of CHS which are grouped into three divisions, each with distinct domain structures (Choquer et al., 2004; Mandel et al., 2006) (Figure 1.7). Division 1 contains CHS from classes I, II and III. These CHS do not have the first section of the CS2 domain, though the CON1 region is still conserved, and contain a Chitin synthase 1 domain CS1 (Chitin_synth_1, PF01644) as well as a Chitin synthase N-terminal domain CSN (Chitin_synth_N, PF08407). Division 2 includes CHS classes IV, V and VI. The catalytic CS2 domain in these CHS proteins is usually preceded by a cytochrome b5-binding type domain (Cyt-b5, PF00173). The Classes V and VI contain a myosin motor domain (Myosin_head, PF00063) and a DEK C-terminal domain (DEK_C, PF08766). Division 3 consists only of class VII, with only the CS2 domain shared by all CHS. The CHS proteins encoded for by the class I-III genes tend to be smaller and contain an amino terminal catalytic domain whereas the CHS proteins encoded by class IV-VII genes tend to be larger and the catalytic domain tends to be more towards the carboxy terminal.

The use of different methods of phylogenetic analysis, among other factors, has caused multiple CHS classifications strategies to arise over time, which becomes a problem when comparing results from multiple independent studies (Table 1.1). While many classification types exist, the general class I-VII system is commonly used. But, there have been some discrepancies in the nomenclature for CHSVI and CHSVII. Choquer et al. (2004) classified CHSVI as being in division 2 and CHSVII in division 3. However, in some cases (Niño-Vega et al., 2004; Mandel et al., 2006) the nomenclature is reversed, in that CHSVII is included in division 2 and CHSVI is in division 3. In this study we will be using the classification by Choquer et al. (2004) as it is the most commonly used system.

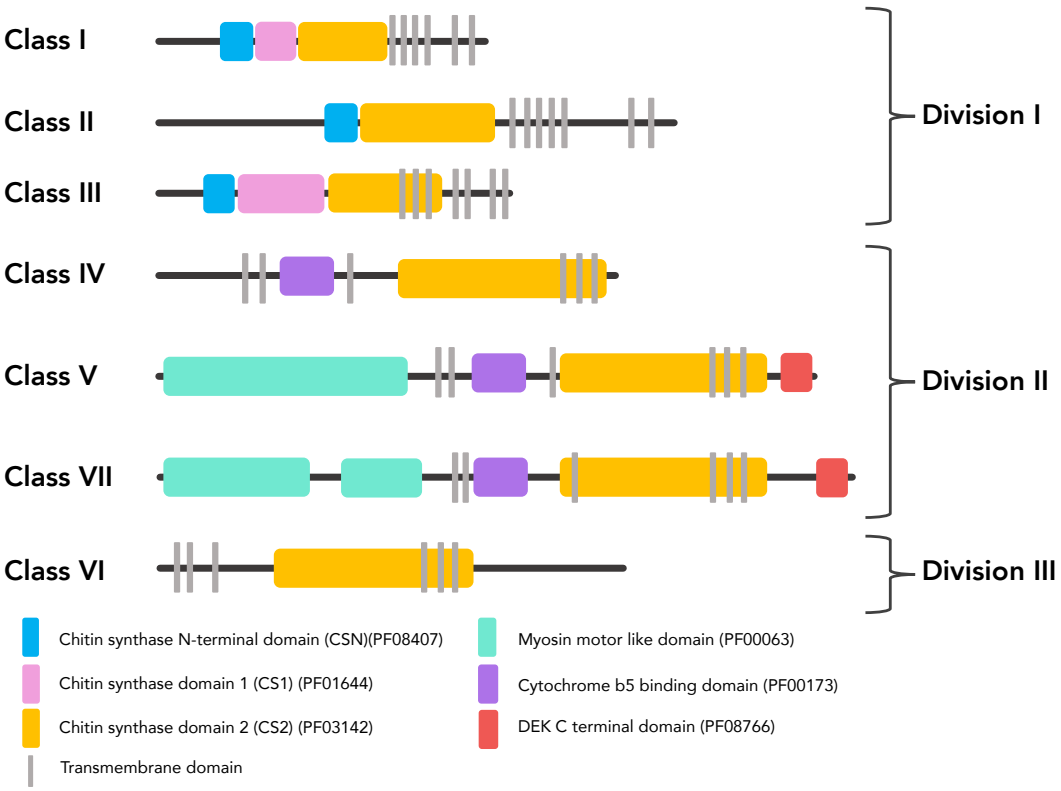

FIGURE 1.7: Schematic representation of the seven CHS classes, types of domain structure of the fungal CHS and their distribution into the three divisions of fungal CHS. This figure was adapted from Fajardo-Somera et al. (2015) and their depiction of the seven CHS proteins in *N. crassa*.

CHS Classifications	Division 1								Division 2								Division 3
Bowen et al. (1992)	I	II	III	-					-								-
Spetch et al (1996) Xoconostle-Cazares et al. (1997)	I	II	III						IV			V					-
Munro and Gow (2001) Roncero (2002) Nino-Vega et al. (2004) Mandel et al. (2006) Zhang et al. (2016)	I	II	III						IV			V	V	VI	-		VI
															VIII	-	-
Chigira et al (2002) Choquer et al (2004)	I	II	III						IV			V	VI		-		- VII
Amnuaykanjanasin and Epstein (2003)	-								IVa	IVb	-	Va	Vb		-		-
Ruiz-Herrera and Ortiz-Castellanos (2010)	I	II	III	IIa			IIb				IV						
Gonçalves et al. (2016)	I	II	III	A	B	C	D	E	IVa	IVb	IVc	Va Vc	Vb Vd	CV	ESV		recChs

TABLE 1.1: Summarised history of chitin synthase protein classifications in fungi (Bowen et al., 1992; Specht et al., 1996; Xoconostle-Cázaresa et al., 1997; Munro and Gow, 2001; Roncero, 2002; Chigira et al., 2002; Amnuaykanjanasin and Epstein, 2003; Niño-Vega et al., 2004; Choquer et al., 2004; Mandel et al., 2006; Ruiz-Herrera and Ortiz-Castellanos, 2010; Zhang et al., 2016; Gonçalves et al., 2016). CV, Chlorovirus-like CHS class. ESV, *Ectocarpus siliculosus*-like CHS class. recCHS, recombined chitin synthase. This figure was adapted from Gonçalves et al. (2016).

The class I, II and IV CHS are present in all fungi, whereas classes III, V, VI and VII are specific to filamentous fungi and certain dimorphic species (Rogg et al., 2012). Considerable efforts have been directed towards characterising the CHS systems in filamentous fungi, however most of the knowledge of CHS comes from yeast, especially *S. cerevisiae*. The precise reason for the expansion of *Chs* genes in filamentous fungi remains unclear. Compared to yeast, filamentous fungi generally possess more complex differentiation patterns. The higher diversity of CHS may be due to the specialisation of each CHS to specific temporal or spatial points during the fungal lifecycle.

Predicting CHS function through homology is not a feasible strategy, as individual classes do not necessarily share the same function across species. The most common strategy to characterise CHS genes is by examining the phenotype of single and multiple *Chs* gene disruptions. However, extrapolating the mutant phenotypes into an exact function is complicated by the functional redundancy of multiple CHS proteins. Additionally, extrapolating from a yeast model species to the context of a filamentous fungi is limited by the widely differing nature of their cell walls and life cycles.

In *S. cerevisiae* the class I CHS acts as a repair enzyme at the site of cytokinesis (Silverman et al., 1988). On the other hand, mutation of the two class I *Chs* genes in *C. albicans* (CHS2 and CHS8) appear to have minimal effects on the overall cell growth and are not vital to repair during cytokinesis (Munro et al., 1998). Similarly, mutations of class I *Chs* genes do not exhibit any obvious phenotypes in *A. nidulans,* and *A. fumigatus* (Motoyama et al., 1994; Munro and Gow, 2001). In contrast expression of the class I CHS is related to morphogenesis in *Botrytis cinerea* (Soulié et al., 2006).

The class II CHS is functionally important in *S. cerevisiae* as it is involved in the construction of the primary septum after cytokinesis (Silverman et al., 1988). It is also essential in *C. albicans* as it produces both septal and lateral wall chitin (Munro et al., 2001). In contrast, the class II CHS has not been shown to be essential in *A. nidulans* or *N. crassa* (Motoyama et al., 1994; Din and Yarden, 1994).

The CHS proteins containing the myosin motor like domain in class V and VI are important in morphogenesis. They have been shown to support hyphal tip growth in the filamentous fungi *A. fumigatus, C. graminicola, N. crassa*, and *Ustilago maydis* (Amnuaykanjanasin and Epstein, 2003; Mellado et al., 2003; Fajardo-Somera et al., 2015; Schuster et al., 2016). The myosin motor like domain is essential for function and polar localisation of the class CHSV (CsmA) in *A. nidulans* (Takeshita et al., 2005). Previous studies have demonstrated that CsmA binds to actin and localises near actin structures at the hyphal tips and septation sites. Mutations to the myosin motor like domain have also demonstrated that interactions between the domain and actin are not only necessary for the proper localisation of CsmA, but also for

CsmA function. In *U. maydis*, the CHSV and CHSVI have been shown to co-locate with β-1,3-glucan synthase in a myosin-CHS-dependent secretion pathway (Schuster et al., 2016).

From gene disruption studies, it is clear that predicting the function of individual *Chs* genes based on homology is not a reliable method. The vast differences between the lifestyles and cell wall compositions of individual fungi affect the role and function of every *Chs* gene in a way that cannot be generalised across species.

1.8 Chemical inhibitors of fungal cell wall synthesis

Fungi are responsible for a multitude of serious diseases that plague the agricultural industry. Disease control is implemented by routine use of fungicides and breeding of resistant genes into desired cultivars. Fungicides have been used in agriculture for well over a century to control disease outbreaks and safeguard crop yield and quality (Thind, 2012). There are a plethora of antifungal agents which target an array of anabolic pathways in the fungal cells that are effective at low dosages and provide a high level of disease control (Russell, 2005; Kathiravan et al., 2012). The fungal cell wall is perhaps the most ideal target for the treatment of fungal pathogens. The enzymes and signal transduction pathways that govern the synthesis of these cell wall components are a prime target for antifungal drug development.

As chitin is a vital component of fungal cell walls, its biosynthesis pathways is a primary target for exploitation in the agriculture and health industries. Several chitin synthase inhibitors have been identified. The most effective and well characterised inhibitors are the peptide nucleoside antibiotics nikkomycin and polyoxin, as well as their synthetic derivatives. Polyoxin and nikkomycin are natural products produced by *Streptomyces cacaoi* and *Streptomyces tendae*, respectively (Hector, 1993). Both compounds are structural analogues of GlcNAc and function by inhibiting chitin synthesis through competitive inhibition with the chitin synthase substrate, UDP-*N*-GlcNAc (Figure 1.8 (b)).

Polyoxin and nikkomycin are extremely effective in hindering chitin synthesis *in vitro*, however treatments *in vivo* are not as potent. The ineffectiveness of the antifungals is thought to be attributable to their peptidyl nucleoside nature as they are susceptible to cleavage by peptidases originating from competing microbial sources or the host. Another reason is due to their limited uptake into the fungal cell. Nikkomycin and polyoxin are required to cross the cell membrane and be delivered to active sites of chitin synthesis in order to be effective, because of this they accumulate poorly in the target fungi.

Polyoxins have demonstrated to be more applicable towards phytopathogenic fungi and oomycetes. However, only a small number of polyoxins have been commercialised for plant protection. Out of the 15 different polyoxins (A-O) the

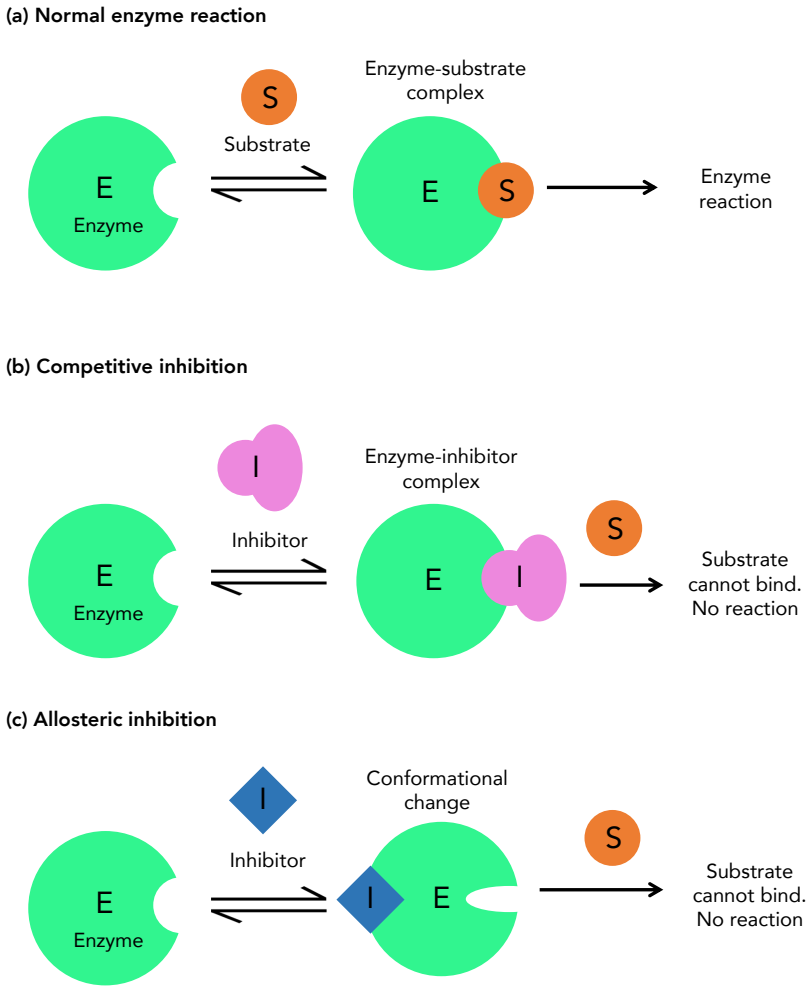

FIGURE 1.8: Schematic diagrams presenting mechanisms of enzyme inhibition. **(a)** Normal enzyme reaction. Substrate binds to enzyme and carries out enzymatic reaction. **(b)** Competitive inhibition. In competitive inhibition the inhibitor resembles the normal substrate that binds to the active site of the enzyme. By mimicking the structure of the substrate, the inhibitor can bind to the active site and prevent the enzyme from utilising the natural substrate by competing with it for the active site. **(c)** Non-competitive (allosteric) inhibition. Non-competitive inhibition reduces the activity of an enzyme without binding to the active site. The most common mechanism of non-competitive inhibition involves the binding of an inhibitor to an allosteric site. When the inhibitor binds to the allosteric site it induces a conformation change in the enzyme in which the substrate can no longer bind to the active site.

one which holds the most agronomic significance is polyoxin D. Polyoxin D has been used to manage phytopathogenic fungi and oomycetes all over the world, from *R. solani*, which causes rice sheath blight in Japan and brown patch in the United States, to *Pythium* sp., which cause blight on turfgrass in Europe (Merzendorfer, 2013).

Unlike polyoxin, nikkomycin has yet to be developed into an antifungal drug. Despite its effective inhibitory activity *in vitro* its application is restricted as the antifungal activity of nikkomycin is limited to a narrow range of fungal species. Nikkomycin is effective against fungi with high chitin content, such as the dimorphic fungal pathogens *Coccidioides immitis, Blastomyces dermatitidis*, and *H. capsulatum*, however it has little effect towards *C. albicans* or *C. tropicalis*, most likely due to the low levels of chitin in these microorganisms (Kathiravan et al., 2012).

Like chitin synthase, the inhibition of β-1,3-glucan synthase is also a highly pursued avenue for antifungal therapies due to the high glucan content in most fungal species. The most notable family of β-1,3-glucan synthase inhibitors are the echinocandins. Echinocandins are a family of large amphiphilic lipopeptides comprised of cyclic hexapeptides modified with lipid side chains. They were approved

for clinical use in 2002 and have been used as antifungals in clinical practice ever since. Echinocandins currently marketed are caspofungin, micafungin, and anidulafungin (Denning, 2003). The echinocandins are secondary metabolites that act as non-competitive inhibitors of β-1,3-glucan synthase (Figure 1.8 (c)), though the exact mechanism of inhibition is not fully understood. Treatment with echinocandins results in cell swelling and lysis at sites of active cell wall synthesis.

Echinocandins are generally administered clinically for aspergillosis and candidiasis (Denning, 2003). While the therapies are normally quite effective there is some apprehension concerning acquisition of resistance that has resulted in treatment failure in some cases. The primary mode of acquired echinocandin resistance are single-base mutations in hot spot regions in the *Fks* sequence (Walker et al., 2010). Additionally, *in vitro* studies have demonstrated that echinocandins can cause paradoxical growth (Wiederhold, 2009). The fungal cell wall is a dynamic structure and obstructing the synthesis of one cell wall component is known to lead to compensatory increases in chitin in order to strengthen the cell wall (Munro et al., 2007). Subsequently the inhibition of β-1,3-glucan synthase leads to a compensatory surge in chitin synthesis in *C. albicans* (Walker et al., 2008, 2013).

While enhanced chitin levels reduce susceptibility to echinocandins, the combinational use of chitin and β-glucan synthase inhibitors show synergistic activity (Walker et al., 2008, 2010). The simultaneous targeting of two cell wall components can greatly enhance cell wall damage to pathogenic fungi. Employing both nikkomycin and echinocandins is effective against *A. fumigatus*. Fungal cultures grown in the presence of echinocandins and nikkomycin showed extensive

cell wall damage and killing activity compared to cultures grown with a single fungicide (Stevens, 2000; Chiou et al., 2001). Additionally, signalling pathways that regulate synthase expression and activity can also act as potential targets in combinational treatments. The calcineurin pathway, protein kinase C (PKC) and high osmolarity glycerol response (HOG) signalling pathway are important in regulating cell wall integrity and may be involved in paradoxical growth (Munro et al., 2007). Consequently, antagonists against these pathways may synergise with β-glucan and chitin inhibitors.

Powdery mildew fungi cause devastating and persistent crop disease in many cereal crops. Intensive breeding programs have introduced numerous race specific resistance genes into modern barley cultivars against *Bgh*, however the resilience of *Bgh* have allowed them to consistently and rapidly overcome the resistance mechanisms of the barley cultivars. Similarly, powdery mildews have also exhibited a propensity to progressively develop resistance towards fungicides (Lucas et al., 2015). Several fungicides targeting different processes has been used in the past to control the spread of *Bgh*, such as seed treatment with ethirimol (Thind, 2012), azoles to inhibit the synthesis of ergosterol (Wolfe, 1984), the quinone outside inhibitor which inhibits respiration by binding to the cytochrome bc_1 complex (Chin et al., 2001; Bäumler et al., 2003; Zhang et al., 2005), and the quinolines (quinoxyfen and proquinazid) which target signal transduction (Hollomon et al., 1997; Gilbert et al., 2009). Overtime *Bgh* quickly lost sensitivity to these fungicides and many were eventually withdrawn from use within a few years.

1.9 Resources available for *Bgh* research

As one of the leading causes of yield losses in barley, the economic impact of *Bgh* drives research at all levels. Despite their significance, very little is known about these pathogens at the molecular level. Analysis of gene function in *Bgh* has fallen considerably behind other filamentous and phytopathogenic fungi, though this is not due to lack of effort (Zhang et al., 2005). Obligate biotrophs are notoriously difficult to work with as modern methods of genetic manipulation cannot be applied to them due to the fact that the fungus depends entirely on the host for survival. Therefore, genetic manipulation techniques such as transformation for overexpressing, silencing, or tagging genes are not available. Additionally, it is difficult to acquire sufficient fungal material to extract stage-specific mRNA or proteins for any adequate analysis.

Elucidating the molecular basis of the sophisticated interactions between obligate biotrophs and their host plants has also proven to be a difficult trial. No reliable transformation protocols have been established yet for *Bgh*, imposing phenomenal challenges for using them as experimental systems. Early attempts at transient transformation protocols for *Bgh* using biolistics were reported to produce stable

transformants (Christiansen et al., 1995; Chaure et al., 2000), however lack of any reproducibility led this to be a nonviable technique.

The majority of analyses conducted on *Bgh* are done using *in planta* systems. Segments of barley leaves are inoculated with *Bgh* conidia and the epidermal layer is peeled to be used in various assays. Candidate effectors are identified by investigating gene regulation during infection and examining proteins associated with the haustoria. The recent sequencing of the *Bgh* genome has also allowed bioinformatic surveys to identify numerous candidate secreted effector proteins, the supposed arsenal of effectors in *Bgh* pathogenesis (Spanu et al., 2010; Pedersen et al., 2012).

The *Bgh* genome is estimated to be approximately 120 Mb, which is four times the average size of other Ascomycete genomes. However, the actual number of predicted genes was nearly 6000, which is in the lower range in comparison to other fungal genomes. Approximately 64% of the genome consisted of transposable elements, which were evenly distributed throughout the *Bgh* genome. A range of secondary metabolites are generally produced by filamentous fungi, some of which participate in pathogenesis. However, the number of key enzymes involved in secondary metabolite pathways are drastically reduced (Spanu et al., 2010). Similar trends have been observed in other biotrophic fungi, such as *U. maydis* and *Tuber melanosporum*.

Even though the genomic information reveals features about the biotrophic lifestyle, it does not reveal any information about gene expression, the protein arsenal and how they interact with each other. To mitigate this, other studies have extensively studied the transcript and proteomic profiles of *Bgh* during different developmental stages (Both et al., 2005a; Bindschedler et al., 2009; Noir et al., 2009; Hacquard et al., 2013).

The absence of a reliable and reproducible transformation system for *Bgh* precludes genetic validation of genes of interest. This has been somewhat circumvented with the development of host-induced gene silencing (HIGS). HIGS is implemented in barley by utilising a biolistic delivery system to bombard barley epidermal cells with particles to introduce and transiently express constructs encoding hairpin RNAs corresponding to targeted *Bgh* transcripts. The barley is then inoculated and the effect on pathogen development is observed by measuring the haustorial index (Nowara et al., 2010; Zhang et al., 2012; Pliego et al., 2013). Although it is beneficial that gene silencing can now be employed to study some effector functions in *Bgh* it may not always be a feasible method as the efficiency of HIGS have been quite variable across studies.

1.10 Aims of this work

Reliable control of major diseases is a fundamental requirement in agriculture. Unfortunately, the effectiveness of chemicals introduced to control powdery mildews has frequently been compromised by the development of resistance. In order to establish more reliable tactics towards disease control, a greater understanding of *Bgh* is required. Knowledge of cell wall composition and its biosynthesis will allow more targeted and tailored approaches towards disease control. β-Glucan and chitin in particular are fundamental components in practically all fungal cell walls and their synthesis are ideal targets for inhibition. The development of robust and reliable *in vitro* methods for *Bgh* is paramount. In spite of its standing as a leading barley pathogen virtually nothing is known about *Bgh* at the cell wall level due to its status as an obligate biotroph and the lack of any sustainable *in vitro* systems.

The present study was conducted in order to:

- Characterise the composition of the *Bgh* cell wall
- Identify genes of interest involved in *Bgh* cell wall biosynthesis
- Establish an *in vitro* system to facilitate thorough analysis of pre-penetrative *Bgh* processes
- Characterise the activity of proteins involved in cell wall biosynthesis

Chapter 2 presents a detailed analysis of the CAZy (Carbohydrate-Active enZyme) genes present in *Bgh* and an expression analysis of these genes in the ungerminated *Bgh* conidia. In addition, permethylation glycosidic linkage analysis of ungerminated *Bgh* conidia cell wall reveals the polysaccharide composition of the *Bgh* cell wall for the first time.

Chapter 3 details the establishment of an *in vitro* system to stimulate the development of *Bgh* pre-penetrative processes. Several artificial surfaces were constructed, based on the previous work by Kobayashi et al. (1991) and Hansjakob et al. (2010), to create an effective and efficient method to generate pre-penetrative stage *Bgh* tissue for analysis. As an obligate biotroph *Bgh* is unable to be cultured *in vitro* and must be grown on the host surface. The presence of host material reduces the sensitivity of many assays and limits *Bgh* research. The purpose of establishing a pre-penetrative *Bgh in vitro* system is to produce fungal material without any contamination from the host plant.

Chapter 4 makes use of the *in vitro* system established in Chapter 3 and presents various analyses conducted on *Bgh* using the developed *in vitro* system. The transcriptomic and proteomic profile of ungerminated *Bgh* conidia and appressorial germ tube stage *Bgh* were analysed from *Bgh* grown on artificial surfaces. In addition, permethylation glycosidic linkage analysis of appressorial germ tube stage

Bgh was conducted to discern any compositional cell wall changes that may occur during early germination growth relative to the ungerminated conidia described in Chapter 2.

Chapter 5 presents the work conducted on the heterologous expression of genes related to cell wall development and biosynthesis in *Bgh*. The seven chitin synthases (*ChsI-VII*), a single *β*-1,3-glucan synthase (*FKSI*) and three *β*-1,3-glucanosyltransferase genes (*GelA/B/C*) genes were isolated from *Bgh* and heterologously expressed in *S. cerevisiae* and *Escherichia coli* in order to isolate and purify their proteins for enzyme biochemical analysis.

Chapter 2

Composition and biosynthetic machinery of the *Blumeria graminis* f. sp. *hordei* conidia cell wall

Statement of Authorship

Title of Paper	Composition and biosynthetic machinery of the *Blumeria graminis* f. sp. *hordei* conidia cell wall
Publication Status	☐ Published ☐ Accepted for Publication ☐ Submitted for Publication ☒ Unpublished and Unsubmitted work written in manuscript style
Publication Details	This work has not been submitted yet.

Principal Author

Name of Principal Author (Candidate)	Trang Anh Pham		
Contribution to the Paper	Collected all samples and prepared them for analysis, interpreted data, wrote manuscript and acted as principal author.		
Overall percentage (%)	75%		
Certification:	This paper reports on original research I conducted during the period of my Higher Degree by Research candidature and is not subject to any obligations or contractual agreements with a third party that would constrain its inclusion in this thesis. I am the primary author of this paper.		
Signature		Date	01-11-18

Co-Author Contributions

By signing the Statement of Authorship, each author certifies that:

i. the candidate's stated contribution to the publication is accurate (as detailed above);
ii. permission is granted for the candidate in include the publication in the thesis; and
iii. the sum of all co-author contributions is equal to 100% less the candidate's stated contribution.

Name of Co-Author	Alan Little		
Contribution to the Paper	Supervised development of work, helped in data interpretation, manuscript evaluation and acted as corresponding author.		
Signature		Date	01-11-18

Name of Co-Author	Neil J. Shirley		
Contribution to the Paper	Analysed qPCR transcript profiling and RNAseq dataset.		
Signature		Date	01-11-18

Name of Co-Author	Julian G. Schwerdt		
Contribution to the Paper	Performed genome annotation		
Signature		Date	01-11-18

Name of Co-Author	Vincent Bulone		
Contribution to the Paper	Supervised development of work, helped in data interpretation, manuscript evaluation and acted as corresponding author.		
Signature		Date	02-11-18

Name of Co-Author	Xiaohui Xing		
Contribution to the Paper	Permethylation glycosidic linkage analysis		
Signature		Date	Nov. 1st, 2018

Manuscript draft

Composition and biosynthetic machinery of the *Blumeria graminis* f. sp. *hordei* conidia cell wall

Trang A. T. Pham[1], Julian G. Schwerdt[1], Neil J. Shirley[1], Xiaohui Xing[2], Vincent Bulone[1,2] and Alan Little[1*].

[1]ARC Centre of Excellence in Plant Cell Walls, School of Agriculture, Food and Wine, University of Adelaide, Waite Campus, Urrbrae, SA 5064, Australia.

[2]Adelaide Glycomics, School of Agriculture, Food and Wine, University of Adelaide, Waite Campus, Urrbrae, SA 5064, Australia.

[*]**Corresponding author:** Alan Little

Phone: +61 8313 7260

Fax: +61 8313 7102

Email: alan.little@adelaide.edu.au

Proposed journal: Cell Surface

Keywords: *Blumeria graminis* f. sp. *hordei*, cell wall, glycosyltransferase, glycoside hydrolase.

2.1 Abstract

Infection of barley with the powdery mildew causal agent, *Blumeria graminis* f. sp. *hordei* (*Bgh*), can lead to devastating damage to barley crops. The recent emergence of fungicide resistance imposes a need to develop new antifungal strategies. The enzymes involved in cell wall biosynthesis are ideal targets for the development of fungicides. However, in order to narrow down any target proteins involved in cell wall formation, a greater understanding of the cell wall structure and composition is required. Here, we present a detailed carbohydrate analysis of the *Bgh* conidial cell wall, a full annotation of Carbohydrate Active enZymes (CAZy) in the *Bgh* genome, and a comprehensive expression profile of the genes involved in cell wall metabolism. Glycosidic linkage analysis has revealed that the cell wall of *Bgh* predominantly consists of glucose (63.1%) and has a greater proportion of galactopyranose residues compared to other species (8.5%). Trace amounts of xylose residues were also detected, which is unusual in ascomycetes. Transcripts of the genes involved in cell wall metabolism show high expression of chitin deacetylases, which assist fungi in evading the host defence system by deacetylating chitin to chitosan. Together these data indicate that the characteristic obligate biotrophic CAZy gene profile and the cell wall composition act in concert to shroud the conidia to circumvent the plant host immune response.

2.2 Introduction

Plant pathogens present significant constraints on the yield and quality of agricultural crops. Powdery mildew infestations in barley are caused by *Blumeria graminis* f. sp. *hordei* (*Bgh*), an obligate biotrophic airborne fungus. In many parts of the world powdery mildew has emerged as one of the most economically important barley diseases, as a single outbreak alone can cause up to 20-40% yield loss (Akhkha, 2009; Murray and Brennan, 2010).

One of the most common strategies to control fungal pathogens is by breeding disease resistant cultivars that can specifically detect the pathogen and avoid infection. However, the resistance is usually monogenic and the fungi are eventually able to circumvent the resistant genes within a few years (Wolfe and Mcdermott, 1994). While disease resistant breeding is a viable strategy it is a time-consuming process and may not even benefit in the long run as some resistant cultivars have shown reductions in yield performance. In conjunction with breeding resistant cultivars, an arsenal of fungicides are also used to control disease outbreaks. However, powdery mildew has a propensity towards rapidly developing resistance to the various fungicides. Potential fungicides that could be deployed in the future may not be viable if *Bgh* can overcome their mode of action (Reis et al., 2013; Tucker et al., 2015). The emergence of fungicide-resistant strains is a global issue necessitating the need for new fungicides and antifungal strategies.

Fungal cells are encompassed in a complex network of interconnected polysaccharides and proteins known as the cell wall (Free, 2013; Gow et al., 2017). As the first point of contact between the fungus and the environment, the fungal cell wall influences the interactions with other organisms and holds a critical role in determining if the environmental conditions are hostile or favourable. The cell wall protects the fungi against all manners of environmental adversities, i.e. from desiccation, extreme temperatures, pH changes, oxidative agents, and mechanical injuries (Levin, 2011). In the case of pathogenic fungi, additional stresses may arise from the host defence responses and antifungal agents. The dynamic nature of the cell wall makes it essential during morphogenesis, cell viability, and pathogenesis (Durán and Nombela, 2004). The importance of the cell wall is not to be underestimated as approximately 20% of the *Saccharomyces cerevisiae* genome is dedicated to cell wall metabolism.

In phytopathogenic fungi the cell wall is critical for successful penetration of the plant host. The infection structures that the fungi develop are the focal point for enzymatic activity and increased turgor pressure is required for the fungal penetration peg to breach the host cell wall. It is therefore prudent to disrupt the biosynthesis of the cell wall before it can facilitate these functions. The fungal cell wall contains vital polysaccharides that are not present within the cell walls of

plants. This makes the enzymes involved in the biosynthesis of cell wall components ideal targets for antifungal drugs for disease control.

Fundamentally the overall cell wall structure and architecture is conserved across all fungal species (Coronado et al., 2007). However, while many of the underlying building blocks are conserved other components are species-specific or even morphologically-specific. The cell wall core consists of a conserved network of chitin and β-1,3-glucan along with an outer layer of heterogeneous glycoproteins. The chitin and β-1,3-glucan interconnect together and assemble a load bearing structural foundation and scaffold for the glycoproteins (Klis et al., 2006).

The structure and composition of the oligosaccharide chains attached to the glycoproteins vary significantly between fungi. While many are composed of mannose they can also consist of a multitude of different sugars such as glucose, galactose, and fucose (Free, 2013). Yeast, such as *S. cerevisiae* and *Candida albicans*, possess an outer layer comprised of highly mannosylated glycoproteins (Ruiz-Herrera et al., 2006; Orlean, 2012) whereas the filamentous fungi *Neurospora crassa* and *Aspergillus fumigatus* have an outer layer of galactomannans (Fontaine et al., 2000; Free, 2013). Collectively the glycoproteins generate a chemically inert shield that limits the permeability of the cell wall, defending the internal framework of polysaccharides from degradation (Erwig and Gow, 2016).

In order to successfully design new and efficient fungal cell wall inhibitors, a finer understanding of cell wall structures and their biosynthesis in phytopathogenic fungi is required. To acquire insight into the cell wall composition of *Bgh* we analysed the polysaccharide composition of ungerminated *Bgh* conidia. To complement this, we also examined the Carbohydrate-Active enZymes (CAZy) encoded in the *Bgh* genome and investigated the expression profile of cell wall polysaccharide metabolic genes in the ungerminated *Bgh* conidia.

2.3 Materials and Methods

2.3.1 Fungal material

A field isolate of *Bgh* was kindly donated by Professor Richard Oliver (Curtin University, W.A., Australia). The *Bgh* isolate was maintained on the highly susceptible barley cultivar Baudin. *Bgh* was propagated by inoculating seven-day-old barley seedlings with conidia from previously infected barley seedlings. The inoculated plants were then cultivated in a growth chamber with a 16 h photoperiod at 22°C for a week. *Bgh* conidia were collected by vacuuming them directly from the plants through a 35 μm filter and capturing them on a 5 μm filter.

2.3.2 Preparation of cell walls

The fungal sample was snap frozen in liquid nitrogen and freeze dried. Alcohol insoluble residue (AIR) was prepared from the *Bgh* conidia as previously described (Mélida et al., 2013). The AIR was then de-starched by α-amylase, recovered by ethanol precipitation, and dehydrated under vacuum (Pettolino et al., 2012). The AIR was stored in a desiccator until required.

2.3.3 Permethylation glycosidic linkage analysis

The cell wall sample was treated with acetic anhydride in aqueous, methanolic acetic acid solution to per-N-acetylate amino sugars (Hirano et al., 1976). Uronic acids were converted to their 6,6-dideuterio neutral sugar counterparts using carbodiimide activation at pH 4.75 followed by reduction with sodium borodeuteride ($NaBD_4$) at pH 7.0 (Kim and Carpita, 1992). All carbohydrates in the sample were permethylated (Ciucanu and Kerek, 1984), hydrolysed with trifluoroacetic acid (TFA), reduced with $NaBD_4$, and peracetylated with acetic anhydride to generate partially methylated alditol acetates (PMAAs) (Pettolino et al., 2012). The PMAAs from neutral sugars and amino sugars were separated using gas chromatography as described earlier (Mélida et al., 2013, 2015). An Agilent J&W VF-23ms capillary column (30 m x 0.25 mm i.d.) and an Agilent J&W DB-1ms Ultra Inert (UI) capillary column (30 m x 0.25 mm i.d.) were used for the separation of PMAAs from neutral and amino sugars, respectively, on an Agilent 7890B/5977B GC-MS system coupled with flame ionization detection (FID). The PMAAs were then identified by comparing their MS fragmentation patterns with those of reference derivatives and by referring to the literature (Carpita and Shea, 1988), and quantified based on the FID response (Sweet et al., 1975; Carpita and Shea, 1988). Five separate experiments were conducted.

2.3.4 RNA extraction and RNAseq library creation

One hundred mg of *Bgh* conidia were ground in liquid nitrogen with a mortar and pestle. Total RNA was extracted using the Plant Total RNA Kit (Sigma) as per the manufacturer's instructions. RNA-Seq sequencing and library preparation were performed at the Australian Genome Research Facility Ltd. (AGRF, Melbourne, Victoria). Libraries for three independent biological replicates were prepared using the Illumina Stranded mRNA kit and 100-bp single-ended sequence reads collected using the Illumina HiSeq sequencer. Each run produced up to 20 million reads per biological replicate.

For each of the samples, sequence reads were quality trimmed and then mapped to the genome of *Bgh* DH14 strain (http://www.ebi.ac.uk/ena/data/view/GCA_000151065.3) using the CLC Genomics Workbenchv8.0 (CLC bio, Aarhus, Denmark). Mean gene expression from each sample was expressed as reads per kilobase of transcript per million mapped reads (RPKM). Sequence read data will be lodged at the NCBI sequence read archive (SRA) upon publication.

2.3.5 Quantitative polymerase chain reaction validation

To confirm the reliability of transcript levels, the relative expression levels of 13 cell wall related genes were checked using quantitative polymerase chain reaction (qPCR) evaluation. cDNA was synthesised from total RNA using the SuperScript®III Reverse Transcriptase (RT) enzyme (Life Technologies, Carlsbad, U.S.A.) following the manufacturer's protocol. Transcript profiling was carried out using qPCR as described previously in Burton et al. (2010) using the gene-specific primers listed in Supplementary Table S8. The data were normalised against the geometric mean of four *Bgh* housekeeping genes, namely actin (*bgh00992*), glyceraldehyde 3-phosphate dehydrogenase (*bgh00075*), tubulin (*bgh01972*), and ubiquitin (*bgh03777*).

2.3.6 Transcriptome analysis and genome annotation

Kyoto Encyclopedia of Genes and Genomes (KEGG), Enzyme commission (EC) and PFAM annotations were retrieved from the EnsemblFungi website (http://fungi.ensembl.org/index.html) through the BioMart portal and appended to the *Bgh* DH14 genome (Spanu et al., 2010). Annotations were also downloaded from the Carbohydrate-Active enZymes Database (CAZy) (http://www.cazy.org) and appended to the *Bgh* genome using *Fusarium graminearum* as a reference organism (Little et al., manuscript in preparation).

Genes that are potentially involved in cell wall polysaccharide biosynthesis were partitioned in two ways; the first method involved categorising the genes together

based on their CAZy families. In the, second method the genes were segregated based on their KEGG predicted functions and EC numbers.

2.4 Results

2.4.1 Glycosidic linkage analysis of *Bgh* conidia

Linkage analysis conducted on the *Bgh* conidia showed that a majority of the conidial cell wall is comprised of glucose (Glc) (63.1%) followed by mannose (Man) (16.2%), galactose (Gal) (10.7%), *N*-acetylglucosamine (GlcNAc) (9%), and trace amounts of xylose (1%) (Figure 2.1). The linkage analysis revealed that the Glc fraction of the *Bgh* conidial cell wall was dominated by 1,3-linked Glc residues (56%) followed by 2,3-Glc (11.8%), 1,4-Glc (10%), and terminal Glc residues (9%). Almost all of the GlcNAc fraction of the cell wall consisted of 1,4-linked residues (97.7%), with the remaining fraction in the terminal GlcNAc form (3.3%). The comparatively low presence of terminal GlcNAc suggests that the chitin chains in the *Bgh* cell wall occur with a high degree of polymerisation. Ten and a half percent of the Man fraction was found in the terminal form, followed by a relatively even distribution of 1,2-linked (26.5%), 1,4-linked (32.7%), and 1,6-linked (23.5%) Man residues. The majority of the Gal fraction in the cell wall was present in the pyranose form as 1,4-linked residues (64%) along with some 2,3-linked residues (13%). Both furanose (20.7%) and pyranose (2.8%) terminal forms were also present in the Gal fraction, with a significantly higher proportion of terminal Gal occurring in the furanose form. The trace amount of xylose found in the cell wall was present as 1,4-linked residues.

2.4.2 Annotation of Carbohydrate Active enZymes (CAZy) in the *Bgh* genome

Genes that were potentially involved in the synthesis of *Bgh* cell wall polysaccharides were identified and annotated. The genome of *Bgh* DH14 (Spanu et al., 2010) was appended with KEGG Enzyme Class, PFAM, CAZy annotations and blasted against the annotated *F. graminearum* genome. Putative genes involved in cell wall biosynthesis were sorted based on their KEGG annotations and predicted functions (Figure 2.2). However, as the KEGG classification does not cover all of the CAZy genes, a separate table of all annotated CAZy genes can be found in Supplementary Tables S1-S6. Three hundred and six CAZy genes were identified. These code for predicted auxiliary activity (AA) (25), carbohydrate binding modules (CBM) (41), carbohydrate esterases (CE) (25), glycoside hydrolases (GH) (138), glycosyl transferases (GT) (93), and polysaccharide lyases (PL) (4) (Table 2.1).

Multiple copies of putative chitin synthase genes (*Chs*) (GT2) were identified. Similar to *N. crassa*, seven copies of *Chs* genes were identified in *Bgh* (Sánchez-León et al., 2011), one for each chitin synthase class (*I-VII*). Naming of the *Bgh* chitin synthase genes was based on their class and homology to *F. graminearum* chitin synthases.

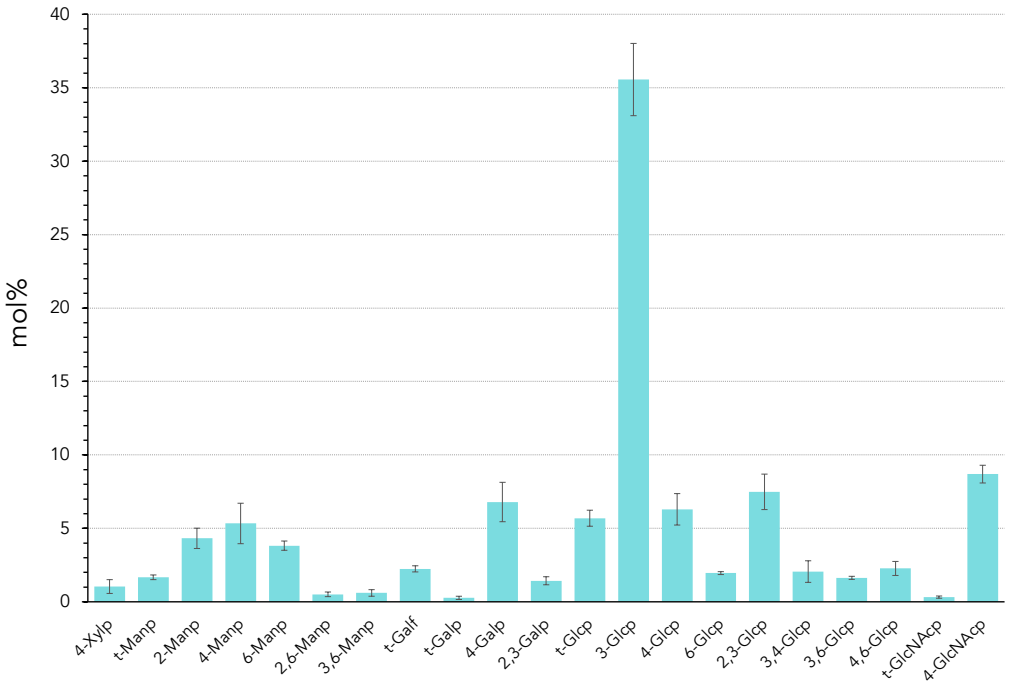

FIGURE 2.1: Permethylation glycosidic linkage analysis (mol%) of the carbohydrate fraction of the cell wall from ungerminated *Blumeria graminis* f. sp. *hordei* conidia. The different glycosidic linkages and pyranose or furanose forms of each monosaccharide were deduced from EI-MS spectra. Gal, galactose; Glc, glucose; GlcNAc, *N*-acetylglucosamine; Man, mannose; Xyl, xylose; 'p' and 'f' at the end of a monosaccharide abbreviation indicate that the residue occurs in the pyranose or furanose form, respectively; 't-' indicates a 'terminal' monosaccharide that occurs at the non-reducing end of a glycan. Error bars indicate standard deviations calculated from three biological replicates.

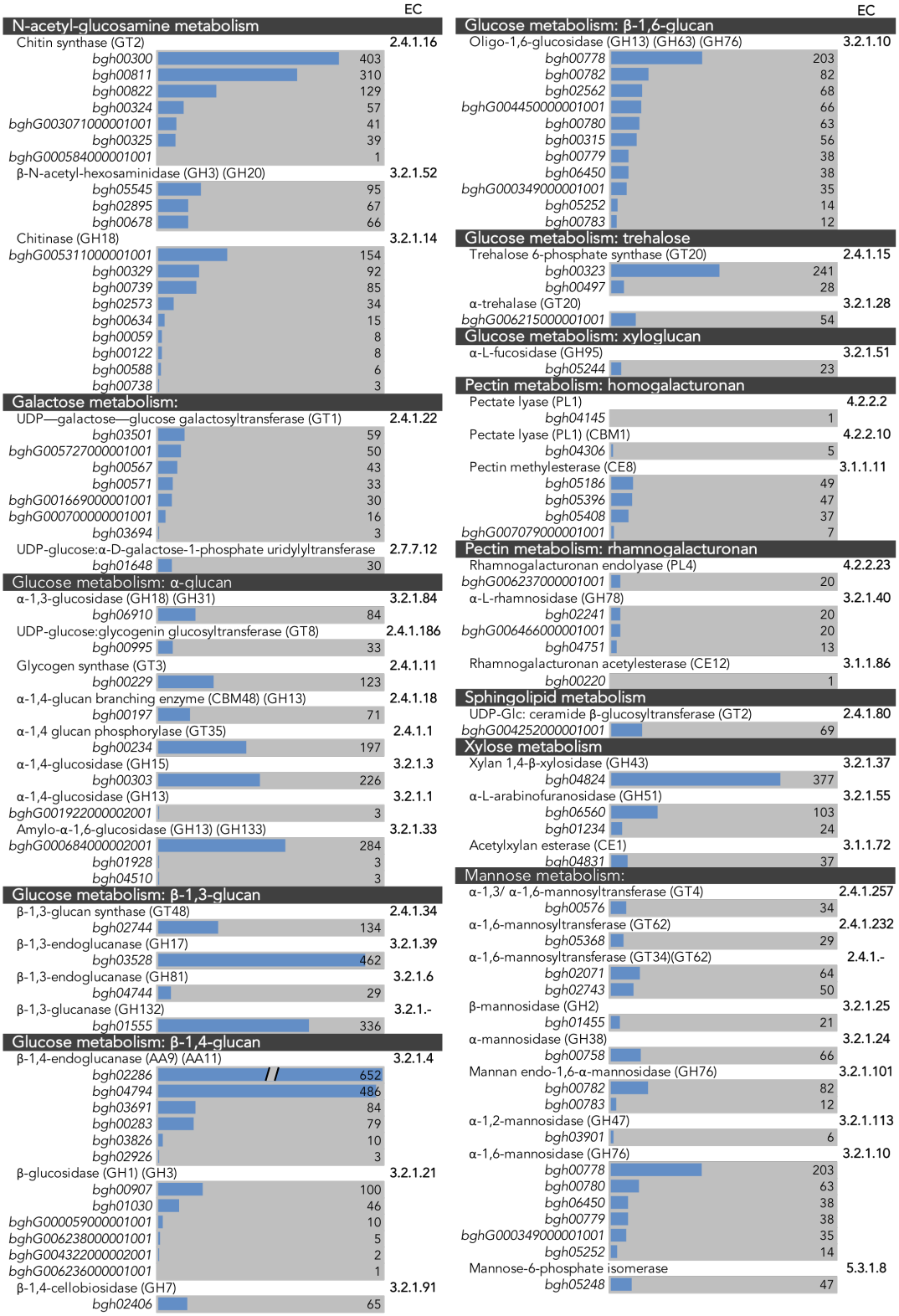

FIGURE 2.2: RNAseq transcript levels of genes involved in cell wall metabolism in the *Blumeria graminis* f. sp. *hordei* ungerminated conidia. Genes are organised by their KEGG predicted roles in cell wall metabolism. Transcript levels are displayed adjacent to the accession numbers of genes as RPKM values. Scale of the bars is 0-500 RPKM, with a few outliers exceeding 500. EC, Enzyme Commission numbers. (Continues on next page).

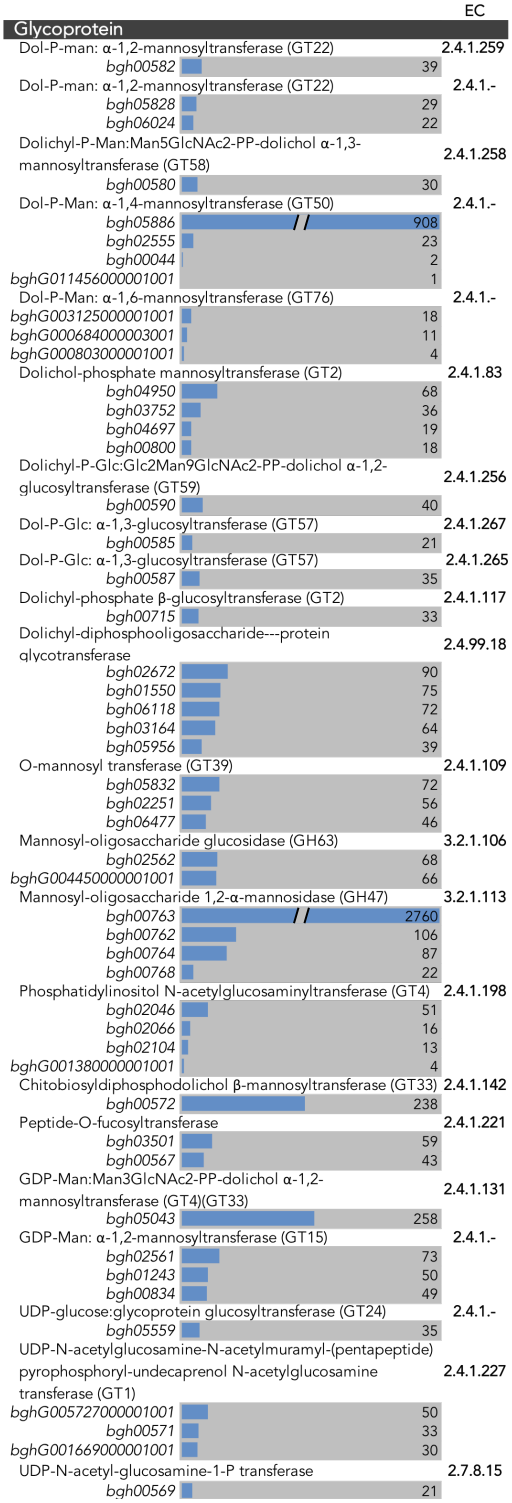

FIGURE 2.2: Continued

TABLE 2.1: Copy number of *Blumeria graminis* f. sp. *hordei* Carbohydrate Active enZymes (CAZy) classified genes in each family. Auxiliary Activity (AA) enzymes, Carbohydrate Binding Modules (CBM), Carbohydrate Esterases (CE), Glycoside Hydrolases (GH), Glycosyl Transferases (GT) and Polysaccharide Lyases (PL).

CAZY Groups	Number of Genes
AA	25
CBM	41
CE	25
GH	138
GT	93
PL	4
total	**326**

A number of enzymes involved in chitin modification were also identified, including three β-*N*-acetyl-hexosaminidase (GH3 and GH20), eleven chitinases (GH18 and CBM18), and four chitin deacetylases (CE4 and CBM18).

The *Bgh* genome encodes one functional copy of a putative β-1,3-glucan synthase (*Fks1*) (GT48). This trend is common in other filamentous fungi, in which a single *Fks1* is potentially responsible for synthesising the entirety of the β-1,3-glucan in the fungal cell wall (Supplementary Table S5). The analysis did not uncover any genes that could be potentially involved in α-1,3-glucan biosynthesis. Nevertheless genes that code for putative transglycosylation α-1,3-glucanosyltransferases (GH57) and α-1,3-glucosidases (GH18) are present within the genome.

Three putative β-1,3-glucanosyltransferases (GH72) were also identified (Supplementary Table S7). Enzymes affiliated with the GH72 family have been annotated as transglycosylases that are predicted to assist in either the formation of β-1,3-glucans with 1,6-branches or the elongation of β-1,3-glucan chains (Hartland et al., 1996; Mouyna et al., 1998). The presence of 1,3,6-linked glucose residues in the *Bgh* cell wall supports the possibility that the GH72 enzymes are involved in β-1,3-glucan branching. Two *Bgh* genes with similarity to the *KRE* genes in *S. cerevisiae*, which have been suggested to be required for β-1,6-glucan synthesis (Kollár et al., 1997), were also found to be present within the genome (Supplementary Table S7). These genes could also be acting in conjunction with candidate chitin β-1,6-glucosyltransferases (*bgh02647* and *bghG001597000001001*) (Supplementary Table S7), which form cross-links between chitin and 1,3-glucan. These candidate genes are GH16 transglycosylases that contain a CBM18, a chitin binding module. The presence of these genes, coupled with the presence of 1,6-linked glucan (Figure 2.1), indicate that β-1,6-glucan may form cross-links with β-1,3-glucan, chitin, and GPI-anchored oligosaccharides in the *Bgh* cell wall. In addition to the anabolic enzymes, there are also mutiple hydrolytic enzymes involved in glucan metabolism. Three copies of exo-β-1,3-glucanases (GH5) were identified, along with four endo-β-1,3-glucanases (GH17 and GH81), and eight β-1,3-glucanases (GH16, GH55, and GH132) (Supplementary Table S7).

A wide range of genes putatively involved in mannan biosynthesis were identified, which supported the presence of the various mannose linkages found in the cell wall analysis. A total of 31 mannosyltransferases were identified, many with overlapping functions in glycoprotein metabolism. There were seven α-1,2-mannosyltransferases (GT4, GT15, GT22 and GT33), one α-1,3-mannosyltransferase (GT58), four α-1,4-mannosyltransferases (GT50), nine α-1,6-mannosyltransferases (GT32, GT34, GT62, GT76), one 1,3/1,6-α-mannosyltransferase (GT4), six mannosyltransferases (GT2 and GT22), and three O-mannosyl transferases (GT39) (Figure 2.2). As only a single GT4 was present, it is likely that it may be responsible for synthesising the 1,3,6-linked mannose residues (Figure 2.1). The hydrolytic enzymes that were predicted to act on mannose structures include one α-mannosidase (GH38), one

β-mannosidase (GH2), seven α-1,2-mannosidases (GH47 and GH92), six α-1,6-mannosidases (GH76), and three endo α-1,6-mannosidases (GH76) (Figure 2.2).

While a large number of gene families were recognised to be involved in the metabolism of the major cell wall polysaccharides, a more limited pool of genes were identified to be putatively involved in galactose and xylose metabolism. A few candidates involved in the UDP-galactose pathway were identified (GT1) along with two galactosyltransferases (GT34) that are believed to transfer galactose residues to acceptor molecules. Although there were no strong candidates identified for synthesis of the xylose in the *Bgh* cell wall, genes encoding the xylan hydrolytic enzymes 1,4-β-xylosidase (GH3 and GH43) and acetylxylan esterase (CE1) were found within the genome. The lack of any candidate genes for the synthesis of xylose is resultant from the KEGG classification system, which depends on previously characterised orthologues in other species. As there is a lack of characterisation of xylose metabolism genes in fungal species this renders the KEGG database insufficient for identifying target genes from this class. Based on the predicted functions of the CAZy classes, candidate synthases for xylose may be found in the GT1, GT4 and GT90 families.

2.4.3 Transcriptome analysis of ungerminated *Bgh* conidia

The majority of the candidate cell wall genes (Figure 2.2 and Supplementary Table S7) were observed to be expressed at detectable levels in the RNA sequence data from the ungerminated *Bgh* conidia. Only the genes that exhibited detectable transcripts in the KEGG sorted list are shown in Figure 2.2, along with the corresponding accession numbers. Supplementary Table S7 displays all the CAZy annotated genes along with their corresponding transcript levels. To validate the RNAseq dataset, qPCR was conducted on a subset of cell wall related genes, chiefly GHs involved in chitin and glucan metabolism (Supplementary Figure S1 and S2). A good correlation was observed between the RNAseq and qPCR expression profiles ($y = 429.14x - 18215; R^2 = 0.93$), indicating the reliability of the RNAseq dataset (Supplementary Figure S3).

All of the seven *Chs* genes are expressed in the ungerminated conidia (Figure 2.2). The *ChsI* (*bgh00300*) displayed the highest expression, which is not unexpected as class I chitin synthases are quite stable and generally expressed at high levels during vegetative growth (Roncero, 2002). Following this, the *ChsVII* (*bgh00811*) exhibited the second highest rate of expression. Following *ChsVII*, *ChsIII* (*bgh00822*) displayed a moderate level of expression. *ChsV* (*bgh00324*) and *ChsVI* (*bgh00325*) showed quite low levels of expression in the conidia.

Transcripts of *ChsII* (*bghG000584000001001*) and *ChsIV* (*bghG003071000001001*) show the lowest levels of expression in the conidia. This could be because in other fungal species these two classes of CHS are generally only active during mating

and sporulation. Class II chitin synthases in particular are associated with septum formation, while class IV chitin synthases are associated with spore maturation (Roncero, 2002). The chitinases generally displayed low levels of expression, however one chitin deacetylase (*bgh06022*) showed considerably high transcript levels, 670 RPKM (Supplementary Table S7). The chitin deacetylases catalyse post-synthetic modifications to chitin by partially or fully deacetylating chitin to form chitosan. As chitosan is a poor elicitor of the plant immune response and resistant to plant chitinases the ungerminated *Bgh* may be masking the cell wall chitin in preparation for pathogenesis (Hadwiger, 2013).

The *Fks1* (*bgh02744*) transcript displays a relatively moderate level of expression (134 RPKM) (Figure 2.2), yet a number of enzymes involved in glucan remodelling are highly expressed in the ungerminated conidia. These include two of the β-1,3-glucanosyltransferases (GH72) (*bgh00776*, and *bgh00774*) (Supplementary Table S7), an exo-β-1-3-glucanase (GH5) (*bgh00086*) (Supplementary Table S7), a β-1,3-endoglucanase (GH17) (*bgh03528*) (Figure 2.2) and a β-1,3-glucanase (GH16 (*bgh00726*) and GH132 (*bgh01555*)) (Supplementary Table S7 and Figure 2.2 respectively). The β-1-3-glucanosyltransferase gene (*bgh00776*) in particular was one of the highest expressed (1185 RPKM). The two GH72 β-1,3-glucanosyltransferases ((*bgh00776*) and *bgh00774*) genes are homologous to the *A. fumigatus GEL1* and *GEL7*, respectively. *GEL1* was highly expressed during mycelial growth and was important in virulence while *GEL7* is implicated in conidiation (Mouyna et al., 2005; Gastebois et al., 2010; Zhao et al., 2014). The elevated transcript levels of the various enzymes involved in glucan metabolism may suggest that a high degree of β-1,3-glucan remodelling occurs in the *Bgh* conidia.

Several genes involved in *N*-glycan biosynthesis and modification of glycan side chains are also highly expressed, including an α-1,2-mannosidase (GH47) (*bgh00763*), a Dol-P-Man: α-1,4-mannosyltransferase (GT50) (*bgh05886*), and a β-1,4-xylosidase (GH3 and GH43) (Figure 2.2). In fact, the gene encoding for the α-1,2-mannosidase is the highest expressed in the conidia (2760 RPKM). Chitobiosyldiphosphodolichol β-mannosyltransferase (GT33) (*bgh00572*) and GDP-Man:Man3GlcNAc2-PP-dolichol α-1,2-mannosyltransferase (GT4) (GT33) (*bgh05043*), which are also involved in *N*-glycan biosynthesis, exhibited moderate levels of expression.

TABLE 2.2: Permethylation glycosidic linkage analysis (mol%) of the carbohydrate fraction of the total cell walls from ungerminated *Blumeria graminis* f. sp. *hordei*, *Neurospora crassa* (Mélida et al., 2015), *Rhynchosporium secalis* (Pettolino et al., 2009), *Aspergillus fumigatus* (Fontaine et al., 2000) (Alcohol insoluble fraction only) and *Saccharomyces cerevisiae*. The different glycosidic linkages and pyranose or furanose forms of each monosaccharide were deduced from EI-MS spectra. Sugar derivatives nomenclature used: Gal, galactose; GalNAc, *N*-acetylgalactosamine; Glc, glucose; GlcA, glucuronic acid; GlcNAc, *N*-acetylglucosamine; Man, mannose; Rha, rhamnose; Xyl, xylose; 'p' and 'f' at the end of a monosaccharide abbreviation indicate that the residue occurs in the pyranose or furanose form, respectively; 't-' indicates a 'terminal' monosaccharide that occurs at the non-reducing end of a glycan.

Linkage	*B. graminis hordei*	*N. crassa*	*R. secalis*	*A. fumigatus*	*S. cereviseae*
t-Galf	2.2	1.0		2.2	
5-Galf			12.0	8.1	
t-Galp	0.3	3.0	2.5		0.2
4-Galp	6.8				
2,3-Galp	1.4				0.4
2,3,4,6-Galp			0.1		
4-GalNAcp				3.9	
t-Glcp	5.7	13.0	13.9	0.3	5.5
2-Glcp			0.1		
3-Glcp	35.6	54.0	11.6	43.3	26.9
4-Glcp	6.3	4.0	17.2	14.2	
6-Glcp	2.0		0.5	0.3	16.0
2,3-Glcp	7.5		1.5		7.0
3,4-Glcp	2.1		0.5	0.3	0.7
3,6-Glcp	1.6	5.0	2.7	1.6	3.0
4,6-Glcp	2.3		0.5		
2,3,4-Glcp			0.1		
3,4,6-Glcp			0.1		
2,3,4,6-Glcp			2.3		
t-GlcNAcp	0.3	0.5			0.1
4-GlcNAcp	8.7	10.0	6.3	17.65	0.6
t-Manp	1.7	1.5	3.1	0.1	15.7
2-Manp	4.3	3.0	4.3	2.4	7.9
3-Manp			2.9		4.0
4-Manp	5.3				0.3
6-Manp	3.8		4.4	1.2	1.2
2,3-Manp			0.9		
2,4-Manp			0.1		
2,6-Manp	0.5	4.0	2.4	1.3	10.2
3,6-Manp	0.6		0.6		0.4
4,6-Manp				0.5	
2,4,6-Manp			0.8		
2,3,4,6-Manp			0.6		
t-Rhap			5.7		
2-Rhap			1.3		
2,3,4,6-Rhap			0.1		
4-Xylp	1		0.1		
Total	100.0	99.0	99.2	97.4	100.1

2.5 Discussion

A comparison of the *Bgh* cell wall against other well characterised species, such as *N. crassa* (Mélida et al., 2015), *A. fumigatus* (Fontaine et al., 2000), *S. cerevisiae* (Little et al., manuscript in preparation), and *Rhynchosporium secalis* (Pettolino et al., 2009), demonstrates the contrasting composition of the *Bgh* cell wall. Despite the significant structural role of chitin, especially in filamentous fungi, it only represents 9% of the total cell wall in the *Bgh* conidia. The chitin deacetylase (*bgh06022*) showed high transcript levels (Supplementary Table S7) in the conidia. This could infer that a majority of the chitin in the conidia cell wall is in a deacetylated state, possibly to reduce the opportunity in eliciting the plant immune response. The relative decrease of chitin in the cell wall is compensated by an increase in glucan content (63.1%). The prevailing form of glucan in the cell wall is 1,3-linked (56%), however, the distribution of alpha and beta linkages is unknown, with both *Fks1* and candidate α-1,3-glucanosyltransferases displaying relatively moderate expression levels in the conidia (Figure 2.2).

Chitin, β-1,3-glucans, and glycoproteins are cross-linked together by β-1,6-glucans in *S. cerevisiae* and *C. albicans* (Kollár et al., 1995, 1997; Netea et al., 2008). The presence of 1,6 (2%) and 1,3,6-linked (1.6%) residues in the *Bgh* cell wall suggests that β-1,3-glucans, chitin, and glycoproteins are cross-linked together by β-1,6-glucans. This is further supported by the presence of putative β-1,3-glucanosyltransferases (GH72) and candidate chitin β-1,6-glucosyltransferases. Not all fungi implement the use of β-1,6-glucan cross-links. For example, species such as *N. crassa*, *R. secalis* and *A. fumigatus*, have extremely low or no detectable amounts of 1,6-linked glucan in their cell wall (Table 2.2), indicating that there may be alternate means of cross-linking cell wall components for structural integrity.

In comparison to the other fungi, the total proportion of mannose in the *Bgh* cell wall is similar to that of *R. secalis*, though the distributions of mannan linkages vary considerably (Table 2.2). *Bgh* has the highest amount of 1,4-linked mannose compared to the other fungi in this table. Chitobiosyldiphosphodolichol β-mannosyltransferase (GT33) (*bgh00572*), a β-1,4-mannosyltransferase, displayed moderate expression in the conidia (238 RPKM), while Dol-P-Man: α-1,4-mannosyltransferase (GT50) (*bgh05886*) was highly expressed (908 RPKM). In addition, α-1,2-mannosyltransferase (*bgh05043*) also exhibited moderate expression and the α-1,2-mannosidase (GH47) gene (*bgh00763*) was one of the highest expressed (Figure 2.2). These genes are all involved in the synthesis of *N*-glycans and may imply that mannan chains are modified during the conidial stage.

The galactose component of the *Bgh* cell wall is primarily composed of 1,4-linked galactopyranose (63.6%), which is seldom present in fungal cell walls. There has only been scarce mentions of galactopyranose in fungal cell wall analysis studies. Though trace amounts of 1,4-linked galactopyranose have been detected in

Magnaporthe grisea (>1%) (Samalova et al., 2016) and galactopyranose residues have been detected in *R. secalis* (Pettolino et al., 2009), these composed a minute portion of the cell wall compared to *Bgh*.

Unlike genes related to the other cell wall polysaccharides, only a few candidate genes involved in galactose metabolism could be identified. The few genes that were identified displayed relatively low levels of expression in the conidia (Figure 2.2). In *Aspergillus*, UDP-galactopyranose mutase converts UDP-galactopyranose to UDP-galactofuranose for the biosynthesis of galactofuranose glycoconjugates. Galactofuranose is an important component of the fungal cell wall that is not found in any mammals or higher plants and has been shown to play an important role in virulence and cell wall structure in *Aspergillus nidulans* and *A. fumigatus* (El-Ganiny et al., 2008; Schmalhorst et al., 2008; Afroz et al., 2011). The diminished presence of galactofuranose in the *Bgh* cell wall could have evolved to avoid eliciting the plant immune response. As an obligate biotroph the survival strategy of *Bgh* is to remain undetected and not harm the host.

Interestingly, 1,4-linked xylose was found to be present in the *Bgh* cell wall. In the past, a hallmark of ascomycetes was the absence of xylose in the cell wall. This monosasccharide has previously been found in basidiomycetes such as *Tremella mesenterica, Ustilago maydis* and *Crytococcus neroformans* (Reid and Bartnicki-Garcia, 1976; Ruiz-Herrera et al., 1996; Park et al., 2012). However, trace amounts of xylose have recently been recorded in ascomycetes, such as *M. grisea* (Samalova et al., 2016). Little is known about the role of xylose in the fungal cell wall. It could potentially be a component of xylomannan, which has been detected in the fungal cell walls of *Flammulina velutipes* and *Trichosporon cutaneum* (Depree et al., 1993; Kawahara et al., 2016) and is found in diverse taxa, ranging from plants, insects, and amphibians (Walters et al., 2011). It has been proposed as an antifreeze molecule that enables organisms to overwinter.

Not enough is known about xylose metabolism in fungi to be able to select strong candidate xylosyltransferase genes from the genome, although the candidate pool may be narrowed down by looking at the predicted functions of various CAZy classes. Only a small number of genes thought to be involved in xylose metabolism were identified, with potential CAZy classes including GT1, GT4, GT34, and GT90, which all have predicted xylosyltransferase functions. Knowledge of the *Bgh* cell wall composition is the first step in understanding its structure. Further experimental evidence will be required to determine how each linkage is incorporated into individual polysaccharides and how they are organised within the cell wall.

Plants possess an innate immune system that are able to identify invading pathogens by recognising evolutionary conserved pathogen or microbial associated molecular patterns (PAMPs or MAMPs) through pattern recognition receptors (PRR) (Ferrari

et al., 2013). Major cell wall components, such as chitin and β-glucans, are strong elicitors and activate PAMP-triggered immunity (PTI). The diverse compositions observed in the fungal cell wall glycoproteins found in the outer cell wall layers of different species may serve to mask the more widespread immunoreactive cell wall components.

A common strategy to evade host detection involves structurally or chemically modifying the cell wall. Relative to chitin and β-glucan, chitosan and α-glucans are much weaker inducers of the defence responses in most plants (Fujikawa et al., 2012; Hadwiger, 2013). By deacetylating chitin to chitosan or accumulating α-1,3-glucan on the outer surface of the cell wall pathogens have a much greater chance of evading detection. As an obligate biotroph *Bgh* would not harm the host and would aim to remain undetected to avoid triggering the PTI. It would stand to reason that the *Bgh* cell wall would reflect this lifestyle as well. With the high expression of chitin deacetylase, it is likely that the majority of the chitin present in the conidial cell wall has been deacetylated to chitosan. The glycoproteins would be cross-linked to the β-1,3-glucan core through β-1,6-glucan and decorated with galactofuranose and xylomannan side chains that are rarely present in fungal cell walls. Considering that 1,3-linked glucose residues were the most abundant polysaccharides in the *Bgh* cell wall, it is also possible that α-1,3-glucans are decorating the exterior of the *Bgh* cell wall as well. The design of the cell wall would conceal the *Bgh* pathogen with the chitosan and rare polysaccharides so that it can live an epiphytic lifestyle without alerting the host.

In the *Bgh* genome, there is a notable reduction in genes encoding enzymes involved in the degradation of the plant cell wall. Genome annotations of other obligate biotrophic pathogens, such as corn smut (*U. maydis*) and rust fungi (*Melampsora laricipopulina* and *Puccinia graminis* f. sp. *tritici*), have also exhibited diminished numbers in cell wall degrading enzymes and hydrolases (Kämper et al., 2006; Duplessis et al., 2011). In comparison with hemibiotrophic and necrotrophic fungi, biotrophic fungi have the smallest array of CAZy genes (Raffaele and Kamoun, 2012; Zhao et al., 2013). The loss of these genes are mirrored in the genomes of numerous unrelated biotrophic fungi and oomycetes, indicating convergent adaptions to the obligate biotrophic lifestyle on plants (Raffaele and Kamoun, 2012). The CAZy annotations of the *Bgh* genome show that there have been expansions and reductions within gene families when compared to other well characterised fungal species (Supplementary Table S1-S6).

Prior analyses of the *Bgh* genome have concluded that *Bgh* had an extreme reduction in enzymes devoted to degrading the plant cell walls (Spanu et al., 2010; de Witt et al., 2012; Hacquard et al., 2013). However, although the number of cell wall degrading genes are diminished, the original analysis had severely underestimated the *Bgh* CAZy gene numbers. Spanu et al. (2010) were unable to identify any candidate cellulose, xylan or pectin degrading enzymes and were only able to

identify 3 GH families (GH16, GH61 and GH81), while de Witt et al. (2012) identified 63 GH genes and a few genes in the CE and CBM families. This is contrary with our data, as we have identified a substantially greater number of genes in all the CAZy families using a combination of CAZy annotations, PFAM, and BLAST searches (Supplementary Table S1-S6). Although diminished compared to other hemibiotrophic and necrotrophic fungi, *Bgh* does possess a significant arsenal of cell wall degrading and modifying enzymes for pathogenesis and cell wall modification.

The largest reduction in gene numbers can be seen with the GH families, especially when compared to *A. fumigatus* and the hemibiotrophic plant pathogen *R. secalis*. Many of the GH families in *Bgh* showed decreased gene numbers or absence compared to the other fungi, with the most dramatic reductions seen in the GH2, GH3 and GH43 families (Supplementary Table S4). The GH2 family is reported to contain β-mannosidase, β-galactosidase, exo-glucosaminidase, and chitosanase activities. The GH3 family contains β-xylosidases and β-glucosidases and the GH43 family contains endo-α-1,5-arabinanase, α-arabinofuranosidase, and β-xylosidase activities.

There was also a reduction within the CE1 and CE5 families, which are associated with acetylxylan esterase and cutinase functions (Supplementary Table S3). In addition, there was a significant reduction in the AA3 and AA9 families. The AA families contain redox enzymes that act in conjunction with hydrolytic CAZy enzymes. The AA3 family mostly contains cellobiose dehydrogenases (Levasseur et al., 2013) while AA9 enzymes have been demonstrated to act as lytic polysaccharide monooxygenases (LPMO), working synergistically with cellulases in cellulose hydrolysis (Kim et al., 2015). While the total number of genes within the GTs was comparable to all the other species there were expansions in GT32, GT33, GT50, and GT76, which are all families associated with mannosyl and galactosyltransferase activities.

The CBMs had notable increases in the CBM1, CBM18, and CBM50 families, which have been demonstrated to bind to cellulose (CBM1) and chitin (CBM18 and CBM50) (Mello and Polikarpov, 2014; Akcapinar and Kappel, 2015; Liu and Stajich, 2015). Expansions in CBMs have been associated with pathogenicity in various fungi by defending the pathogen from the host defence response (Abramyan and Stajich, 2011; Amselem et al., 2011). The increase in chitin-binding modules may assist the *Bgh* in dampening chitin induced PTI. Plants release chitinases as a general protective measure against fungal pathogens and are able to recognise chitin oligomers. To avoid chitin induced PTI, fungi such as *Cladosporium fulvum* secrete the evolutionary conserved LysM(CBM50)-domain containing extracellular effector protein 6 (Ecp6) during infection, which sequesters the chitin fragments and outcompetes the PRRs to avoid detection (de Jonge et al., 2010). To guard against chitinases, *C. fulvum* also secretes the chitin-binding effector Avr4 (CBM14), which binds to the chitin present on the fungal cell wall to protect it from degradation

(van den Burg et al., 2006). It was recently demonstrated that secreted proteins containing a CBM18 also have the capacity to bind to chitin on the cell wall and protect fungi from chitinases (Liu and Stajich, 2015). The expansion of CBM18 has also been observed in other pathogenic fungi (Abramyan and Stajich, 2011; Amselem et al., 2011).

The genomic analysis revealed a comprehensive list of CAZy families involved in polysaccharide metabolism and supports previous speculations of *Bgh* possessing an extensively reduced set of CAZy genes due to its nature as an obligate biotroph. Further analysis demonstrated an expansion of the CBM families, not identified in previous investigations and classified substantially more CAZy genes than were previously thought to be present in the *Bgh* genome.

The conidia are generally considered metabolically inactive structures, developing on the conidiophores and remaining dormant until triggered to germinate. Contrary to this viewpoint, recent studies on dormant conidia have demonstrated that they are metabolically active (Novodvorska et al., 2016). Transcriptome analysis reveals that a multitude of genes associated with polysaccharide metabolism are active in the *Bgh* conidia. The conidia cell wall, while not experiencing any active biosynthesis requirements due to growth, is most likely undergoing many reconstruction and maintenance processes, with the conidia cell wall composition and transcriptome data suggesting that the conidia cell wall was modified to conceal itself from the plant host.

The transcriptome and genome annotations of the *Bgh* cell wall synthetic and hydrolytic machinery will be a useful resource for locating candidate genes involved in polysaccharide metabolism for further analysis to investigate their role in cell wall biosynthesis as well as potential targets for disease control. While knockouts are not a feasible option yet for *Bgh* it is possible to perform gene knockdowns using host-induced gene silencing (HIGS) to silence target cell wall genes and determine their role in cell wall biosynthesis, growth, and survival (Nowara et al., 2010; Pliego et al., 2013). Further investigations should be conducted on the cell wall composition during various stages of *Bgh* pathogenesis in the future. The cell wall is not a static structure and any stage-specific variations in the cell wall during pathogenesis could be potential targets for disease control.

Understanding the fungal cell wall in conjunction with the genes and processes associated with its metabolism is an important milestone in the search for new wall-specific antifungals. In addition to major cell wall elements, the subtle species-specific differences in the cell wall structures and composition may play a significant part in supporting cell wall integrity and could be ideal targets for disease control.

In conclusion, this study presents the composition of the conidial cell wall of *Bgh*, which was correlated to a repertoire of genes involved in polysaccharide metabolism that could be potential targets for the development of novel fungicides.

2.6 Supplementary Figures and Tables

TABLE S1: Copy number of genes classified in Carbohydrate Active enZymes Auxiliary Activity (AA) modules from *Blumeria graminis* f. sp. *hordei*, *Neurospora crassa*, *Rhynchosporium secalis*, *Aspergillus fumigatus* and *Saccharomyces cerevisiae*.

CAZY	*B. graminis hordei*	*N. crassa*	*R. secalis*	*A. fumigatus*	*S. cerevisiae*	CAZY Functions
AA1	7	8	11	2	3	Laccase / p-diphenol:oxygen oxidoreductase / ferroxidase, ; ferroxidase, Laccase-like multicopper oxidase
AA2	3		7		1	manganese peroxidase, versatile peroxidase, lignin peroxidase, peroxidase
AA3	1	2	22	16		cellobiose dehydrogenase, glucose 1-oxidase, aryl alcohol oxidase, alcohol oxidase, pyranose oxidase
AA4	2		5			vanillyl-alcohol oxidase
AA5		1				Oxidase with oxygen as acceptor, galactose oxidase, glyoxal oxidase
AA6			3		2	1,4-benzoquinone reductase
AA7	4		11			glucooligosaccharide oxidase, chitooligosaccharide oxidase
AA8		2		2		Iron reductase domain
AA9	4	14	13	9		AA9 (formerly GH61) proteins are copper-dependent lytic polysaccharide monooxygenases (LPMOs); cleavage of cellulose
AA10		4		2		AA10 (formerly CBM33) proteins are copper-dependent lytic polysaccharide monooxygenases
AA11	4	3	1			AA11 proteins are copper-dependent lytic polysaccharide monooxygenases
AA12		1		2		pyrroloquinoline quinone-dependent oxidoreductase
AA13		8		2	3	AA13 proteins are copper-dependent lytic polysaccharide monooxygenases
AA total	**25**	**35**	**73**	**33**	**6**	

TABLE S2: Copy number of genes classified in Carbohydrate Active enZymes Carbohydrate Binding Modules (CBM) from *Blumeria graminis* f. sp. *hordei*, *Neurospora crassa*, *Rhynchosporium secalis*, *Aspergillus fumigatus* and *Saccharomyces cerevisiae*.

CAZY	*B. graminis hordei*	*N. crassa*	*R. secalis*	*A. fumigatus*	*S. cerevisiae*	CAZY Functions
CBM1	12	19	5	7		Modules of approx. 40 residues found almost exclusively in fungi. The cellulose-binding function has been demonstrated in many cases
CBM6						The cellulose-binding function has been demonstrated in one case on amorphous cellulose and β-1,4-xylan
CBM13	1	2				While in the plant lectins this module binds mannose, binding to xylan has been demonstrated in the Streptomyces lividans xylanase A and arabinofuranosidase B
CBM14				1		The chitin-binding function has been demonstrated in several cases
CBM18	15	3	11	12	2	The chitin-binding function has been demonstrated in many cases
CBM19					1	Modules of 60-70 residues with chitin-binding function
CBM20	1	2		4		The granular starch-binding function has been demonstrated in several cases
CBM21	1	1	1	1	4	The granular starch-binding function has been demonstrated in one case
CBM24		3		1		α-1,3-glucan (mutan)-binding function demonstrated in two cases
CBM32		1				Binding to galactose and lactose has been demonstrated for the module of Micromonospora viridifaciens sialidase. Binding to polygalacturonic acid has been shown for a Yersinia
CBM35				3		A module that is conserved in three Cellvibrio xylan-degrading enzymes binds to xylan
CBM38		1				The inulin-binding function has been demonstrated
CBM42				1		Binding to arabinofuranose (present in arabinoxylan) has been demonstrated
CBM43	1	1		3	2	The β-1,3-glucan binding function has been demonstrated with the olive pollen protein Ole e 10
CBM48	2	1	1	1	3	Modules of approx. 100 residues with glycogen-binding function
CBM50	6	1	9	2		Binding to chitopentaose demonstrated
CBM52		1				Binding to β-1,3-glucan demonstrated for Schizosaccharomyces pombe
CBM63	2			1		expansin EXLX1 has been shown to bind cellulose.
CBM total	**41**	**36**	**27**	**37**	**12**	

TABLE S3: Copy number of genes classified in Carbohydrate Active enZymes Carbohydrate Esterase (CE) modules from *Blumeria graminis* f. sp. *hordei*, *Neurospora crassa*, *Rhynchosporium secalis*, *Aspergillus fumigatus* and *Saccharomyces cerevisiae*.

CAZY	*B. graminis hordei*	*N. crassa*	*R. secalis*	*A. fumigatus*	*S. cerevisiae*	CAZY Functions
CE1	1	6	4	2		acetyl xylan esterase, cinnamoyl esterase, feruloyl esterase, carboxylesterase, S-formylglutathione hydrolase, diacylglycerol O-acyltransferase, trehalose 6-O-mycolyltransferase
CE2	3		9			acetyl xylan esterase
CE3	3	3	1	5		acetyl xylan esterase
CE4	5	4	1	7	2	acetyl xylan esterase, chitin deacetylase, chitooligosaccharide deacetylase, peptidoglycan GlcNAc deacetylase, peptidoglycan N-acetylmuramic acid deacetylase
CE5	3	3	12	4		acetyl xylan esterase, cutinase
CE8	4	1	5	3		pectin methylesterase
CE9		1		1		N-acetylglucosamine 6-phosphate deacetylase, N-acetylglucosamine 6-phosphate deacetylase
CE12	5	1	5	2		pectin acetylesterase, rhamnogalacturonan acetylesterase, acetyl xylan esterase
CE15		1				4-O-methyl-glucuronoyl methylesterase
CE16	1	1		3		acetylesterase
CEnc		1		4		
CE total	**25**	**22**	**37**	**31**	**2**	

TABLE S4: Copy number of genes classified in Carbohydrate Active enZymes Glycoside Hydrolase (GH) modules from *Blumeria graminis* f. sp. *hordei*, *Neurospora crassa*, *Rhynchosporium secalis*, *Aspergillus fumigatus* and *Saccharomyces cerevisiae*.

CAZY	*B. graminis hordei*	*N. crassa*	*R. secalis*	*A. fumigatus*	*S. cerevisiae*	CAZY Functions
GH1	2	1	1	3		β-glucosidase, β-galactosidase, β-mannosidase, β-glucuronidase, β-xylosidase, β-D-fucosidase, phlorizin hydrolase, exo-β-1,4-glucanase, 6-phospho-β-galactosidase, 6-phospho-β-glucosidase, strictosidine β-glucosidase, lactase, amygdalin β-glucosidase, prunasin β-glucosidase, vicianin hydrolase, raucaffricine β-glucosidase, thioglucosidase, β-primeverosidase, isoflavonoid 7-O-β-apiosyl-β-glucosidase, ABA-specific β-glucosidase, DIMBOA β-glucosidase, β-glycosidase, hydroxyisourate hydrolase,
GH2	1	5	2	10		β-galactosidase, β-glucuronidase, α-L-arabinofuranosidase, mannosylglycoprotein endo-β-mannosidase, exo-β-glucosaminidase,
GH3	5	9	15	20		β-glucosidase, xylan 1,4-β-xylosidase, β-glucosylceramidase, β-N-acetylhexosaminidase, α-L-arabinofuranosidase, glucan 1,3-β-glucosidase, glucan 1,4-β-glucosidase, isoprimeverose-producing oligoxyloglucan hydrolase, coniferin β-glucosidase, exo-1,3-1,4-glucanase, β-N-acetylglucosaminide phosphorylases,
GH5	10	7	13	15	5	endo-β-1,4-glucanase / cellulase, endo-β-1,4-xylanase, β-glucosidase, β-mannosidase, β-glucosylceramidase, glucan β-1,3-glucosidase, licheninase, exo-β-1,4-glucanase / cellodextrinase, glucan endo-1,6-β-glucosidase, mannan endo-β-1,4-mannosidase, cellulose β-1,4-cellobiosidase, steryl β-glucosidase, endoglycoceramidase, chitosanase, β-primeverosidase, xyloglucan-specific endo-β-1,4-glucanase, endo-β-1,6-galactanase, hesperidin 6-O-α-L-rhamnosyl-β-glucosidase, β-1,3-mannanase, arabinoxylan-specific endo-β-1,4-xylanase, mannan transglycosylase,
GH6		3	1	2		endoglucanase, cellobiohydrolase,
GH7	1	5	6	3		endo-β-1,4-glucanase, reducing end-acting cellobiohydrolase, chitosanase, endo-β-1,3-1,4-glucanase,
GH10	1	4	5	3		endo-1,4-β-xylanase, endo-1,3-β-xylanase, tomatinase, xylan endotransglycosylase,
GH11		2	6	2		endo-β-1,4-xylanase, endo-β-1,3-xylanase,
GH12		1	5	1		endoglucanase, xyloglucan hydrolase, β-1,3-1,4-glucanase, xyloglucan endotransglycosylase,
GH13	8	10	5	14	9	α-amylase, pullulanase, cyclomaltodextrin glucanotransferase, cyclomaltodextrinase, trehalose-6-phosphate hydrolase, oligo-α-glucosidase, maltogenic amylase, neopullulanase, α-glucosidase, maltotetraose-forming α-amylase, isoamylase, glucodextranase, maltohexaose-forming α-amylase, maltotriose-forming α-amylase, branching enzyme, trehalose synthase, 4-α-glucanotransferase, maltopentaose-forming α-amylase, malto-oligosyltrehalose trehalohydrolase, isomaltulose synthase, malto-oligosyltrehalose synthase, amylo-α-1,6-glucosidase, α-1,4-glucan: phosphate α-maltosyltransferase, 6?-P-sucrose phosphorylase, amino acid transporter
GH15	1	2	2	2	1	glucoamylase, glucodextranase, α,α-trehalase,

TABLE S4: Continued

CAZY	*B. graminis hordei*	*N. crassa*	*R. secalis*	*A. fumigatus*	*S. cerevisiae*	CAZY Functions
GH16	16	14	11	13	5	xyloglucan:xyloglucosyltransferase, keratan-sulfate endo-1,4-β-galactosidase, endo-1,3-β-glucanase, endo-1,3(4)-β-glucanase, licheninase, β-agarase, κ-carrageenase, xyloglucanase, endo-β-1,3-galactanase, β-porphyranase, hyaluronidase, endo-β-1,4-galactosidase, chitin β-1,6-glucanosyltransferase, endo-β-1,4-galactosidase,
GH17	7	4		5	4	glucan endo-1,3-β-glucosidase, glucan 1,3-β-glucosidase, licheninase, ABA-specific β-glucosidase, β-1,3-glucanosyltransglycosylase,
GH18	12	12	15	19	2	chitinase, lysozyme, endo-β-N-acetylglucosaminidase, peptidoglycan hydrolase with endo-β-N-acetylglucosaminidase specificity, Nod factor hydrolase, xylanase inhibitor concanavalin B narbonin
GH20	2	1	2	2		β-hexosaminidase, lacto-N-biosidase, β-1,6-N-acetylglucosaminidase), β-6-SO3-N-acetylglucosaminidase,
GH24	1		1	1		lysozyme
GH25		1		3		lysozyme
GH26		1		3		β-mannanase, exo-β-1,4-mannobiohydrolase, β-1,3-xylanase, lichenase / endo-β-1,3-1,4-glucanase, mannobiose-producing exo-β-mannanase
GH27			6	3		α-galactosidase, α-N-acetylgalactosaminidase, isomalto-dextranase, β-L-arabinopyranosidase, galactan:galactan galactosyltransferase
GH28		2	3	9	1	polygalacturonase, exo-polygalacturonase, exo-polygalacturonosidase, rhamnogalacturonase, rhamnogalacturonan α-1,2-galacturonohydrolase, rhamnogalacturonan α-L-rhamnopyranohydrolase, endo-xylogalacturonan hydrolase
GH29			1			α-L-fucosidase, α-1,3/1,4-L-fucosidase
GH30		2	2			endo-β-1,4-xylanase, β-glucosidase (3.2.1.21) β-glucuronidase, β-xylosidase, β-fucosidase, glucosylceramidase, β-1,6-glucanase, glucuronoarabinoxylan endo-β-1,4-xylanase, endo-β-1,6-galactanase, [reducing end] β-xylosidase
GH31	5	5	7	10	1	α-glucosidase, α-galactosidase, α-mannosidase, α-1,3-glucosidase, sucrase-isomaltase, α-xylosidase, α-glucan lyase, isomaltosyltransferase, oligosaccharide α-1,4-glucosyltransferase
GH32		1	2	2	1	invertase, endo-inulinase, β-2,6-fructan 6-levanbiohydrolase, endo-levanase, exo-inulinase, fructan β-(2,1)-fructosidase/1-exohydrolase, fructan β-(2,6)-fructosidase/6-exohydrolase, sucrose:sucrose 1-fructosyltransferase, fructan:fructan 1-fructosyltransferase, sucrose:fructan 6-fructosyltransferase, fructan:fructan 6G-fructosyltransferase, levan fructosyltransferase, [retaining] sucrose:sucrose 6-fructosyltransferase (6-SST), cycloinulo-oligosaccharide fructanotransferase
GH33						sialidase or neuraminidase, trans-sialidase, 2-keto-3-deoxynononic acid sialidase, anhydrosialidase
GH35		2	3	4		β-galactosidase, exo-β-glucosaminidase, exo-β-1,4-galactanase, β-1,3-galactosidase
GH36	5	1	1	4		α-galactosidase, α-N-acetylgalactosaminidase, stachyose synthase, raffinose synthase

TABLE S4: Continued

CAZY	*B. graminis hordei*	*N. crassa*	*R. secalis*	*A. fumigatus*	*S. cerevisiae*	CAZY Functions
GH37	1	2	1	1	2	α,α-trehalase
GH38	1	1	2	1	1	α-mannosidase, mannosyl-oligosaccharide α-1,2-mannosidase, mannosyl-oligosaccharide α-1,3-1,6-mannosidase, α-2-O-mannosylglycerate hydrolase, mannosyl-oligosaccharide α-1,3-mannosidase
GH39	1			1		α-L-iduronidase, β-xylosidase
GH43	2	7	10	15		β-xylosidase, α-L-arabinofuranosidase, arabinanase, xylanase, galactan 1,3-β-galactosidase, α-1,2-L-arabinofuranosidase, exo-α-1,5-L-arabinofuranosidase, [inverting] exo-α-1,5-L-arabinanase, β-1,3-xylosidase
GH45		1	1	1		endoglucanase
GH47	5	8	6	7	3	α-mannosidase
GH51	3	1	3	2		endoglucanase, endo-β-1,4-xylanase, β-xylosidase, α-L-arabinofuranosidase
GH53		1	1	1		endo-β-1,4-galactanase
GH54		1	3	1		α-L-arabinofuranosidase, β-xylosidase
GH55	3	6		6		exo-β-1,3-glucanase, endo-β-1,3-glucanase
GH62			1	2		α-L-arabinofuranosidase
GH63	2	1	2	1	1	processing α-glucosidase, α-1,3-glucosidase, α-glucosidase, mannosylglycerate α-mannosidase / mannosylglycerate hydrolase
GH64		2				β-1,3-glucanase
GH65				1	1	α,α-trehalase, maltose phosphorylase, trehalose phosphorylase, kojibiose phosphorylase, trehalose-6-phosphate phosphorylase, nigerose phosphorylase, 3-O-α-glucopyranosyl-L-rhamnose phosphorylase, 2-O-α-glucopyranosylglycerol: phosphate β-glucosyltransferase, α-glucosyl-1,2-β-galactosyl-L-hydroxylysine α-glucosidase
GH67		1	1	1		α-glucuronidase, xylan α-1,2-glucuronidase
GH71	5	6	5	5		α-1,3-glucanase
GH72	4	5	7	5	5	β-1,3-glucanosyltransglycosylase
GH74		1		2		endoglucanase, oligoxyloglucan reducing end-specific cellobiohydrolase, xyloglucanase
GH75		1	1	2		chitosanase
GH76	9	10	11	7	2	α-1,6-mannanase
GH78	4		5	8		α-L-rhamnosidase
GH79		2		1		β-glucuronidase, hyaluronoglucuronidase, heparanase, baicalin β-glucuronidase, β-4-O-methyl-glucuronidase
GH81	1	1	1	2	2	endo-β-1,3-glucanase
GH88				2		d-4,5-unsaturated β-glucuronyl hydrolase
GH92	2	2	3	5		mannosyl-oligosaccharide α-1,2-mannosidase, mannosyl-oligosaccharide α-1,3-mannosidase, mannosyl-oligosaccharide α-1,6-mannosidase, α-mannosidase, α-1,2-mannosidase, α-1,3-mannosidase, α-1,4-mannosidase, mannosyl-1-phosphodiester α-1,P-mannosidase
GH93		2		2		exo-α-L-1,5-arabinanase
GH94		1				cellobiose phosphorylase, laminaribiose phosphorylase, cellodextrin phosphorylase, chitobiose phosphorylase, cyclic β-1,2-glucan synthase, cellobionic acid phosphorylase, β-1,2-oligoglucan phosphorylase

TABLE S4: Continued

CAZY	*B. graminis hordei*	*N. crassa*	*R. secalis*	*A. fumigatus*	*S. cerevisiae*	CAZY Functions
GH95	1			3		α-L-fucosidase, α-1,2-L-fucosidase, α-L-galactosidase
GH105		1	1	3		unsaturated rhamnogalacturonyl hydrolase, d-4,5-unsaturated β-glucuronyl hydrolase
GH114	2	1	1	2		endo-α-1,4-polygalactosaminidase
GH115		1		1		xylan α-1,2-glucuronidase, α-[4-O-methyl]-glucuronidase
GH125	3	3	3	1		exo-α-1,6-mannosidase
GH127	1		1	1		β-L-arabinofuranosidase
GH128	3	2	5	2		β-1,3-glucanase
GH131		3		1		broad specificity exo-β-1,3/1,6-glucanase with endo-β-1,4-glucanase activity
GH132	2	2	2	2	5	Activity on β-1,3-glucan [curdlan]
GH133	3	1		2	1	amylo-α-1,6-glucosidase
GH134				4		β-mannanase
GH135	1		4	3		α-1,4-galactosaminogalactan hydrolase
GHnc	2	4		4	5	
GH total	**138**	**176**	**198**	**264**	**57**	

TABLE S5: Copy number of genes classified in Carbohydrate Active enZymes Glycosyl Transferase (GT) modules from *Blumeria graminis* f. sp. *hordei*, *Neurospora crassa*, *Rhynchosporium secalis*, *Aspergillus fumigatus* and *Saccharomyces cerevisiae*.

CAZY	*B. graminis hordei*	*N. crassa*	*R. secalis*	*A. fumigatus*	*S. cerevisiae*	CAZY Functions
GT1	7	6	8	9	2	UDP-glucuronosyltransferase, zeatin O-β-xylosyltransferase, 2-hydroxyacylsphingosine 1-β-galactosyltransferase, N-acylsphingosine galactosyltransferase, flavonol 3-O-glucosyltransferase, anthocyanidin 3-O-glucosyltransferase, sinapate 1-glucosyltransferase, indole-3-acetate β-glucosyltransferase, flavonol L-rhamnosyltransferase, sterol glucosyltransferase, UDP-Glc: 4-hydroxybenzoate 4-O-β-glucosyltransferase, zeatin O-β-glucosyltransferase, limonoid glucosyltransferase, UDP-GlcA: baicalein 7-O-β-glucuronosyltransferase, UDP-Glc: chalcone 4?-O-β-glucosyltransferase, ecdysteroid UDP-glucosyltransferase, salicylic acid β-glucosyltransferase, anthocyanin 3-O-galactosyltransferase, anthocyanin 5-O-glucosyltransferase, dTDP-β-2-deoxy-L-fucose: α-L-2-deoxyfucosyltransferase, UDP-β-L-rhamnose: α-L-rhamnosyltransferase, zeaxanthin glucosyltransferase
GT2	16	11	15	12	5	cellulose synthase, chitin synthase, dolichyl-phosphate β-D-mannosyltransferase, dolichyl-phosphate β-glucosyltransferase, N-acetylglucosaminyltransferase, N-acetylgalactosaminyltransferase, hyaluronan synthase, chitin oligosaccharide synthase, β-1,3-glucan synthase, β-1,4-mannan synthase, β-mannosylphosphodecaprenol-mannooligosaccharide α-1,6-mannosyltransferase, UDP-Galf: rhamnopyranosyl-N-acetylglucosaminyl-PP-decaprenol β-1,4/1,5-galactofuranosyltransferase, UDP-Galf: galactofuranosyl-galactofuranosyl-rhamnosyl-N-acetylglucosaminyl-PP-decaprenol β-1,5/1,6-galactofuranosyltransferase, dTDP-L-Rha: N-acetylglucosaminyl-PP-decaprenol α-1,3-L-rhamnosyltransferase
GT3	1	1	1	1	2	glycogen synthase
GT4	5	6	6	7	3	sucrose synthase, sucrose-phosphate synthase, α-glucosyltransferase, lipopolysaccharide N-acetylglucosaminyltransferase, phosphatidylinositol α-mannosyltransferase, GDP-Man: Man1GlcNAc2-PP-dolichol α-1,3-mannosyltransferase, GDP-Man: Man3GlcNAc2-PP-dolichol/Man4GlcNAc2-PP-dolichol α-1,2-mannosyltransferase, digalactosyldiacylglycerol synthase, 1,2-diacylglycerol 3-glucosyltransferase, diglucosyl diacylglycerol synthase, trehalose phosphorylase, NDP-Glc: α-glucose α-glucosyltransferase / α,α-trehalose synthase, GDP-Man: Man2GlcNAc2-PP-dolichol α-1,6-mannosyltransferase, UDP-GlcNAc: 2-deoxystreptamine α-N-acetylglucosaminyltransferase, UDP-GlcNAc: ribostamycin α-N-acetylglucosaminyltransferase, UDP-Gal α-galactosyltransferase, UDP-Xyl α-xylosyltransferase, UDP-GlcA α-glucuronyltransferase, UDP-Glc α-glucosyltransferase,

TABLE S5: Continued

CAZY	*B. graminis hordei*	*N. crassa*	*R. secalis*	*A. fumigatus*	*S. cerevisiae*	CAZY Functions
GT5		2		2		UDP-Glc: glycogen glucosyltransferase, ADP-Glc: starch glucosyltransferase, NDP-Glc: starch glucosyltransferase, UDP-Glc: α-1,3-glucan synthase, UDP-Glc: α-1,4-glucan synthase
GT8	2	2	3	4	3	lipopolysaccharide α-1,3-galactosyltransferase, UDP-Glc: (glucosyl)lipopolysaccharide α-1,2-glucosyltransferase, lipopolysaccharide glucosyltransferase 1, glycogenin glucosyltransferase, inositol 1-α-galactosyltransferase (galactinol synthase), homogalacturonan α-1,4-galacturonosyltransferase, UDP-GlcA: xylan α-glucuronyltransferase
GT15	3	5	4	3	9	glycolipid 2-α-mannosyltransferase, GDP-Man: α-1,2-mannosyltransferase
GT17		1				β-1,4-mannosyl-glycoprotein β-1,4-N-acetylglucosaminyltransferase
GT20	3	3	3	3	4	α,α-trehalose-phosphate synthase [UDP-forming], Glucosylglycerol-phosphate synthase, trehalose-6-P phosphatase, [retaining] GDP-valeniol: validamine 7-phosphate valeniolyltransferase
GT21	1	1		1		UDP-Glc: ceramide β-glucosyltransferase
GT22	4	3	4	4	4	Dol-P-Man: Man6GlcNAc2-PP-Dol α-1,2-mannosyltransferase, Dol-P-Man: Man8GlcNAc2-PP-Dol α-1,2-mannosyltransferase, Dol-P-Man: Man2-GlcNAc-phosphatidylinositol α-1,2-mannosyltransferase, Dol-P-Man: Man3-GlcNAc-phosphatidylinositol α-1,2-mannosyltransferase
GT24	1	1	1	1	1	UDP-Glc: glycoprotein α-glucosyltransferase
GT25		1		4		lipopolysaccharide β-1,4-galactosyltransferase, β-1,3-glucosyltransferase, β-1,2-glucosyltransferase, β-1,2-galactosyltransferase, LPS β-1,4-galactosyltransferase, occidiofungin β-xylosyltransferase, UDP-Gal:procollagen β-galactosyltransferase
GT31	5	3	5	5		N-acetyllactosaminide β-1,3-N-acetylglucosaminyltransferase, Glycoprotein-N-acetylgalactosamine 3-β-galactosyltransferase, fucose-specific β-1,3-N-acetylglucosaminyltransferase, globotriosylceramide β-1,3-GalNAc transferase, chondroitin synthase (β-1,3-GlcUA and β-1,4-GalNAc transferase, chondroitin β-1,3-glucuronyltransferase, chondroitin β-1,4-N-acetylgalactosaminyltransferase, UDP-Gal: β-galactosylxylosylprotein β-1,3-galactosyltransferase, UDP-GlcNAc: O-fucosylpeptide β-1,3-N-acetylglucosaminyltransferase
GT32	10	4	10	7	4	α-1,6-mannosyltransferase, α-1,4-N-acetylglucosaminyltransferase, α-1,4-N-acetylgalactosaminyltransferase, GDP-Man: inositol-phosphorylceramide transferase, UDP-Gal: β-galactoside α-1,4-galactosyltransferase, UDP-Gal: lactose/N-acetyl-lactosamine α-1,4-galactosyltransferase
GT33	3	1	1	1	1	GDP-Man: chitobiosyldiphosphodolichol β-mannosyltransferase

TABLE S5: Continued

CAZY	*B. graminis hordei*	*N. crassa*	*R. secalis*	*A. fumigatus*	*S. cerevisiae*	CAZY Functions
GT34	2	2	2	3	2	UDP-Gal: galactomannan α-1,6-galactosyltransferase, UDP-Xyl: xyloglucan α-1,6-xylosyltransferase, α-1,2-galactosyltransferase
GT35	1	1	1	1	1	glycogen or starch phosphorylase
GT39	3	3	3	3	7	Dol-P-Man: protein α-mannosyltransferase
GT41	1	1		1		UDP-GlcNAc: peptide β-N-acetylglucosaminyltransferase, UDP-Glc: peptide N-β-glucosyltransferase
GT48	1	1	1	1	3	1,3-β-glucan synthase
GT50	4	1	1	1	1	Dol-P-Man α-1,4-mannosyltransferase
GT55		1				GDP-Man: mannosyl-3-phosphoglycerate synthase
GT57	2	2	2	2	2	Dol-P-Glc: α-1,3-glucosyltransferase
GT58	1	1	1	1	1	Dol-P-Man: Man5GlcNAc2-PP-Dol α-1,3-mannosyltransferase
GT59	1	1	1	1	1	Dol-P-Glc: Glc2Man9GlcNAc2-PP-Dol α-1,2-glucosyltransferase
GT62	3	3	3	3	3	α-1,2-mannosyltransferase, α-1,6-mannosyltransferase
GT64	1		1			UDP-GlcNAc: heparan α-N-acetylhexosaminyltransferase
GT66	1	1	1	1	1	dolichyl-diphosphooligosaccharide—protein glycotransferase, undecaprenyl-diphosphooligosaccharide—protein glycotransferase
GT69	1	2	1	3		GDP-Man: α-1,3-mannosyltransferase
GT71		1		2	6	α-mannosyltransferase
GT76	4	1	1		1	Dol-P-Man: α-1,6-mannosyltransferase
GT77			2			α-xylosyltransferase, α-1,3-galactosyltransferase, arabinosyltransferase, arabinosyltransferase
GT90	3	3	4	2		UDP-Xyl: (mannosyl) glucuronoxylomannan/ galactoxylomannan β-1,2-xylosyltransferase, UDP-Glc: protein O-β-glucosyltransferase, UDP-Xyl: protein O-β-xylosyltransferase
GTnc	3	2	6	3		
GT total	**93**	**78**	**89**	**92**	**67**	

TABLE S6: Copy number of genes classified in Carbohydrate Active enZymes Polysaccharide Lyase (PL) modules from *Blumeria graminis* f. sp. *hordei*, *Neurospora crassa*, *Rhynchosporium secalis*, *Aspergillus fumigatus* and *Saccharomyces cerevisiae*.

CAZY	*B. graminis hordei*	*N. crassa*	*R. secalis*	*A. fumigatus*	*S. cerevisiae*	CAZY Functions
PL1	2	1	2	8		pectate lyase, exo-pectate lyase, pectin lyase
PL3		1	3	5		pectate lyase
PL4	1	1	3	4		rhamnogalacturonan lyase
PL9	1			1		pectate lyase, exopolygalacturonate lyase, thiopeptidoglycan lyase
PL11			1	1		rhamnogalacturonan lyase, exo-unsaturated rhamnogalacturonan lyase
PL20		1	1	2		endo-β-1,4-glucuronan lyase
PL total	**4**	**4**	**10**	**21**	**0**	

TABLE S7: RNAseq transcripts of all Carbohydrate Active enZymes groups in ungerminated *Bgh*. Transcripts are displayed as RPKM values.

Accession	CAZy	Multiple CAZys	Annotation	0 h RPKM
bgh05596	AA1		Uncharacterized protein	1264
bgh00674	AA1		Iron transport multicopper oxidase	77
bgh01709	AA1		Cytochrome b561	75
bgh06849	AA1		Uncharacterized protein	27
bgh00673	AA1		CELP0013 Effector like protein	5
bgh05270	AA1		Putative candidate secreted effector protein	4
bghG00272200 0001001	AA1		Serine/threonine protein kinase domain protein	
bgh02286	AA11		Uncharacterized protein	652
bgh00283	AA11		Uncharacterized protein	79
bgh00773	AA11		Endoglucanase	63
bghG00020900 0001001	AA11		CT20 family protein	
bgh05777	AA2		Peroxidase/catalase	1106
bgh02379	AA2		Peroxidase	134
bgh00659	AA2		Peroxidase	102
bgh06259	AA3		Uncharacterized protein	166
bgh01229	AA4		D-2-hydroxyglutarate dehydrogenase	162
bgh04548	AA4		D-lactate dehydrogenase	31
bgh04741	AA7		FAD binding oxidoreductase	56
bgh01694	AA7		/alba domain containing protein	40
bgh06327	AA7		Putative cytochrome P450 monooxygenase/cypX	15
bgh04053	AA7		24-dehydrocholesterol reductase	10
bgh03826	AA9	AA9, CBM1	Uncharacterized protein	10
bgh04794	AA9		CELP0027 Effector like protein	486
bgh03691	AA9		CSEP0132 putative effector protein	84
bgh02926	AA9		EKA-like protein	3
bgh03826	CBM1	AA9, CBM1	Uncharacterized protein	10
bgh02406	CBM1	CBM1, GH7	Uncharacterized protein	65
bgh04306	CBM1	PL1, CBM1	EKA-like protein	5
bgh04082	CBM1		Putative candidate secreted effector protein	0
bghG00209700 0002001	CBM1		Putative effector protein	
bghG00210200 0001001	CBM1		Putative effector protein	
bghG00210600 0001001	CBM1		Putative effector protein	
bghG00211800 0001001	CBM1		Putative effector protein	
bghG00212700 0001001	CBM1		Uncharacterized protein	
bghG00633500 0001001	CBM1		Putative effector protein	

TABLE S7: Continued

Accession	CAZy	Multiple CAZys	Annotation	0 h RPKM
bghG006337000001001	CBM1		Putative effector protein	
bghG009519000001001	CBM1		Putative effector protein	
bgh06361	CBM13	CBM13, GHnc	Uncharacterized protein	18
bgh06022	CBM18	CBM18, CE4	Bifunctional xylanase/chitin deacetylase	670
bgh00857	CBM18	CBM18, CE4	Chitin diacetylase	166
bgh00731	CBM18	CBM18, GH16	CELP0014 Effector like protein	28
bgh05372	CBM18	CBM18, GH18	CELP0030 Effector like protein	6
bgh00588	CBM18	CBM18, GH18	Extracellular chitinase	6
bgh02647	CBM18	CBM18, GH16	ER membrane protein Wsc4	257
bghG001597000001001	CBM18	CBM18, GH16	WSC domain containing protein	
bgh03986	CBM18	CBM50, CBM18, CBM63	Rare lipoprotein A (RlpA)-like double-psi beta-barrel domain-containing	2251
bghG002265000001001	CBM18	CBM50, CBM18, CBM63	Uncharacterized protein	
bgh03691	CBM18		CSEP0132 putative effector protein	84
bgh03613	CBM18		Putative candidate secreted effector protein	41
bgh02573	CBM18		Phosphatase 1 regulatory subunit 11	34
bgh02278	CBM18		Glyoxal oxidase	4
bghG000925000001001	CBM18		Putative candidate secreted effector protein	
bghG003954000001001	CBM18		CSEP0395 putative effector protein	
bgh00303	CBM20	CBM20, GH15	Glucoamylase	226
bgh05717	CBM21		Uncharacterized protein	289
bgh00774	CBM43	CBM43, GH72	1,3-beta-glucanosyltransferase (GELC)	480
bgh00197	CBM48	CBM48, GH13	Glycogen branching enzyme	71
bgh01946	CBM48		Putative Snf1 serine/threonine protein kinase complex	84
bgh03986	CBM50	CBM50, CBM18, CBM63	Rare lipoprotein A (RlpA)-like double-psi beta-barrel domain-containing	2251
bghG002265000001001	CBM50	CBM50, CBM18, CBM63	Uncharacterized protein	
bgh02573	CBM50		Phosphatase 1 regulatory subunit 11	34
bgh05775	CBM50		Tubulin-specific chaperone D	10
bgh00843	CBM50		Uncharacterized protein	9
bghG003954000001001	CBM50		CSEP0395 putative effector protein	
bgh03986	CBM63	CBM50, CBM18, CBM63	Rare lipoprotein A (RlpA)-like double-psi beta-barrel domain-containing	2251
bghG002265000001001	CBM63	CBM50, CBM18, CBM63	Uncharacterized protein	
bgh04831	CE1		Uncharacterized protein	37

TABLE S7: Continued

Accession	CAZy	Multiple CAZys	Annotation	0 h RPKM
bgh06427	CE12	CE2, CE12	GDSL Lipase/Acylhydrolase family protein	19
bgh00208	CE12	CE2, CE12	GDSL-like lipase/acylhydrolase	18
bgh03781	CE12	CE2, CE12	GDSL-like Lipase	17
bgh05093	CE12		Putative GDSL lipase/acylhydrolase family protein	14
bgh00220	CE12		BEC 6-4/similar to beta 1,3 glucanohydrolase	1
bgh04143	CE16		Uncharacterized protein	17
bgh06427	CE2	CE2, CE12	GDSL Lipase/Acylhydrolase family protein	19
bgh00208	CE2	CE2, CE12	GDSL-like lipase/acylhydrolase	18
bgh03781	CE2	CE2, CE12	GDSL-like Lipase	17
bgh00732	CE3		Beta-1,6 glucan synthetase	81
bgh06065	CE3		CELP0008 Effector like protein	5
bghG000636000001001	CE3		Putative Bgh-specific protein	
bgh06022	CE4	CBM18, CE4	Bifunctional xylanase/chitin deacetylase	670
bgh00857	CE4	CBM18, CE4	Chitin diacetylase	166
bgh00591	CE4		Cda1/Chitin deacetylase	47
bgh05283	CE4		Chitin deacetylase	23
bghG000925000001001	CE4		Putative candidate secreted effector protein	
bgh00226	CE5		Cutinase	102
bgh00227	CE5		Cutinase	23
bgh01726	CE5		Uncharacterized protein	9
bgh05186	CE8		QCR10 domain-containing protein	49
bgh05396	CE8		GTPase activating protein	47
bgh05408	CE8		Uncharacterized protein	37
bghG007079000001001	CE8		PfkB family carbohydrate kinase (Mak32)/MAK32 kinase	
bgh01030	GH1		Putative MSF multidrug transporter	46
bghG004322000002001	GH1		CSEP0405 putative effector protein	
bgh04082	GH10		Putative candidate secreted effector protein	0
bgh02045	GH114		Uncharacterized protein	35
bgh01639	GH114		Putative endo alpha-1,4 polygalactosaminidase	15
bgh00747	GH125		DUF1237 domain protein	66
bgh03821	GH125		DNA-directed RNA polymerase III subunit	27
bgh02390	GH125		DUF1237 domain protein	13
bghG006029000001001	GH127		Putative effector protein	
bgh02974	GH128		Uncharacterized protein	401
bgh04733	GH128		Uncharacterized protein	41
bghG002926000001001	GH128		Putative candidate secreted effector protein	

TABLE S7: Continued

Accession	CAZy	Multiple CAZys	Annotation	0 h RPKM
bgh00197	GH13	CBM48, GH13	Glycogen branching enzyme	71
bgh04510	GH13	GH13, GH133	CSEP0211 putative effector protein	3
bghG00068400 0002001	GH13	GH13, GH133	Glycogen debranching enzyme	
bgh00315	GH13		Maltase/alpha-glucosidase	56
bgh01928	GH13		Cytochrome P450/P450	3
bgh04675	GH13		Uncharacterized protein	0
bghG00006100 0002001	GH13		Alpha-amylase	
bghG00192200 0002001	GH13		CSEP0338 putative effector protein	
bgh01040	GH132	GH132, GH5	Putative SUN domain protein (Adg3) (glucanase)	903
bgh01555	GH132		SUN domain protein, putative (glucanase)	336
bgh04510	GH133	GH13, GH133	CSEP0211 putative effector protein	3
bghG00068400 0002001	GH133	GH13,GH133	Glycogen debranching enzyme	
bgh01928	GH133		Cytochrome P450/P450	3
bgh02654	GH135		Spherulin domain protein	1
bgh00303	GH15	CBM20, GH15	Glucoamylase	226
bgh00731	GH16	CBM18, GH16	CELP0014 Effector like protein	28
bgh02647	GH16	CBM18, GH16	ER membrane protein Wsc4	257
bghG00159700 0001001	GH16	CBM18, GH16	WSC domain containing protein	
bgh00726	GH16		Beta-glucosidase/glycosyl hydrolase family 16/cell wall glucanase	474
bgh05640	GH16		Beta-glucosidase/glycosyl hydrolase family 16/cell wall glucanase	185
bgh00720	GH16		Beta-glucosidase/glycosyl hydrolase family 16	62
bgh04565	GH16		Sterigmatocystin 8-O-methyltransferase	44
bgh01147	GH16		Uncharacterized protein	39
bgh05042	GH16		Endo-1,3(4)-beta-glucanase	32
bgh00729	GH16		Beta-glucosidase/glycosyl hydrolase family 16/cell wall glucanase	29
bgh01441	GH16		Beta-1,3-glucanase	12
bgh00719	GH16		Beta-1,3-glucanase	9
bgh02575	GH16		EKA-like protein	1
bgh04167	GH16		Uncharacterized protein	1
bghG00101400 0001001	GH16		Uncharacterized protein	
bghG00282200 0002001	GH16		CSEP0369 putative effector protein	
bgh03528	GH17		GPI-anchored cell wall beta-1,3-endoglucanase EglC	462
bgh01668	GH17		Uncharacterized protein	41

TABLE S7: Continued

Accession	CAZy	Multiple CAZys	Annotation	0 h RPKM
bgh00736	GH17		Endo-beta-1,3-glucanase	40
bgh06777	GH17		Beta 1,3 glucanase/similar to BEC6 and BEC6-2	26
bgh01858	GH17		HIT finger domain protein	7
bgh05070	GH17		CELP0029 Effector like protein	1
bghG00208400 0001001	GH17		CSEP0342 putative effector protein	
bgh05372	GH18	CBM18, GH18	CELP0030 Effector like protein	6
bgh00588	GH18	CBM18, GH18	Extracellular chitinase	6
bgh06910	GH18	GH18, GH31	Alpha glucosidase II	84
bgh00329	GH18		Chitinase	92
bgh00739	GH18		Endochitinase	85
bgh00737	GH18		Chitinase	17
bgh00634	GH18		Endochitinase class V/CH18 chitinase	15
bgh00059	GH18		Chi1/extracellular endochitinase	8
bgh00122	GH18		Endochitinase	8
bgh00738	GH18		Class III chitinase	3
bgh03470	GH18		Putative candidate secreted effector protein	0
bghG00531100 0001001	GH18		Uncharacterized protein	
bgh01455	GH2		Putative RING finger domain-containing protein	21
bgh05545	GH20		Beta-hexosaminidase	95
bgh02895	GH20		Uncharacterized protein	67
bgh02236	GH24		Serine/threonine-protein phosphatase 4 regulatory subunit	40
bgh00907	GH3		Uncharacterized protein	100
bgh00678	GH3		Beta-N-acetylglucosaminidase	66
bghG00005900 0001001	GH3		CSEP0278 putative effector protein	
bghG00623600 0001001	GH3		Putative effector protein	
bghG00623800 0001001	GH3		CSEP0455 putative effector protein	
bgh06910	GH31	GH18, GH31	Alpha glucosidase II	84
bgh00034	GH31		Putative candidate secreted effector protein	2
bghG00079900 0001001	GH31		Putative candidate secreted effector protein	
bghG00083400 0001001	GH31		Putative effector protein	
bghG00424000 0001001	GH31		Putative effector protein	
bgh00508	GH36		EKA-like protein	1
bgh00613	GH36		EKA-like protein	1
bgh00619	GH36		EKA-like protein	1
bgh03897	GH36		EKA-like protein	0

TABLE S7: Continued

Accession	CAZy	Multiple CAZys	Annotation	0 h RPKM
bgh04497	GH36		EKA-like protein	0
bghG006215000001001	GH37		Alpha-trehalose glucohydrolase	
bgh00758	GH38		Alpha-mannosidase	66
bghG001764000002001	GH39		Uncharacterized protein	
bgh04824	GH43		Uncharacterized protein	377
bgh01111	GH43		Uncharacterized protein	22
bgh00763	GH47		alpha-1,2-Mannosidase	2760
bgh00762	GH47		alpha-1,2-Mannosidase	106
bgh00764	GH47		alpha-1,2-Mannosidase	87
bgh00768	GH47		alpha-1,2-Mannosidase	22
bgh03901	GH47		Putative candidate secreted effector protein	6
bgh01040	GH5	GH132, GH5	Putative SUN domain protein (Adg3)	903
bgh00086	GH5		Exo-1,3-beta-glucanase	674
bgh04952	GH5		Uncharacterized protein	86
bgh06688	GH5		Glycosyl hydrolase family 5	62
bgh06275	GH5		Uncharacterized protein	39
bgh06810	GH5		Exo 1,3 beta glucanase	5
bgh00680	GH5		Exo-1,3-beta-glucanase	1
bghG004981000001001	GH5		Putative effector protein	
bghG005088000001001	GH5		Serine/threonine protein kinase domain protein	
bghG006240000001001	GH5		CSEP0457 putative effector protein	
bgh06560	GH51		Uncharacterized protein	103
bgh01234	GH51		Structure-specific endonuclease subunit SLX1	24
bghG004928000001001	GH51		Secreted protein (Signalp)/blumeria specific	
bgh04507	GH55		Mitochondrial ATPase inhibitor	176
bgh00683	GH55		APT1/Adenine phosphoribosyltransferase	65
bgh00772	GH55		1,3-beta glucanase	55
bgh02562	GH63		Glycoside hydrolase family 63 protein	68
bghG004450000001001	GH63		Mannosyl-oligosaccharide glucosidase	
bgh02406	GH7	CBM1, GH7	Uncharacterized protein	65
bgh00865	GH71		Putative aspartyl aminopeptidase	91
bgh05452	GH71		Putative ABC transporter	53
bgh05700	GH71		Ubiquinone biosynthesis protein	42
bgh00842	GH71		Putative ubiquinone biosynthesis protein	25
bgh03852	GH71		ABC1 domain protein	16
bgh00774	GH72	CBM43, GH72	1,3-beta-glucanosyltransferase (GELC)	480

TABLE S7: Continued

Accession	CAZy	Multiple CAZys	Annotation	0 h RPKM
bgh00776	GH72		1,3-beta-glucanosyltransferase (GELA)	1185
bgh00775	GH72		1,3-beta-glucanosyltransferase (GELB)	93
bgh04747	GH72		Uncharacterized protein	24
bgh00778	GH76		Glycosyl hydrolase family 76	203
bgh00782	GH76		Mannan endo-1,6-alpha-mannosidase	82
bgh00780	GH76		Glycosyl hydrolase family 76	63
bgh00779	GH76		Glycosyl hydrolase	38
bgh06450	GH76		Glycosyl hydrolase family 76	38
bgh05252	GH76		Glycosyl hydrolase family 76	14
bgh00783	GH76		Mannan endo-1,6-alpha-mannosidase	12
bgh06197	GH76		Extracellular solute-binding protein	0
bghG00034900 0001001	GH76		Glycosyl hydrolase	
bgh02241	GH78		Putative tRNA-specific adenosine deaminase	20
bgh04751	GH78		Uncharacterized protein	13
bghG00068400 0001001	GH78		Alpha-L-rhamnosidase	
bghG00646600 0001001	GH78		Putative effector protein	
bgh04744	GH81		Endo-1,3-beta-glucanase	29
bgh00795	GH92		Alpha-1,2-mannosidase	8
bghG00607400 0001001	GH92		Alpha-1,2-mannosidase	
bgh05244	GH95		Uncharacterized protein	23
bgh06361	GHnc	CBM13, GHnc	Uncharacterized protein	18
bgh02562	GHnc		Glycoside hydrolase family 63 protein	68
bgh00570	GT1		Asparagine-linked glycosylation protein 14	36
bgh00571	GT1		Asparagine-linked glycosylation protein 13	33
bgh03694	GT1		Putative candidate secreted effector protein	3
bgh05060	GT1		Putative powdery mildew-specific protein	0
bghG00166900 0001001	GT1		Autophagy-related protein 26	
bghG00572700 0001001	GT1		UDP-glucose,sterol transferase	
bghG00070000 0001001	GT1		Uncharacterized protein	
bgh02561	GT15		Alpha-1,2-mannosyltransferase	73
bgh01243	GT15		Putative alpha-1,2 mannosyltransferase KTR1	50
bgh00834	GT15		RNAse qde2	49
bgh00300	GT2		Uncharacterized protein	403
bgh00811	GT2		Class VII chitin synthase	310
bgh00822	GT2		Class III chitin synthase	129
bgh00324	GT2		Chitin synthase	57

TABLE S7: Continued

Accession	CAZy	Multiple CAZys	Annotation	0 h RPKM
bgh00325	GT2		Chitin synthase	39
bgh03871	GT2		Signal recognition particle 14kD protein	37
bgh00715	GT2		Dolichyl-phosphate beta-glucosyltransferase	33
bgh00800	GT2		Dolichol-phosphate mannosyltransferase	18
bgh05140	GT2		Lysophospholipase	18
bgh02840	GT2		Pyrroline-5-carboxylate reductase	10
bgh00809	GT2		Polysaccharide synthase	3
bgh04125	GT2		EKA-like protein	0
bghG00058400 0001001	GT2		Class II chitin synthase	
bghG00307100 0001001	GT2		Class IV chitin synthase	
bghG00425200 0001001	GT2		Ceramide glucosyltransferase	
bghG00810000 0001001	GT2		Mannose phospho-dolichol synthase	
bgh00497	GT20	GT20, GTnc	Trehalose-6-phosphate synthase	28
bgh00323	GT20		Trehalose-6-phosphate synthase	241
bghG00163400 0001001	GT20		UDP-glucose-glucosephosphate glucosyltransferase	
bghG00425200 0001001	GT21		Ceramide glucosyltransferase	
bgh00584	GT22		Mannosyltransferase	56
bgh00582	GT22		Mannosyltransferase	39
bgh05828	GT22		Mannosyltransferase	29
bgh06024	GT22		Mannosyltransferase	22
bgh05559	GT24		UDP-glucoseglycoprotein glucosyltransferase	35
bgh00229	GT3		Glycogen [starch] synthase	123
bgh00172	GT31		Uncharacterized protein	79
bgh05045	GT31		Glycosyltransferase Family 31	62
bgh02741	GT31		Glycosyltransferase family 31	41
bghG00190900 0003001	GT31		Bgh-specific protein	
bghG00389600 0002001	GT31		pH-response regulator protein palI/RIM9	
bgh03157	GT32		Uncharacterized protein	155
bgh02742	GT32		Alpha 1,6 mannosyltransferase	125
bgh01309	GT32		Putative solute carrier family 35 member E3	47
bgh01119	GT32		Putative GDP-mannose transporter	46
bgh01145	GT32		Acyltransferase	44
bgh01073	GT32		Triose-phosphate Transporter family protein	33
bgh05574	GT32		Uncharacterized protein	33
bgh01180	GT32		Putative nucleotide-sugar transporter	26

TABLE S7: Continued

Accession	CAZy	Multiple CAZys	Annotation	0 h RPKM
bgh02603	GT32		Uncharacterized protein	6
bghG001852000001001	GT32		Glycosyl transferase	
bgh05043	GT33	GT4, GT33	Alpha-1,2-mannosyltransferase ALG11	258
bgh03319	GT33	GT4, GT33	Glycosyl transferase/glycosyl transferase group 1 family protein	1
bgh00572	GT33		ALG1/Alg1/Mannosyltransferase/Dol-PP-GlcNAc2Man transferase/beta-1,4-mannosyltransferase	238
bgh02743	GT34		Alpha-1, 6-mannosyltransferase/galactosyltransferase	50
bgh01096	GT34		Alpha-1,2-galactosyltransferase/putative alpha-1,6-mannosyltransferase subunit	44
bgh00234	GT35		Alpha-1,4 glucan phosphorylase	197
bgh05832	GT39		Protein O-mannosyl-transferase 1	72
bgh02251	GT39		O-mannosyl transferase	56
bgh06477	GT39		Dolichyl-phosphate-mannose-protein mannosyltransferase	46
bgh05043	GT4	GT4, GT33	Alpha-1,2-mannosyltransferase ALG11	258
bgh03319	GT4	GT4, GT33	Glycosyl transferase/glycosyl transferase group 1 family protein	1
bgh00576	GT4		Glycolipid 6-alpha-mannosyltransferase/glycolipid 3-alpha-mannosyltransferase/ALG2	34
bgh02104	GT4		N-acetylglucosaminyl-phosphatidylinositol biosynthetic protein	13
bghG003847000001001	GT4		CSEP0391 putative effector protein	
bgh04852	GT41		UDP-N-acetylglucosaminyltransferase	23
bgh02744	GT48		1,3-beta glucan synthase	134
bgh05886	GT50		Extracellular matrix protein	908
bgh02555	GT50		GPI mannosyltransferase	23
bgh00044	GT50		Putative candidate secreted effector protein	2
bghG011456000001001	GT50		Putative candidate secreted effector protein	
bgh00587	GT57		Alpha-1,3-glucosyltransferase	35
bgh00585	GT57		Alpha-1,3-glucosyltransferase	21
bgh00580	GT58		Dol-P-Man:Man(5)GlcNAc(2)-PP-Dol alpha-1,3-mannosyltransferase	30
bgh00590	GT59		Dolichyl-phosphoglucose-dependent alpha-1,2 glucosyltransferase/ALG10/DIE2	40
bgh03496	GT62		Mannan polymerase II complex ANP1 subunit	93
bgh02071	GT62		Mannan polymerase II complex ANP1 subunit	64
bgh05368	GT62		Mannan polymerase complexes MNN9 subunit	29
bgh04567	GT64		Peptidyl-tRNA hydrolase/Pth2p	25
bgh02672	GT66		Dolichyl-diphosphooligosaccharide--protein glycosyltransferase subunit STT3	90
bgh05865	GT69		Uncharacterized protein	29

TABLE S7: Continued

Accession	CAZy	Multiple CAZys	Annotation	0 h RPKM
bghG00312500 0001001	GT76		GPI mannosyltransferase 2	
bghG00068400 0003001	GT76		Uncharacterized protein	
bghG00080300 0001001	GT76		Putative effector protein	
bghG00747600 0001001	GT76		Uncharacterized protein	
bgh00995	GT8		GLG1/glycogen synthesis initiator (Glycogenin)	33
bgh02441	GT8		Glycosyl transferase	6
bgh01321	GT90		Capsular associated protein	34
bgh01272	GT90		Capsular associated protein	18
bgh04640	GT90		Capsule-associated protein CAP1	10
bgh02097	GTnc	GT20, GTnc	Uncharacterized protein	28
bgh02625	GTnc		Tom6/TOM core complex subunit Tom6	168
bgh00969	GTnc		Ubiquitin conjugating enzyme	156
bgh04306	PL1	PL1, CBM1	EKA-like protein	5
bgh04145	PL1		EKA-like protein	1
bghG00623700 0001001	PL4		Uncharacterized protein	20
bghG00188600 0002001	PL9		Serine/threonine protein kinase Sgk2	11

TABLE S8: Oligonucleotides used for qPCR of *Bgh* cell wall related genes.

Primer	Sequence 5′ → 3′
CHSI_Fq	AGGGTCCCATCGATAACCCT
CHSI_Rq	ATACCCCACGGAACATACGC
CHSII_Fq	GTCGTTGTCTCGTGGATGGT
CHSII_Rq	GCCGCTACCAATTGCCCTAA
CHSIII_Fq	ACTGGCACGATGTCTCATGG
CHSIII_Rq	CCGTCGCTTCGAACTGACTA
CHSIV_Fq	TCGTAAGACAGACGGCGAAA
CHSIV_Rq	CCGGGAAGCCCAGAAAAGTT
CHSV_Fq	AATGTCCAACCTTCCTGGGC
CHSV_Rq	CTCCTTGCATCCAGTGGAACA
CHSVI_Fq	GGATCTTTCGGTGGGGAGAC
CHSVI_Rq	CAACCAGAGCGTGAACTTGTTTC
CHSVII_Fq	ACTACCGATCTCAATCAGCCA
CHSVII_Rq	GGACTCCTACCCCCAACTCT
FKSI_Fq	CGCGGGGTCGATGATAATTGAT
FKSI_Rq	AATCTGTGCTGGTTCCCGTTTC
GELA_Fq	ACTTTGCTGCCCTCAAGTCA
GELA_Rq	CTGCACTTGGTATGGCTGGA
GELB_Fq	CAACCGAGCCCTACAGACAC
GELB_Rq	TGATCCGCTGGATTTCGTGT
GELC_Fq	AGCGCCAATGCTACTACTGG
GELC_Rq	TGCGGATTGGATCTTCGCAT
KRE6_Fq	GCAGTCATTCCAAGCTGCTC
KRE6_Rq	TCGTTGTTGAGCCAGGTCAC
KRE9_Fq	GCCCACTGCTATAACTGCCA
KRE9_Rq	TCTTTCCAGCGGTTCAGAAAC

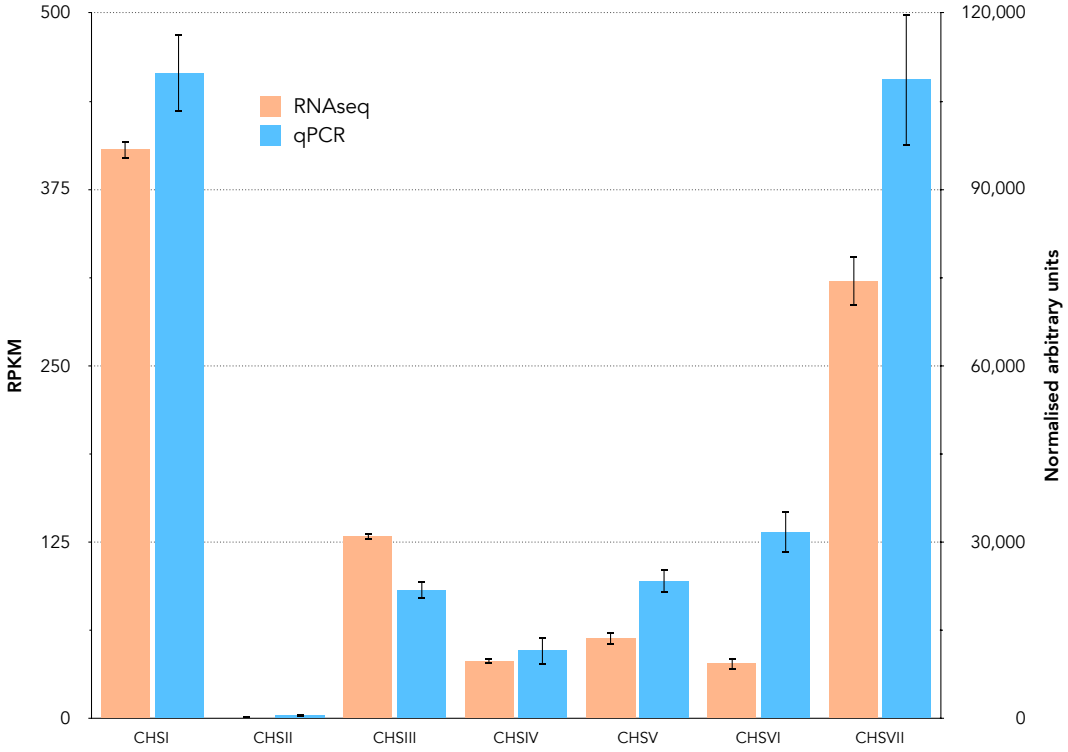

FIGURE S1: Comparison of chitin synthase RNAseq (RPKM) and qPCR (normalised arbitrary units) transcript levels in *Blumeria graminis* f. sp. *hordei* conidia. Data are given as means of three replications ± SD.

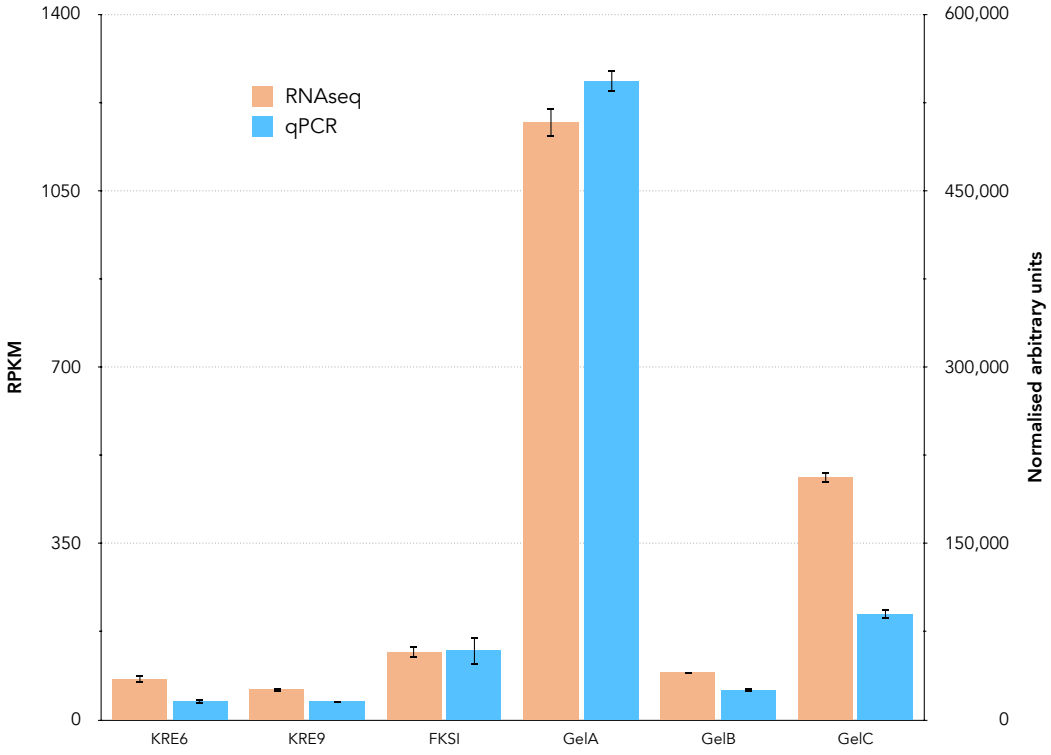

FIGURE S2: Comparison of RNAseq (RPKM) and qPCR (normalised arbitrary units) transcript levels in *Blumeria graminis* f. sp. *hordei* conidia of various genes implicated in glucan metabolism. Data are given as means of three replications ± SD.

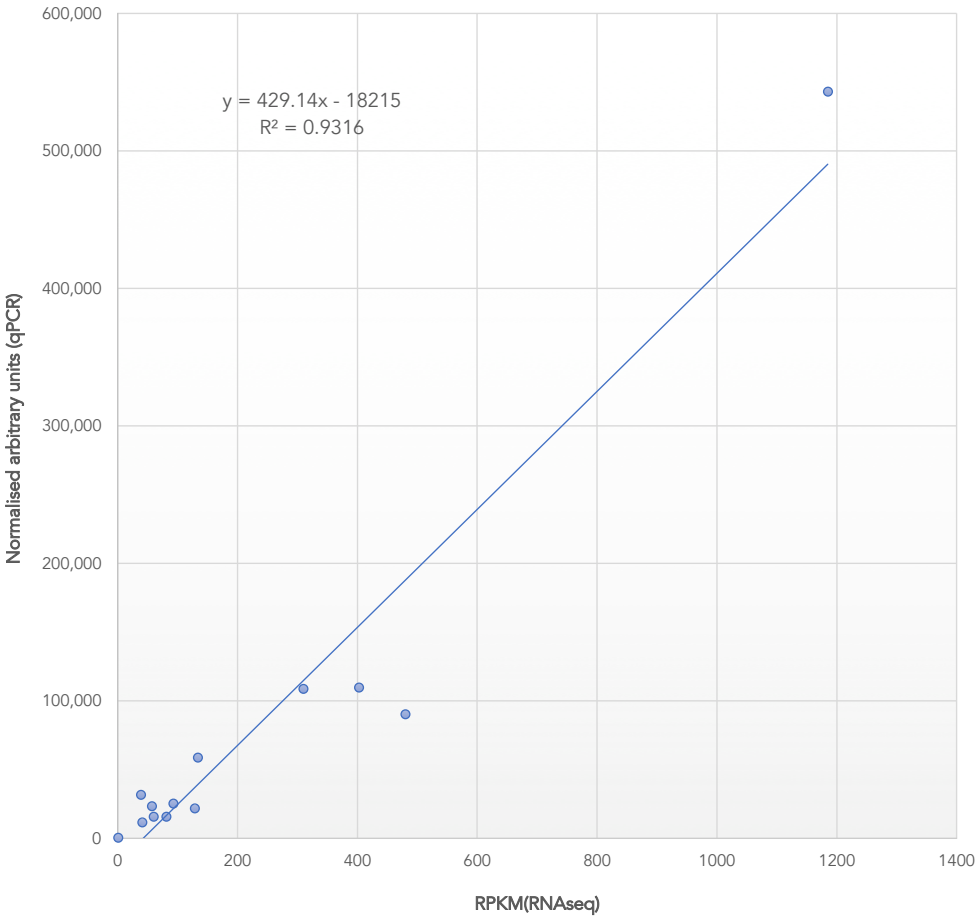

FIGURE S3: Correlation between RNAseq (RPKM) and qPCR (normalised arbitrary units) from *Blumeria graminis* f. sp. *hordei* conidia. Genes chosen were GHs involved in chitin and glucan metabolism

Chapter 3

Establishment of an *in vitro* germination system for analysis of *Blumeria graminis* f. sp. *hordei* pre-penetrative events

3.1 Introduction

As an obligate biotroph *Blumeria graminis* f. sp. *hordei* (*Bgh*) cannot be cultured *in vitro*, which severely limits the repertoire of classical molecular techniques that can be employed, such as genetic manipulation. Because of this, analysis of *Bgh* at the molecular level has lagged considerably compared to other filamentous pathogenic fungi. The conventional method for analysing the *Bgh* infection process involves peeling the epidermal layers from infected host tissues (Both et al., 2005a; Chowdhury et al., 2014; Zeng et al., 2017). This method leads to a significant reduction in the sensitivity of many assays due to the presence of the host material despite the collection of the single cell-thick epidermal layer. The goal of this study was to construct an artificial surface that mimics aspects of the surface of a barley leaf to cultivate *Bgh in vitro*. The purpose of developing this *in vitro* system is to create a fast and efficient method to critically analyse the molecular events that take place during pre-penetration while also eliminating contamination from the host plant.

The first barrier that phytopathogenic microbes must overcome for successful infection is the leaf cuticle. The cuticle is a protective sheath surrounding aerial plant surfaces, forming the direct interface between the plant and its environment. The central physiological role of the cuticle is to prevent non-stomatal water loss (Yeats and Rose, 2013). It is also involved in shielding against UV radiation and as a defence against herbivores, insects, and fungal and bacterial pathogens. The cuticle provides mechanical protection against invading pathogens, affecting pathogen adhesion, and host recognition.

The cuticle is comprised of cutin, a polymer matrix, and cuticular waxes, solvent-soluble lipids. Cutin is composed of esterified hydroxy and epoxy C_{16}, and C_{18} fatty acids while the cuticular waxes consist of aliphatic very long chain fatty acid derivatives, such as primary and secondary alcohols, aldehydes, esters, ketones, alkanes, and cyclic compounds like triterpenoids and phenylpropanoids (Jetter et al., 2000, 2007).

Cuticular waxes are well known to contain substances that affect the germination and differentiation of several pathogenic plant fungi, including *Bgh* (Carver and Thomas, 1990; Tsuba et al., 2002; Gniwotta et al., 2005; Mendoza-Mendoza et al., 2009). The pre-penetrative phase during early infection is a critical part of the fungal life cycle. The process begins when airborne *Bgh* conidia land on the host surface, the conidia form a short primary germ tube (pgt) and attaches itself to the leaf surface (Edwards, 2002). A secondary germ tube (sgt) subsequently emerges and differentiates into an appressorial germ tube (agt). The agt matures into a lobed apical appressorium and a penetration peg develops under the appressorium to pierce through the host cuticle and cell wall. Establishing the appressorium and breaching through the cuticular barrier are necessary steps to a successful infection. Consequently, there is considerable appeal in understanding the events leading to successful appressorium formation and identifying potential surface effectors that trigger pre-penetration events in *Bgh*.

Bgh conidia have been observed to germinate when suspended on threads or on artificial surfaces, such as agar and glass. However, sgt and mature agt only developed when the suspended conidia were transferred to coleoptiles, suggesting that the pgt perceives a stimulus from the plant to trigger sgt elongation and differentiation (Carver and Ingerson, 1987). Kobayashi et al. (1991) found that cellulose films induced rates of germination and differentiation similar to that on barley coleoptiles and suggested that cellulose films placed on agar could be used as an *in vitro* model system. Early studies first examined the impact of cuticular waxes on the pre-penetrative process using *eceriferum* (*cer*) barley mutants, which had an altered cuticular composition and physical structure (Yang and Ellingboe, 1972). While *Bgh* conidia germinated and matured effectively on native host surfaces, scarcely any mature appressoria were observed on host surfaces stripped off the cuticle. Malformed appressoria were prevalent on *cer*-mutant leaves and artificial surfaces (reconstructed wax layers on 2% agar). The impeded germination and maturation of *Bgh* on the mutant and artificial surfaces indicated that the pre-penetration processes were dependent on the cuticular layer.

Mechanical removal of the cuticular wax on the leaf resulted in standard *Bgh* development, indicating that the morphological features of the cuticular waxes have little effect on pre-penetration processes (Carver and Thomas, 1990). Instead, Francis et al. (1996) proposed that cutin monomers are involved in stimulating agt development. The barley cuticular wax constituent *n*-hexacosanal, a C_{26} aldehyde,

has been found to strongly induce appressorium formation in *Bgh* (Tsuba et al., 2002). Examination of the constituents of the barley cuticle *in vitro* has revealed that even numbered very-long-chain-aldehydes (C_{22}-C_{30}) promote *Bgh* germination and differentiation in a dose and chain-length dependent manner, though *n*-hexacosanal was still the most effective (Hansjakob et al., 2010).

In addition to chemical cues from the plant, other environmental parameters such as surface hydrophobicity and atmospheric humidity can significantly affect the pre-penetrative processes. Zabka et al. (2008) ascertained that a sufficiently high level of surface hydrophobicity was necessary to stimulate *Bgh* germination and differentiation on *n*-hexacosanal coated glass slides.

The aim of the present study was to develop an *in vitro* system to investigate the molecular processes that occur during the *Bgh* pre-penetrative phases, with a strong focus on cell wall biosynthesis. While there is a large body of work dedicated to elucidating the intricacies involved in triggering *Bgh* germination and differentiation no-one has exploited this knowledge to investigate the changes in the conidial cell wall and corresponding biosynthetic machinery during the pre-penetrative stages. For this purpose, the *Bgh in vitro* system developed by Hansjakob et al. (2010) was adapted here to develop a method to generate *Bgh* material suitable for cell wall analysis. The hypothesis proposed by Kobayashi et al. (1991) in regard to the validity of cultivating *Bgh* on cellulose films on agar was also tested to determine if it is a viable method. By developing an *in vitro* system this opens up more avenues for *Bgh* research and allows a comprehensive examination of the pre-penetrative *Bgh* processes.

3.2 Materials and Methods

3.2.1 Fungal and plant material

Hordeum vulgare (cv. Baudin) was sown in plastic pots containing cocopeat soil. The plants were kept in a glasshouse with a 16 h photoperiod. For barley cuticular wax analysis, seven-day-old leaves were harvested for extraction.

A field isolate of *Bgh* was kindly donated by Professor Richard Oliver (Curtin University, W.A., Australia). *Bgh* was propagated by inoculating seven-day old Baudin seedlings with conidia from previously infected seedlings. The inoculated plants were then cultivated in a growth chamber with a 16 h photoperiod at 22°C for a week.

3.2.2 Synthesis of n-hexacosanal

Synthesis of *n*-hexacosanal was conducted by Dr Yves Hsieh as previously described by Hansjakob et al. (2010).

3.2.3 Preparation of artificial surfaces

In order to facilitate analysis of pre-penetrative processes in *Bgh*, various surface media were constructed to stimulate *Bgh* germination *in vitro*. These methods were adapted from the work done by Hansjakob et al. (2010) and Kobayashi et al. (1991). Cellophane discs (cellulose acetate), 2% agar and glass slides were each used separately as support media for the artificial surfaces. Agar was prepared in polypropylene plates to prevent damage from downstream chloroform treatments.

Two different treatments were utilised for coating the support media. The first involved total leaf wax extracts that were acquired by soaking seven-day old barley leaves in 10 mL of chloroform and then supplemented with 0.5% Formvar®resin. The second involved *n*-hexacosanal that was dissolved in chloroform containing 0.5% Formvar®resin. A serial dilution of the *n*-hexacosanal at different concentrations was used to coat the glass slides and agar [7×10^{-4}, 7×10^{-5}, 7×10^{-6}, 7×10^{-7}, 7×10^{-8} mol/L]. The barley cuticle extract and *n*-hexacosanal solutions were used to coat the support media and subsequently left to dry for 30 minutes.

3.2.4 *Bgh* pre-penetrative process observations

Artificial surfaces were inoculated with conidia from seven-day-old infected barley by shaking fresh conidia from infected barley seedlings. A settling tower was used in order to obtain a uniform distribution of conidia. After inoculation, agar plates were sealed closed, while glass slides were kept in a sealed box with moist sponges underneath to maintain humidity. Samples were incubated in the dark and taken out for observation at specific time points (2 h, 4 h, 6 h, 16 h and 24 h).

Bgh conidia on each surface were analysed by light microscopy to determine whether they had germinated and, if so, whether they had formed a primary germ tube (pgt), a secondary germ tube (sgt) or a appressorial germ tube (agt) (Figure 3.1). Only single, well separated conidia were counted at each observation to eliminate the possibility of inhibition caused by crowding.

3.2.5 Light microscopy

n-Hexacosanal/Formvar®resin coated glass slides were inoculated with *Bgh* conidia and left to incubate until specific time points (2h, 4h, 6h and 24h). Fungal structures were then labelled with wheat germ agglutinin (WGA), which selectively binds to *N*-acetylglucosamine residues in the fungal cell wall, coupled with Alexa Fluor™-555 (Life Technologies, Carlsbad, CA, USA) following the manufacturer's protocol. For calcofluor white labelling, slides were incubated with 300 mM sodium hydroxide (NaOH) for 1 h prior to labelling with 0.01% calcofluor white for 10 minutes. Labelled *Bgh* was observed with a Carl Zeiss fluorescence microscope (Axio Imager M2; Carl Zeiss; Oberkochen, Germany). Signals from the conjugated WGA were observed with the dsRED filter set at 545/25 nm excitation and 605/70 nm emission wavelengths. Signals from calcofluor white were observed with the DAPI filter set at 365 nm excitation and 445/50 nm emission wavelengths.

3.2.6 Large scale *Bgh* sample collection for downstream analysis

Trays of 2% agar (29 x 29 cm) were coated with 7 x 10^{-4} mol/L *n*-hexacosanal + 0.5% Formvar®resin. Trays were inoculated with *Bgh* conidia and left to incubate in the dark. *Bgh* was harvested by peeling the Formvar®resin film off the agar at 0 h (ungerminated conidia), 2 h (pgt), 4 h (sgt) and 6 h (agt), snap frozen with liquid nitrogen and then stored at -20°C.

Ungerminated *Bgh* conidia were collected by vacuuming the conidium directly from seven-day old infected barley through a 35 μm filter and captured on a 5 μm filter.

3.2.7 RNA extraction

Pure ungerminated *Bgh* conidia (0 h) and germinated *Bgh* conidia (6 h) on formvar resin were ground in liquid nitrogen with a mortar and pestle. Total RNA was extracted using the Plant Total RNA Kit (Sigma-Aldrich) as per the manufacturer's instructions.

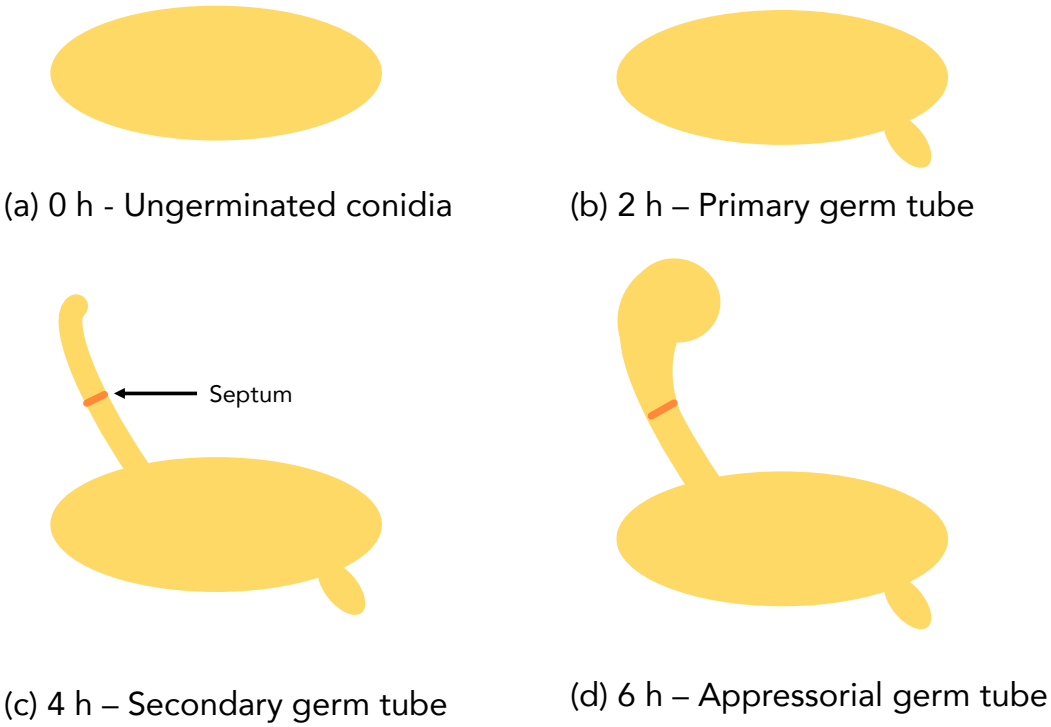

FIGURE 3.1: Stages of *Blumeria graminis* f. sp. *hordei* development during pre-penetrative growth. Timeline of development correspond to the expected time points of growth during *in vivo* growth on the barley leaf and are expected to be replicated on the artificial surfaces. h, hours.

3.3 Results

3.3.1 *Bgh* germination and differentiation analysis on artificial surfaces

Germination and differentiation of *Bgh* conidia on artificial surfaces coated with barley wax extracts and *n*-hexacosanal were assayed to investigate the optimal method to perform *in vitro* assays for the collection of the pre-penetrative *Bgh* growth stage samples.

The agar plates with a layer of cellophane on top coated with either the barley wax/Formvar®resin or *n*-hexacosanal/Formvar®resin [7 x 10^{-5} mol/L] were difficult to work with and barely induced any of the *Bgh* conidia to germinate, even after an extended incubation period (7-days). The cellophane often wrinkled upon exposure to the chloroform solution and produced ridges on the surface that were not optimal for *Bgh* germination. Over time, many of the conidia on the surface shrivelled and dessicated with very few conidia producing a pgt. The levels of *Bgh* germination were equivalent to those on uncoated cellophane agar plates.

The glass slides and agar plates coated with barley wax/Formvar®resin displayed variable rates of germination. While there was an increase in *Bgh* germination and differentiation it was patchy and inconsistent. The barley wax did not seem to coat the surfaces evenly as there were certain zones of germination and zones where the conidia did not germinate at all even after an extended time (7-days).

This result is contrary to the results acquired by Hansjakob et al. (2010), in which consistent and effective *Bgh* germination rates were achieved. In their study, wax was extracted from 14-day-old barley and sprayed onto glass slides with a glass chromatography sprayer. This method would be expected to provide a more even coating.

During our tests the *n*-hexacosanal/Formvar®resin [7 x 10^{-5} mol/L] coating was, by far, the most effective and consistent approach to cultivating *Bgh in vitro* (Figure 3.2). It was equally effective at inducing germination and differentiation on both glass slides and agar, although the conidia were far less likely to burst or dessicate on the coated agar surface due to the increased humidity and available surface moisture. Unlike with the barley wax, the results from the *n*-hexacosanal coatings were reproducible and consistent. The majority of the *Bgh* conidia formed agt after 24 h, with very few sgt remaining undifferentiated. Penetration pegs occasionally developed under the appressorium, though they were sparse at best and difficult to identify without labelling with specific probes (Chapter 4, Figure 4.5 (24 h)).

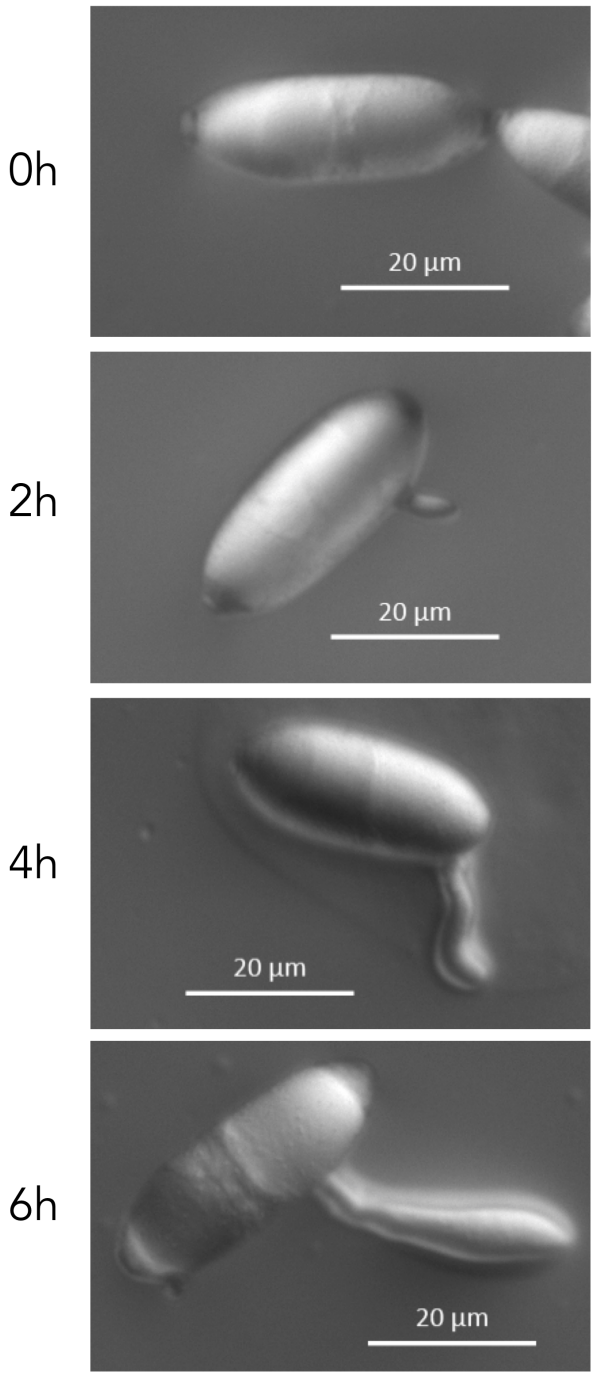

FIGURE 3.2: Differential interference contrast microscopy of *Blumeria graminis* f. sp. *hordei* germination and differentiation over the course of 6 hours on glass slides coated with Formvar®resin

3.3.2 *n*-Hexacosanal dilution series

n-Hexacosanal, a major component of the aldehyde fraction of the barley leaf cuticular wax, is one of the most effective components in the barley cuticular wax to stimulate *Bgh* germination (Tsuba et al., 2002; Zabka et al., 2008; Hansjakob et al., 2010). To study these effects in more detail, conidial germination was analysed in the presence of varying concentrations of *n*-hexacosanal.

Glass slides were coated with a dilution series of *n*-hexacosanal + 0.5% Formvar®resin [7 x 10^{-8}, 7 x 10^{-7}, 7 x 10^{-6}, 7 x 10^{-5} and 7 x 10^{-4} mol/L] along with a control slide coated with just Formvar®resin. The slides were inoculated with *Bgh* and left to incubate for 6 h. The rate of germination and differentiation on the slides were then scored using light microscopy. Success rates were scored based on whether the conidia remained ungerminated, formed a pgt, sgt or an agt (Figure 3.1).

Maximal germination and differentiation rates were seen with the highest concentration of *n*-hexacosanal [7 x 10^{-4}] (Figure 3.3). As the concentration of *n*-hexacosanal was increased the rate of germination and differentiation elevated. At the lowest concentration [7 x 10^{-8} mol/L] scarcely any of the *Bgh* differentiated to the agt stage (3.5%), with the vast majority remaining ungerminated (87%). With the increasing concentrations more sgt differentiated into agt while the number of conidia that remained ungerminated diminished. At the highest concentration [7 x 10^{-4} mol/L] 52.1% conidia differentiated to the agt stage while only 8.5% remained ungerminated.

3.3.3 RNA extraction and qPCR

To determine if the Formvar®resin would impede total RNA extraction, a side-by-side extraction was executed with *Bgh* conidia and ungerminated *Bgh* conidia on the *n*-hexacosanal/Formvar®resin medium. An agar plate coated with *n*-hexacosanal/Formvar®resin was inoculated with *Bgh* and then immediately peeled off to produce ungerminated *Bgh* on a resin membrane. Analysis by gel electrophoresis showed that the RNA extraction on Formvar®resin was successful and that the RNA remained intact (Figure 3.4). Once it was determined that RNA extractions with Formvar®resin was feasible, total RNA was extracted from *Bgh* germinated *in vitro* and harvested at different stage specific times, i.e. 2 h (pgt), 4 h (sgt), and 6 h (agt). To ascertain if the RNA extracted from *Bgh* cultivated *in vitro* was viable for quantitative analysis, the mRNA levels of several cell wall related genes were measured using quantitative polymerase chain reaction (qPCR). Results from the qPCR analysis were integrated into Chapter 4 (Figure 4.8).

3.3.4 Cell wall chitin labelling

Results from the labelling of the chitin on the developing *Bgh* cell wall were integrated into Chapter 4 (Figure 4.5 and 4.6). For cell wall labelling glass slides coated with *n*-hexacosanal/Formvar®resin was used as it was easier to handle.

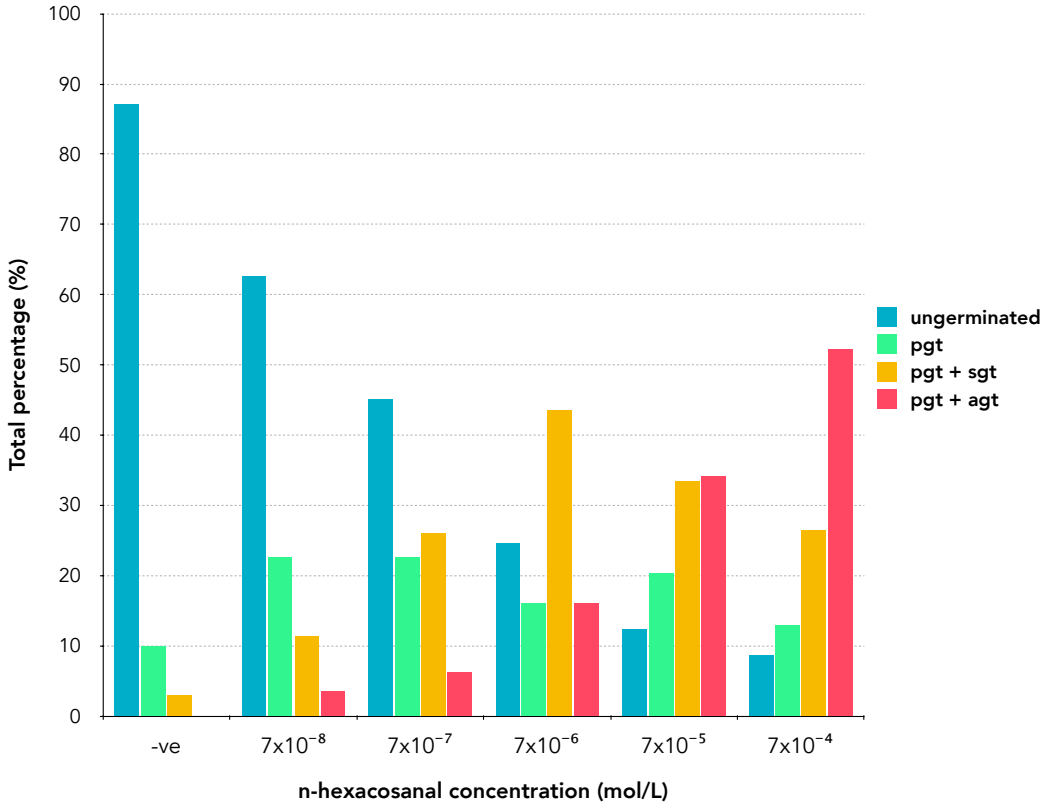

FIGURE 3.3: *Blumeria graminis* f. sp. *hordei* development after 6 hours on glass slides coated with Formvar®resin supplemented with different concentrations of *n*-hexacosanal. Data is a single replication.

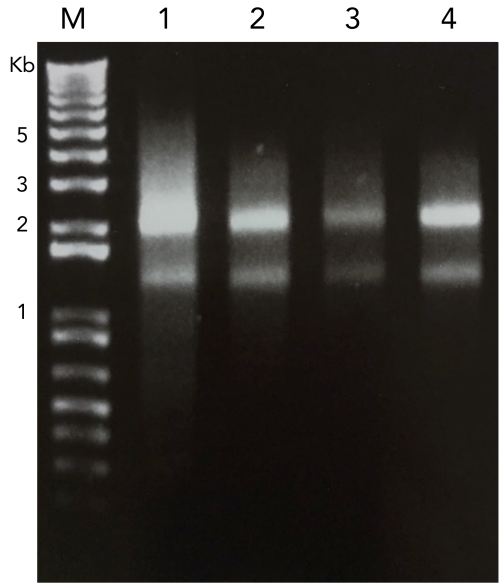

FIGURE 3.4: Agarose gel (2%) analysis of RNA extracted from *Blumeria graminis* f. sp. *hordei* (*Bgh*) conidia. M, DNA molecular size markers. 1: RNA extracted from *Bgh* conidia, first elution, 2: RNA extracted from *Bgh* conidia on Formvar®resin, first elution, 3: RNA extracted from *Bgh* conidia, second elution, 4: RNA extracted from *Bgh* conidia on Formvar®resin, second elution.

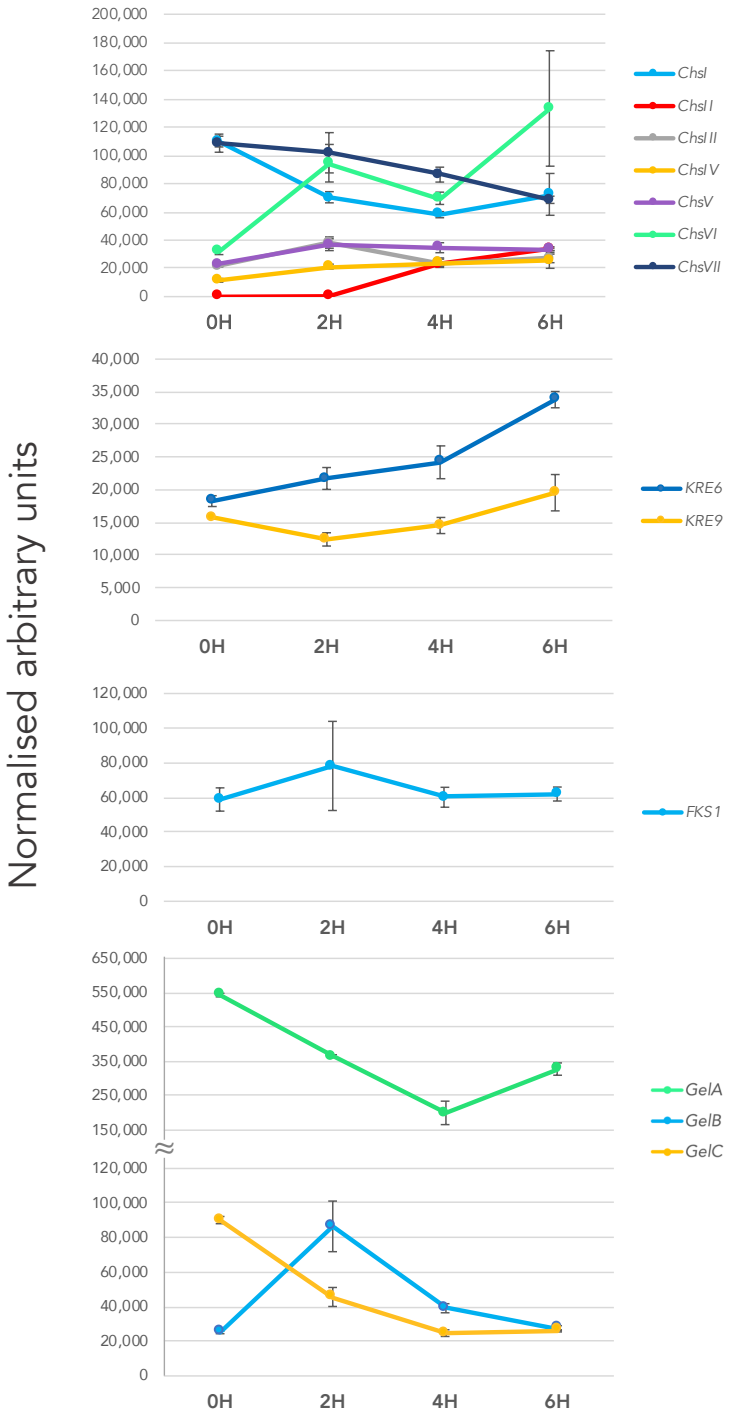

FIGURE 3.5: Transcript profile (qPCR) of cell wall related genes in *Blumeria graminis* f. sp. *hordei* cell cultivated *in vitro* during early germination (0-6 h). Data are given as means of three replications ± SD.

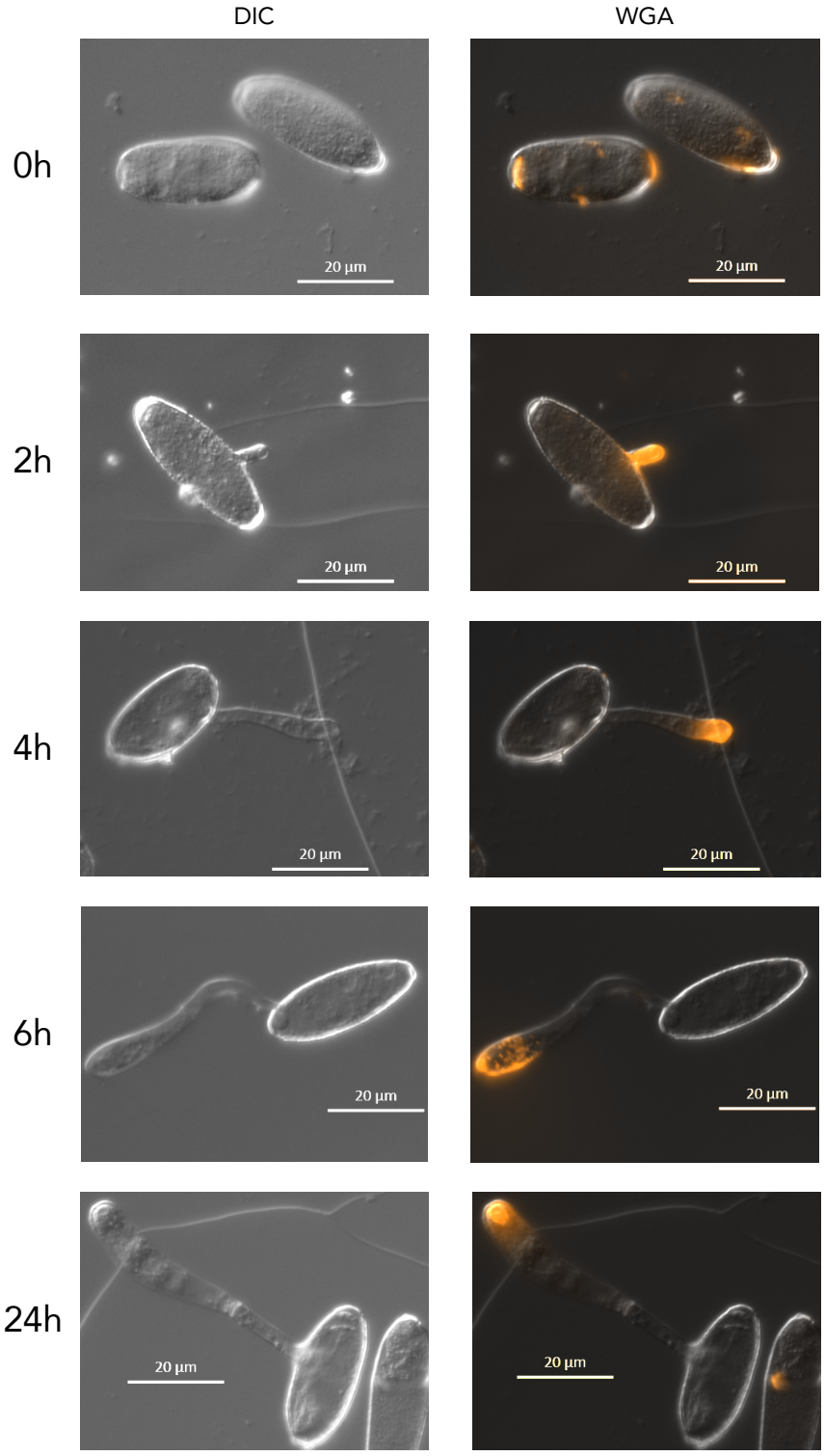

FIGURE 3.6: Light microscopy of *Blumeria graminis* f. sp. *hordei* development on glass slides coated with *n*-hexacosanal/Formvar®resin labelled with wheat germ agglutinin conjugated to Alexa Fluor 555 (WGA-AF555). 0 h: Conidium immediately after inoculation, 2 h: emergence of primary germ tube (pgt), 4 h: development of secondary germ tube (sgt), 6 h: differentiation of sgt to appressorial germ tube (agt), 24 h development of a penetration peg under the appressorium. DIC, differential interference contrast; dsRED filter to observe WGA-AF555 labels.

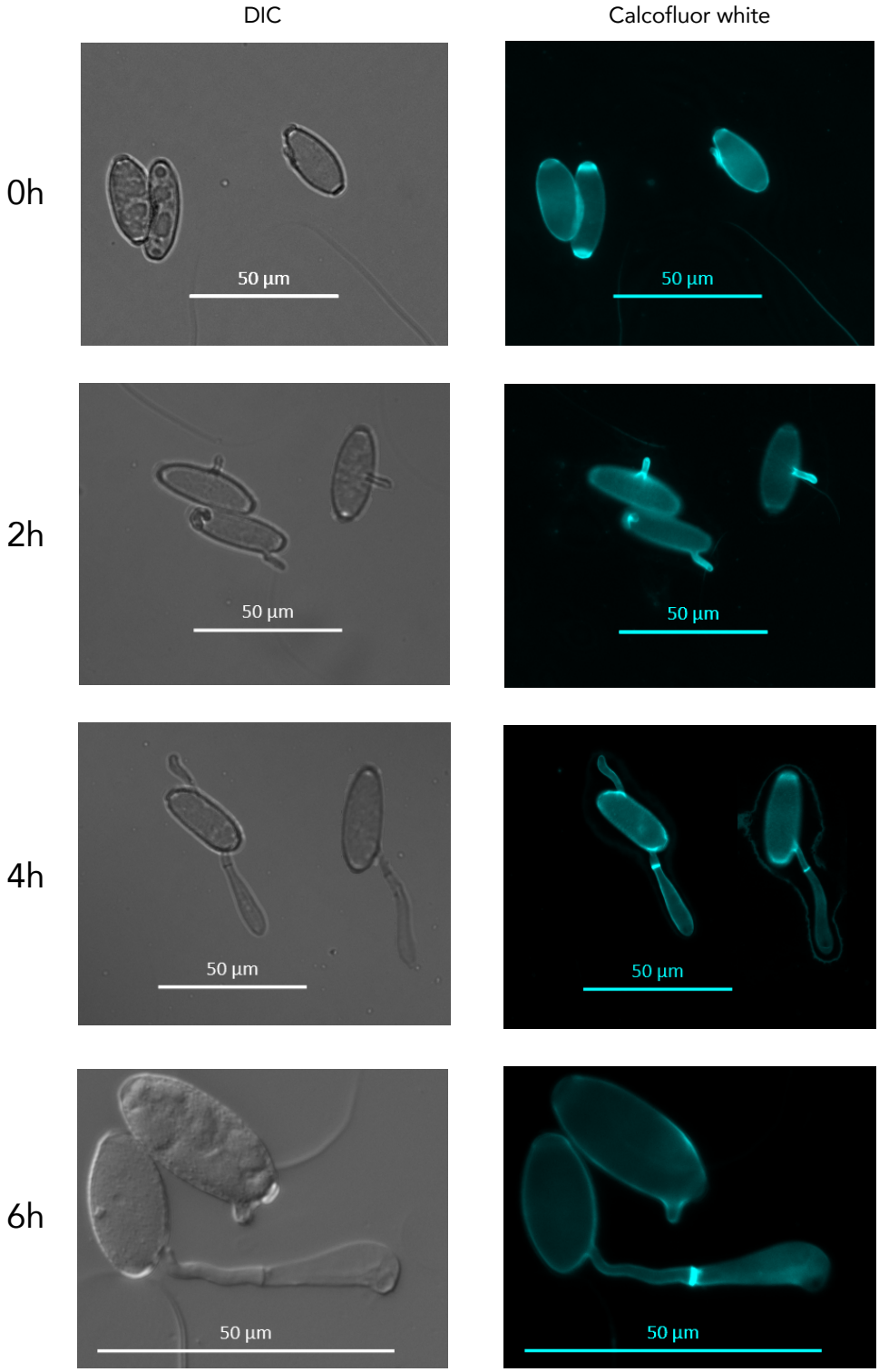

FIGURE 3.7: Light microscopy of *Blumeria graminis* f. sp. *hordei* development on glass slides coated with *n*-hexacosanal/Formvar®resin labelled with calcofluor white. 0 h: Conidium immediately after inoculation, 2 h: emergence of primary germ tube (pgt), 4 h: development of secondary germ tube (sgt), 6 h: differentiation of sgt to appressorial germ tube (agt). At 4 h and 6 h a septum is present between the conidium and sgt/agt. DIC, differential interference contrast; DAPI filter to observe calcofluor white.

3.4 Discussion

The plant cuticle is the first site of contact that airborne fungal pathogens land on. The cuticle is generally composed of very long chain aliphatic compounds such as primary and secondary alcohols, aldehydes, esters, ketones, and alkanes (Yeats and Rose, 2013). The substances that compose the cuticle are known to affect the germination and differentiation of several pathogenic fungi. *Bgh* conidial germination and differentiation are known to be triggered by the C_{26} aldehyde *n*-hexacosanal, a minor constituent of the barley leaf cuticle. Using the previous work conducted on *Bgh* interactions with the barley cuticle as a basis, the goal of this study was to develop an easy *in vitro* method to germinate *Bgh* to investigate pre-penetrative processes. To do this, various artificial surfaces were constructed to ascertain which system would provide optimal induction of *Bgh* conidia germination and differentiation.

Cellophane coated in *n*-hexacosanal/Formvar®resin on 2% agar was originally considered a viable candidate as the cellophane layer would allow easier harvesting whilst mimicking the surface of a leaf. The regenerated cellulose base of the cellophane would act as a faux cell wall while the *n*-hexacosanal/Formvar®resin outer layer would be the 'cuticle' that would stimulate germination and the 2% agar would provide humidity. This did not end up working in practice as the chloroform used to dissolve the *n*-hexacosanal/Formvar®resin caused the cellophane to shrivel while the moisture from the agar was unable to permeate through the cellophane and caused the *Bgh* conidia to become desiccated due to the low humidity. Our experiences with the cellophane is contrary to the hypothesis proposed by Kobayashi et al. (1991), who originally postulated that a cellulose film on agar without any extra cuticle coating would produce a feasible *in vitro* system for *Bgh*.

While the *Bgh* germinated quite well on the *n*-hexacosanal/Formvar®resin coated glass slides, the procedure to remove the coating from the glass slide was quite delicate. The technical data sheet from a Formvar®resin supplier (SPI Supplies) recommends scoring around the edge of the slide to break the coating and then floating it off on top of a clean water surface. Hansjakob et al. (2012) adapted this method and coated a glass slide with polyvinylpyrrolidone 40 (PVP40), a water-soluble polymer, before coating it in a Formvar®resin solution supplemented with barley wax or *n*-hexacosanal. The edges of the slides were scratched with sandpaper and the coating was carefully released into distilled water. This treatment led to solubilisation of the PVP40 coating and the subsequent release of the Formvar®resin coating onto the surface of the water. Cultivating *Bgh* on coated glass slides for *in vitro* analysis and microscopy could work, but large scale collection required for downstream analysis is limited.

Preliminary attempts to remove the Formvar®resin coating from glass slides proved to be arduous and time consuming. Not only was it difficult to remove the coatings,

but once detached the thin film of Formvar®resin was difficult to remove from the water's surface and often became submerged. The amount of time required to separate the coating from the glass slides means that it would be difficult to harvest time specific samples as it would take too long to collect them. The conventional barley epidermal peel method would actually be much faster than attempting to remove the Formvar®resin coating. In addition, the chances of the samples becoming compromised is relatively high due to the difficultly in separating it from the water. All in all, harvesting *in vitro* germinated *Bgh* from glass slides was not an easy task to accomplish and would not be a recommended method to use for large scale *Bgh* harvest.

The best artificial surface to cultivate *Bgh in vitro* was also associated with the easiest method to harvest the cells. This was the 2% agar coated with *n*-hexacosanal/Formvar®resin. As the coating was hydrophobic, the *n*-hexacosanal/Formvar®resin film was incredibly easy to detach and peel away from the agar. *Bgh* cultivated on the coated agar germinated and differentiated to the agt stage incredibly well. In addition, *Bgh* cultivated on agar were less prone to damage and desiccation than was noted to occur on the coated glass slide counterpart. After sampling a range of *n*-hexacosanal concentrations, it was determined that 7 x 10^{-4} mol/L was the best concentration to use to gain optimal germination and differentiation.

The rate of efficiency is similar to that achieved by Hansjakob et al. (2010) (Figure 3.8). In their study, a *n*-hexacosanal concentration of 7 x 10^{-5} mol/L resulted in an agt differentiation rate of 79% after 16 h of incubation. With a slightly higher concentration of 7 x 10^{-4} mol/L we were able to achieve an appressorial differentiation rate of 87% after 24 h.

The *n*-hexacosanal/Formvar®resin film was peeled off the agar and snap frozen in liquid nitrogen. This method made it less difficult to collect large scale stage specific *Bgh* samples. Using this, it was possible to extract stage-specific RNA during pre-penetration from the *in vitro* cultivated *Bgh* without any contamination from plants. From this, the expression profile of several cell wall related genes were analysed over the course of 6 hours (0 h, 2 h, 4 h and 6 h) (Chapter 4, Figure 4.7).

The coated glass slides were the easiest for performing microscopy analysis of *Bgh* germination due to the ease of handling the slides and the flat optically transparent surface. The conventional method for whole mount tissue preparation for light microscopy requires decolouring leaves in methanol or ethanol solutions before labelling can be done (Both et al., 2005a; Chowdhury et al., 2014; Zeng et al., 2017). By inoculating glass slides this bypasses the step in between required to clear the leaf. The *in vitro* light microscopy with the two chitin stains, WGA and calcofluor white, showed that it is possible to observe cell wall changes over the course of pre-penetration (Chapter 4, Figure 4.5 and 4.6). This system can also be utilised to study

cytological processes as well. Hansjakob et al. (2012) used their *in vitro* method to determine if appressorium morphogenesis and cell cycle progression were linked by adding cell cycle inhibitors to agar and observing the migration of the nucleus with 4',6-diamidino-2-phenylindole (DAPI) staining.

3.5 Conclusion

This work demonstrates that it is possible to use *Bgh* cultivated *in vitro* to study the pre-penetrative processes of *Bgh*. It also makes sample collection and microscopy preparation a much simpler procedure compared to conventional methods. Current techniques for the collection of fungal tissues from barley leaves require coating leaves in cellulose acetate followed by peeling off the leaf epidermis. For microscopy, leaf segments need to be cleared before anything can be done (Both et al., 2005a; Chowdhury et al., 2014; Zeng et al., 2017). Although this *in vitro* system is limited to pre-penetration stages of *in vitro* growth and differentiation, it facilitates extensive analysis due to the simplicity of tissue collection and handling, while also eliminating any host tissue contamination.

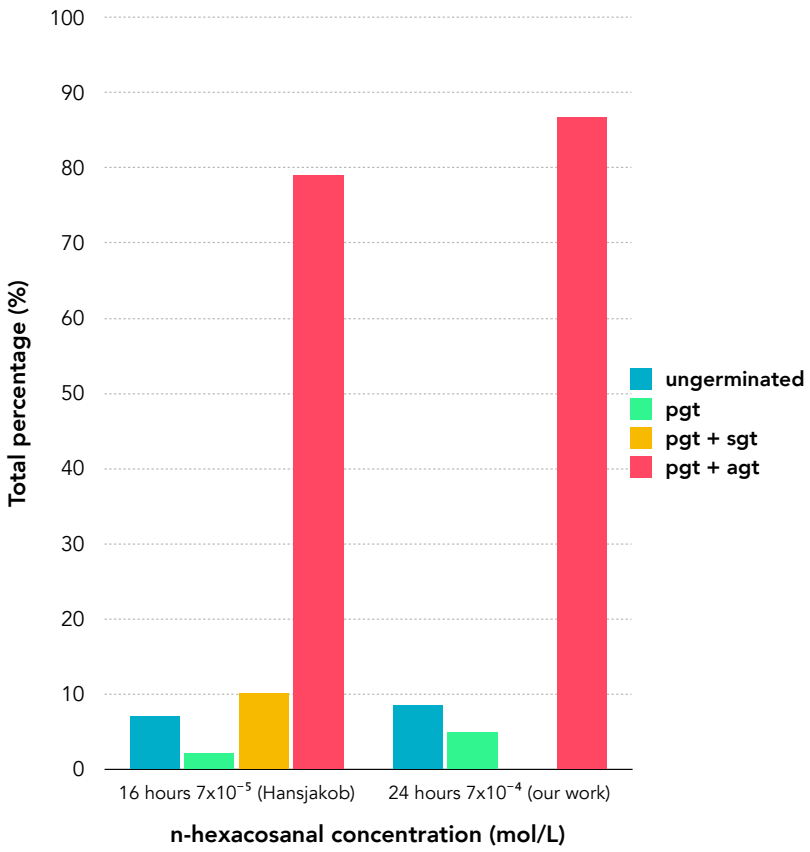

FIGURE 3.8: Comparison of *Blumeria graminis* f. sp. *hordei* (*Bgh*) germination and differentiation efficiency on *n*-hexacosanal/Formvar®resin coated slides between Hansjakob et al. (2010) and our group. Hansjakob et al. (2010) coated their glass slides with 7 x 10^{-5} mol/L + 0.5% Formvar®resin and left the *Bgh* to incubate for 16 h while we coated our glass slides with 7 x 10^{-4} mol/L + 0.5% Formvar®resin and left the *Bgh* to incubate for 24 h.

Chapter 4

Analysis of cell wall synthesis and metabolism during early germination of *Blumeria graminis* f. sp. *hordei*

Statement of Authorship

Title of Paper	Analysis of cell wall synthesis and metabolism during early germination of *Blumeria graminis* f. sp. *hordei*
Publication Status	☐ Published ☐ Accepted for Publication ☐ Submitted for Publication ☒ Unpublished and Unsubmitted work written in manuscript style
Publication Details	This work has not been submitted yet.

Principal Author

Name of Principal Author (Candidate)	Trang Anh Pham		
Contribution to the Paper	Collected all samples and prepared them for analysis, interpreted data, wrote manuscript and acted as principal author.		
Overall percentage (%)	70%		
Certification:	This paper reports on original research I conducted during the period of my Higher Degree by Research candidature and is not subject to any obligations or contractual agreements with a third party that would constrain its inclusion in this thesis. I am the primary author of this paper.		
Signature		Date	01-11-18

Co-Author Contributions

By signing the Statement of Authorship, each author certifies that:

i. the candidate's stated contribution to the publication is accurate (as detailed above);
ii. permission is granted for the candidate in include the publication in the thesis; and
iii. the sum of all co-author contributions is equal to 100% less the candidate's stated contribution.

Name of Co-Author	Alan Little		
Contribution to the Paper	Supervised development of work, helped in data interpretation, manuscript evaluation and acted as corresponding author.		
Signature		Date	01-11-18

Name of Co-Author	Neil J. Shirley		
Contribution to the Paper	Analysed qPCR transcript profiling and RNAseq dataset.		
Signature		Date	01-11-18

Name of Co-Author	Julian G. Schwerdt		
Contribution to the Paper	Performed genome annotation		
Signature		Date	01-11-18

Name of Co-Author	Vincent Bulone		
Contribution to the Paper	Supervised development of work, helped in data interpretation, manuscript evaluation and acted as corresponding author.		
Signature		Date	02-11-18

Name of Co-Author	Xiaohui Xing		
Contribution to the Paper	Permethylation glycosidic linkage analysis		
Signature		Date	Nov. 1st, 2018

Name of Co-Author	Vaibhav Srivastava		
Contribution to the Paper	Sample preparation, mass spectrometry, data analysis		
Signature		Date	1-11-2018

Name of Co-Author	Yves S. Y. Hsieh		
Contribution to the Paper	Chemical synthesis of long chain aldehyde the hexacosanol		
Signature		Date	31/Oct/2018

Manuscript draft

Analysis of cell wall synthesis and metabolism during early germination of *Blumeria graminis* f. sp. *hordei*

Trang A. T. Pham[1], Julian G. Schwerdt[1], Neil J. Shirley[1], Xiaohui Xing[2], Yves S. Y. Hsieh[3], Vaibhav Srivastava[3], Vincent Bulone[1,2,3*] and Alan Little[1*].

[1]ARC Centre of Excellence in Plant Cell Walls, School of Agriculture, Food and Wine, University of Adelaide, Waite Campus, Urrbrae, SA 5064, Australia.

[2]Adelaide Glycomics, School of Agriculture, Food and Wine, University of Adelaide, Waite Campus, Urrbrae, SA 5064, Australia.

[3]Division of Glycoscience, School of Engineering Sciences in Chemistry, Biotechnology and Health, Royal Institute of Technology (KTH), AlbaNova University Centre, 106 91 Stockholm, Sweden.

[*]**Corresponding authors:** Alan Little and Vincent Bulone

Proposed journal: Cell Surface

Keywords: *Blumeria graminis* f. sp. *hordei*, cell wall, metabolism, pathogenesis, pre-penetration.

Note: Supplementary data includes excel spreadsheets that will not be present in this thesis.

4.1 Link to previous chapters

This study utilises the *in vitro* system presented in Chapter 3 for cultivating *Blumeria graminis* f. sp. *hordei* (*Bgh*) up until the appressorial germ tube stage to extend the work conducted in Chapter 2. By cultivating *Bgh* on an artificial surface there is no contamination from plant material that generally occurs when *Bgh* is cultivated on a host plant. By employing the *in vitro* system, the composition of the cell wall during the appressorial germ tube stage was elucidated as well as the transcriptomic profile of the enzymes associated with cell wall metabolism that were identified in Chapter 2.

4.2 Abstract

As an obligate biotroph, *Blumeria graminis* f. sp. *hordei* (*Bgh*) cannot be grown in an axenic culture, and instead must be cultivated on its host species, *Hordeum vulgare* (barley). In this study an *in vitro* system utilizing *n*-hexacosanal, a constituent of the barley cuticle and known inducer of *Bgh* germination, was used to cultivate *Bgh* and differentiate conidia up to the appressorial germ tube stage for analysis. Transcriptomic and proteomic profiling of the appressorial germ tube stage reveal that there was a significant shift towards energy and protein production during the pre-penetrative phase of development, with an up-regulation of enzymes associated with cellular respiration and protein synthesis, modification, and transport. Permethylation glycosidic linkage analysis of the cell wall demonstrated that during appressorial development an increase in 1,3- and 1,4-linked glucose and branched 1,4 xylose were detected in the cell wall along with a significant decrease in galactose. The use of this *in vitro* cultivation method demonstrates that it is possible to analyse the pre-penetrative processes of *Bgh* development in the absence of a plant host.

4.3 Introduction

The barley powdery mildew, *Blumeria graminis* f. sp. *hordei* (*Bgh*), is a widespread pathogen that causes tremendous damage to barley fields. Like all powdery mildews *Bgh* are obligate biotrophic pathogens, meaning they cannot be grown in culture and are entirely dependent on the living host for growth and propagation.

Failure to control outbreaks can result in widespread damage and severe harvest losses. Disease control is implemented by the routine use of fungicides and intensive breeding of novel resistant varieties. However, the resilience of *Bgh* has allowed the fungus to rapidly develop fungicide resistance and overcome breed resistance (Wolfe, 1984; Wolfe and Mcdermott, 1994; Chin et al., 2001). New approaches and techniques are required if *Bgh* is to be effectively controlled. This involves the development of new classes of fungicides and the introgression of novel disease resistance genes. To develop these approaches a finer understanding of the molecular and physiological changes that occur in *Bgh* during conidial germination and pathogenesis is required.

The asexual lifestyle of *Bgh* proceeds in a highly controlled and synchronous manner (Both et al., 2005a). Pathogenesis starts when an airborne conidium makes contact with the leaf surface. Following this, the conidium releases an extracellular matrix and a short primary germ tube emerges (Edwards, 2002). Subsequently, a secondary germ tube emerges which develops into an appressorial germ tube (agt). A penetration peg forms under the appressorium and forces its way through the host cell wall with a combination of enzymatic degradation and turgor pressure generated in the appressorium (Pryce-Jones et al., 1999). A haustorium develops in the periplasmatic space of the epidermal cell and allows the *Bgh* cell to take up nutrients from the host. Once a functional haustorium is established epiphytic mycelium proliferates and assemble additional secondary appressoria that breach the cells and form more haustoria.

The *Bgh* pathogen is one of the most intensively studied fungal powdery mildews. In spite of the economic and agricultural significance of *Bgh*, analysis at the molecular level has lagged considerably compared to other filamentous pathogenic fungi (Zhang et al., 2005). As an obligate biotroph *Bgh* cannot be cultured *in vitro*, severely limiting the repertoire of classical molecular techniques that can be employed, such as genetic manipulation. Standard extraction of *Bgh* material relies on stripping the fungal tissues from plant tissue coated with nail polish for examination (Both et al., 2005a; Zhang et al., 2000; Zeng et al., 2017). Although this technique is *in planta* it reduces the sensitivity and reliability of many assays due to contamination from the host plant. In addition, the nail polish is made of cellulose acetate, which interferes significantly with downstream cell wall analysis.

Only a few studies have focussed on the pre-penetrative events that occur before the *Bgh* pathogen infects the host, with most other research focusing on resistance

responses of the plant host. Two studies have examined the global gene expression throughout the *Bgh* asexual development cycle, from the ungerminated conidia all the way to maturity at five days post infection, i.e. when conidiophores start to develop (Both et al., 2005a,b). One study focused on the dynamic changes that occur during primary metabolism and found that several glycolytic enzymes were co-ordinately up-regulated during the development of the appressoria while transcripts for lipid degradation were abundant in the conidia and diminished significantly during the later developmental stages (Both et al., 2005a). A second study focused on potential virulent determinants and revealed that transcripts related to protein biosynthesis exhibited a substantial increase in expression during post-penetrative stages (Both et al., 2005b).

Analyses of the proteomic profile of *Bgh* conidia have revealed that the vast majority of the proteins in the conidia are classified as metabolic proteins, involved in carbohydrate, lipid, amino acid, and protein metabolism (Noir et al., 2009; Bindschedler et al., 2009). Similar profiles have been observed in other phytopathogenic spores and it has been suggested that phytopathogenic spores are mobile protein factories that are primed to start germination immediately upon physical contact without needing to expend limited energy resources on *de novo* synthesis (Cooper et al., 2007).

The pre-penetrative processes during the early stages of infection are essential periods of the *Bgh* lifecycle. The early stages of pathogenesis require recognising the plant surface, growing to a suitable penetration point, developing the right infection structures to overcome the host barriers made up of the cuticular layer and the plant cell wall, followed by successfully establishing a haustorium feeding structure. Characterising the complex physiological and molecular changes that occur during the pre-penetrative phases before the *Bgh* has invaded the host is an important step towards disease control.

Previous analysis of the *Bgh* conidial cell wall revealed that the cell wall is predominantly composed of glucose (63.1%) and had a greater proportion of galactopyranose residues compared to other species. In addition, trace amounts of xylose residues were also detected in the cell wall, which is an unusual observation in ascomycetes (Chapter 2). Annotation of the Carbohydrate Active enZymes (CAZy) in the *Bgh* genome revealed several more CAZy genes than was previously identified (Spanu et al., 2010; de Witt et al., 2012; Hacquard et al., 2013) and has also identified several key enzymes involved in cell wall metabolism. The cell wall is a dynamic structure, continuously expanding and changing throughout the fungal life cycle. To understand these dynamic changes the processes involved in cell wall metabolism need to be examined during key stages of pathogenesis.

The cuticular waxes that cover the surfaces of plants are well known to contain substances that affect the germination and differentiation of several pathogenic

plant fungi, including *Bgh* (Carver and Thomas, 1990; Tsuba et al., 2002; Gniwotta et al., 2005; Mendoza-Mendoza et al., 2009). *n*-Hexacosanal, an aldehyde and minor constituent of the barley leaf cuticle, is a strong inducer of germination and differentiation in *Bgh* (Tsuba et al., 2002; Hansjakob et al., 2010). An *in vitro* system to cultivate the pre-penetrative stages of *Bgh* using *n*-hexacosanal was developed by Hansjakob et al. (2010) and used to investigate if appressorium morphogenesis and cell cycle progression were linked.

In this study we have adapted their method to analyse the molecular events that occur during *Bgh* pre-penetrative development *in vitro*. Using this, *Bgh* conidia at specific developmental stages were able to be collected without any contamination from the host plant for analysis of the fungal cell wall composition and associated transcriptomic and proteomic changes.

4.4 Materials and Methods

4.4.1 Fungal material

The *Bgh* used in the experiments was a field isolate donated by Professor Richard Oliver (Curtin University, W.A., Australia). The *Bgh* isolate was maintained on the highly susceptible barley cultivar Baudin. *Bgh* was propagated by inoculating seven-day-old barley seedlings with conidia from previously infected barley seedlings. The inoculated plants were then cultivated in a growth chamber with a 16 h photoperiod at 22°C for a week. *Bgh* conidia were collected by vacuuming the conidium directly from the plants through a 35 μm filter and captured on a 5 μm filter.

4.4.2 *In vitro* growth of *Bgh*

Bgh was cultivated on 2% agar coated with a Formvar [0.5%]/*n*-hexacosanal [7 x 10^{-4} mol/L] membrane and harvested after 2 h, 4 h, and 6 h of incubation. This method was adapted from Hansjakob et al. (2010). Synthesis of *n*-hexacosanal was conducted as previously described by Hansjakob et al. (2010).

4.4.3 Preparation of *Bgh* cell wall samples

The fungal samples were snap frozen in liquid nitrogen and freeze dried. Alcohol insoluble residue (AIR) was prepared from the *Bgh* conidium as previously described (Mélida et al., 2013). The AIR was then de-starched by α-amylase, recovered by ethanol precipitation, and dehydrated under vacuum (Pettolino et al., 2012). The AIR was stored in a desiccator until required.

4.4.4 Permethylation glycosidic linkage analysis

The cell wall sample was treated with acetic anhydride in aqueous, methanolic acetic acid solution to per-N-acetylate amino sugars (Hirano et al., 1976). Uronic acids were converted to their 6,6-dideuterio neutral sugar counterparts using carbodiimide activation at pH 4.75 followed by reduction with sodium borodeuteride ($NaBD_4$) at pH 7.0 (Kim and Carpita, 1992). All carbohydrates in the sample were permethylated (Ciucanu and Kerek, 1984), hydrolysed with trifluoroacetic acid (TFA), reduced with $NaBD_4$, and peracetylated with acetic anhydride to generate partially methylated alditol acetates (PMAAs) (Pettolino et al., 2012). The PMAAs from neutral sugars and amino sugars were separated using gas chromatography as described earlier (Mélida et al., 2013, 2015). An Agilent J&W VF-23ms capillary column (30 m x 0.25 mm i.d.) and an Agilent J&W DB-1ms Ultra Inert (UI) capillary column (30 m x 0.25 mm i.d.) were used for the separation of PMAAs from neutral and amino sugars, respectively, on an Agilent 7890B/5977B GC-MS system coupled with flame ionization detection (FID). The PMAAs were then identified by

comparing their MS fragmentation patterns with those of reference derivatives and by referring to the literature (Carpita and Shea, 1988), and quantified based on the FID response (Sweet et al., 1975; Carpita and Shea, 1988). Five separate experiments were conducted.

Data of the cell wall composition are reported as the mean ±SE. Differences in P values that were <0.05 were considered significant. P values were calculated by paired sample t-test.

4.4.5 RNA extraction

Frozen ungerminated *Bgh* conidia (0 h) and germinated *Bgh* (2 h, 4 h and 6 h) on *n*-hexacosanal/Formvar®resin were ground in liquid nitrogen with a mortar and pestle. Total RNA was extracted using the Plant Total RNA Kit (Sigma-Aldrich) as per the manufacturer's instructions.

4.4.6 RNAseq library creation

RNA-Seq sequencing and library preparation were performed at the Australian Genome Research Facility Ltd. (AGRF, Melbourne, Victoria). Libraries for three independent biological replicates were prepared using the Illumina Stranded mRNA kit and 100-bp single-ended sequence reads collected using the Illumina HiSeq sequencer. Each run produced up to 20 million reads per biological replicate.

For each of the samples, sequence reads were quality trimmed and then mapped to the genome of *Bgh* DH14 strain (http://www.ebi.ac.uk/ena/data/view/GCA_000151065.3) using the CLC Genomics Workbenchv8.0 (CLC bio, Aarhus, Denmark). Mean gene expression from each sample was expressed as reads per kilobase of transcript per million mapped reads (RPKM).

4.4.7 Quantitative polymerase chain reaction (qPCR) validation

To confirm the reliability of transcript levels, the relative expression levels of 13 cell wall related genes were checked using qPCR evaluation. cDNA was synthesised from total RNA using the SuperScript®III Reverse Transcriptase (RT) enzyme (Life Technologies, Carlsbad, U.S.A.) following the manufacturer's protocol. Transcript profiling was carried out using qPCR as described previously in Burton et al. (2010) using the gene-specific primers listed in Supplementary Table S1. The data were normalised against the geometric mean of four housekeeping genes, actin (*bgh00992*), glyceraldehyde 3-phosphate dehydrogenase (*bgh00075*), tubulin (*bgh01972*) and ubiquitin (*bgh03777*).

4.4.8 Transcriptome analysis

Transcriptome analysis was conducted as previously described (Pham et al., 2019; Chapter 2). Kyoto Encyclopedia of Genes and Genomes (KEGG), Enzyme Commission (EC), Gene Ontology (GO), and PFAM annotations were retrieved from the EnsemblFungi website (http://fungi.ensembl.org/index.html) through the BioMart portal and appended to the *Bgh* DH14 genome (Spanu et al., 2010). Annotations were also downloaded from the Carbohydrate-Active enZymes Database (CAZy) (http://www.cazy.org) and appended to the *Bgh* genome using *Fusarium graminearum* as a reference organism.

4.4.9 Protein extraction and sample preparation for proteomics

The protein extraction method used was adapted from Noir et al. (2009). Approximately 200 mg of 0 h conidia and 6 h germinated *Bgh* were ground in liquid nitrogen with a mortar and pestle. Samples were then suspended in 1 ml of extraction buffer [50 mM Tris-Base pH 8.0, 10 mM ethylenediaminetetraacetic acid (EDTA), 0.5% 3-[(3-cholamidopropyl)dimethylammonio]-1-propanesulphonate (CHAPS), 10 mM dithiothreitol (DTT), 1x cOmplete™EDTA-free Protease Inhibitor Cocktail (Sigma-Aldrich)]. Protein extraction was done by five repetitions of vortexing for 30 s, with short pauses on ice for 30 s in between. The solution was centrifuged at 16,000g for 5 min at 4°C, and the supernatant was removed and then stored on ice. The extraction procedure was repeated on the pellet using 500 μl of extraction buffer. The supernatant was then freeze dried and stored at -20°C.

Proteins were resuspended in denaturing buffer [3% sodium deoxycholate (SDC), 100 mM tetraethylammonium bromide (TEAB)], loaded onto Microcon YM-10 filters and centrifuged for 15 mins at 12,000 rpm at room temperature. All subsequent centrifugations involving the YM-10 filters were performed at 12,000 rpm at room temperature. 250 μl of reducing solution [20 mM dithiothreitol, 3% SDC, 100 mM TEAB] was added to the filters and the mixtures were incubated at 60°C for 1 h. 100 μl of alkylation solution [80 mM iodoacetamide, 3% SDC, 100 mM TEAB] was added and left to alkylate the reduced proteins at 37°C in the dark for 30 min. The solution was then centrifuged for 20 min and 300 μl of 100 mM TEAB was added to the filters. The samples were centrifuged for 15 min and the procedure was repeated. 300 μl of 100 mM TEAB containing trypsin at an enzyme to substrate ratio of 1:50 was added to the filter and the preparations were incubated overnight at 37°C. The solutions were then centrifuged for 10 min to extract the peptide fragments. 50 μl of 100 mM TEAB was added to the filters and spun for 10 min. The procedure was repeated 3 more times to extract all of the peptides.

The total pooled peptide fractions were acidified by adding TFA to a final concentration of 0.5%. The solution was then vortexed, causing the SDC to precipitate. The samples were centrifuged at 14,000 rpm for 10 min to remove the

SDC pellet. The supernatant was transferred to a new column and peptides were purified using a pep clean column. The eluate was dried down under vacuum (SpeedVac) and the peptide was resuspended in 10 μl of 0.1% formic acid and stored at -20°C.

4.4.10 Nano-LC-MS/MS analysis of samples subjected to iTRAQ labelling

The peptide samples were analysed after iTraq labelling as previously described (Srivastava et al., 2013, 2018). Peptide analysis was performed with reverse-phase liquid chromatography-electrospray ionization-tandem mass spectrometry (LC–ESI–MS/MS) using a nanoACQUITY Ultra Performance Liquid Chromatography system coupled to a Q-TOF mass spectrometer. iTraq labelling was performed as described earlier in Srivastava et al. (2013). The peptide fractions were resuspended in 0.1% TFA, loaded onto a C18 trap column (Symmetry 180 μm × 20 mm, 5 μm; Waters, Milford, MA) and then washed with 0.1% (v/v) formic acid at a rate of 15 μl/min for 10 min. The eluted sample was then separated on a C18 analytical column (75 μm × 200 mm, 1.7 μm; Waters, Milford, MA) at 225 nl/min using 0.1% formic acid as solvent A and 0.1% formic acid in acetonitrile as solvent B in a stepwise gradient: 0.1–8% B (0–5 min), 8–25% B (5–185 min), 25–45% B (185–201 min), 45–90% B (201–205 min), 90% B (205–213 min), and 90–0.1% B (213–215 min). The eluting peptides were sprayed into the mass spectrometer with the capillary and cone voltages set to 2.3 kV and 45 V respectively. The five most abundant signals from a survey scan (400–1300 m/z range, 1s scan time) were then selected by charge state, and collision energy was applied appropriately for sequential MS/MS fragmentation scanning (50–1800 m/z range, 1s scan time).

4.4.11 Data processing and protein identification

For data processing and protein identification the Automated Proteomics Pipeline (APP) was used to analyse the MS data (Malm et al., 2014). APP automates the processing of proteomics tasks such as peptide identification, validation and quantitation from LC-MS/MS data and allows easy integration of many separate proteomics tools. The raw MS data file was first processed using the Mascot Distiller software (version 2.4.3.2, Matrix Science, London, UK). The resulting mgf files were subsequently converted into the mzXML file format using msconvert (Kessner et al., 2008). The data were searched against the *Bgh* genome using several search engines in parallel and the following settings: trypsin specific digestion with two missed cleavages allowed; peptide tolerance of 200 ppm; fragment tolerance of 0.5 Da; methylthio on Cys and iTRAQ 4-plex for peptide N-t and Lys used as fixed modifications; oxidized Met and Tyr for iTRAQ 4-plex analysis in variable mode. PeptideProphet was used to validate the results from the searches (Keller et al., 2002).

4.4.12 Light microscopy

n-Hexacosanal/Formvar®resin coated glass slides were inoculated with *Bgh* conidia and moist sponges were placed underneath to maintain humidity. Samples were incubated in the dark and taken out for observation at specific time points (0 h, 2 h, 4 h and 6 h). Fungal structures were then labelled with wheat germ agglutinin (WGA), which selectively binds to *N*-acetylglucosamine residues in the fungal cell wall, coupled with Alexa Fluor™-555 (Life Technologies, Carlsbad, CA, USA) following the manufacturer's protocol. For calcofluor white labelling, slides were incubated with 300 mM sodium hydroxide (NaOH) for 1 h prior to labelling with 0.01% calcofluor white for 10 min. The labelled *Bgh* cells were observed with a Carl Zeiss fluorescence microscope (Axio Imager M2; Carl Zeiss; Oberkochen, Germany). Signals from the conjugated WGA were observed with the dsRED filter set at 545/25 nm excitation and 605/70 nm emission wavelengths. Signals from calcofluor white were observed with the DAPI filter set at 365 nm excitation and 445/50 nm emission wavelengths.

4.5 Results

4.5.1 Transcriptomic and proteomic analysis

The expression profile of *Bgh* during the pre-penetrative phase of pathogenesis was investigated by analysing the transcriptomes of the ungerminated *Bgh* conidia and agt stage using Illumina RNA sequencing (Supplementary Table S2). Genes were sorted into functional categories based on Gene Ontology (GO) as shown in Figure 4.1. A multiple t-test identified the genes differentially expressed between the *Bgh* conidia and agt stage. The categories which had the largest number of differentially expressed genes during the agt stage were transcription, protein biosynthesis, and lipid metabolism.

Overall there was a switch towards energy and protein production during the agt stage, with a large up-regulation of genes involved in cellular respiration and protein biosynthesis.

Key regulators in glycolysis such as phosphofructokinase (*bgh00033*) and pyruvate kinase (*bgh00037*) were up-regulated during the agt stage while regulatory enzymes in gluconeogenesis, such as glucose 6-phosphatase (*bgh05280*), fructose 1,6-bisphosphatase (*bgh02549*), phosphoenolpyruvate carboxykinase (*bgh06596*), and pyruvate carboxylase (*bgh00049*) were down-regulated (Supplementary Figure S1). Similarly, many of the genes up-regulated in the lipid metabolism group were involved in lipid and fatty acid catabolism while the vast majority of down regulated genes were associated with lipid, fatty acid, and long chain fatty acid biosynthesis. Genes involved in oxidative phosphorylation, such as ATP synthases and ATPases, were also highly up-regulated (Figure 4.2, transporters).

The most up-regulated genes were those involved in transcription and protein biosynthesis. The differential expression between the two developmental stages indicates that there is a shift towards pathogenic specific transcription and translation factors and complexes. The bZIP transcription factor *HacA* (*bgh02519*) was up-regulated during the agt stage (Figure 4.2). *HacA* is orthologous to the *Neurospora crassa hac-1* and is an important transcription factor to the unfolded protein response (Montenegro-Montero et al., 2015), which activates when the folding capacity of the endoplasmic reticulum is exceeded, such as during germination when enzymes are secreted. In addition, the C_2H_2 transcription factor *Seb1* (*bgh05556*) displayed relatively high expression during both developmental phases. *Seb1* is orthologous to the *Saccharomyces cerevisiae Msn2*, a general stress response transcription factor of the high osmolarity glycerol (HOG) pathway. Orthologues of *Msn2* have been found to be important to hyphal growth, conidiation, and virulence in several pathogenic fungi (Zhang et al., 2014; Luo et al., 2015; Tian et al., 2017).

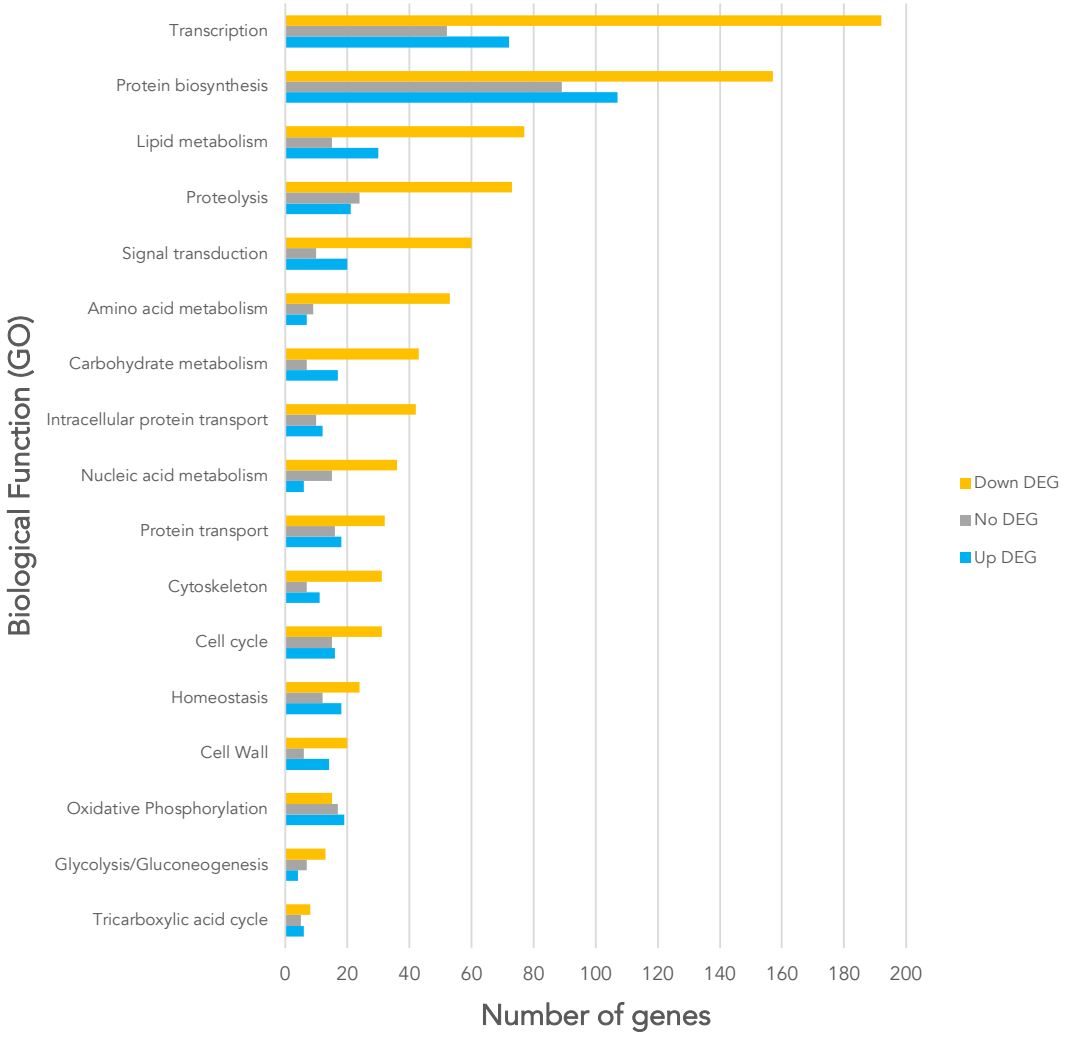

FIGURE 4.1: Functional classification of differentially expressed genes (DEG) in *Blumeria graminis* f. sp. *hordei* conidia and during the appressorial germ tube stage. Genes were categories based on Gene Ontology (GO). Number of genes up-regulated during the appressorial germ tube stage are in blue while the orange bars are the genes that are down regulated. Genes that displayed relatively stable expression during both stages are in grey.

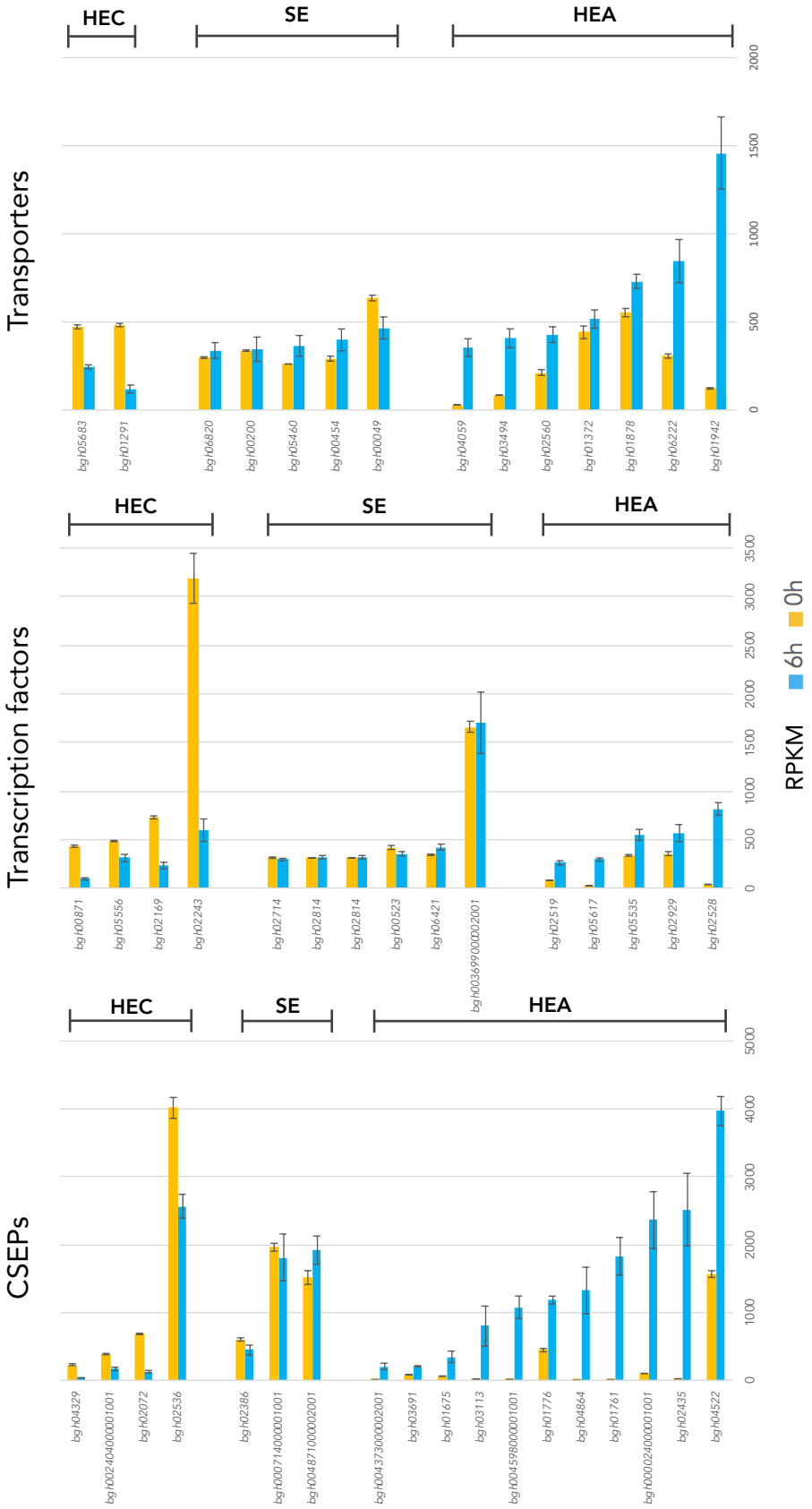

FIGURE 4.2: Highest expressed candidate secreted effector proteins (CSEP), transporter, and transcription factor transcripts in the *Blumeria graminis* f. sp. *hordei* conidia (0 h) and agt stage (6 h). HEC, high expression in conidia. SE, stable expression in the conidia and agt. HEA, high expression in the agt. Data are given as means of three replications ± SD.

To complement the transcriptome analyses, the proteomic profile of *Bgh* was analysed during the conidial and agt stage. The identified proteins were sorted into broad categories based on their GO annotations. A total of 542 proteins were identified, with 326 proteins detected in the ungerminated conidia (0 h) and 460 detected at the agt stage of *Bgh* (6 h) (Figure 4.3). 244 of these proteins were common to both stages while 82 were unique to the conidia and 216 were unique to the agt stage. The majority of proteins identified were classified as metabolic proteins, representing approximately 60% of total proteins during both the conidial and agt stages. Many of the metabolic proteins identified were involved in amino acid, carbohydrate, lipid, nucleotide, and protein metabolism.

Similar to the transcriptomic analysis, a transition towards energy and protein production during the agt stage was observed in the proteomic profile of *Bgh*. The largest number of proteins identified, aside from those of unknown function, are represented by protein metabolism and modification as well as carbohydrate metabolism. The amount of proteins involved in oxidative phosphorylation increased by 1.5-fold during the agt stage while those involved in protein biosynthesis increased by 2-fold. The greatest shift in proteins identified were those involved with lipid metabolism and protein transport, which increased by 3-fold. In regard to transport proteins, there was a high increase in proteins involved in membrane vesicle trafficking and protein transport.

Several candidate secreted effector proteins (CSEPs) are differentially expressed during the conidial and agt stage (Figure 4.2). The majority of the highest expressed CSEPs were the same as the highest expressed transcripts measured in *Bgh* cultivated *in planta* on *Arabidopsis* at 6 h (Figure 4.2) (Hacquard et al., 2013). In addition, several CSEPs were also found to be highly expressed in the conidia (*bgh02536, bgh02072, bghG002404000001001* and *bgh04329*). The CSEPs detected in the *Bgh* proteome did not correlate well with the transcriptomic data. While eight CSEPs proteins were detected, their transcripts were expressed at low levels during both developmental stages, aside from CSEP0041 (*bgh02072*) (Supplementary Table S2).

Several transporters involved in multidrug resistance were also detected in the transcriptome and proteome. During the conidial stage, the transporters with the highest transcript expression were two putative major facilitator superfamily (MFS) multidrug transporters (*bgh01291* and *bgh05683*) (Figure 4.2). Additionally, a few stage specific ATP-binding cassette (ABC) transport proteins were detected during the agt stage (*bgh01226, bgh00933*, and *bgh01627*). Both ABC and MFS transporters are superfamilies that are one of the most prominent contributors to multidrug resistance and virulence, playing important roles in antibiotic-mediated interactions between bacteria and fungi in plant-associated environments (Schoonbeek et al., 2002; Costa et al., 2014).

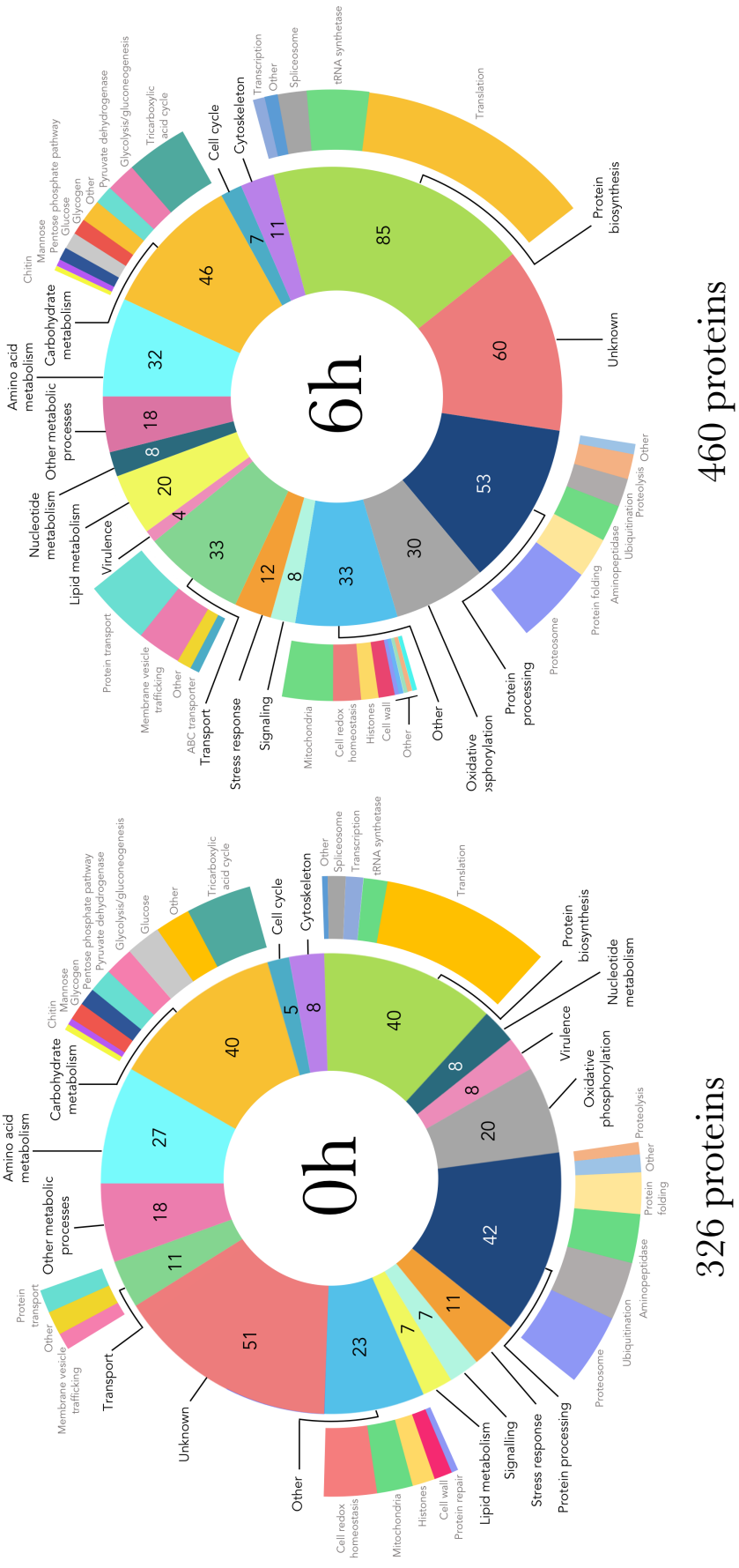

FIGURE 4.3: Caption on the following page

FIGURE 4.3: Pie chart representing the functional classifications of the identified proteins from *Blumeria graminis* f. sp. *hordei* conidia and appressorial germ tube stage. The diagram shows the number of proteins identified in various functional categories based on their GO annotations. The outer layer of the pie chart provides additional information to some of the broader categories.

4.5.2 Compositional analysis of *Bgh* cell wall

Analysis of the cell wall polysaccharides of ungerminated (Pham et al., 2019; Chapter 2) and agt stage *Bgh* revealed that a majority of the fungal cell wall was comprised of glucose, *N*-acetylglucosamine mannose, galactose, and trace amounts of xylose (Figure 4.4). The total amount of glucose, mannose, and *N*-acetylglucosamine remained relatively stable between the two developmental stages. However, while the proportions of the mannose and *N*-acetylglucosamine linkage types were the same, there were some changes in the proportion of glucose linkage types. Compared to the conidial stage the 1,3- and 1,4-linked glucose residues increased by 12.8% and 57% respectively during the agt stage while the 1,6-linked, and branched 1,2,3 and 1,3,4-linked residues decreased by 70.4%, 29%, and 18.4% respectively.

The galactose proportion of the cell wall experienced the most dramatic decrease during the agt stage, with a total decrease of 73.5% of the galactose residues during the agt stage compared to the conidial stage. The terminal galactofuranose was reduced by 53% while 1,4-linked galactopyranose decreased by 101.7%. The xylose proportion was the only monosaccharide that experienced an overall increase in content, with the total xylose content increasing by 3-fold. The 1,4-linked xylose residue increased by 2-fold during the agt stage. In addition, the presence of branched 2,4- and 3,4-linked xylose was detected specifically during the agt stage.

4.5.3 *Bgh* cell wall labelling

Developing *Bgh* cells were labelled with the chitin-binding probes, WGA and calcofluor white. Calcofluor white is a fluorescent stain known to strongly bind to chitin while WGA is a lectin that binds to the *N*-acetylglucosaminyl residues that compose the chitin in fungal cell walls. WGA was applied directly to the germinating *Bgh* cells and bound to newly developing structures (Figure 4.5). On freshly inoculated slides (0 h) WGA labelled the buds scars at the ends of the conidia, though over time it can be observed that the labelling of the scars dissipates (2-6 h). *Bgh* conidia develop on a structure called conidiophores, a chain of linear conidia connected to each other. Bud scars form between the conidia during conidiation, an asexual reproduction process in filamentous fungi. As the conidia develop, the connections constrict and eventually weaken to the point that they can be broken by wind stress, releasing the conidia from the conidiophore and exposing the scars.

At 2 h WGA binds to newly emerged primary germ tubes. However, after 2 h it appears that WGA does not bind to the primary germ tubes anymore. In fact, at 4 h and 6 h the WGA only labels the tips of the developing secondary germ tubes and agt respectively. After 24 h WGA only labels the *Bgh* cells that developed a penetration peg under the appressorium. From these observations, it can be concluded that the

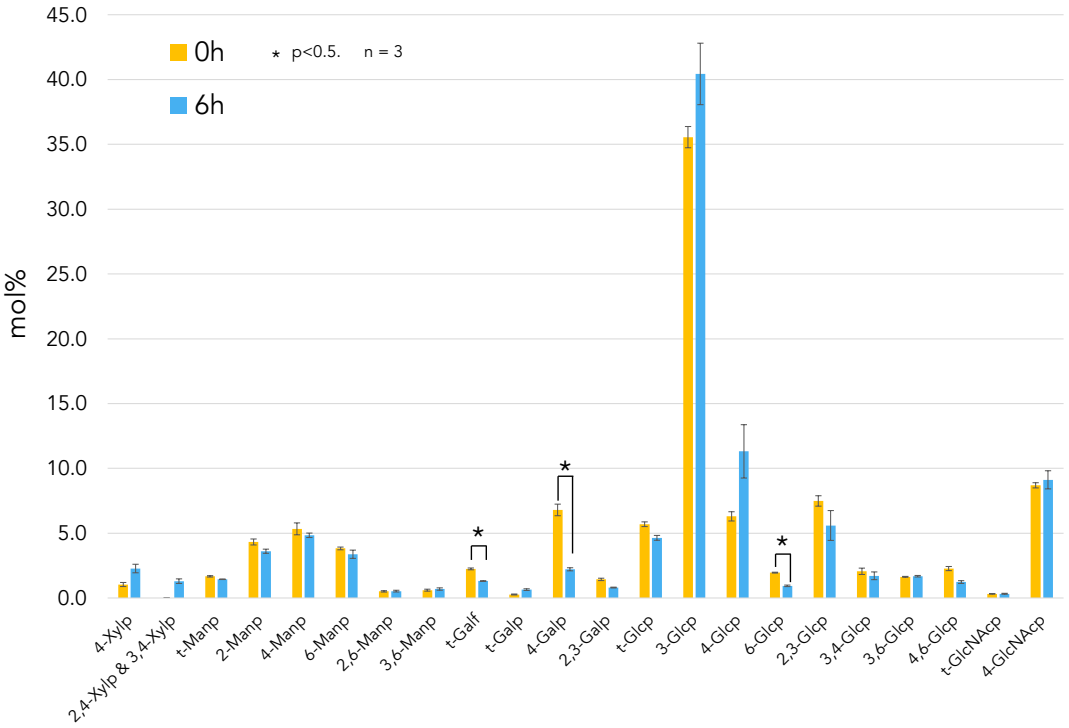

FIGURE 4.4: *Blumeria graminis* f. sp. *hordei* glycosidic linkage analysis (mol%) of the carbohydrate fraction of the cell wall from ungerminated conidia (0h) and the appressorial germ tube stage (6h). The different glycosidic linkages and pyranose or furanose forms of each monosaccharide were deduced from EI-MS spectra. Gal, galactose; Glc, glucose; GlcNAc, *N*-acetylglucosamine; Man, mannose; Xyl, xylose; 'p' and 'f' at the end of a monosaccharide abbreviation indicate that the residue occurs in the pyranose or furanose form, respectively; 't-' indicates a 'terminal' monosaccharide that occurs at the non-reducing end of a glycan. Error bars indicate standard deviations calculated from three biological replicates.

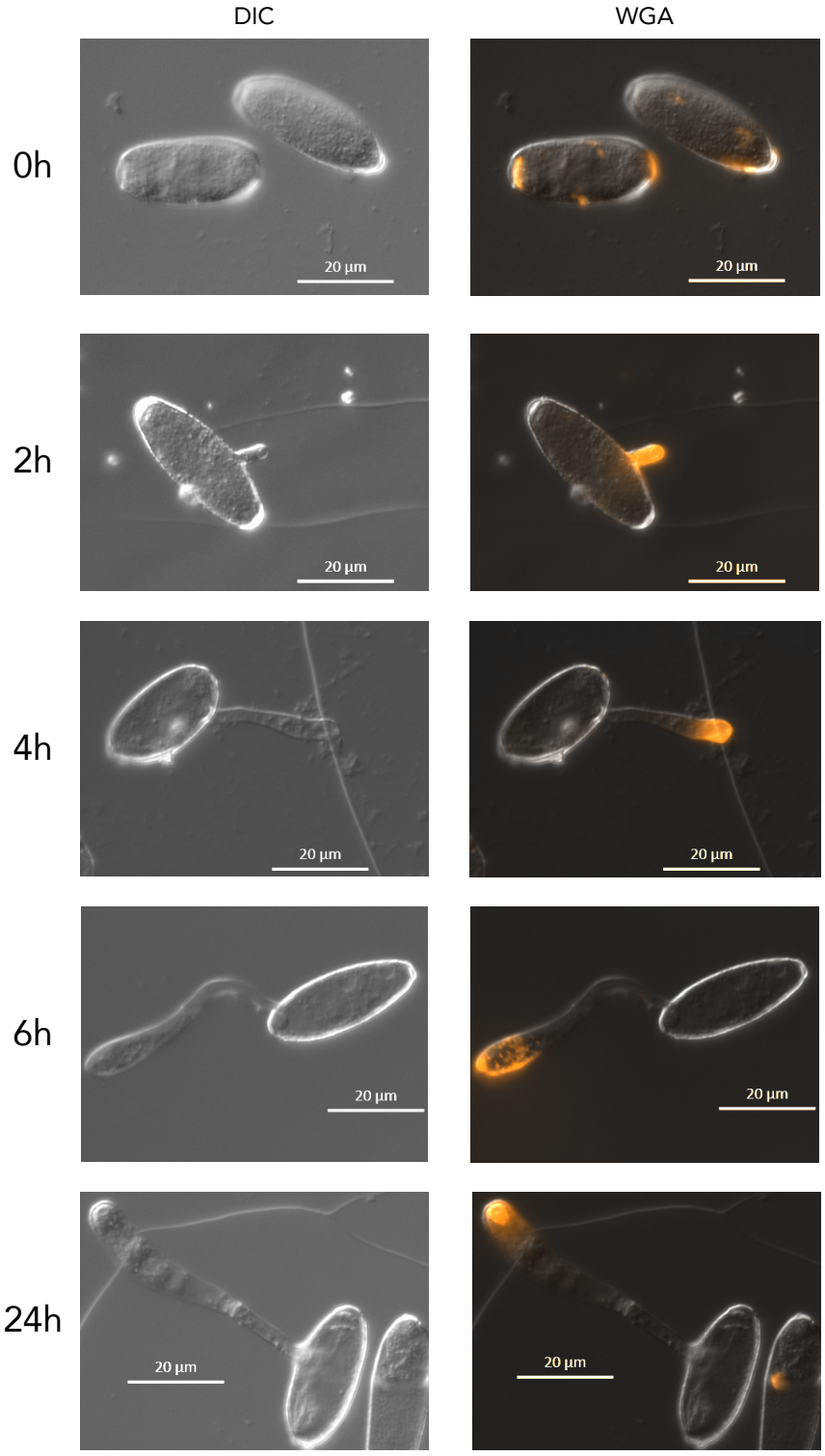

FIGURE 4.5: Light microscopy of *Blumeria graminis* f. sp. *hordei* development on glass slides coated with *n*-hexacosanal/Formvar®resin labelled with wheat germ agglutinin conjugated to Alexa Fluor 555 (WGA-AF555). 0 h: Conidium immediately after inoculation, 2 h: emergence of primary germ tube (pgt), 4 h: development of secondary germ tube (sgt), 6 h: differentiation of sgt to appressorial germ tube (agt), 24 h development of a penetration peg under the appressorium. DIC, differential interference contrast; dsRED filter to observe WGA-AF555 labels.

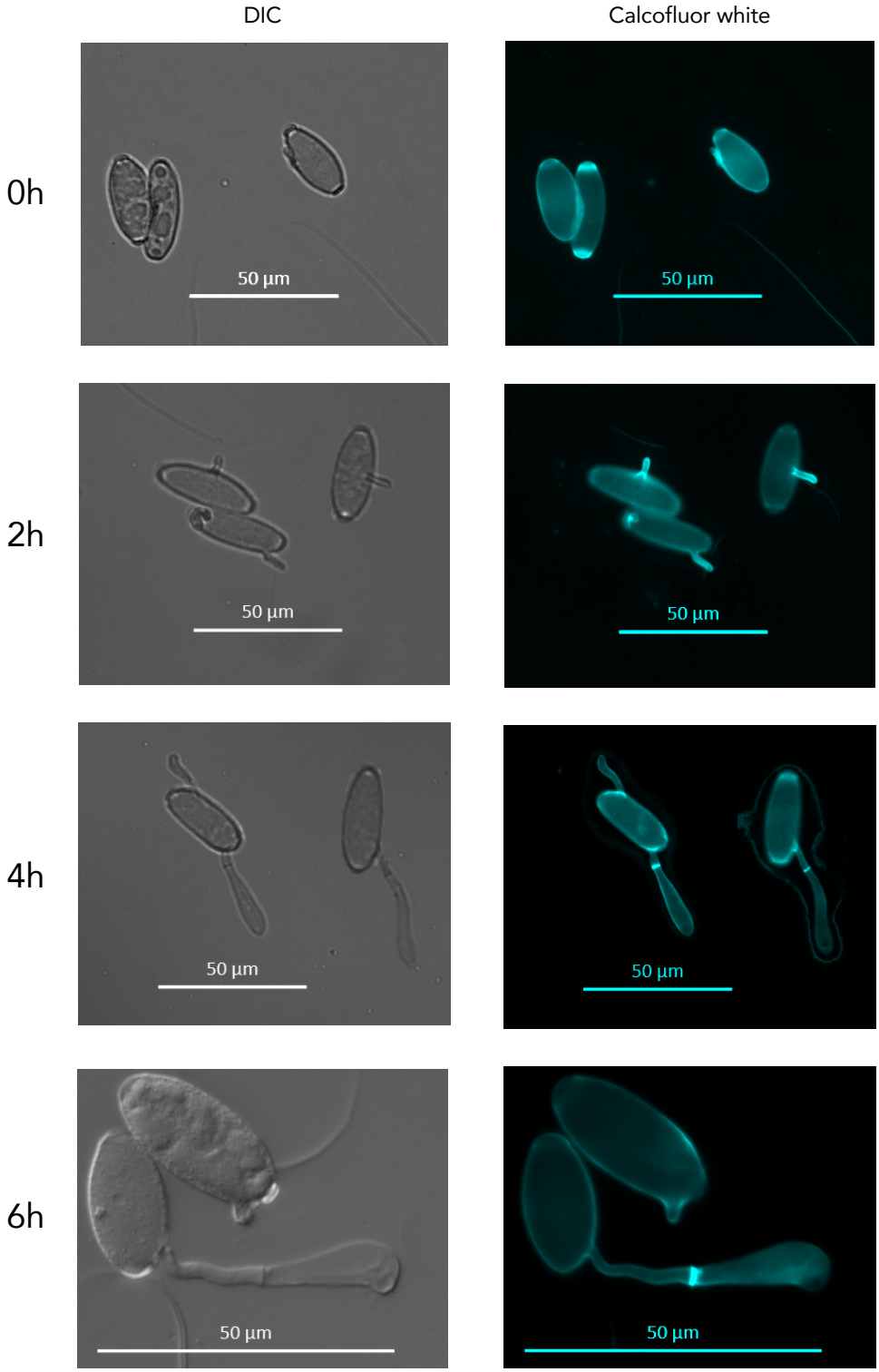

FIGURE 4.6: Light microscopy of *Blumeria graminis* f. sp. *hordei* development on glass slides coated with *n*-hexacosanal/Formvar®resin labelled with calcofluor white. 0 h: Conidium immediately after inoculation, 2 h: emergence of primary germ tube (pgt), 4 h: development of secondary germ tube (sgt), 6 h: differentiation of sgt to appressorial germ tube (agt). At 4 h and 6 h a septum is present between the conidium and sgt/agt. DIC, differential interference contrast; DAPI filter to observe calcofluor white.

WGA is only able to label newly emerging structures and that the *Bgh* works swiftly to mask any exposed chitin as over time these structures are no longer labelled. To label the internal structures, the developing *Bgh* cells were permeabilised with NaOH so that calcofluor white could penetrate through the cell wall. This allowed calcofluor white to label the entire *Bgh* structure, from the conidia to the developing germ tubes (Figure 4.6). Similar to WGA, the bud scars are seen at 0 h and then recede over time. The internal labelling reveals the septum that forms in the secondary germ tubes (4 h) and assists in the development of the agt (6 h).

4.5.4 *Bgh* cell wall metabolism

A table displaying the transcriptomic profile of genes involved in cell wall metabolism was constructed (Figure 4.7). The classifications of the genes were based on CAZy and KEGG annotations. Aside from a few exceptions, there was a general down-regulation of genes involved in cell wall metabolism.

Only a few genes, such as chitinase (*bgh00059*), chitin deacetylase (*bgh00857*), β-1,3-glucanase (*bgh02974*), pectin methytransferase (*bgh05186*), and galactosyltransferase (*bgh03501*) displayed increased expression profiles during the agt stage. A UDP-glucose/galactose transporter was also up-regulated during the agt stage (*bgh04059*) (Figure 4.2). These genes may play an important role in cell wall development during germination.

Several genes maintained high expression during both the conidia and agt stages, such as chitin deacetylase (*bgh06022*), Dol-P-Man: α-1,4-mannosyltransferase (*bgh00763*), β-1,3-glucanase (*bgh01040*), and β-1,3-glucanosyltransferase (*bgh00776*), indicating possible key roles in cell wall maintenance and development during early developmental stages.

A few agt specific proteins involved in cell wall processes were detected as well, such as the cell wall biogenesis protein phosphatase Ssd1. Ssd1 is an important regulator of fungal cell wall biogenesis and composition, and is also important in mediating resistance to osmotin in a cell wall-dependent manner in *S. cerevisiae, Colletotrichum lagenarium*, and *Magnaporthe grisea* (Ibeas et al., 2001; Tanaka et al., 2007). Osmotin is a plant defence antifungal protein belonging to the pathogenesis-related (PR)-5 family. Additionally, the chitinase with high expression in the transcriptome (*bgh00059*) was also detected in the proteome. Chitinases have been implicating in assisting cell wall growth by plasticising the cell wall (Tzelepis et al., 2012).

The expression profile of enzymes involved in chitin synthesis (*ChsI-VII*) and β-1,3-glucan synthesis and remodelling (*Fks1, GELA/B/C, KRE6* and *KRE9*) were measured during the pre-penetrative phases of *Bgh* pathogenesis (0 h, 2 h, 4 h and 6 h) by qPCR (Figure 4.8).

The chitin synthase genes displayed variable profiles over the course of 6 h. While some remained stable (*ChsIII, IV* and *V*), others were decreasing (*ChsI* and *VII*). The

only chitin synthases that were up-regulated were *ChsII* and *ChsVI*. *ChsII* had no expression at 0 h and 2 h, and only begun to display expression at 4 h with an increased expression at 6 h. This coincided with the formation of the septum in the secondary germ tube at 4 h and could possibly be associated with septum formation and development (Figure 4.6). *ChsVI* expression increased over the course of the 6 h and may indicate involvement in germination and secondary/appressorial germ tube development.

There was a general down regulation of the β-1,3-glucanosyltransferases (*GELA/B/C*) over time, though *GELA* was still the highest expressing gene over the course of 6 h. *GELB* expression peaked at 2 h and then decreased. This may indicate that *GELB* is involved in primary germ tube development. The expression of the β-1,3-glucan synthase (*Fks1*) and the putative β-1,6-glucan synthase (*KRE9*) remained relatively stable (Figure 4.8) while the *KRE6* exhibited a general trend of up-regulation, indicating possible involvement in early development.

The qPCR results were used to validate the RNAseq dataset. A good correlation was observed between the $\log_2$ of the fold change ratios (6 h/0 h) of the RNAseq and qPCR expression profiles ($y = 0.6659x - 0.859; R^2 = 0.8973$), indicating the reliability of the RNAseq dataset (Supplementary Figure S2).

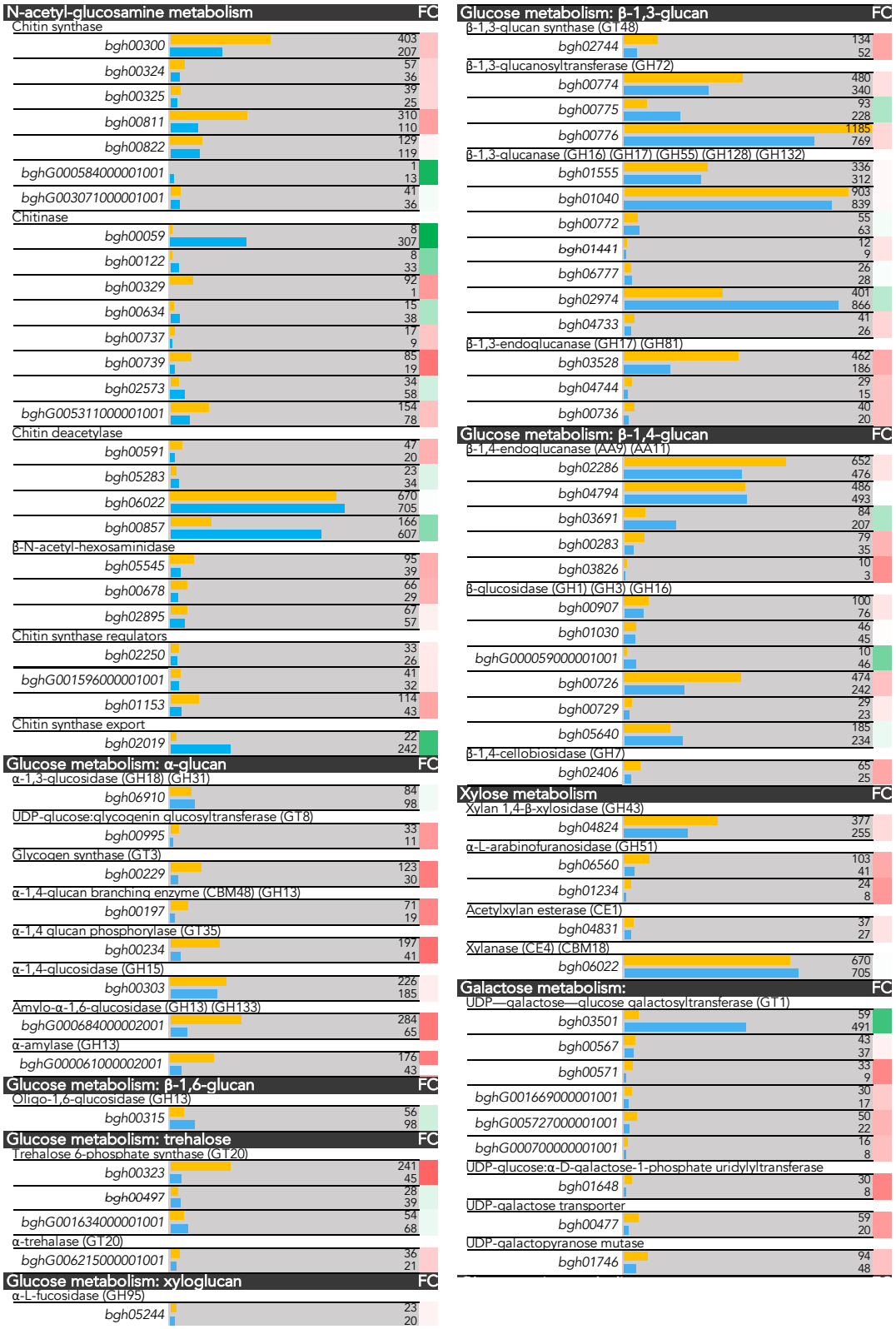

FIGURE 4.7: Continues on next page

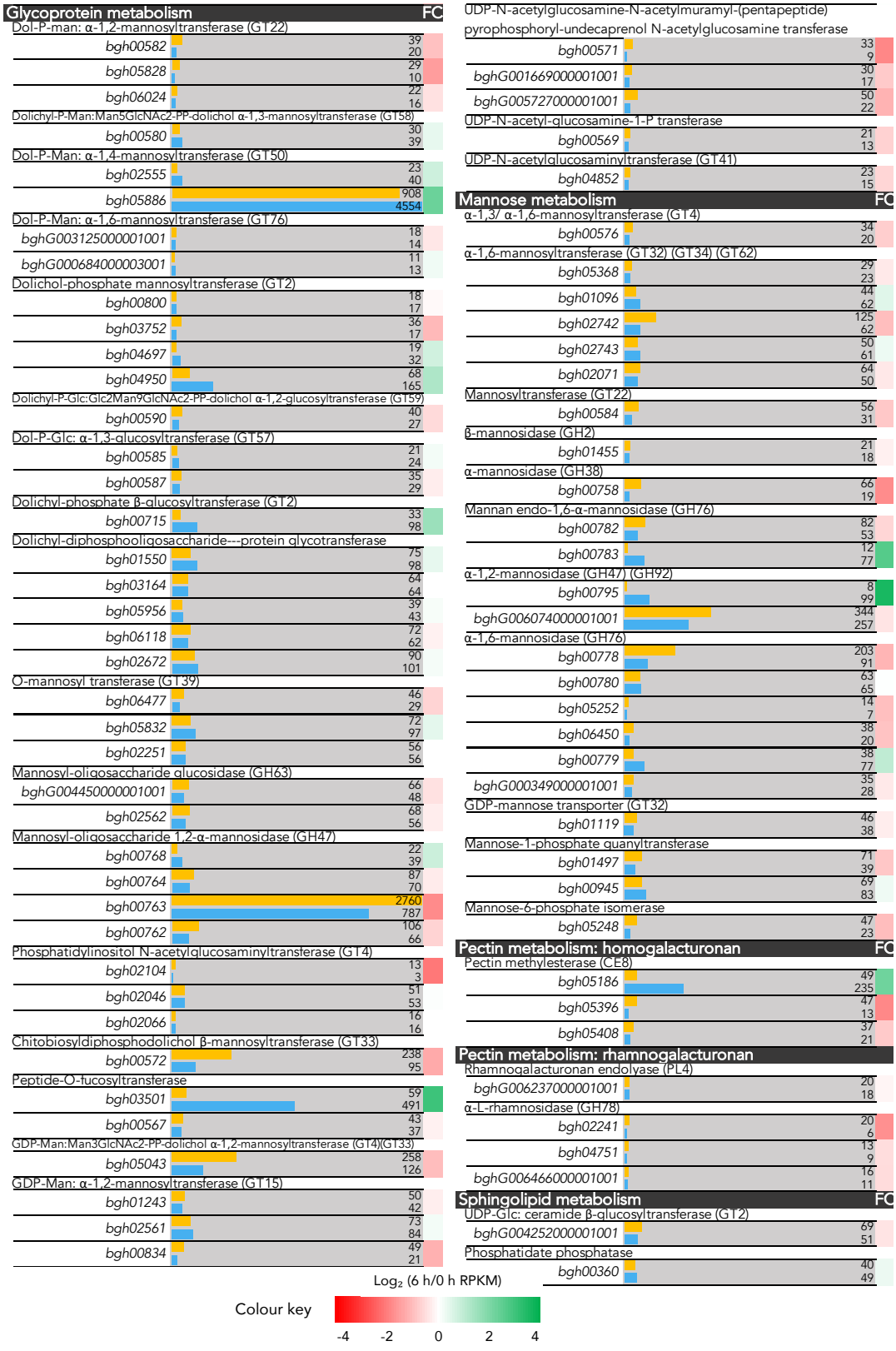

FIGURE 4.7: Continued. Caption on the following page

FIGURE 4.7: RNAseq transcript levels of genes involved in cell wall metabolism in *Blumeria graminis* f. sp. *hordei* conidia (0 h – orange) and during the appressorial germ tube stage (6 h – blue). Genes are organised based on which part of the cell wall metabolism they are involved in. Transcript levels are displayed adjacent to the accession numbers of the genes as RPKM values. Scale of the bar is 0-1000 RPKM, with a few outliers exceeding 1000. FC, $\log_2$ fold change between the conidia (0 h) and appressorial germ tube stage (6 h).

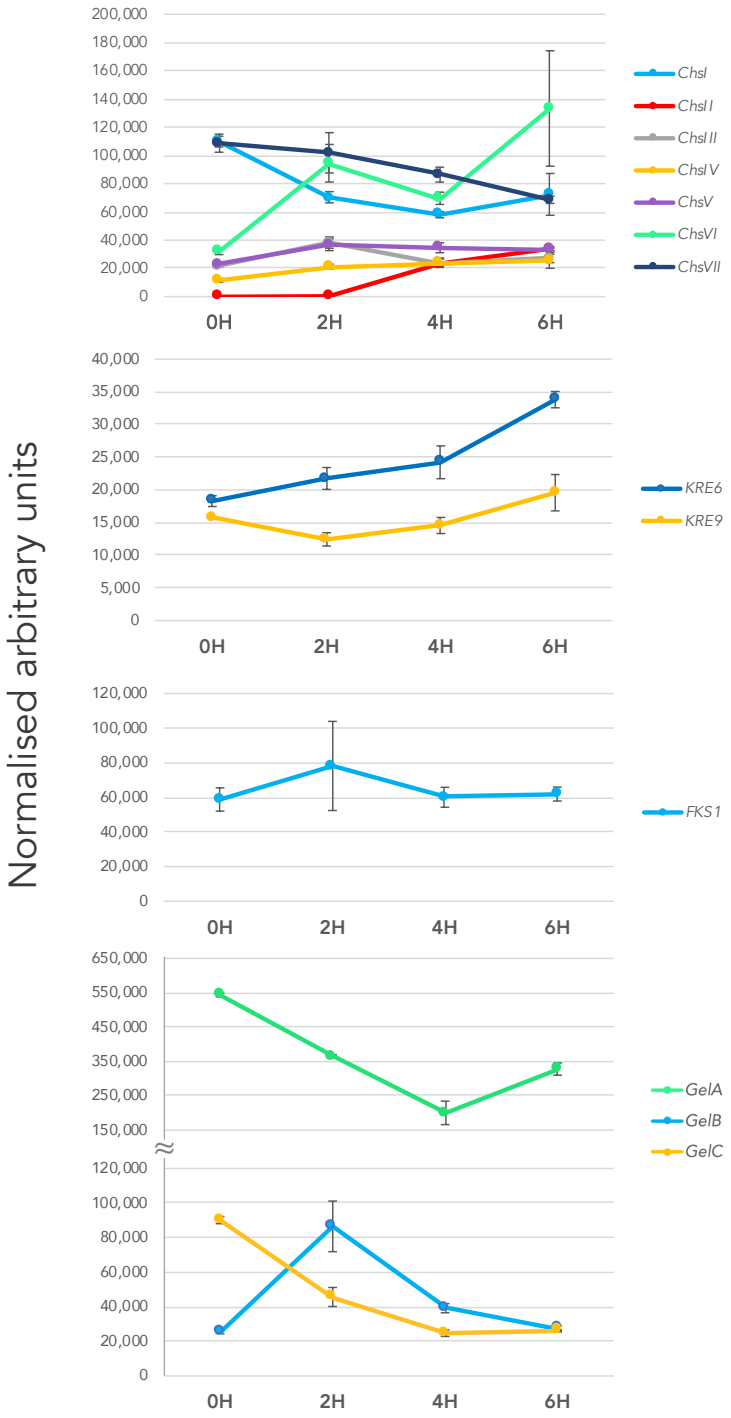

FIGURE 4.8: Transcript profile (qPCR) of cell wall related genes in *Blumeria graminis* f. sp. *hordei* cell cultivated *in vitro* during early germination (0-6 h). Data are given as means of three replications ± SD.

4.6 Discussion

Characterising the complex physiological and molecular changes that occur during pathogenesis is an important step towards disease control. As an obligate biotroph the range of molecular techniques applicable to *Bgh* is severely limited, as it cannot be cultured completely *in vitro*. In this study, we used a method adapted from Hansjakob et al. (2010) to cultivate *Bgh in vitro* up to the pre-penetrative stages of pathogenesis to examine the physiological and molecular shifts that occur during germination by analysing the transcriptome, proteome, and cell wall composition.

Transcriptomic analysis of the metabolic processes in *Bgh* reveal that there is a shift towards energy and protein production during the agt stage. After 6 h many genes involved in cellular respiration and protein synthesis were up-regulated. Key regulators in glycolysis and enzymes involved in lipid catabolism were up-regulated during the agt stage. This coincided with the expression profile of *Bgh* primary metabolism previously conducted by Both et al. (2005a), as they too observed an increase in glycolytic processes and lipid metabolism during pre-penetrative development. The processes of glycolysis and lipid metabolism consist of catabolic activities that generate energy to make use of the glycogen and lipid droplets stored in the *Bgh* conidia (Both et al., 2005a). Several enzymes involved in oxidative phosphorylation were also up-regulated. The majority of the highest expressing transporters were various ATP synthases and ATPases that were also highly up-regulated at 6 h *in planta* on *Arabidopsis* (Hacquard et al., 2013).

Genes involved in transcription and protein synthesis were by far the most up-regulated during the agt stage. Several of the transcription factors up-regulated seemed to be important transcription factors to virulence development. The *Seb1* transcription factor (*bgh05556*) was highly expressed during both the conidial and agt stages of development. Orthologues of *Seb1* have been found to be important to hyphal growth and virulence in other pathogenic fungi (Zhang et al., 2014; Luo et al., 2015; Tian et al., 2017). The *N. crassa hac-1* has an important role in aiding the secretion of enzymes during ER stress conditions (Montenegro-Montero et al., 2015). The *Bgh* orthologue *HacA* (*bgh02519*) was up-regulated during the agt stage and likely assists in the secretion of plant cell wall degrading enzymes that facilitate the penetration process.

The proteome from the agt stage supports the results from the transcriptomic analysis. During the agt stage, there was a significant increase in proteins involved in lipid metabolism and protein biosynthesis, processing, and transport. There was a greater increase in proteins involved in lipid metabolism than glycolysis. This was likely more energy efficient as, compared to carbohydrates, the breakdown of fatty acids yields more ATP when there are completely oxidised by β-oxidation and the tricarboxylic acid cycle. The sheer volume of proteins identified to be involved in protein biosynthesis points to a rapid need to generate more proteins

during pathogenesis. This is also accompanied by a significant increase in proteins associated with membrane vesicle trafficking and protein transport.

As the agt stage precedes penetration it is likely that a great supply of energy is necessary to generate the turgor pressure in the appressoria to penetrate the plant cell wall and to also fuel the synthesis of new proteins for virulence factors and the development of the haustoria.

Bgh is constantly growing and developing new structures throughout the process of pathogenesis. As the fungus grows there is a constant demand for more protein production. Previous proteomic analyses of the *Bgh* conidia, haustoria and sporulating hyphae have shown that proteins associated with protein biosynthesis, modification, and metabolism are present in high levels throughout all developmental stages (Bindschedler et al., 2009; Godfrey et al., 2009).

A few studies have previously analysed the *Bgh* conidia (Bindschedler et al., 2009; Noir et al., 2009), with some able to analyse the *in planta* proteome of *Bgh* haustoria and sporulating hyphae thanks to the sequencing of the *Bgh* genome (Bindschedler et al., 2009; Godfrey et al., 2009). The majority of the proteins identified in the conidia were classified as metabolic proteins (62%). Metabolic proteins are generally well represented in proteomic studies as they are highly abundant and soluble. *Bgh* is not the only phytopathogenic fungus to exhibit this profile in the conidia as spores from the fungal plant pathogen *Uromyces appendiculatus* also mainly consisted of metabolic proteins (66%) (Cooper et al., 2006). It has been suggested that asexual fungal spores preform metabolic proteins to be prepared to rapidly produce proteins upon contact with the host surface without expending limited energy resources on *de novo* assembly (Cooper et al., 2006; Loginov and Šebela, 2016).

Pathogens are able to suppress the host innate immune mechanisms and manipulate host cellular functions to redirect nutrients by secreting effector molecules (Win et al., 2012). In *Bgh*, this is achieved by CSEPs. Over 500 CSEPs have been identified in *Bgh* (Spanu et al., 2010), though only a few have been shown to play a role in virulence (Aguilar et al., 2016; Ahmed et al., 2016). Analysis of the CSEP transcripts reveal that several CSEPs are highly expressed in the conidia and agt stages. Hacquard et al. (2013) examined the transcript profile of CSEPs from *Bgh* infected *Arabidopsis* from 6 h onward. The majority of the highest expressed CSEPs in their study were the same as those detected on the *in vitro* surface. In addition, several CSEPs were found to be highly expressed in the *Bgh* conidia. However, aside from CSEP0041 (*bgh02072*), none of the highly expressed CSEPs were detected in the proteomic analysis. Eight CSEP proteins detected in the conidia and expressed at low levels during both developmental stages (*bgh05118, bgh02337, bgh04522, bgh03855, bgh05117, bghG003669000001001*, and *bgh00804*) (aside from CSEP0041). These conidia specific CSEPs are likely involved in the early stages of pathogenesis and are possibly secreted in the extracellular matrix that is released when *Bgh*

conidia land on a surface. Of these eight CSEPs, four were also detected during the agt stage (*bgh05118*, *bgh02072*, *bgh02337*, and *bgh04522*) and possibly have roles in interfering with important plant processes during host penetration or haustorium development.

Permethylation analysis of the *Bgh* cellallowed the identification of the polysaccharides present in their cell walls (Figure 4.4). Previous analysis of the *Bgh* conidial cell wall revealed that it was primarily composed of glucose, had a greater proportion of galactopyranose residues compared to other species, and had 1,4-linked xylose (Pham et al., 2019; Chapter 2). After 6 h there was a shift in the glucosyl linkages, with an increase in 1,3- and 1,4-linked glucose residues and a decrease in 1,6-linked residues. While the galactose portion of the cell wall experienced a large decrease in content (54%), its function is unknown as the biosynthesis of galactose as well as its biological role and importance for fungal viability are currently undefined. The xylose proportion of the cell wall increasing by 3-fold, with the 1,4-linked xylose residues doubling and forming branches. The presence of branched 1,4 xylose is quite novel and has not yet been reported in fungi. It was previously suggested that xylose residues in the cell wall may form xylomannan, an antifreeze molecule (Pham et al., 2019; Chapter 2), as xylomannan has been detected in the cell walls of other fungal species (Walters et al., 2011; Kawahara et al., 2016).

The agt stage consists of a secondary germ tube emerging from the side of the *Bgh* conidia that has differentiated into an appressorium (Figure 4.6, 6 h). The germ tube itself would contribute less than 5% of the total cell wall mass, with minimal changes expected to occur compared to the composition of the ungerminated conidium cell wall. Therefore, it may be possible to extrapolate the composition of the germ tube from the difference between the conidial and agt stages. The cell wall of the germ tube would likely have a chitin and β-1,3-glucan foundation, like the majority of fungal cell walls. As there was an increase in 1,3- and 1,4-linked glucosyl residues as well as branched 1,4-xylose, it can be inferred that the majority of the new polysaccharides synthesised would be in the agt.

In terms of cell wall metabolism, some of the highest expressed genes were chitinase (*bgh00059*) and chitin deacetylases (Figure 4.7). The expression of these genes could be an important element during pre-penetrative development. Not only was chitinase highly expressed but the protein was also detected during the agt stage. Chitinases have been shown to be important during polar growth and have been suggested to have a plasticising function in *N. crassa* during hyphal development (Tzelepis et al., 2012).

Chitin deacetylase are important to virulence as they catalyse post-synthetic modifications to chitin by deacetylating it to form chitosan. Chitosan is a weak inducer and assists in evading the host defence system (Fujikawa et al., 2012; Hadwiger, 2013). Labelling the chitin of the cell walls revealed that while exposed

bud scars and newly emerging structures are labelled, over time the WGA would cease binding to these structures as they were most likely swiftly deacetylated to chitosan to avoid triggering plant immunity (Figure 4.6).

Chitin deacetylases have recently been associated with inducing appressorium differentiation in *Magnaporthe oryzae* (Kuroki et al., 2017). It has been proposed that chitin deacetylase not only functions in avoidance of the host defence system, but is also involved in signalling, as exogenous sources of chitosan were able to induce appressorial formation in *M. oryzae* (Geoghegan and Gurr, 2016). In addition, chitin deacetylase deletions in *M. oryzae* resulted in compromised appressoria. The chitin deacetylases expressed during the agt stage could be an important factor to pathogenesis and agt development in *Bgh*.

Analysis of the *Bgh* chitin synthases by qPCR over the course of 6 h revealed that *ChsII* may be involved in septum formation, as its expression coincides with the formation of the septum in the agt, while *ChsVI* may contribute to germ tube development, as it was the only CHS enzyme to be up-regulated over 6 h (Figure 4.6 and 4.8). Class II chitin synthases, such as *Bgh ChsII*, have been associated with septum formation and lateral cell wall integrity in *Candida albicans* (Roncero, 2002). The *Bgh ChsVI* is orthologous to the *Ustilago maydis Chs6*, which has been found to be important in elongating hyphal tips and co-transporting β-1,3-glucan synthase to sites of growth (Schuster et al., 2016). Both *ChsII* and *ChsVI* may hold important roles in cell wall development during early pathogenesis.

Bgh is one of the most destructive foliar pathogens to barley. Despite the economic and agricultural significance of *Bgh*, molecular analysis of the pathogen has fallen significantly behind that of other filamentous pathogenic fungi, with a gap in knowledge surrounding the events during appressorial development. Due to its nature as an obligate biotroph the range of molecular techniques that can be carried out on *Bgh* is severely limited.

This study demonstrates that it is possible to cultivate *Bgh in vitro* up to the pre-penetrative stage of development to generate fungal material for molecular analysis without the problems associated with *in planta* studies. Transcriptomic profiling of the glycolytic processes, lipid metabolism, transcription factors, transporters, and virulence factors (CSEPs) also corroborate with *in planta Bgh* expression profiles from previous studies (Both et al., 2005a; Hacquard et al., 2013), demonstrating that pre-penetrative *in vitro* events can serve as a viable approximation for pre-penetrative *in planta* events.

4.7 Supplementary Figures and Tables

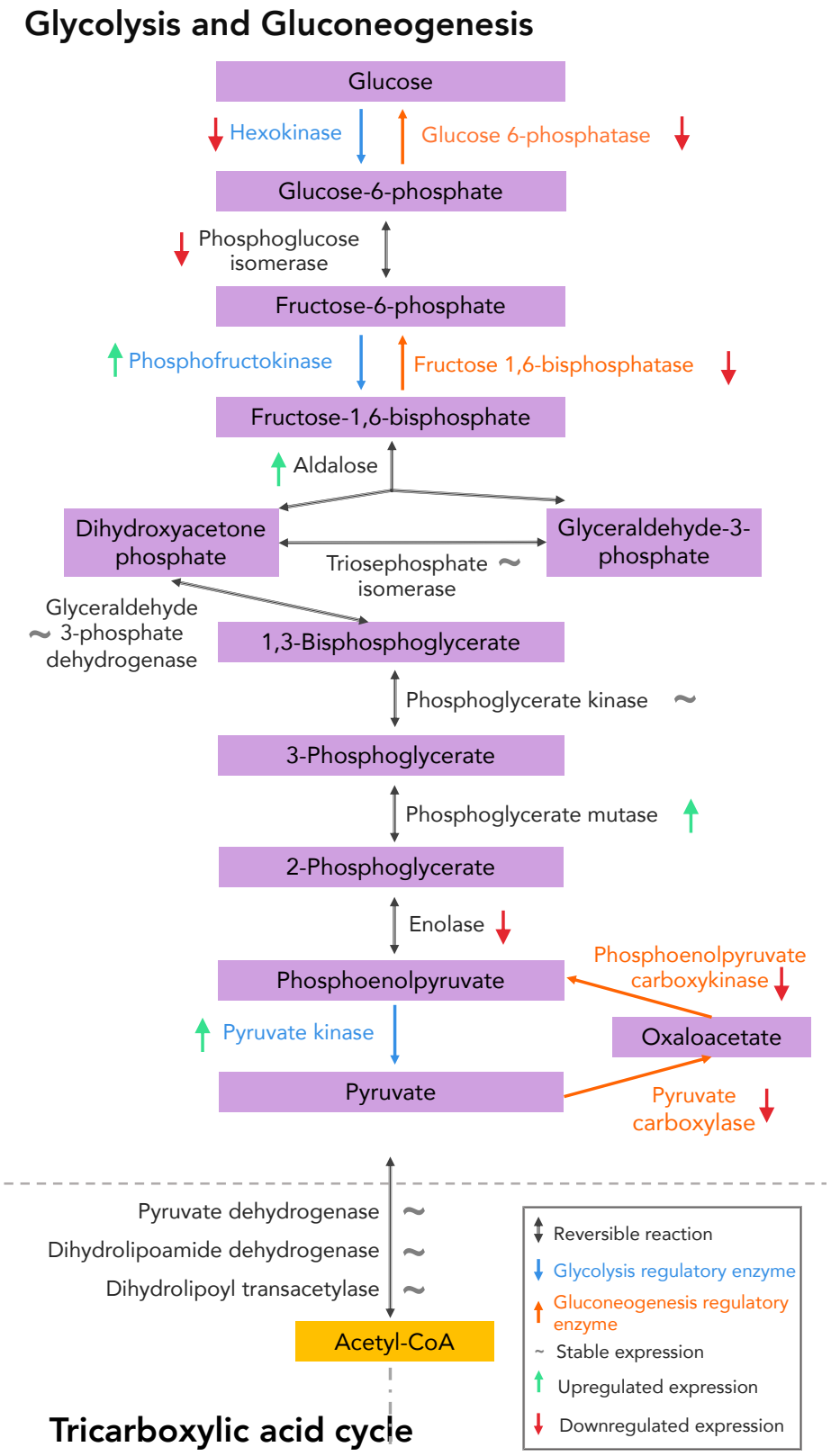

FIGURE S1: Caption on the following page.

FIGURE S1: Diagram of the metabolic pathway of glycolysis and the relative expression of the corresponding enzymes during the appressorial germ tube stage of *Blumeria graminis* f. sp. *hordei* development. Glycolysis is the process in which glucose is converted to pyruvate. Key glycolytic enzymes are highlighted by the blue text and arrows. Gluconeogenesis is the opposite of glycolysis and is a process that results in the generation of glucose. As it is the reverse process, glycolysis and gluconeogenesis share many enzymes that have reversible activity. Key enzymes in gluconeogenesis are denoted by the orange arrows and text. Arrows denote the direction of the enzymatic reaction. Double headed arrows mean that the enzymatic reaction is reversible while single direction arrows indicate that the reaction is irreversible. Enzyme up-regulation and down-regulation are designated by the green and red arrows respectively while stable expression is indicated by tildes.

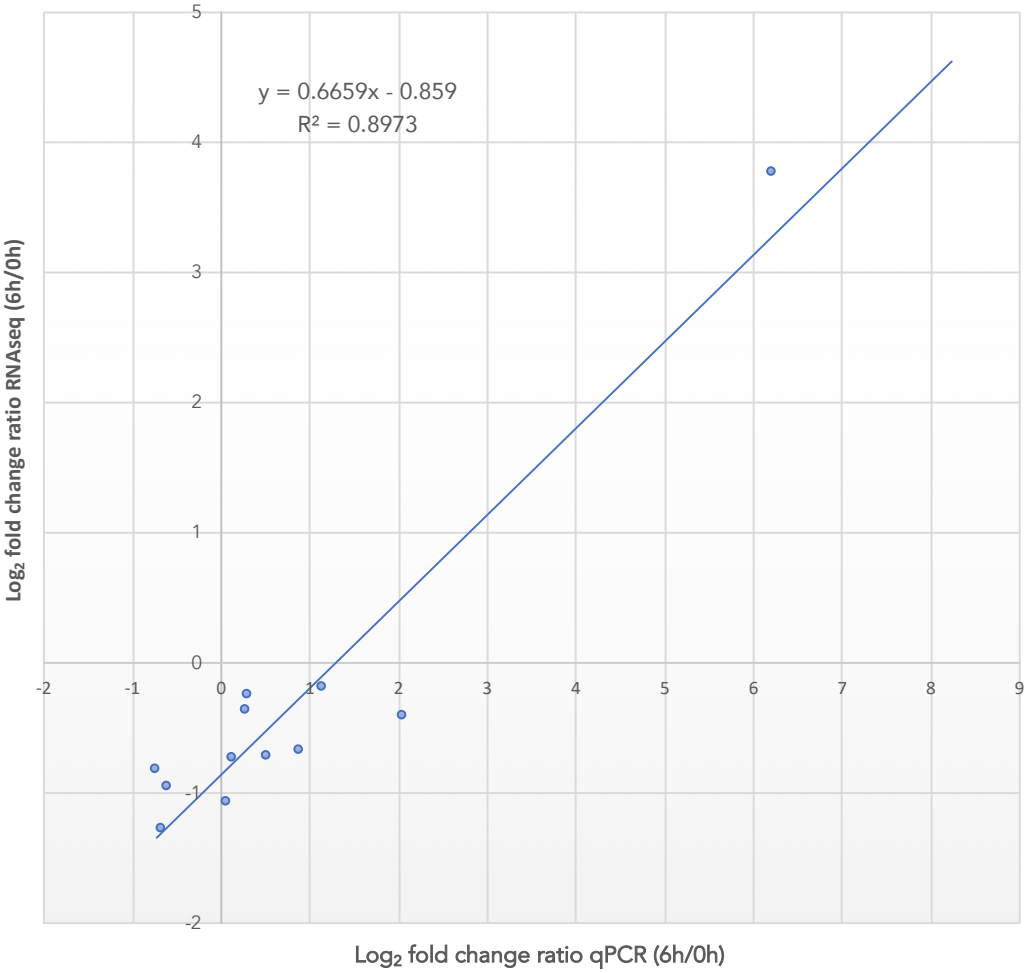

FIGURE S2: Correlation of the $\log_2$ of the fold change (6 h/0 h) between RNAseq (RPKM) and qPCR (normalised arbitrary units) from *Blumeria graminis* f. sp. *hordei* conidia (0 h) and appressorial germ tube (6 h).

TABLE S1: Primers for qPCR of *Blumeria graminis* f. sp. *hordei* cell wall related genes

Primer	Sequence 5′ → 3′
CHSI_Fq	AGGGTCCCATCGATAACCCT
CHSI_Rq	ATACCCCACGGAACATACGC
CHSII_Fq	GTCGTTGTCTCGTGGATGGT
CHSII_Rq	GCCGCTACCAATTGCCCTAA
CHSIII_Fq	ACTGGCACGATGTCTCATGG
CHSIII_Rq	CCGTCGCTTCGAACTGACTA
CHSIV_Fq	TCGTAAGACAGACGGCGAAA
CHSIV_Rq	CCGGGAAGCCCAGAAAAGTT
CHSV_Fq	AATGTCCAACCTTCCTGGGC
CHSV_Rq	CTCCTTGCATCCAGTGGAACA
CHSVI_Fq	GGATCTTTCGGTGGGGAGAC
CHSVI_Rq	CAACCAGAGCGTGAACTTGTTTC
CHSVII_Fq	ACTACCGATCTCAATCAGCCA
CHSVII_Rq	GGACTCCTACCCCCAACTCT
FKSI_Fq	CGCGGGGTCGATGATAATTGAT
FKSI_Rq	AATCTGTGCTGGTTCCCGTTTC
GELA_Fq	ACTTTGCTGCCCTCAAGTCA
GELA_Rq	CTGCACTTGGTATGGCTGGA
GELB_Fq	CAACCGAGCCCTACAGACAC
GELB_Rq	TGATCCGCTGGATTTCGTGT
GELC_Fq	AGCGCCAATGCTACTACTGG
GELC_Rq	TGCGGATTGGATCTTCGCAT
KRE6_Fq	GCAGTCATTCCAAGCTGCTC
KRE6_Rq	TCGTTGTTGAGCCAGGTCAC
KRE9_Fq	GCCCACTGCTATAACTGCCA
KRE9_Rq	TCTTTCCAGCGGTTCAGAAAC

TABLE S2: Summary of RNAseq data of *Blumeria graminis* f. sp. *hordei* during the conidial and agt stages of development on an *in vitro* surface. Supplementary table is an excel spread sheet, this figure displays a portion of the spreadsheet.

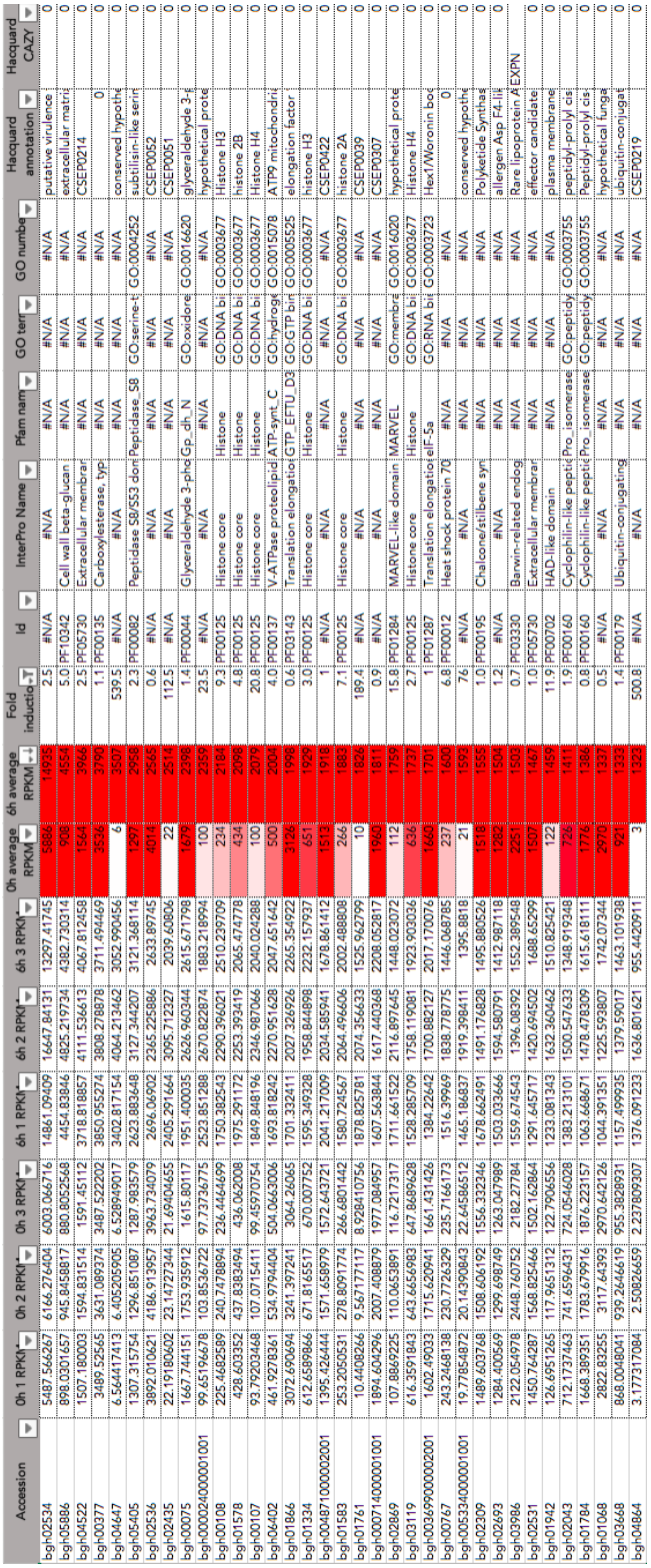

Accession	0h 1 RPKM	0h 2 RPKM	0h 3 RPKM	6h 1 RPKM	6h 2 RPKM	6h 3 RPKM	0h average RPKM	6h average RPKM	Fold induction	Id	InterPro Name	Pfam name	GO terms	GO numbers	Hacquard annotation	Hacquard CAZY
bgh02534	5487.546267	6166.274404	6003.046716	1486.109409	16447.84131	13297.41745	5882	14248	2.5	#N/A	#N/A	#N/A	#N/A	#N/A	putative virulence	0
bgh05986	898.0301657	945.8458817	880.8052568	4454.838846	4825.219734	4382.730314	908	4554	5.0	PF10342	Cell wall beta-glucan	#N/A	#N/A	#N/A	extracellular matri	0
bgh04522	1507.180003	1594.831514	1591.45112	3718.818857	4111.536613	4067.812458	1564	3966	2.5	PF05730	Extracellular membrar	#N/A	#N/A	#N/A	CSEP0214	0
bgh00377	3489.52565	3631.089374	3487.522202	3850.955274	3808.278878	3711.494469	3536	3790	1.1	PF00135	Carboxylesterase, typ	#N/A	#N/A	#N/A	0	0
bgh04647	6.544417413	6.405205905	6.528949017	3402.817154	4064.213462	3052.990456	6	3507	539.5	#N/A	#N/A	#N/A	#N/A	#N/A	conserved hypothe	0
bgh05405	1307.315754	1296.851087	1287.983579	2623.883648	3127.344207	3121.368114	1297	2957	2.3	PF00082	Peptidase_S8/S53 dom	Peptidase_S8	GO:serine-t	GO:0004252	subtilisin-like serir	0
bgh02536	3892.010621	4186.913957	3963.734079	2696.06902	2365.225886	2633.897745	4014	2548	0.6	#N/A	#N/A	#N/A	#N/A	#N/A	CSEP0052	0
bgh02435	22.19180602	23.14727344	21.69404655	2405.291664	3095.712327	2039.608061	22	2514	112.5	#N/A	#N/A	#N/A	#N/A	#N/A	CSEP0051	0
bgh00075	1667.744151	1753.935912	1615.80117	1951.400035	2626.960344	2615.671798	1679	2398	1.4	PF00044	Glyceraldehyde 3-phos	Gp_dh_N	GO:oxidore	GO:0016620	glyceraldehyde 3-p	0
bgh00024000001001	99.65196678	103.8536722	97.73736775	2522.851288	2670.822874	1883.218994	100	2358	23.5	#N/A	#N/A	#N/A	#N/A	#N/A	hypothetical prote	0
bgh00108	225.4682589	240.7478894	236.4464699	1750.382543	2290.396021	2510.239709	234	2164	9.3	PF00125	Histone core	Histone	GO:DNA bi	GO:0003677	Histone H3	0
bgh01578	428.603352	437.8383494	436.062008	1975.291172	2253.393419	2065.474778	434	2098	4.8	PF00125	Histone core	Histone	GO:DNA bi	GO:0003677	histone 2B	0
bgh00107	93.79203468	107.0715411	99.45970754	1849.848196	2344.987066	2040.024288	100	2079	20.8	PF00125	Histone core	Histone	GO:DNA bi	GO:0003677	Histone H4	0
bgh04402	461.9278361	504.9794404	504.0643006	1693.818242	2270.951628	2047.651642	500	2006	4.0	PF00137	V-ATPase proteolipid	ATP-synt_C	GO:hydrogt	GO:0015078	ATP9 mitochondri	0
bgh01866	3072.690694	3241.397241	3064.26085	1701.332411	2027.326926	2265.354922	3126	1998	0.6	PF03143	Translation elongatior	GTP_EFTU_D3	GO:GTP bin	GO:0005525	elongation factor	0
bgh01334	612.6589866	671.8165517	670.007752	1595.349328	1958.844896	2232.157937	651	1929	3.0	PF00125	Histone core	Histone	GO:DNA bi	GO:0003677	histone H3	0
bgh00487000002001	1395.426444	1571.658079	1572.643721	2041.217009	2034.585941	1678.861412	1513	1918	1	#N/A	#N/A	#N/A	#N/A	#N/A	CSEP0422	0
bgh01583	253.2050531	278.8091774	266.4801442	1580.724567	2064.496404	2002.488808	264	1883	7.1	PF00125	Histone core	Histone	GO:DNA bi	GO:0003677	histone 2A	0
bgh01761	10.4408266	9.567177117	8.928410756	1878.825781	2074.356633	1525.962799	10	1828	189.4	#N/A	#N/A	#N/A	#N/A	#N/A	CSEP0039	0
bgh00714000001001	1894.604296	2007.408879	1977.084957	1607.563844	1617.440368	2208.052817	1960	1811	0.9	#N/A	#N/A	#N/A	#N/A	#N/A	CSEP0307	0
bgh02869	107.8869225	110.0653891	116.7217317	1711.661522	2116.897645	1448.023072	112	1759	15.8	PF01284	MARVEL-like domain	MARVEL	GO:membra	GO:0016020	hypothetical prote	0
bgh03119	616.3591843	643.6656983	647.8689628	1528.285709	1758.119081	1923.903036	634	1773	2.7	PF00125	Histone core	Histone	GO:DNA bi	GO:0003677	Histone H4	0
bgh00369900002001	1602.49033	1715.620941	1641.431428	1384.22642	1700.882127	2017.170076	1640	1701	1	PF01287	Translation elongatior	eIF-5a	GO:RNA bi	GO:0003723	Hex1/Woronin boc	0
bgh00767	243.2468138	230.7726329	235.7166173	1516.39969	1838.778775	1446.068785	237	1600	6.8	PF00012	Heat shock protein 70	#N/A	#N/A	#N/A	0	0
bgh00533400000101	19.77854872	20.14390843	22.64586512	1465.186837	1919.398411	1395.8818	21	1593	76	#N/A	#N/A	#N/A	#N/A	#N/A	conserved hypothe	0
bgh02309	1489.603768	1508.606192	1554.332346	1678.662491	1491.176828	1495.880526	1510	1555	1.0	PF00195	Chalcone/stilbene syn	#N/A	#N/A	#N/A	Polyketide Synthas	0
bgh02693	1284.400569	1299.698749	1263.047989	1503.033666	1594.580791	1412.987118	1282	1530	1.2	#N/A	#N/A	#N/A	#N/A	#N/A	allergen Asp F4-lik	0
bgh03986	2122.054978	2448.760752	2182.27784	1559.674543	1396.08392	1552.389548	2251	1503	0.7	PF03330	Barwin-related endog	#N/A	#N/A	#N/A	Rare lipoprotein A	EXPN
bgh02531	1450.764287	1568.825466	1502.162864	1291.645717	1420.694502	1688.65299	1507	1467	1.0	PF05730	Extracellular membrar	#N/A	#N/A	#N/A	effector candidate	0
bgh01942	126.6951265	117.9651312	122.7906556	1233.081343	1632.360462	1510.825421	122	1459	11.9	PF00702	HAD-like domain	#N/A	#N/A	#N/A	plasma membrane	0
bgh02043	712.1737463	741.6586431	724.0544028	1383.213101	1503.547633	1348.919248	724	1411	1.9	PF00160	Cyclophilin-like peptic	Pro_isomerase	GO:peptidy	GO:0003755	peptidyl-prolyl cis	0
bgh01784	1668.389351	1783.679916	1876.223157	1063.668671	1478.478309	1615.618111	1776	1386	0.8	PF00160	Cyclophilin-like peptic	Pro_isomerase	GO:peptidy	GO:0003755	Peptidyl-prolyl cis	0
bgh01068	2822.83255	3117.64393	2970.642126	1044.391351	1225.593807	1742.07344	2970	1337	0.5	#N/A	#N/A	#N/A	#N/A	#N/A	hypothetical funga	0
bgh03668	868.0048041	939.2646619	955.3828931	1157.499935	1379.59017	1463.101938	921	1333	1.4	PF00179	Ubiquitin-conjugating	#N/A	#N/A	#N/A	ubiquitin-conjugat	0
bgh04864	3.177317084	2.508226459	2.237809307	1376.091233	1636.801621	955.4420911	3	1328	500.8	#N/A	#N/A	#N/A	#N/A	#N/A	CSEP0219	0

Chapter 5

Biochemical characterisation of *Blumeria graminis* f. sp. *hordei* cell wall biosynthetic enzymes

5.1 Introduction

Typical techniques employed to analyse the function of a particular gene of interest involve transcriptional analysis, reverse genetics or bioinformatics. However, the information discerned from these techniques is often limited and does not always reveal the specific protein activity. The analysis of transcript levels does not always correlate to protein levels or activity (Maier et al., 2009; Liu et al., 2016). In addition, gene disruption studies sometimes display no discernible phenotype at all due to functional redundancies and compensatory pathways within the cell (Mellado et al., 1996b,a; Rogg et al., 2011). While bioinformatics sequence analysis can reveal possible functions based on homology to other characterised genes it is all conjecture unless linked to solid evidence about the protein structure or the specific function that the protein plays in the organism.

In order to validate the predicted gene functions, the corresponding proteins need to be purified for biochemical analysis and, if possible, elucidation of protein structure. Recombinant production of proteins is one of the most powerful techniques available in biological research. Successful production and purification of a recombinant protein can allow detailed characterisation and functional analysis through well-defined assays. The procedure for recombinant protein expression is relatively simple. Target gene sequences are cloned into an expression vector and introduced into a host system to express the desired protein. These proteins are often tagged with a short peptide or small protein domain that serves to facilitate purification (Cutler, 2004; Walls and Loughran, 2017).

While sounding easy, in practice recombinant protein expression and purification can be extremely challenging as a multitude of factors can affect and influence the outcome of the procedure. Depending on the choice of host, the proteins

may not fold in the correct conformation. In addition, some proteins require post-translational modifications for activation which may not be available in some host systems. Some proteins may also be toxic to the host and impair host viability (Rosano and Ceccarelli, 2014). Even once an active protein is expressed the purification process is another hurdle to overcome. Expressed proteins can aggregate and form inclusion bodies, which require extensive processing to produce the active proteins. Poor expression and degradation of target proteins can also result in suboptimal protein quality and yield. The conditions of the purification process and composition of the buffers may also not be conducive to purification, requiring extensive testing of various buffers and processes to determine the optimal conditions (Cutler, 2004; Walls and Loughran, 2017).

The biosynthesis and remodelling of the fungal cell wall involves numerous biosynthetic pathways. Despite the importance of the cell wall, its composition, structure and synthesis are poorly understood. More is known about the genes encoding carbohydrate active enzymes than the specific activity of the proteins themselves. The structure of the enzymes and molecular mechanism in which β-1,3-glucans and chitin are synthesised are still to be determined.

Chitin and glucan are the most structurally important polysaccharides in the fungal cell wall. The glucan proportion of the cell wall is predominantly present as long chains and branches in fungal cell walls. The β-1,3-glucan is synthesised by the FKS1 complex at the plasma membrane. Using intracellular UDP-glucose as a substrate, linear β-1,3-glucan chains are extruded into the cell wall space (Latgé, 2007). β-1,3-Glucanosyltransferases of the glycoside hydrolase 72 family (GH72) are known to catalyse the elongation of β-1,3-glucan chains and also contribute to the formation of lateral branches by elongating branching points, β-1,6-glucan residues, that are created by branching enzymes (Klis et al., 2002).

Chitin is a linear polysaccharide of *N*-acetylglucosamine (GlcNAc) units linked together through β-1,4 glycosidic bonds. Due to its crystalline nature, the chitin polymers have high tensile strength and contribute significantly to the strength and rigidity of the fungal cell wall (Latgé and Calderone, 2006). The synthesis of chitin is mediated by chitin synthases, integral membrane proteins that catalyse the transfer of GlcNAc from UDP-*N*-acetylglucosamine (UDP-GlcNAc) to an elongating chitin chain. Chitin in fungal cell walls plays a vital role in maintaining cell wall integrity. The disruption of chitin synthesis, either by drugs or gene deletion, has diverse effects on fungi, causing the cell wall to become disordered, malformed, and osmotically unstable. These findings have come to give rise to the hypothesis that the chitin synthesis processes are an ideal target for antifungal agents.

In this study several genes related to cell wall synthesis in *Blumeria graminis* f. sp. *hordei* (*Bgh*) were chosen to be heterologously expressed due to the importance of their putative products to the integrity of the cell wall. Like other

filamentous ascomycete fungi, only one β-1,3-glucan synthase gene (*Fks1*) belonging to the glycosyltransferase family 48 (GT48) was identified in *Bgh*. Three β-1,3-glucanosyltransferase genes belonging to the GH72 family were identified (*GELA*, *GELB* and *GELC*) in the *Bgh* genome, which are believed to contribute to the synthesis of β-1,3-glucans. Seven chitin synthase (*Chs*) genes were also selected from the GT2 family, one for each *CHS* class.

As these enzymes are involved in the synthesis of vital components of the fungal cell wall many studies in the past have worked to characterise these enzymes in other fungi. Out of these enzymes, only the GH72 genes has a history of successful protein purification and characterisation (Mouyna et al., 2000; Carotti et al., 2004; de Medina-Redondo et al., 2010; Kováčová et al., 2015). This is likely due to the fact that GH72 β-1,3-glucanosyltransferases are small soluble proteins (~50 kDa), as opposed to FKS1 (>200 kDa) and CHS (80-200 kDa). Both FKS1 and CHS are generally large proteins with several transmembrane regions that span the membrane.

Fungal GH72 proteins have been best expressed in *Pichia pastoris*. Active β-1,3-glucanosyltransferases from *Candida albicans, Aspergillus fumigatus, Saccharomyces cerevisiae*, and *Schizosaccharomyces pombe* have been expressed and purified for biochemical analysis using *P. pastoris* systems (Mouyna et al., 2000; Carotti et al., 2004; de Medina-Redondo et al., 2010; Kováčová et al., 2015). The biochemical activity of GH72 β-1,3-glucanosyltransferase enzymes was first demonstrated with the GEL1 β-1,3-glucanosyltransferase from *A. fumigatus* (Mouyna et al., 2000). By characterising purified GEL1 protein in conjunction with mutational analysis, it was determined that GEL1 contributed to the catalysis of the β-1,3-glucanosyltransferase reaction by first cleaving the glycosidic linkage of a donor β-1,3-glucan chain and then transferring the exposed reducing end to the non-reducing end of an acceptor β-1,3-glucan chain, resulting in its elongation. In addition, a purified β-1,3-glucanosyltransferase protein from *S. cerevisiae* (GAS1) was found to be resistant to heat treatment (Carotti et al., 2004). Structural changes induced in the GAS1 protein after heating to 80°C were completely reversible upon cooling down to 20°C, a feat that is unusual for most enzymes.

The expression of both CHS and FKS1 has had very limited success in past studies, encountering many of the traditional problems associated with the purification of large membrane proteins. The exact biochemical mechanisms by which β-1,3-glucans and chitin are synthesised are still poorly understood. In many cases, kinetic assays have been performed using partially expressed proteins or crude extracts.

The β-1,3-glucan synthases complexes have been characterised almost exclusively in the yeast *S. cerevisiae*. The complex was shown to be composed of the catalytic subunit FKS1, a large enzyme (>200 kDa) with 16 transmembrane domains, and the RHO1 regulatory subunit that stimulates β-1,3-glucan synthase activity (Mazur et al., 1995; Inoue et al., 1999; Douglas, 2001). While extensively studied in yeast,

the β-1,3-glucan synthase complexes have been poorly analysed in filamentous fungi. The β-1,3-glucan synthase complexes of various *Aspergillus* species have been intermittently isolated in the past (Kelly et al., 1996; Beauvais et al., 2001) while the catalytic region of *Paracoccidioides brasiliensis* β-1,3-glucan synthase has been expressed in *E. coli* (Tomazett et al., 2010).

With seven classes of CHS, there is a large range of *Chs* genes present within a single fungal species, all requiring different reaction conditions for full function. Figure 5.1 shows the topology of the *Bgh* CHS enzymes, demonstrating the vastly different sizes and structures of all the different enzymes. The success rate of CHS purification has been quite limited, with several reports of unsuccessful attempts to purify active CHS from several different fungi (Durán and Cabib, 1978; Lending et al., 1991; Uchida et al., 1996). There have been reports of successful partial purifications of the *Wangiella dermatitidis* class V CHS as well as a small CHS from *Rhizopus oryzae* (Abramczyk and Szaniszlo, 2009; Salgado-Lugo et al., 2016). However, in both these cases the yield was low due to protein degradation and the formation of inclusion bodies, respectively.

The work in this chapter relates to attempts to heterologously express *Bgh* genes related to the synthesis of key cell wall polysaccharides, chitin and β-1,3-glucan (*GELA/B/C, FKS1* and *ChsI-VII*), and characterising their biosynthetic activity using *in vitro* biochemical assays.

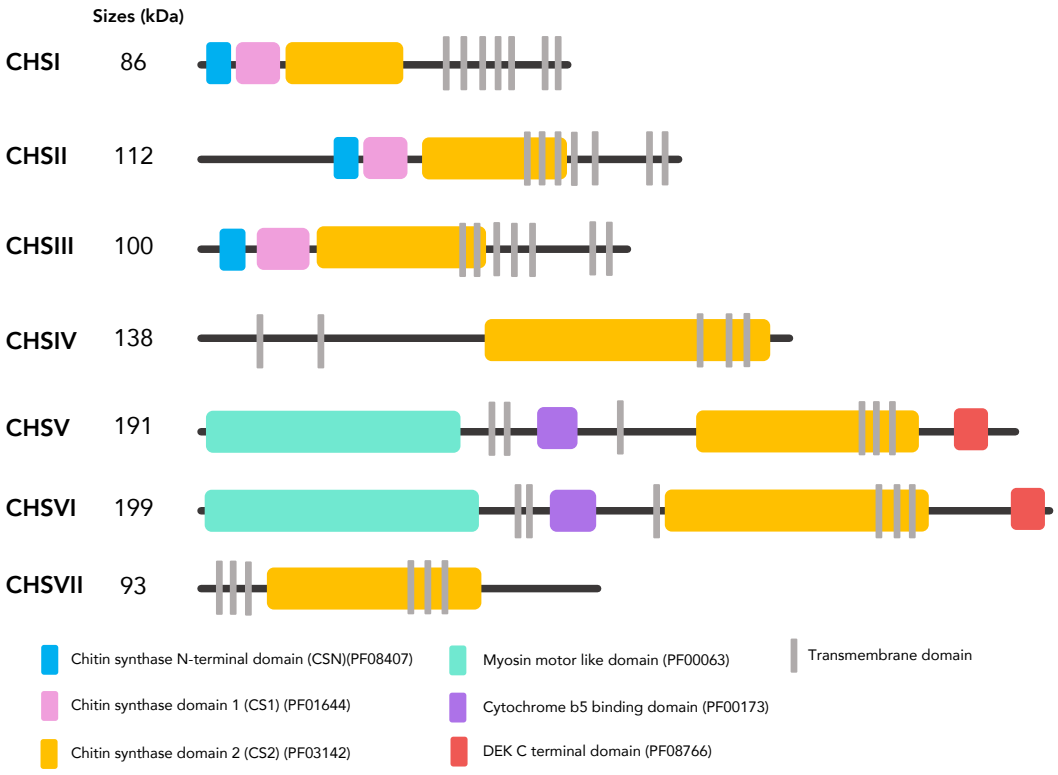

FIGURE 5.1: Domain organisation of the seven *Bgh* chitin synthase proteins. Each protein is named after its respective chitin synthase class.

5.2 Materials and Methods

5.2.1 Fungal material

A field isolate of *Bgh* was kindly donated by Professor Richard Oliver (Curtin University, W.A., Australia). The *Bgh* isolate was maintained on the highly susceptible *Hordeum vulgare* cultivar Baudin. *Bgh* was propagated by inoculating seven-day old Baudin seedlings with conidium from previously infected barley seedlings. The inoculated plants were then cultivated in a growth chamber with a 16 h photoperiod at 22°C for a week. *Bgh* conidia were collected by vacuuming the conidium directly from the plants through a 35 μm filter and captured on a 5 μm filter.

5.2.2 Cloning of target *Bgh* genes and sequence validation

One hundred mg of *Bgh* conidia were ground in liquid nitrogen with a mortar and pestle. Total RNA was extracted using the Plant Total RNA Kit (Sigma-Aldrich) as per the manufacturer's instructions. cDNA was synthesised from total RNA using the SuperScript® III Reverse Transcriptase (RT) enzyme (Life Technologies) following the manufacturer's protocol. Genes were amplified from cDNA using the Phusion® High-Fidelity PCR Master Mix (New England Biolabs) following the manufacturer's protocol using the gene specific primers listed in Table 5.1 and designed based on the *Bgh* DH14 genome (Spanu et al., 2010).

The PCR products were analysed by agarose gel electrophoresis. Gene fragments were excised from the gel and purified using the NucleoSpin® Gel and PCR Clean-up kit (Machery-Nagel GmbH & Co. KG) according to the manufacturer's instructions. The purified DNA fragments were cloned into the pCR8 plasmid and transformed into *Escherichia coli* using the pCR™8/GW/TOPO™TA Cloning Kit with One Shot™TOP10 Chemically Competent *E. coli* following the manufacturer's protocol (Figure 5.2). Plasmids were purified from positive colonies using the Isolate II Plasmid Mini Kit (Bioline) and digested in 20 μl with 0.5 μl of various restrictions enzyme and 1x reaction buffer at 37°C for 2 h. Restriction digests were analysed by 1% agarose gel electrophoresis. Positive plasmids were sent to AGRF Sanger Sequencing services (AGRF, Australia) with the sequencing primers listed in Table 5.2.

5.2.3 Subcloning and expression of target *Bgh* proteins in *E. coli*

Primers for the *GELA, B* and *C* genes were designed with overhang sequences corresponding to the pET3a plasmid vector (Figure 5.3 and Table 5.3). Two sets of

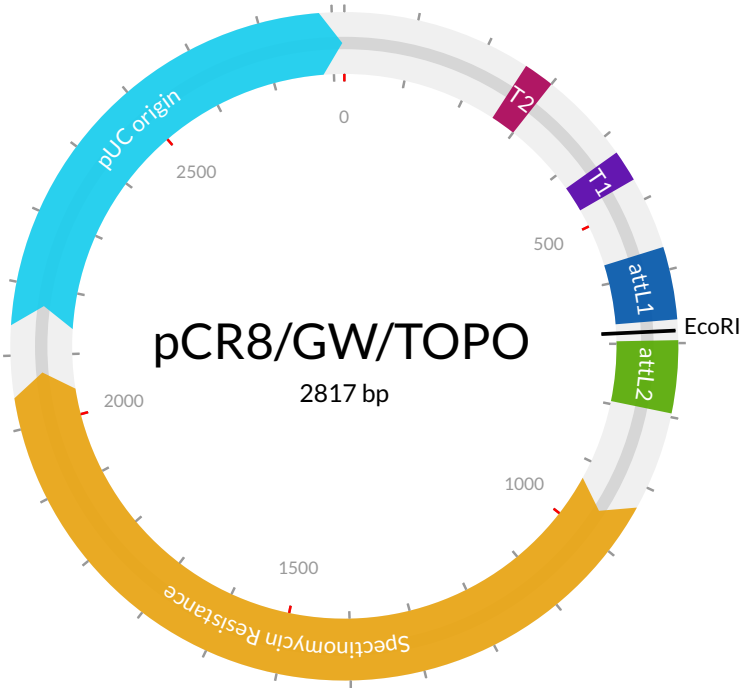

Comments for pCR8®/GW/TOPO®

*rrn*B T2 transcription termination sequence: 268-295
*rrn*B T1 transcription termination sequence: 427-470
M13 forward (-20) priming site: 537-552
*att*L1: 569-668
GW1 priming site: *607-631*
TOPO® recognition site 1: 678-682
TOPO® recognition site 2: 683-687
*att*L2: 696-795
GW2 priming site: 733-757
T7 Promoter/priming site: 812 (c)
M13 reverse priming site: 836-852
Spectinomycin promoter: 930-1063
Spectinomycin resistance gene (Spn^R): 1064-2074

FIGURE 5.2: pCR8/GW/TOPO cloning vector.

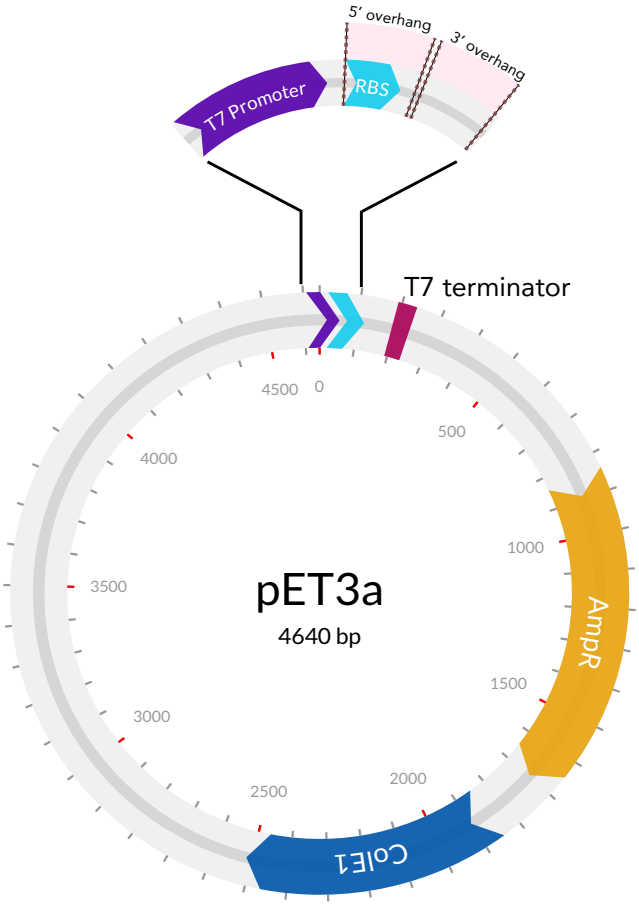

Comments for pET3a

T7 Promoter: 1-19
Ribosome binding site (RBS): 66-72
T7 gene 10 translater leader: 81-113
T7 terminator: 191-237
Ampicillin resistance ORF (Amp ^{R}): 840-1697
pBR322 origin of replication -type ColE1: 1848-2515

FIGURE 5.3: pET3a *E. coli* expression vector. The *Bgh GELA, GELB* and *GELC* genes were cloned into the pET3a vector to be expressed in *E. coli*. The vector does not contain any tags, so a 6xhis-tag was incorporated into the target genes during PCR amplification.

primers were designed for each gene, one set included a 5′ his-tag while the other set contained a 3′ his-tag. The genes were amplified from the relevant pCR8 vector, containing the sequence validated gene of interest, using the Phusion® High-Fidelity PCR Master Mix (New England Biolabs) following the manufacturer's protocol. The *GELA/B/C* genes were subcloned into the pET3a vector using the In-Fusion HD Cloning Plus Kit (Takara, USA) and transformed into One Shot™TOP10 Chemically Competent *E. coli* cells (Thermo Fisher Scientific) following the manufacturer's protocol. The plasmids were purified from positive colonies using the Isolate II Plasmid Mini Kit (Bioline) and digested in 20 μl containing 0.5 μl of various restriction enzymes and 1x reaction buffer at 37°C for 2 h. Restriction digests were analysed by 1% agarose gel electrophoresis. Positive plasmid screens were sent to AGRF Sanger Sequencing services (AGRF, Australia) with the sequencing primers listed in Table 5.2.

Verified plasmids were transformed into One Shot® BL21 Star™ (DE3) Chemically Competent *E. coli* cells (Thermo Fisher Scientific) and plated on lysogeny broth (LB) agar plates containing 100 μg/ml ampicillin. Plasmids were also transformed into BL21-CodonPlus(DE3) -RIL Competent Cells (Agilent Technologies) following the manufacturer's protocol. Isolated colonies were cultured in LB containing 100 μg/ml ampicillin at 37°C with shaking. Overnight cultures were used to seed 10 ml to an OD_{600} = 0.1. Cultures were grown at 37°C with shaking until an OD_{600} = 0.6 was reached. IPTG was added to a final concentration of 0.5 mM in the cultures to induce protein expression and the cultures were subsequently incubated overnight at 18°C with shaking.

5.2.4 Protein extraction and Western blot analysis

Cells were pelleted by brief centrifugation, resuspended in 100 μl xTractor™ Buffer (Takara) and left to lyse for 30 min. The samples were then centrifuged at 16,000g for 5 min. Aliquots of supernatant were taken and mixed with NuPAGE™ LDS Sample Buffer (4X) (Invitrogen). Proteins were prepared for electrophoresis by boiling for 3 min and then separated by SDS-PAGE in NuPAGE™ 4-12% Bis-Tris protein gels (Invitrogen).

Proteins were transferred from polyacrylamide gels to nitrocellulose membranes (0.2 μm) at 120 mA for 90 min. The membranes were submerged in blocking buffer [50 mM Tris-HCl, 150 mM NaCl, 0.5% (w/v) milk] for 1 h at room temperature. Membranes were washed three times in 1x TBS [50 mM Tris-HCl, 150 mM NaCl] for 10 min. The primary antibody [6xhis Monoclonal Antibody (Albumin Free) (Clontech)] was diluted 1:10,000 in 1x TBS and then incubated with the membranes for 1h at room temperature. This was followed by three consecutive 10 min washes with 1x TBS. The membranes were incubated with the secondary antibody [Anti-Mouse IgG (whole molecule)–Peroxidase antibody produced in goat (Sigma-Aldrich)] in a 1:10,000 dilution with 1x TBS for 1 h at room temperature. The

membranes were then washed three times in 1x TBS for 10 min and protein bands were visualised by rinsing the membranes with the BCIP®/NBT-Purple Liquid Substrate System for Membranes (Sigma-Aldrich).

5.2.5 Cloning and transformation of target *Bgh* proteins into *S. cerevisiae*

The transformation protocol was adapted from Drew et al. (2008). Primers for *ChsI-VII* and *Fks1* were designed with overhang sequences corresponding to the pDDGFP-2 plasmid vector (Figure 5.4 and Table 5.4). The primers were used to amplify the genes from the relevant pCR8 vectors, containing the gene of interest, using Phusion® High-Fidelity PCR Master Mix (New England Biolabs) following the manufacturer's protocol. PCR products were then purified using the PCR clean-up protocol from NucleoSpin® Gel and PCR Clean-up kit (Machery-Nagel GmbH & Co. KG). The pDDGFP-2 plasmid was linearised with *Sma*I, isolated by 1% electrophoresis, and then purified using the NucleoSpin® Gel and PCR Clean-up kit (Machery-Nagel GmbH & Co. KG).

A 250 ml culture of *S. cerevisiae* [BY4742 Δ*ChsI*Δ*ChsIII*Δ*pep* and BY4742 Δ*Fks1*] in YPD medium was grown at 30°C in an orbital shaker at 280 rpm until an OD_{600} = 0.6 was reached. The cells were then pelleted by centrifugation at 3,000g for 5 min at 4°C. The supernatant was discarded, and the cells were resuspended in 25 ml of ice-cold sterile milli-Q water. Centrifugation was repeated, and the cells were resuspended in 1 ml of ice-cold sterile 100 mM lithium acetate. The cell suspension was then centrifuged at 8,000g for 15 s and resuspended in 400 μl of 100 mM lithium acetate. 50 μl of the chemically competent yeast cells was then added to 240 μl of ice-cold 50% PEG 3350 and vortexed for 5 s. 50 μg of single stranded carrier DNA [Deoxyribonucleic acid sodium salt from salmon testes (Sigma-Aldrich)] was added to the mix and vortexed for 5 s. A 50 μl DNA mix [75 ng of *Sma*I-digested pDDGFP-2 vector, 750 ng PCR fragments] was added to the mix and vortexed for 5 s.

The mix was left to incubate for 30 min at 30°C and then heat shocked at 42°C for 25 min. Cells were then centrifuged at 8,000g for 15 s at room temperature, the supernatant was discarded, and the cells were resuspended in 100 μl of sterile milli-Q water. The cell suspensions were then plated on URA selective plates and incubated for 2-3 days at 30°C.

5.2.6 Expression and screening of *Bgh* target proteins in *S. cerevisiae*

The expression screening protocol was adapted from Drew et al. (2008). Positive colonies were culture in aerated tubes containing URA medium with 2% glucose overnight at 30°C and 280 rpm. Overnight cultures were diluted to an OD_{600} = 0.12

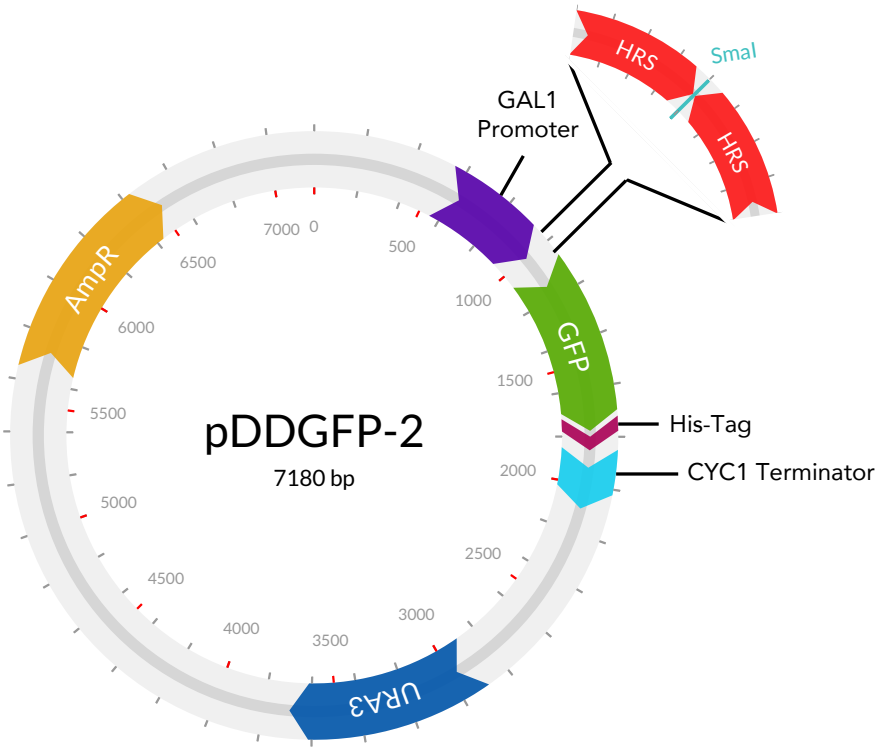

Comments for pDDGFP-2

GAL1 Promoter sequence: 551-1002
Homologous recombination site (HRS) 1: 1003-1032
Homologous recombination site (HRS) 2: 1036-1038
GFP tag: 1066-1776
His-Tag: 1777-1800
CYC1 Terminator: 1849-2101
URA3 Selection marker: 2890-3693
Ampicillin resistance gene (Amp ^{R}): 5652-6512

FIGURE 5.4: pDDGFP-2 *S. cerevisiae* expression vector. The *ChsI-VII* and *Fks1* gene fragments were incorporated into the pDDGFP-2 vector by homologous recombination during transformation. The recombination creates a construct that, when expressed, contains the *ChsI-VII* and *Fks1* proteins with a 3′ GFP and 6xhis-tag.

in URA medium with 0.1% glucose and grown at 30°C and 280 rpm until an OD_{600} = 0.6 was reached. Expression of the membrane protein-GFP fusion was induced by adding 20% galactose to a final concentration of 2% in the culture. Twenty-two h after induction, the cells were harvested by centrifugation at 3,000g for 5 min. The supernatant was removed, and the cells were resuspended in 200 μl of YSB [50 mM Tris-HCl pH 7.6, 5 mM EDTA, 10% glycerol, 1x cOmplete™, EDTA-free Protease Inhibitor Cocktail (Sigma-Aldrich)]. The cell suspension was transferred to a 1.5 ml tube along with glass beads and an additional 500 μl of YSB. Yeast cells were then lysed with a Retsch mill set at 30 Hz for 7 min at 4°C and 30 s intervals.

Unbroken cells were removed by centrifugation at 22,000g for 5 s at 4°C. The supernatant was transferred to a new tube and cell lysis was repeated with 500 μl of YSB. The supernatant was pooled together and centrifuged at 20,000g for 1 h at 4°C. The supernatant was discarded, and crude membrane pellets were resuspended in 50 μl of YSB. Fiften μl of crude membranes were combined with 15 μl sample buffer [50 mM Tris-HCl pH 7.6, 5% glycerol, 5 mM EDTA, 0.02% bromophenol blue, 4% sodium dodecyl sulphate (SDS), 50 mM dithiothreitol] and left to incubate for 5 min at 37°C.

Proteins were loaded for SDS-PAGE analysis on a Tris-glycine 4-15% Mini-PROTEAN TGX™ Precast Gel (Biorad). Gels were rinsed with milli-Q water and viewed by in-gel fluorescence upon exposure to a blue light set at 460 nm through a filter of 515 nm. The gels were stained overnight in Coomassie Brilliant Blue R in methanol (20%), ethanol (20%) and acetic acid (10%), and destained in the same solution devoid of the dye.

5.2.7 In-gel proteolysis and mass spectrometry

After SDS-PAGE, fluorescent protein bands were excised and hydrolysed with trypsin in-gel, and prepared for mass spectrometry (MS). After every step, gel fragments were centrifuged at 1,000 rpm for 1 min and the solution was removed. Gel fragments were cut into smaller pieces and reduced in 200 μl reduction buffer [10 mM dithiothreitol (DTT), 50 mM ammonium bicarbonate (NH_4HCO_3)] for 1 h at 56°C. Proteins then underwent alkylation [55 mM indole-3-acetic acid (IAA), 50 mM NH_4HCO_3] for 45 min in the dark at room temperature and the gel fragments were washed with 200 μl 5 mM NH_4HCO_3. The samples were then dehydrated with 200 μl dehydration buffer [50% 5 mM NH_4HCO_3, 50% ACN] for 15 min and the procedure was repeated. Twenty-five μl trypsin solution [10 ng/μl trypsin, 5 mM NH_4HCO_3] was added and left for 15 min on ice. An additional 20 μl of 5 mM NH_4HCO_3 was added and proteins were left to digest at 37°C for 16 h. The samples were acidified with 5 μl of 5% formic acid (FA) and proteins were extracted with 50 μl of 1% FA, the samples were sonicated for 30 min and the solution was transferred to another tube. This was then repeated a second time. A third extraction was done with [50% ACN, 49% H_2O, 1% FA] and sonicated for 30 min. Fifty μl of 100% ACN

was added to the gel fragments and sonicated for 15 min, the solution was removed and transferred to another tube and the steps were repeated. The pool of peptide extracts was then lyophilised and sent to Adelaide Glycomics (Australia) to run on the MS to identify the peptides.

5.2.8 Preparation of solubilised membrane fractions for chitin synthase assays

Isolated colonies with verified expression were cultured in flasks containing URA medium with 2% glucose overnight at 30°C and 280 rpm. Overnight cultures were diluted to an OD_{600} = 0.12 in 1L of URA medium with 0.1% glucose and grown at 30°C and 280 rpm until an OD_{600} = 0.6 was reached. Expression of the membrane protein-GFP fusion was induced by adding 20% galactose to a final concentration of 2% to the culture. Twenty-two h after induction, the cells were harvested by centrifugation at 4,000g for 10 min at 4°C. The supernatant was decanted, and yeast pellets were frozen with liquid nitrogen and stored at -80°C for future use.

Yeast pellets were resuspended in 25 ml of CRB [50 mM Tris-HCl pH 7.6, 1mM EDTA, 600 mM sorbitol, 1x cOmplete™, EDTA-free Protease Inhibitor Cocktail (Sigma-Aldrich)] per litre of original culture. The cell suspension was poured into a bead homogeniser and lysed on ice for 10 min at 30 s intervals. Unbroken cells and debris were removed by centrifugation at 10,000g for 10 min at 4°C and filtered through Miracloth.

The cell lysate was then centrifuged at 150,000g for 2 h at 4°C. The supernatant was discarded, and the pellet was resuspended to a final volume of 6 ml/L of original culture in MRB [10 mM Tris-HCl pH 7, 10% glycerol, 1x cOmplete™, EDTA-free Protease Inhibitor Cocktail (Sigma-Aldrich)] using a 10 ml syringe with a 21-gauge needle. Protein concentration was determined using a Qubit fluorometer and adjusted to 3 mg/ml. Proteins were then incubated on ice with 0.5% digitonin and gentle agitation for 30 min. The solution was centrifuged at 150,000g for 30 min at 4°C and the supernatant was used for activity assays.

5.2.9 His-tagged protein purification

The initial protein purification follows the same method as described above, however the protein pellet after ultracentrifugation is resuspended in SEW buffer [10 mM PBS pH 7.4, 150 mM NaCl, 30 mM imidazole, 10% glycrol, 1x cOmplete™, EDTA-free Protease Inhibitor Cocktail (Sigma-Aldrich)]. After solubilisation in digitonin and centrifugation, the solution was added to 5 ml of Ni-NTA His•Bind® Resin (Merck) with gentle agitation at 4°C for 2-3h (or overnight).

The slurry was poured into a glass Econo-Column (Biorad) and the solution was allowed to flow through. The column was then washed with 100 ml/L original culture of SEW buffer + 0.1% digitonin. Fusion proteins were eluted with 30 ml

of elution buffer [SEW Buffer, 180 mM imidazole, 0.05% digitonin]. The proteins were concentrated down using an Amicon Ultra-15 30K Centrifugal Filter Device (Millipore) at 4,000g at 4°C. When the volume was 200-500 μl, 15 ml of exchange buffer [10 mM Tris-HCl pH 7, 10% glycerol, 0.05% digitonin, 1x cOmplete™, EDTA-free Protease Inhibitor Cocktail (Sigma-Aldrich)] was added and the samples were centrifuged in the same conditions until the desired volume was reached. Concentrated proteins were then used for activity assays.

5.2.10 Chitin synthase activity assay

Chitin synthase activity assays were performed as described previously (Bulone et al., 1992). Briefly, 10-50 μl of enzyme preparation was added to the reaction buffer [10 mM Tris-HCl pH 7.4, 10 mM $MgCl_2$, 20 mM *N*-acetyl-D-glucosamine, 1 μg/ml trypsin, 0.5 mM UDP-*N*-acetyl-D-glucosamine, 434 nM *N*-acetyl-D-[U$-^{14}$C]-glucosamine (300 mCi/mmol) or UDP-*N*-acetyl-D-[1$-^{14}$C]glucosamine (55 mCi/mmol) (American Radiolabelled Chemicals, Inc., USA)] to a final volume of 200 μl. The reaction was incubated at room temperature overnight and stopped with 400 μl of ethanol for ethanol-insoluble carbohydrates and 300 μl of chloroform for ethanol-soluble carbohydrates.

The method used to recover the radioactive carbohydrates synthesised was as previously described (Brown et al., 2012). To measure the formation of ethanol-insoluble carbohydrates, samples were left to precipitate for 2 h at -20°C and the insoluble polysaccharides were recovered on Whatman GF/C glass fibre filters and washed successively with 66% ethanol, water, and 66% ethanol. To measure the formation of ethanol-soluble carbohydrates, reaction mixutres were centrifuged for 10 min at 13,000g and the upper phases containing the water-soluble radioactive products were collected. The aqueous phases were loaded onto anion-exchange mini-columns which were washed successively with 60 μl, 125 μl, and 310 μl of ultra-pure water and the eluates were collect in scintillation vials placed under the mini-columns. The incorporation of radioactivity was quantified by liquid scintillation counting and enzyme activity was expressed as nmol of GlcNAc incorporated per mg of protein.

5.3 Results

5.3.1 Expression of GEL proteins in *E. coli*

The putative *GELA/B/C* genes were cloned from *Bgh* cDNA using primers designed from the *Bgh* DH14 genome (Spanu et al., 2010). Sequencing results revealed that the cloned *GELA/B/C* genes matched the consensus sequences from the genome. The *GELA/B/C* genes were then inserted into the pET3a expression vector with a 6xhis-tag on 5′ and 3′ end of the genes on two separate constructs (Figure 5.6 (A, B)). Restriction enzyme digestion of the plasmids and additional sequencing showed that the correct genes were inserted into the vector (Figure 5.6 (C)).

Constructs were initially transformed into BL21 Star (DE3) (Thermo Fisher Scientific) *E. coli* for expression. Expression of the GEL proteins was induced in *E. coli* by the addition of IPTG, a lactose analogue, to the culture media and analysed by western blot. The size of the GELA/B/C proteins were expected to be 47 kDa, 55 kDa and 57 kDa, respectively. However, no visible bands were observed in the induced samples for any of the *GEL* genes (data not shown). Following this, a range of induction temperatures (16°C, 25°C, and 37°C) and IPTG (0.05-1 mM) concentrations were tested and the LB medium was exchanged for terrific broth (TB). None of the different conditions tested led to visible protein expression (data not shown).

Expression vectors were subsequently transformed into the codon optimised BL21-CodonPlus(DE3) *E. coli* strain (Agilent Technologies) due to the presence of a few rare codons found in the *Bgh GEL* sequences. In spite of this, protein expression was not detected at all. Using the same range of induction conditions as previously mentioned the proteins failed to appear under western blot analysis (data not shown).

5.3.2 Expression of chitin synthases and β-1,3-glucan synthase in *S. cerevisiae*

Putative *ChsI-VII* and *Fks1* genes were cloned from *Bgh* cDNA using primers designed from the *Bgh* DH14 genome (Spanu et al., 2010). Sequencing results revealed that the genes matched the consensus sequence from the genome (data not shown). The linearised pDDGFP-2 expression vector and amplified genes with pDDGFP-2 overhangs were transformed into the *S. cerevisiae* expression strains (Figure 5.7). Successful transformants were generated for *ChsI, ChsIV, ChsVI* and *ChsVII*. Despite repeated transformations with the other genes, there were no visible colonies on any of the plates.

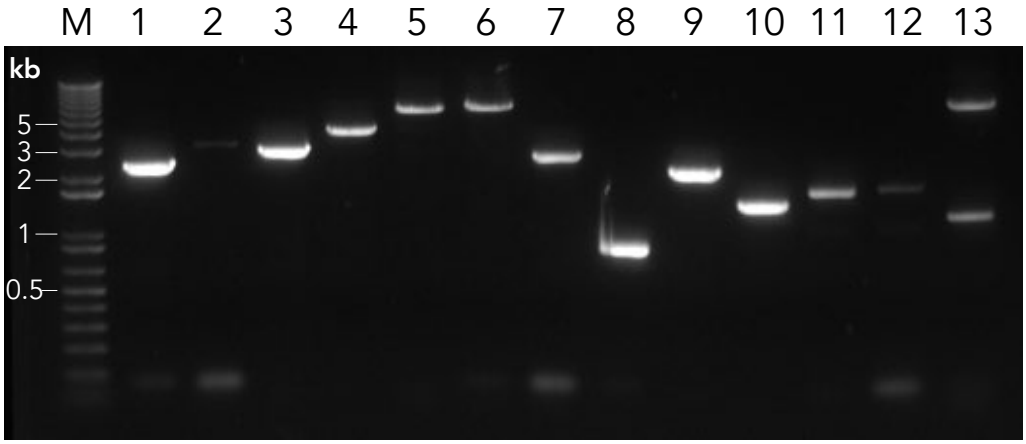

FIGURE 5.5: PCR products of cell wall related genes amplified from *Bgh* cDNA. M: DNA molecular size markers, 1: *ChsI* (2.3 kb), 2: *ChsII* (3.0 kb), 3: *ChsIII* (2.7 kb), 4: *ChsIV* (3.7 kb), 5: *ChsV* (5.1 kb), 6: *ChsVI* (5.4 kb), 7: *ChsVII* (2.5 kb), 8: *KRE9* (0.7 kb), 9: *KRE6* (2.0 kb), 10: *GELA* (1.3 kb), 11: *GELB* (1.5 kb), 12: *GELC* (1.6 kb), 13: *Fks1*. (6.0 kb)

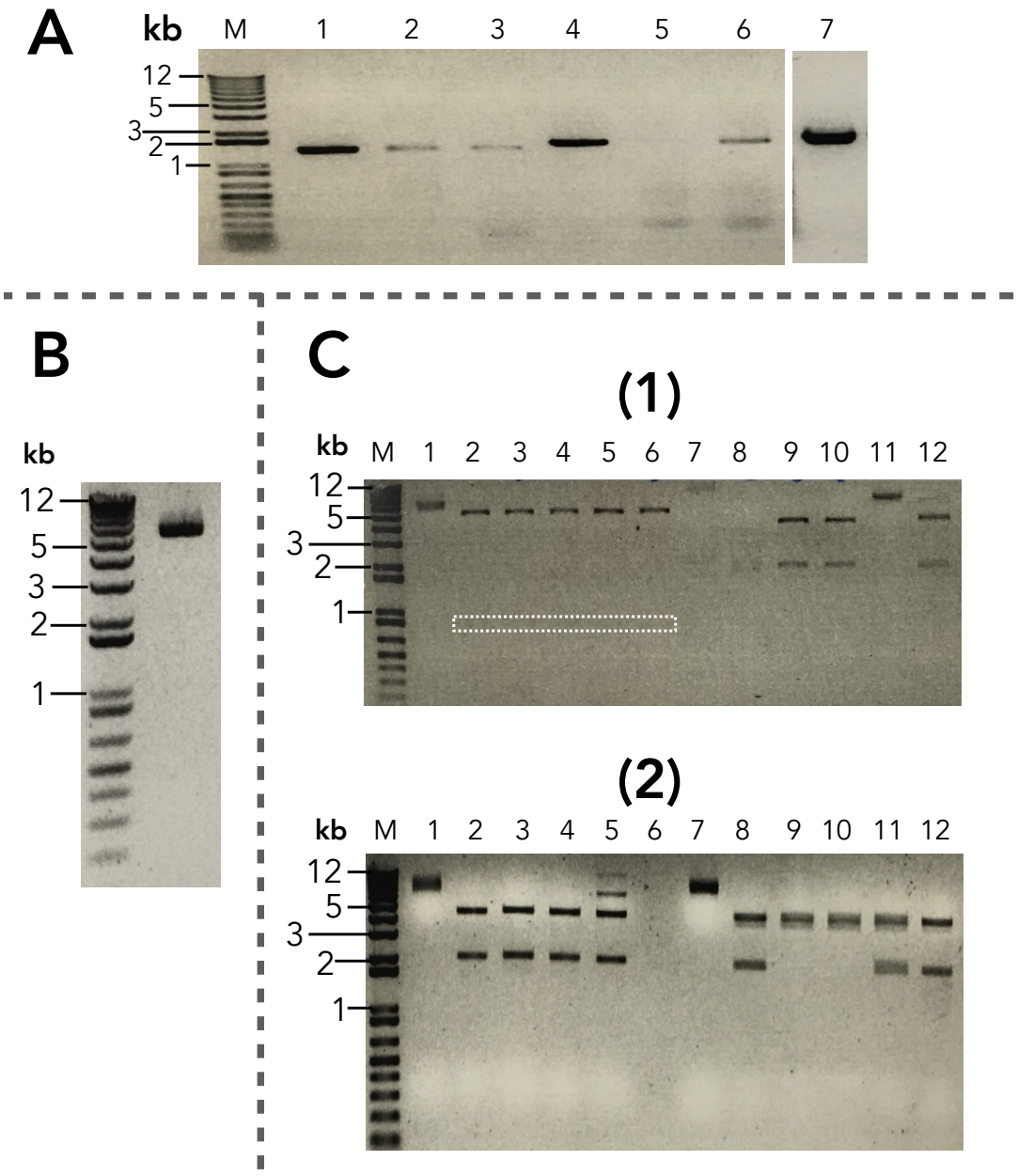

FIGURE 5.6: **(A)** Agarose gel containing PCR amplififed *GELA/B/C* products incorporating pET3a overhang sequences for In-Fusion. 1: *GELA* PCR product (+ve control), 2: *GELA* overhang PCR + 5′ 6xhis-tag, 3: *GELA* overhang PCR + 3′ 6xhis-tag, 4: *GELB* PCR product (+ve control), 5: *GELB* overhang PCR + 5′ 6xhis-tag, 6: *GELB* overhang PCR + 3′ 6xhis-tag. 7: *GELB* overhang PCR + 5′ 6xhis-tag. **(B)** Agarose gel loaded with linearised pET3a plasmid. **(C)** Restriction digestion verification of *GELA/B/C* gene inserts into the pET3a vector. (1) Faint bands are present in lanes 2-6 in the outlined section. 1: (-) pET3a-*GELA*, 2-3: (+) pET3a-*GELA* 5′, 4-6: (+) pET3a-*GELA* 3′, 7: (-) pET3a-*GELB* 5′, 8: (-) pET3a-*GELB* 5′, 9-10: (+) pET3a-*GELB* 3′, 11: (-) pET3a-*GELC* 5′, 12: (+) pET3a-*GELC* 5′. (2) 1: (-) pET3a-*GELB* 5′, 2-5: (+) pET3a-*GELB* 5′, 6: (-) pET3a-*GELC* 5′, 7-8: (+) pET3a-*GELC* 3′, 9-11: (+) pET3a-*GELC* 5′. 5′, 6x-his-tag at the 5′ end. 3′, 6x-his-tag at the 3′ end. (-), undigested plasmids, (+), digested plasmids. *GELA* plasmids were digested with *Nru*I, *GELB* plasmids were digested with *Cla*I and *GELC* plasmids were digested with *Sph*I. M: DNA molecular markers.

Expression of the recombinant proteins was induced in *S. cerevisiae* by the addition of galactose to the culture medias. After 22 h protein expression can be visually confirmed by the green fluorescence of the GFP tag under blue light box (460 nm) through a 515 nm filter. To confirm that the proteins were whole and the correct size, several colonies corresponding to each gene were screened by running crude extracts from induced cultures on an SDS-PAGE gel and viewed by in-gel fluorescence.

The expected sizes of the CHSI, CHSIV, CHSV CHSVI and CHSVII are 86 kDa, 138 kDa, 199 kDa, 191 kDa, and 93 kDa, respectively. However, the GFP tag adds an additional 28 kDa to the total protein size. The in-gel fluorescence experiments all showed bands corresponding to the predicted protein sizes, except for CHSV, along with a constant autofluorescence band observed in all samples at approximately 70 kDa (Figure 5.8).

Despite the positive colonies and the visible green fluorescence visible in the culture medium of the induced CHSV colonies, no bands were seen in the SDS-PAGE gel. The CHSIV and CHSVI bands were quite faint on the gels, indicating low protein expression levels. The low expression is likely due to the size of the proteins as they are both quite large compared to the other proteins. For example, CHSI and CHSVII have stronger bands, and have much smaller predicted protein sizes. With one of the induced CHSIV colonies there was an extremely dark band at approximately 30 kDa instead of the expected 166 kDa band. The culture from this colony was far brighter than any other cultures. At first it was thought that it was a transformant displaying high levels of expression, however the band is the same size as a single GFP protein and may have resulted from a re-ligation of the pDDGFP-2 vector without an insert, resulting in the expression of GFP only.

Fluorescent protein bands were excised from the gels and analysed by MS to confirm the presence of peptides from the target protein. The sequence coverage for the CHSI, CHSVI and CHSVII was quite low, with approximately 7% coverage (data not shown). On the other hand, CHSIV peptides were not detected at all. As the protein samples were crude *S. cerevisiae* protein extracts, there was an abundance of other proteins mixed into the excised gel fragments that diluted the already small amount of fusion proteins. The absence of CHSIV peptide fragments was probably due to a low quantity of fusion protein rather than an absence of protein (Figure 5.8 (B)).

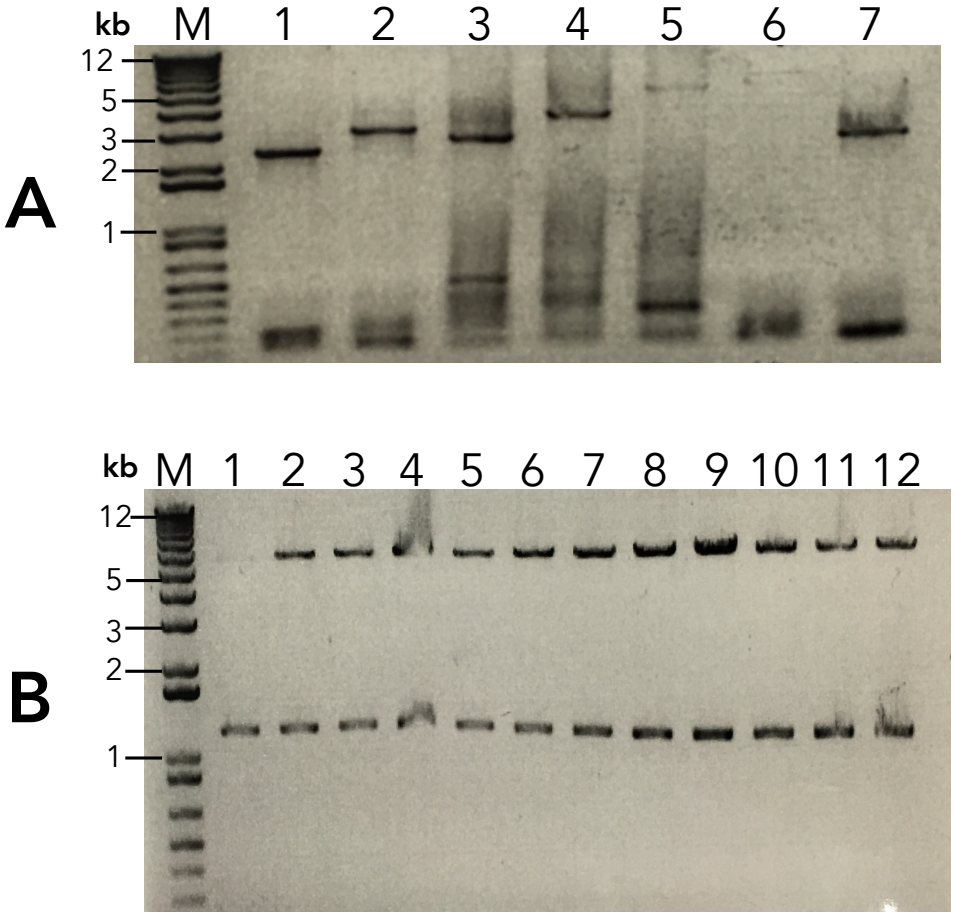

FIGURE 5.7: Agarose gel containing PCR amplified *ChsI-VII* and *Fks1* incorporating overhang homologous recombination site sequences for the pDDGFP-2 vector. **(A)** 1: *ChsI* (2.3 kb), 2: *ChsII* (3.0 kb), 3: *ChsIII* (2.7 kb), 4: *ChsIV* (3.7 kb), 5: *ChsV* (5.1 kb), 6: *ChsVI* (5.4 kb), 7: *ChsVII* (2.5 kb). **(B)** Temperature gradient of *Fks1* PCR (6.0 kb), ranging from 60-71°C. M, DNA molecular markers.

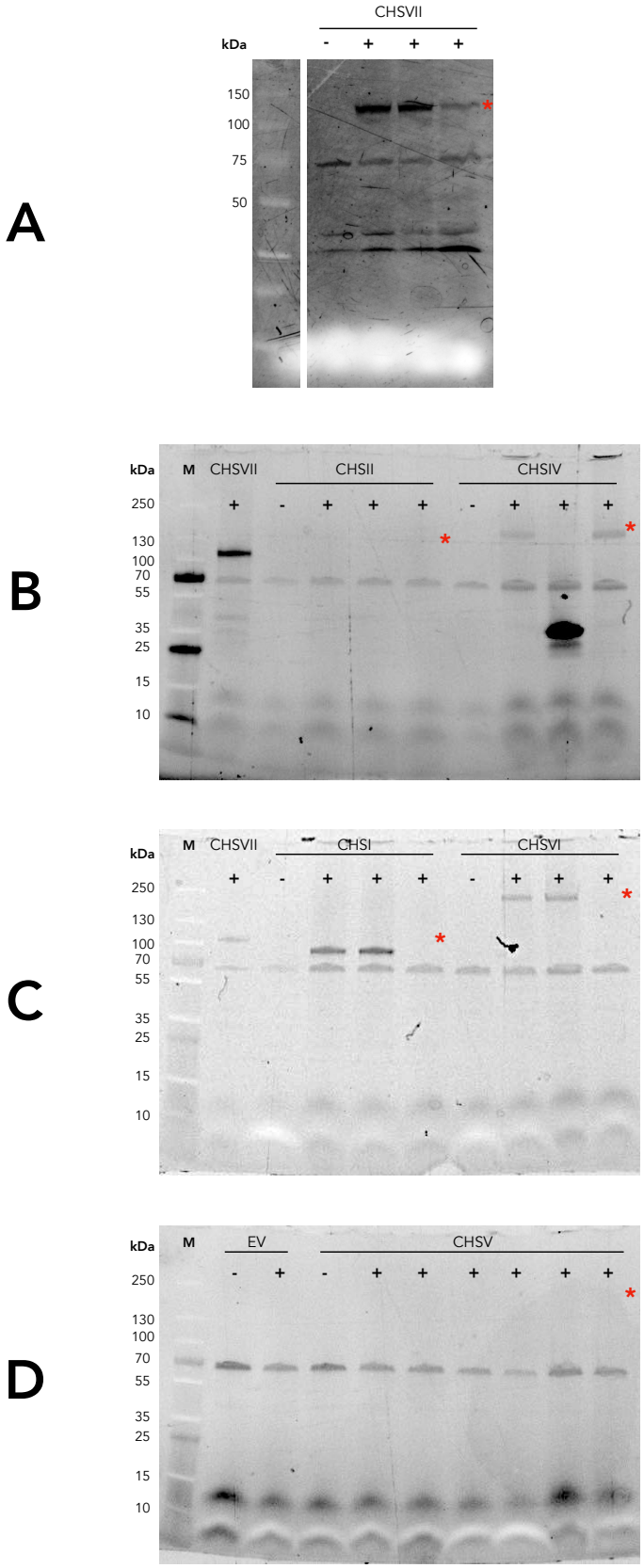

FIGURE 5.8: In-gel fluorescence screenings of CHS-GFP fusion protein expressed in *S. cerevisiae*. **(A)** CHSVII (120 kDa). **(B)** CHSII (139 kDa) and CHSIV (165 kDa). **(C)** CHSI (113 kDa) and CHSVI (226 kDa). **(D)** CHSV. M, protein molecular markers. EV, empty vector control. (-) protein expression is not induced. (+) protein expression is induced with 2% galactose.

5.3.3 Activity of solubilised membrane fractions in chitin synthase assays

Chitin synthase activity was determined through the use of a radiolabelled nucleotide sugar substrate. Chitin is a linear polymer of β-1,4-*N*-acetylglucosamine. By measuring the incorporation of radioactive linked GlcNAc from the nucleotide sugar substrate, UDP-[^{14}C]GlcNAc, the activity of the chitin synthase proteins can be measured. Protein activity was evaluated using detergent-solubilised membrane fractions and measuring the ethanol-soluble chitooligosaccharides and the ethanol-insoluble chitin polymers. Background levels of chitin synthase activity were normalised against extracts from *S. cerevisiae* transformed with an empty pDD plasmid.

In order to learn the techniques and methods required for *S. cerevisiae* yeast transformation, protein purification, and the chitin synthase activity assay, I visited the Division of Glycoscience at the Royal Institute of Technology (KTH) where the technique had already been established. After two months I returned to our Adelaide based laboratory to establish the techniques and study the *Bgh* CHS proteins.

Initial activity assays done at KTH for ethanol-insoluble products with CHSIV and CHSVII extracts displayed a low level of activity (Figure 5.9 (A)). However, subsequent activity assays back at our Adelaide based laboratory could not repeat the initial activity detected in CHSIV and CHSVII (data not shown for CHSIV) (Figure 5.9 (B)). The CHSVI also displayed no signs of activity in any of the assays. The only protein that exhibited consistently high levels of activity was CHSI (Figure 5.9 (B)).

It is standard to add trypsin to chitin synthase activity assays as most CHS proteins can be activated by proteolysis, however not all CHS proteins require activation by proteolysis (Ruiz-Herrera et al., 1997, 1992). To ascertain whether or not the *Bgh* CHSI requires proteolysis activation, assays were conducted with and without trypsin. From this, it was found that the CHSI activity was higher when trypsin was not present (Figure 5.9 (C)), therefore no trypsin was added in subsequent experiments.

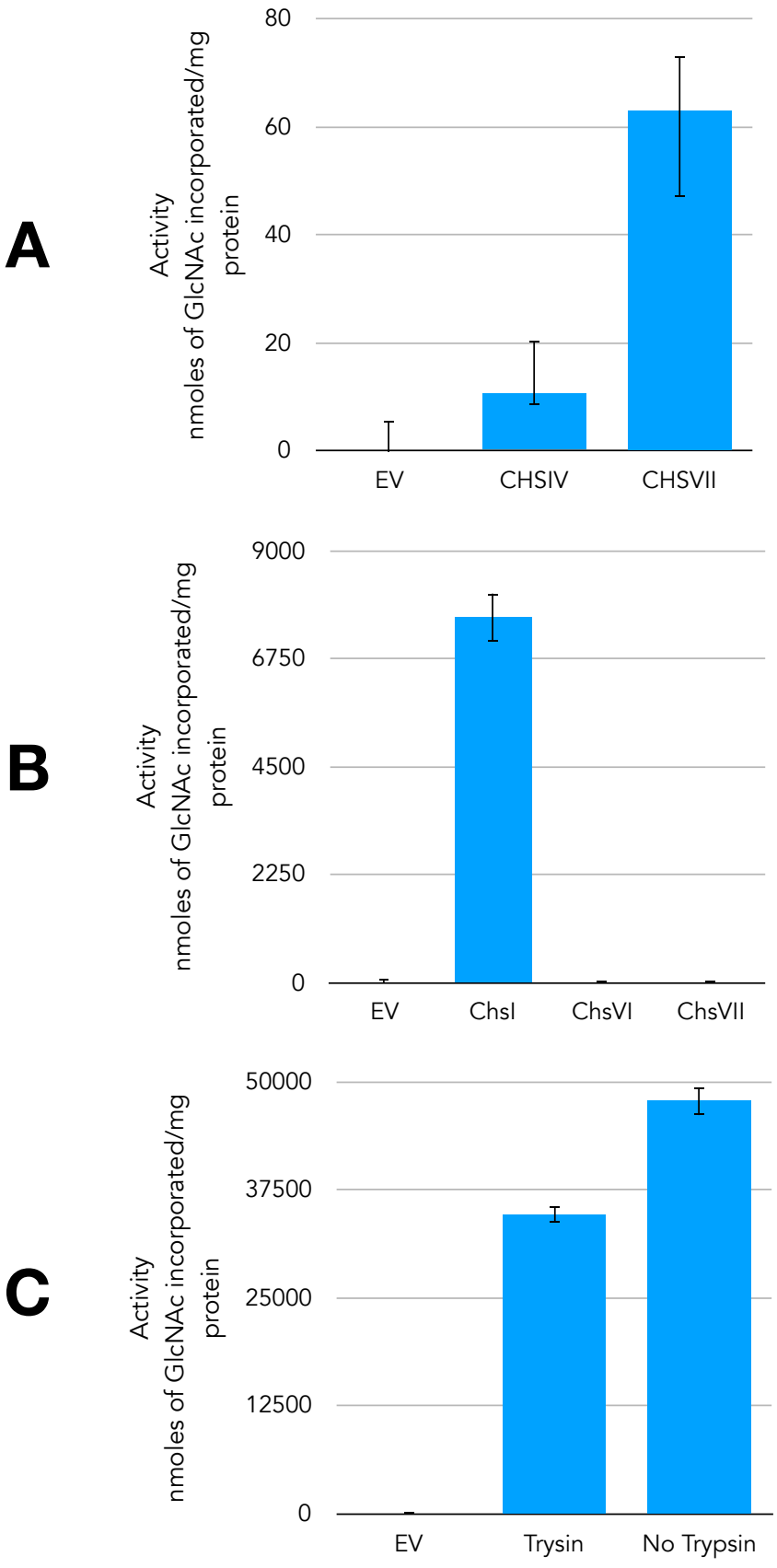

FIGURE 5.9: Caption on the following page.

FIGURE 5.9: Chitin synthase assays conducted on solubilised membrane fractions of recombinant *Bgh* CHS. **(A)** CHSIV and CHSVII synthase assays. **(B)** CHSI, CHSVI and CHSVII synthase assays. **(C)** CHSI in the absence and presence of trypsin. All negative controls are a microsomal membrane preparation from *S. cerevisiae* containing an empty pDDGFP-2 vector (EV). Chitin synthase activity was assayed in the presence of ^{14}C-labelled UDP-GlcNAc. Data are given as means of three replications $\pm$ SD.

5.3.4 Purification of *Bgh* CHSI

In order to carry out biochemical assays, pure CHSI enzyme is required. Purification of the 6xhis-tagged CHSI-GFP fusion proteins was attempted using affinity chromatography. The histidine tagged protein would bind to the chelating nickel resin, which allows the separation and purification of the protein. Unbound proteins would be washed through the column and the bound 6xhis-tagged CHSI proteins would be eluted from the column with high concentrations of imidazole (180 mM). Throughout the purification process, aliquots of proteins were taken to track the CHSI through fluorescent measurements using a real time PCR thermo cycler (Utermark and Karlovsky, 2006) (Figure 5.10).

Protein elutions were concentrated using a molecular weight cutoff centrifugal filter (Amicon) and quantified by measuring the GFP fluorescence. Fluorescent measurements of the concentrated purified product did not show any sign of the protein being present (Figure 5.10 (A)) and in-gel fluorescence of the purified protein did not display any visible enrichment of the CHSI protein (Figure 5.11).

As the CHSI protein purification failed, there were many points of the purification process to examine to determine where the protein was being lost. A common point of failure is the protein failing to bind to the Ni-NTA resin or binding so weakly that the protein is eluted off during the washing step with weak imidazole. While fluorescent measurements indicated that there was a fluorescent protein present within the flow through and wash solutions (Figure 5.10), subsequent SDS-PAGE and activity assays revealed that the CHSI protein was in neither of these fractions. Following this, another possible scenario is that the CHSI protein was binding too strongly to the Ni-NTA resin and was not eluting. To test this, proteins were eluted with 500 mM imidazole. Fluorescent measurements of the purified fraction were unable to detect any protein, however an activity assay revealed that an incredibly small amount of CHSI protein was present in the purified product (data not shown).

As the purification process was initially conducted over a two-day period, it is possible that the extended purification time was causing the CHSI protein to degrade. To modify this, the solubilised fraction was mixed with the Ni-NTA resin for 2-3h, instead of overnight, shortening the purification process to one day. A visibly enriched band matching the size of CHSI-GFP was seen in the purified product with in-gel fluorescence (Figure 5.12, lane 8) and there was a sufficient amount of protein to be detected by fluorescence (Figure 5.10 (B)). Activity assays with the purified CHSI showed high levels of activity (Figure 5.13 (day 1)). The purified CHSI protein was stored at -20°C and was able to maintain activity after one month of frozen storage (Figure 5.13 (30 days)).

The total amount of purified protein was extremely low (16 μg from 1 L of culture). It was suspected that fungal proteases released during the lysis process were affecting the yield of the purification. Phenylmethane sulphonyl fluoride (PMSF) was added

(0.5 mM) to all the buffers while 1 mM of EDTA and EGTA was included in the lysis buffer. PMSF is an inhibitor of serine proteases while EDTA and EGTA inhibit metalloproteases. Purification with these additives appeared to have a negative effect on the whole process. Not only did the protein fail to purify, but the solubilised protein fraction showed no activity.

Another method to remove proteases is through washing during membrane preparation. The membrane fraction would be repeatedly washed in a high salt buffer [1 M NaCl, 50 mM Tris-HCl pH 7.6, 1mM EDTA, 600 mM sorbitol, 1x cOmplete™, EDTA-free Protease Inhibitor Cocktail (Sigma-Aldrich)] prior to the solubilisation step to wash out the proteases. However, this method also negatively affected the purification process and failed to yield any product. A different lysing method was also tested. Yeast pellets were ground in liquid nitrogen (N_2) for 2 h, resuspended in CRB and the protein was purified. This method also failed to enrich the CHSI protein.

Recombinant CHSI fusion proteins were able to be purified when the purification process was done within one day and eluted with 500 mM imidazole, however the total amount of protein recovered from a 1L cell culture was not sufficient enough to carry out a full enzyme kinetic analysis. Attempts to enrich the protein further failed to improve the yield and often had a negative impact on the process.

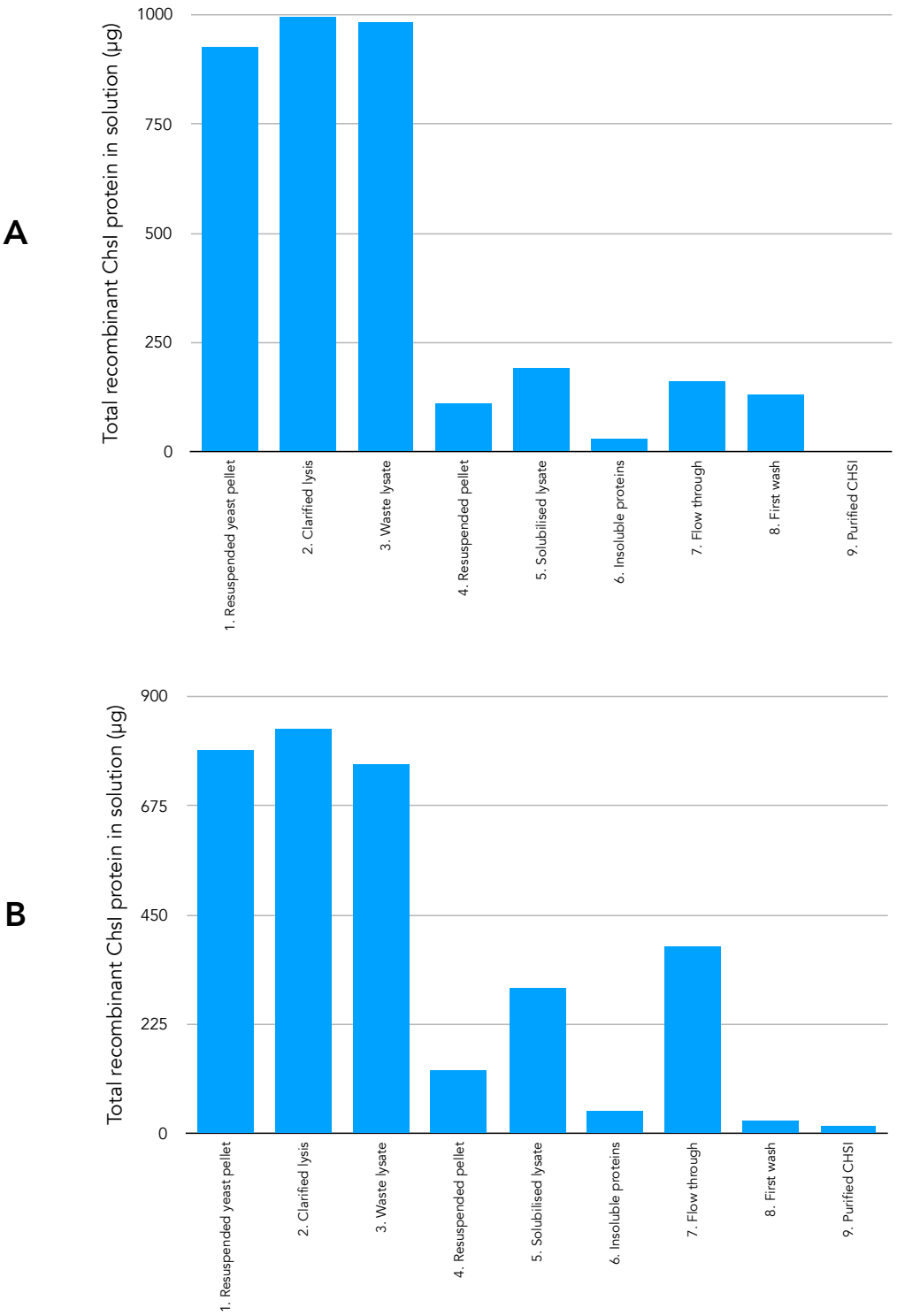

FIGURE 5.10: Total recombinant CHSI present in solutions throughout the purification process calculated from fluorescence measurements of GFP. (A) CHSI purification process over the course of two days. (B) CHSI purification process in a single day. 1, 1L yeast pellet resuspended in lysis buffer. 2, Clarified solution after cell lysis. 3, Waste lysate after ultracentrifugation of membrane proteins. 4, Membrane proteins resuspended. 5, Solubilised membranes after ultracentrifugation. 6, Insoluble protein fraction. 7, Flow-through of proteins after Ni-NTA incubation. 8, First column wash. 9, Purified CHSI.

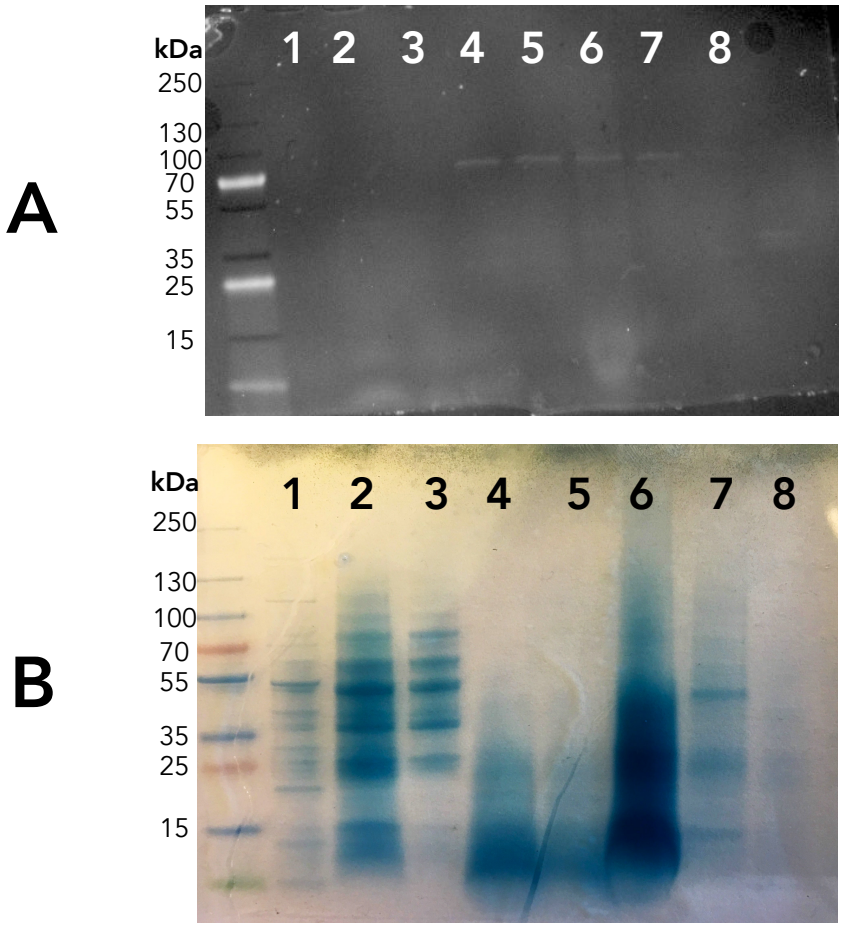

FIGURE 5.11: SDS-PAGE gel as analysed by in-gel fluorescence (A) and Coomassie staining (B) for the purification of CHSI conducted over two days. 1, Stained protein ladder (B). 2, Clarified solution after cell lysis. 3, Waste lysate after ultracentrifugation of membrane proteins. 4, Membrane proteins resuspended. 5, Solubilised membranes after ultracentrifugation. 6, Insoluble protein fraction. 7, Flow-through of proteins after Ni-NTA incubation. 8, Purified CHSI. The expected size of the CHSI-GFP protein is 113 kDa. The band present at 70 kDa is an autofluorescent protein band from the *S. cerevisiae* and not the expressed protein.

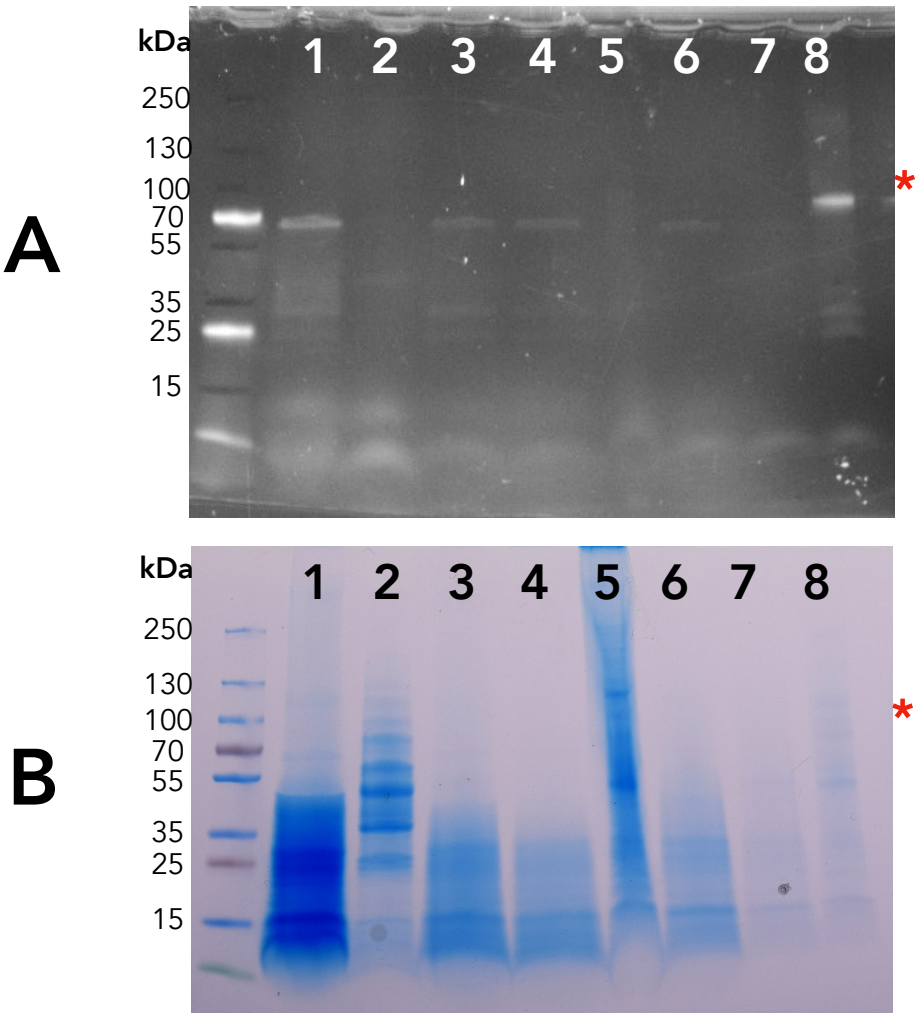

FIGURE 5.12: SDS-PAGE gel as analysed by in-gel fluorescence (A) and Coomassie staining (B) for the purification of CHSI conducted within one day. 1, Clarified solution after cell lysis. 2, Waste lysate after ultracentrifugation of membrane proteins. 3, Membrane proteins resuspended. 4, Solubilised membranes after ultracentrifugation. 5, Insoluble protein fraction. 6, Flow-through of proteins after Ni-NTA incubation. 7, First column wash. 8, Purified CHSI. The expected size of the CHSI-GFP protein is 113 kDa. The band present at 70 kDa is an autofluorescent protein band from the *S. cerevisiae* and not the expressed protein.

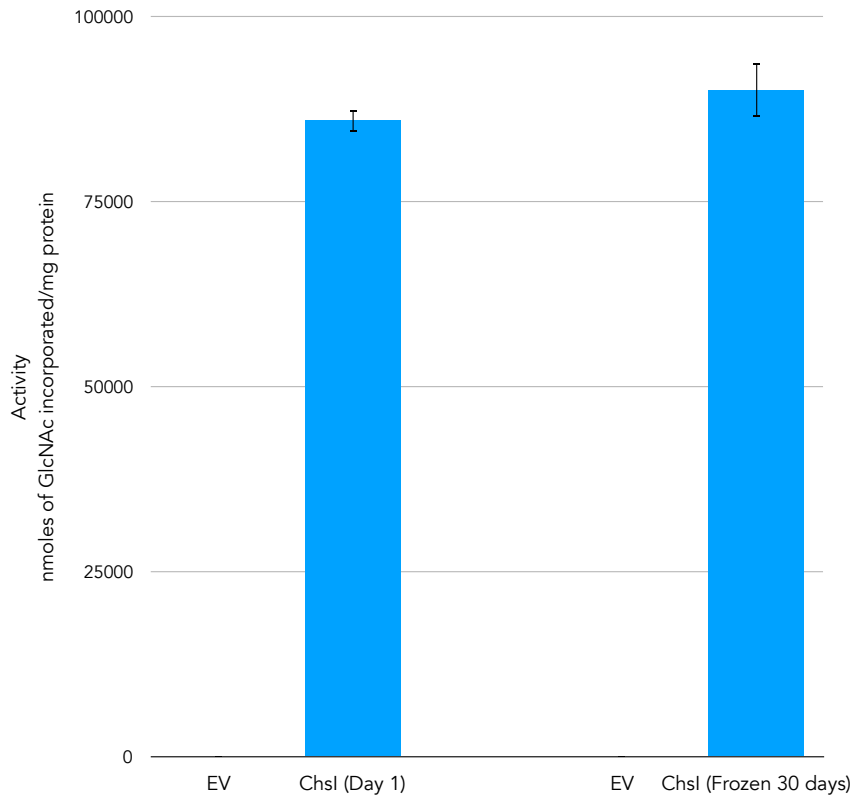

FIGURE 5.13: Purified *Bgh* CHSI activity assay. The first assay was done straight after purification (day 1) while the second assay was performed on purified CHSI that had been stored at -20°C for one month (frozen 30 days). The negative control corresponds to a purification from *S. cerevisiae* containing an empty pDDGFP-2 vector (EV). Chitin synthase activity was assayed in the presence of ^{14}C-labelled UDP-GlcNAc. Data are given as means of three replications $\pm$ SD.

5.4 Discussion

Despite all the information accumulated about the fungal cell wall structure, the enzymes and processes responsible for cell wall synthesis and remodelling remain largely unknown. In an effort to understand the mechanisms involved in *Bgh* cell wall assembly and maintenance, enzymes involved in β-glucan and chitin biosynthesis were heterologously expressed.

5.4.1 Heterologous expression of *Bgh* FKS1 and GEL proteins

In order to undertake a biochemical characterisation of enzymes involved in β-1,3-glucan synthesis and remodelling, the *Bgh GELA/B/C* gene sequences were isolated and expressed in *E. coli* while *Fks1* was expressed in *S. cerevisiae*. However, all of the *GELA/B/C* genes failed to express protein. Modifications to the induction conditions failed to remedy the situation, while *Fks1* failed to even transform into *S. cerevisiae*.

Protein toxicity has been known to arise in *E. coli*, as some recombinant proteins can detrimentally affect cellular function in the host cell (Rosano and Ceccarelli, 2014). Recombinant proteins can interfere with normal proliferation and homeostasis, resulting in slower growth rates, low cell density, and cell death. Monitoring of cell growth before and after induction eliminated the possibility of protein toxicity. Codon bias may have also affected the expression of the *GELA/B/C* genes. Codon bias occurs when the frequency of codons in the foreign DNA is significantly different from that of the host. Low abundant tRNAs are depleted during protein synthesis and can lead to amino acid misincorporation or truncation (Rosano and Ceccarelli, 2014). Analysis of the *GEL* sequences reveal that rare arginine (Arg) codons were present in the sequences. The *GELA/B/C* genes were transformed into the BL21 (DE3) CodonPlus *E. coli* strain which contains rare codons. Unfortunately, this did not affect expression and no GEL proteins were expressed.

It is unknown why the *Bgh* GEL proteins were not expressed. The expression of fungal GH72 β-1,3-glucanosyltransferase proteins is not a novel problem. The *P. brasiliensis* β-1,3-glucanosyltransferases 1, 2 and 3 (*Pb*Gel1p, *Pb*Gel2p and *Pb*Gel3p) have been expressed in *E. coli* (Castro et al., 2009; de Sousa Lima et al., 2012). Though it is unknown whether or not the β-1,3-glucanosyltransferases were active as the proteins were used to generate antibodies and no activity assays were performed. β-1,3-Glucanosyltransferases are more commonly expressed in *Pichia pastoris*, with several instances of active β-1,3-glucanosyltransferases being expressed and purified in the past from *C. albicans, A. fumigatus*, and *S. pombe* (Mouyna et al., 2000; Carotti et al., 2004; de Medina-Redondo et al., 2010; Kováčová et al., 2015). With hindsight, using *P. pastoris* would have been a more optimal system as the heterologous expression of *GEL/GAS/PHR* genes are well documented in *P. pastoris*.

5.4.2 Heterologous expression of *Bgh* CHS proteins

The purification of a fungal CHS is required to determine the structure, molecular organisation, and catalytic mechanisms of the enzyme. The purification of active CHS proteins have been impaired due to the hydrophobicity of CHS, multiple transmembrane domains, and size. Although there have not been any successful purifications of CHS, there have been reports of partial purifications.

The CHS5 from *W. dermatitidis* (WdCHS5) was expressed in a native *W. dermatitidis* system and partially purified using affinity chromatography with polyclonal antibodies. However, the yields were quite low, and it was observed that the purified WdCHS5 was sensitive to degradation (Abramczyk and Szaniszlo, 2009). The small CHS1 from *R. oryzae* was also able to be partially purified recently. While the CHS1 had minimal hydrophobic motifs, it was only able to be expressed in *E. coli* after the deletion of a short hydrophobic stretch at the C-terminus. Unfortunately, most of the CHS1 protein aggregated into inclusion bodies and only a small amount could be purified when solubilised in urea (Salgado-Lugo et al., 2016).

The goal of this research was to solubilise and purify an enzymatically active CHS proteins from *Bgh*. Seven CHS have been identified in *Bgh*, one for each chitin synthase class. Out of those seven, only four were successfully expressed (CHSI, CHSIV, CHSVI and CHSVII), and of those four CHSI was the only active enzyme.

While protein expression was positive for some of the *Chs* genes, that does not guarantee that they were in an active state. It is possible that the proteins were not folding properly in the host expression system. In order to fold properly, proteins often require crucial interactions with other proteins, such as chaperones, that the host systems are missing (Rosano and Ceccarelli, 2014). In addition, post-translational modifications required to activate the enzymes could also be absent in the expression system.

As CHSI was the only active enzyme, we progressed to the purification stage. While CHSI purification was successful, the total yield was low. During initial purification trials, it was suspected that there were issues involved with expression as the CHSI band was not present in the in-gel fluorescence of any of the aliquots taken during the purification process (Figure 5.11). This was proven false as the solubilised membrane protein fraction consistently displayed high levels of chitin synthase activity (data not shown).

Coomassie stains during the purification process showed a large amount of low molecular weight proteins and barely any larger molecular weight proteins. This led to the conclusion that a significant amount of protein degradation was occurring during the purification process. To remedy this, the incubation of solubilised membrane proteins with the Ni-NTA resin was shortened to 2-3h (instead of overnight) to allow the time frame of the purification process to be shortened to one day. Shortening the purification time resulted in CHSI being enriched enough

that the GFP was visible in solution and the 114 kDa CHSI fusion protein band was visible in the in-gel fluorescence (Figure 5.12, lane 8). Upon calculating the protein concentration, it was determined that a total of 16 μg of recombinant CHSI was purified from 1 L of culture.

The low yield suggested that a significant amount of degradation was still occurring throughout the purification process. Attempts to protect CHSI against this degradation by using protease inhibitors (EDTA, EGTA, PMSF, and 2x protease cocktail inhibitors), membrane washing, and an alternate lysing method (liquid N_2 grinding) were unsuccessful.

The analysis of membrane proteins is a significant technical challenge compared to soluble proteins. Expression of membrane proteins are generally quite low. In addition, integral membrane proteins are hydrophobic, causing them to form aggregates. Once solubilised, membrane proteins are often more susceptible to degradation by proteases. Both Abramczyk and Szaniszlo (2009) and Salgado-Lugo et al. (2016) also had difficulty in purifying sufficient amounts of CHS protein, experiencing issues with protein degradation and solubilisation, respectively.

Although endeavours to increase CHSI yield failed to produce any results, preliminary enzymatic activity assays with the solubilised membrane fraction and purified product have discerned some rudimentary properties of the enzyme. Activity assays without trypsin reveal that protease treatment was not required to activate the CHSI. In fact trypsin negatively impacted enzymatic activity (Figure 5.9 (C)). This indicates that CHSI is not synthesised as a zymogen, but instead synthesised in an active state. Proteases have variable effects on CHS activity. In some cases, CHS require proteases for activation (Durán and Cabib, 1978), whereas in other instances the CHS are not activated and instead proteolysed and inactivated (Ruiz-Herrera et al., 1997, 1992). The CHS1 partially purified by Salgado-Lugo et al. (2016) from *R. oryzae* did not require activation by trypsin either.

Proper protein storage is an important element in protein studies. Depending on the protein, different temperatures and solution conditions are required for the protein in order to remain stable. While some proteins remain stable at room temperature and at 4°C others continue to deteriorate even when stored at -80°C. In these cases, proteins are lyophilised in order to remove water and effectively prevent protein degradation (Cutler, 2004; Walls and Loughran, 2017). Storage of solubilised membranes and purified CHSI in varying conditions has allowed some basic storage conditions of CHSI to be deduced. The CHSI protein can be stored at -20° and retain activity (Figure 5.13). On the other hand, CHSI is unstable when stored at room temperature and 4°C, with severely decreased activity due to protein degradation.

Detailed characterisation of the *Bgh* CHSI properties will require additional purification with significantly greater amounts of protein. This study is one of the few works where a fungal CHS was expressed in a heterologous system and

purified in an active state. While attempts to increase protein yields failed to produce any results, the work from this study represents an important step towards characterising *Bgh* CHSI and its potential use as a target for antifungal drug development.

5.5 Primer Tables

TABLE 5.1: PCR primer pairs for amplification of *Bgh* cell wall related genes. F, forward primer. R, reverse primer.

Primer	Sequence 5′ → 3′
CHSI_F	ATGACGCCATCTCCTGCC
CHSI_R	TCATACCCCACGGAACATACG
CHSII_F	ATGGATCGACCATCAACACCC
CHSII_R	TTACCCTCGGACACTTGAGG
CHSIII_F	ATGGCCGGATACCAAGGC
CHSIII_R	TTACCGCCTGATAAAGCAGCA
CHSIV_F	ATGTCATTACCTAAAAGACCTGATGC
CHSIV_R	TTAGTTAAAGTTTTCCGAAATCCA
CHSV_F	ATGGAGGGCTTCCAACTCTTC
CHSV_R	TCAAATTTGCTCCGTTTTTAATGA
CHSVI_F	ATGGCCGGGACTCAGCGAAT
CHSVI_R	TCACATATTGGCCAATTCCGTG
CHSVII_F	ATGGCCATTAAGTACGATACGTCA
CHSVII_R	TTACCGTGATGGATGAGACT
FKSI_F	ATGTCGGGCCATCCACAAC
FKSI_R	TTAAATCAGCCTGAGTTTCTCTGA
GELA_F	ATGAAATCAAACGCAATTGC
GELA_R	TTACAAAGCTATAGCCCCAA
GELB_F	ATGGTATCAAAGATCATTTTAGCGA
GELB_R	TTAATTACTCAAATAAAGCATTATCAAGGC
GELC_F	ATGCAGCCTCTCGGGC
GELC_R	CTACAACAGAATCATGCATGCCC
KRE6_F	ATGGCGTCAAATAGGTTACAACA
KRE6_R	TCATGTACATTCATGGAGCAGACT
KRE9_F	ATGCTCGTCGGATCAAAACTCT
KRE9_R	TTAATCTTTCCAGCGGTTCAGA

TABLE 5.2: Sequencing primers for *Bgh* cell wall related genes.

Primer	Sequence 5′ → 3′
pCR8_GW1_primer	GTTGCAACAAATTGATGAGCAATGC
CHSI_F2	ATATATACGAGTACACAACCCAGG
CHSI_F3	GAGAAAATGCACGGCTCCAACG
CHSI_F4	CGTTGCCTACATTTCTATGGTTCT
CHSI_F5	TGACTACTACCGAGGCTTTCG
CHSII_F2	TCCTAGACCCGGTACTCCATCT
CHSII_F3	CTGAGCTATTTATCTGCGTGACTATG
CHSII_F4	CTAAGCCGGGTGGTAACTCACT
CHSII_F5	CTGCGGTCTACTCCCTAGTTCA
CHSII_F6	GCTGGTCAGTACTTTCTCCTC
CHSIII_F2	GCTGGTGGATTAAAGCGATTTGC
CHSIII_F3	GAGACCGTTGCTCACATATTTGAAT
CHSIII_F3	GAGACCGTTGCTCACATATTTGAAT
CHSIII_F4	TTCATGGCGATCATACTCTTTCGA
CHSIII_F5	CCATCCTAAAGTACCTCTATCTAG
CHSIV_F2	CAACTGGCAATGATCCCATTCTAG
CHSIV_F3	CTCTTCGGCTTCGCGTCAATC
CHSIV_F4	CAAGAACTTAGCAACAGGGGTAG
CHSIV_F5	TCTAAGGTTGGACGCACTCAGC
CHSIV_F6	GCTGGTTTCTATGACTATGGTGC
CHSIV_F7	ACCCAAGGGAGGCCAGAATTATT
CHSIV_F8	TACTCACTGCTCATCGATGGTCA
CHSV_F2	CCTAGTAGCCTATGTAATGGAGTG
CHSV_F3	CGCGGGTGAGGTAGATTATTTAATC
CHSV_F4	GGATTGCAGAGATTAGTCAGCGAT
CHSV_F5	GTTCCGAAATCTTGACACAAGGC

TABLE 5.2: Continued

Primer	Sequence 5′ → 3′
CHSV_F6	ATGTCCACAAACACGAGCGGC
CHSV_F7	CTTGCGATGTCAGTTTGCGGAATA
CHSV_F8	CTTAAACAGAGTGCACTACAACGC
CHSV_F9	ACCACTCTGCTAATGAAGCACCA
CHSV_F10	GACCCAGATTCTATCCCCCATAA
CHSV_F11	ACTGGATGCAAGGAGAGCATAC
CHSVI_F2	TGAATCTTCGCCCTCTTTGCTTG
CHSVI_F3	ACTTGGGAACACCCTCAGCTTTA
CHSVI_F4	GAACATCAACGAGATCGACGGGA
CHSVI_F5	CGATTTGAAGCCGTTAGATGACC
CHSVI_F6	CTGATGTCCGAATGGCTTGGAG
CHSVI_F7	AGCAAGTGAGGGTCAAGACGATA
CHSVI_F8	ACTCTTTAACCGCTCTTCAGTACG
CHSVI_F9	GATTGCTGGCATTTGTGGTGAGACT
CHSVI_F10	ATTCTACCTGCCACCTGTGCATAT
CHSVI_F11	CGTGGAACAGGGTTAGCCTATTT
CHSVII_F2	TGCAGCTCTTCTCACTATCCCAT
CHSVII_F3	GGTAACAGCAGAGATATGCTTGC
CHSVII_F4	CATTCTAGCTCTGGTGCGATTCA
CHSVII_F5	TGACTCTGTGGTAAGCTCATCG
FKSI_F2	TCAGAGACATTCAGCGACTTCAC
FKSI_F3	GTACTTTGCAGCCCATCTCGAT
FKSI_F4	TAGGCTACGATGACTGCAACCAA
FKSI_F5	GCATTAGCCACATTCTTCTTCTTCG
FKSI_F6	ATCTGGACTCCTTGGCGGAATAT
FKSI_F7	GGACACCGCTAAGAGCAAAATTG
FKSI_F8	CTTTCAGGCAATCCAATTCTCGG
FKSI_F9	TGGAGGACGTATAAAGCACTGC
FKSI_F10	GTGTCAAATCTACGCAAACGCATTC
FKSI_F11	TGTGGCTGTAACGCTTGTACCTT

TABLE 5.2: Continued

Primer	Sequence 5′ → 3′
FKSI_F12	CACAGAGTTAGGAATGTTTGCCG
GELA_F2	CAAATACTCTCTCAACCGAGCAAC
GELA_F3	GACTAGTGTTTACTCTGGAGGC
GELB_F2	CGACGTTAACTCACCACTTTCG
GELB_F3	CAGCGAAGTTCCGGCAATTTATG
GELC_F2	CATCAATAAACCGAGACACACCGA
GELC_F3	CCGAGGTTCAAGCCATATATGGT
KRE6_F2	ACAGCCCATTTGGATCACCCTT
KRE6_F3	GATGAGTTCAATAAAGATGGGCGC
KRE6_F4	GTCTAGATCCTCTCCCGAAATC
KRE6_F5	TTGCACAATCTTGCCCAGCTCAT
KRE9_F2	ACCCTCACTGGAATGACTGGTA

TABLE 5.3: *GELA*, *GELB* and *GELC* PCR primers with overhang sequences corresponding to pET3a for cloning. Green segments correspond to the 5′ end of pET3a while the red segments correspond to the 3′ end of the plasmid. Purple segments correspond to a 6xhis-tag incorporated into the 5′ and 3′ end of the genes. F, forward primer. R, reverse primer.

Primer	Sequence 5′ → 3′
GELA_F1	GAAGGAGATATACATATGAAATCAAACGCAATTGC
GELA_R1_3'Histag	TTAGCAGCCGGATCCGTGATGGTGATGGTGATGCAAAGCTATAGCCCCAA
GELA_F2_5'Histag	GAAGGAGATATACATCATCACCATCACCATCACATGAAATCAAACGCAATTGC
GELA_R2	TTAGCAGCCGGATCCTTACAAAGCTATAGCCCCAA
GELB_F1	GAAGGAGATATACATATGGTATCAAAGATCATTTTAGCGA
GELB_R1_3'Histag	TTAGCAGCCGGATCCGTGATGGTGATGGTGATGATTACTCAAATAAAGCATTATCAAGGC
GELB_F2_5'Histag	GAAGGAGATATACATCATCACCATCACCATCACATGGTATCAAAGATCATTTTAGCGA
GELB_R2	TTAGCAGCCGGATCCTTAATTACTCAAATAAAGCATTATCAAGGC
GELC_F1	GAAGGAGATATACATATGCAGCCTCTCGGGC
GELC_R1_3'Histag	TTAGCAGCCGGATCCGTGATGGTGATGGTGATGCAACAGAATCATGCATGCCC
GELC_F2_5'Histag	GAAGGAGATATACATCATCACCATCACCATCACATGCAGCCTCTCGGGC
GELC_R2	TTAGCAGCCGGATCCCTACAACAGAATCATGCATGCCC

TABLE 5.4: *CHSI-VII* and *Fks1* PCR primers with overhang sequences corresponding to pDDGFP-2 for cloning during transformation. Green segments are the recombination sequences corresponding to the 5′ ends of pDDGFP-2 while the red segments are the recombination sequences corresponding to the 3′ ends of the plasmid. F, forward primer. R, reverse primer.

Primer	Sequence 5′ → 3′
CHSI_F_pDD	ACCCCGGATTCTAGAACTAGTGGATCCCCCATGACGCCATCTCCTGCC
CHSI_R_pDD	AAATTGACCTTGAAAATATAAATTTTCCCCTACCCCACGGAACATACG
CHSII_F_pDD	ACCCCGGATTCTAGAACTAGTGGATCCCCCATGGATCGACCATCAACACCC
CHSII_R_pDD	AAATTGACCTTGAAAATATAAATTTTCCCCCCCTCGGACACTTGAGG
CHSIII_F_pDD	ACCCCGGATTCTAGAACTAGTGGATCCCCCATGGCCGGATACCAAGGC
CHSIII_R_pDD	AAATTGACCTTGAAAATATAAATTTTCCCCCCGCCTGATAAAGCAGCA
CHSIV_F_pDD	ACCCCGGATTCTAGAACTAGTGGATCCCCCATGTCATTACCTAAAAGACCTGATGC
CHSIV_R_pDD	AAATTGACCTTGAAAATATAAATTTTCCCCGTTAAAGTTTTCCGAAAATCCA
CHSV_F_pDD	ACCCCGGATTCTAGAACTAGTGGATCCCCCATGGAGGGCTTCCAACTCTTC
CHSV_R_pDD	AAATTGACCTTGAAAATATAAATTTTCCCCAATTTGCTCCGTTTTTAATGA
CHSVI_F_pDD	ACCCCGGATTCTAGAACTAGTGGATCCCCCATGGCCGGGACTCAGCGAAT
CHSVI_R_pDD	AAATTGACCTTGAAAATATAAATTTTCCCCCATATTGGCCAATTCCGTG
CHSVII_F_pDD	ACCCCGGATTCTAGAACTAGTGGATCCCCCATGGCCATTAAGTACGATACGTCA
CHSVII_R_pDD	AAATTGACCTTGAAAATATAAATTTTCCCCCCGTGATGGATGAGACT
FKSI_F_pDD	ACCCCGGATTCTAGAACTAGTGGATCCCCCATGTCGGGCCATCCACAAC
FKSI_R_pDD	AAATTGACCTTGAAAATATAAATTTTCCCCAATCAGCCTGAGTTTCTCTGA

Chapter 6

Conclusion

The goal of this work was to investigate the cell wall structure and related processes of *Blumeria graminis* f. sp. *hordei* (*Bgh*), a major fungal pathogen to *Hordeum vulgare* (barley). Aside from the reverse transcription polymerase chain reaction (RT-PCR) of two chitin synthases (Zhang et al., 2000) and the examination of the *Bgh* conidia ultrastructure through transmission electron microscopy (Roberts et al., 1996) there has been little work done on the *Bgh* cell wall. Zhang et al. (2000) identified two chitin synthase genes, which they designated Bg*Chs1* (class I) and Bg*Chs2* (class V) and examined their expression over time by RT-PCR. Bg*Chs1* was up-regulated during both the primary and appressorial germ tube stages while Bg*Chs2* was up-regulated during the primary germ tube stage. Additionally these authors examined the effects of the chitin substrate analogues nikkomycin Z and polyoxin D on conidial morphogenesis and found that both caused the appressorial germ tube to swell abnormally and burst after 12 h. Roberts et al. (1996) examined the ultrastructure of the *Bgh* conidia and found that the conidium was surrounded by a two-layered wall of chitin when labelled with gold-conjugated wheat germ agglutinin-ovomucoid.

Our study aimed to understand the *Bgh* cell wall structure by examining its composition in the conidia and identify enzymes related to cell wall metabolism (Chapter 2). As *Bgh* cannot be cultured, we derived an *in vitro* system using *n*-hexacosanal to cultivate *Bgh* up until the appressorial germ tube stage from a previous study (Hansjakob et al., 2010) (Chapter 3). The *in vitro* system allowed further characterisation of the *Bgh* cell wall composition during the pre-penetrative stages of pathogenesis as well as examination of the trancriptomic and proteomic profiles (Chapter 4). In order to understand how the *Bgh* cell wall is constructed, key enzymes involved in glucan and chitin synthesis and remodelling that were identified in Chapter 2 were expressed in heterologous systems for biochemical characterisation (Chapter 5).

Permethylation glycosidic linkage analysis conducted on the *Bgh* conidia revealed the composition of the *Bgh* cell wall for the first time (Chapter 2). The conidial cell wall was composed of glucose (63.1%) followed by mannose (16.2%), galactose

(10.7%), *N*-acetylglucosamine (9%), and trace amounts of xylose (1%). The presence of xylose in the *Bgh* is interesting as xylose residues are rarely seen in ascomycete cell walls.

Analysis of the sequenced *Bgh* genome has also expanded upon the Carbohydrate-Active enZymes (CAZy) profile of *Bgh*. Obligate biotrophs, such as powdery mildews, downy mildews and rust fungi, have a reduced set of genes responsible for degrading the plant cell wall (Kämper et al., 2006; Duplessis et al., 2011) compared to hemibiotrophic and necrotrophic fungi (Raffaele and Kamoun, 2012; Zhao et al., 2013). As such, it was expected that *Bgh* would have a reduced set of CAZy genes. However, prior analysis of the *Bgh* genome has barely identified any CAZy genes (Spanu et al., 2010; de Witt et al., 2012; Hacquard et al., 2013). Our analysis identified a substantially larger number of CAZY genes compared to the previous studies, a total of 326 genes. The list of CAZy genes not only contain genes involved in degrading the plant cell wall, but also genes involved in fungal cell wall biosynthesis and remodelling. Several genes implicated in fungal cell wall metabolism were identified. Of particular interest were the seven chitin synthases (*ChsI-VII*) (GT2), a single β-1,3-glucan synthase (*Fks1*) (GT48) and three β-1,3-glucanosyltransferases (*GELA/B/C*) (GH72).

The substances that compose the cuticle on the host plant surface are known to trigger the germination and differentiation of several pathogenic fungi (Carver and Thomas, 1990; Tsuba et al., 2002; Gniwotta et al., 2005; Mendoza-Mendoza et al., 2009). *n*-Hexacosanal, an aldehyde constituent of the barley cutin, has been identified as a strong inducer of germination and differentiation in *Bgh* (Tsuba et al., 2002; Hansjakob et al., 2010, 2011). Utilising the previous work done by Hansjakob et al. (2010), an *in vitro* system was developed using *n*-hexacosanal to cultivate *Bgh* during the pre-penetrative stages of development (Chapter 3). Using this, *Bgh* were able to be collected for analysis without any contamination from the host plant to extend the work done in Chapter 2. Permethylation glycosidic linkage analysis and proteomic analysis became possible on *Bgh* during the appressorial germ tube stage (Chapter 4).

Permethylation glycosidic linkage analysis of the cell wall appressorial germ tube stage revealed increases in 1,3- and 1,4-linked glucosyl residues and significant decreases in the galactose component of the cell wall. Additionally, branched 1,2,4- and 1,3,4-xylose residues was also detected in the cell wall during appressorial development.

The transcriptomic and proteomic profiling of the *Bgh* revealed that there was a shift towards energy production and protein production during the agt stage. An increase in proteins and transcripts involved in cellular respiration and protein synthesis, modification, and transport were observed during the appressorial germ tube stage of development. Many of the highly expressed transcripts on the *in vitro*

surface were also highly expressed on previous *in planta* studies (Both et al., 2005a; Hacquard et al., 2013), demonstrating that the pre-penetrative *in vitro* events are a good approximation for the *in planta* pre-penetrative events.

The isolation and function analysis of *Bgh* chitin synthases (CHSI-VII), β-1,3-glucan synthase and three β-1,3-glucanosyltransferases were pursued using *Escherichia coli* and *Saccharomyces cerevisiae* expression systems. The *Bgh* CHSI protein was successfully purified and showed high levels of enzymatic activity. Unfortunately, due to time contraints biochemical activity assays to characterise the enzyme properties further could not be carried out.

To date there have not been any publications demonstrating successful purification and enzymatic activity of CHS proteins. As a large hydrophobic membrane protein with several transmembrane domains, numerous complications have arisen in previous attempts to express and purify active CHS (Durán and Cabib, 1978; Lending et al., 1991; Uchida et al., 1996). The biochemical properties and molecular mechanisms of fungal CHS remain largely unknown. Additional work to refine the purification of the *Bgh* CHSI will expand knowledge about chitin synthesis processes and possibly assist in the design of antifungal agents.

Additional work is required to refine the purification process for the *Bgh* CHSI. With more time, different techniques and reagent combinations could have been tested to try and improve the process. Once sufficient CHSI is purified, enzyme kinetic analysis can be carried out and novel antifungals could be trialed to see how they would affect activity. Resources could also be devoted for troubleshooting the expression of the other genes. Expression of a few other additional chitin synthases was achieved, though none were active *in vitro*. It is possible that those proteins were either misfolded or perhaps required special conditions in order to activate.

While the permethylation glycosidic linkage analysis has revealed the cell wall composition of the *Bgh* conidial and appressorial germ tube stages, the cell wall architecture still remains unknown. Linkage analysis combined with nuclear magnetic resonance (NMR) spectroscopy could help to reveal some aspects of the structure and architecture of the *Bgh* cell wall as has been done for other fungi (Ahrazem et al., 2003; Kang et al., 2018). Further work on deciphering the structure of the *Bgh* cell wall will perhaps reveal where the galactopyranose and xylose residues fit into the cell wall network.

The results from the analysis performed on *Bgh* samples cultivated using the *in vitro* system proved that it is a viable method for analysing the *Bgh* pre-penetrative stages of development. The adoption of this simplified system could improve analysis of the molecular and cytological processes that occur in *Bgh* before it can establish infection in the host. While there are not many protocols available for manipulating the *Bgh* genes, it may be possible to do a gene knock down with RNA interference (RNAi) with the *in vitro* system. Chemically synthesised short double stranded RNA

(siRNA) can be exogenously applied to the *Bgh in vitro* to knock down genes of interest, such as those involved in cell wall metabolism. The application of siRNA under *in vitro* conditions has been utilised in *Aspergillus nidulans* and *Aspergillus fumigatus* studies and have shown to be effective (Eslami et al., 2014; Mousavi et al., 2015).

The *in vitro* method could also be used to characterise and monitor the compositional changes in cell surface carbohydrates during the pre-penetrative stages of *Bgh* using various probes and antibodies. Further characterisation of the cell wall could also be carried out by immunogold labelling cross sections of *Bgh* to determine the location of specific carbohydrates within the cell wall. In addition, it could be possible to also characterise the cell surface protein profiles during the *Bgh* pre-penetrative stages by extracting the surface proteins.

This study serves as a foundation for future investigations into the *Bgh* cell wall, which has thus far been incredibly lacking. Considering the economic impact of *Bgh*, the importance of the cell wall, and the fact that it is a hotspot for targeted antifungal development, it is surprising that it has remained understudied.

References

Abe, M., Qadota, H., Hirata, A., and Ohya, Y. (2003). Lack of GTP-bound Rho1p in secretory vesicles of Saccharomyces cerevisiae. *Journal of Cell Biology*, 162(1):85–97.

Abramczyk, D. and Szaniszlo, P. J. (2009). Immunoaffinity purification of the class V chitin synthase of Wangiella (Exophiala) dermatitidis. *Preparative Biochemistry and Biotechnology*, 39(3):277–288.

Abramyan, J. and Stajich, J. E. (2011). Species-specific chitin-binding module 18 expansion in the amphibian pathogen Batrachochytrium dendrobatidis. *mBio*, 3(3).

Afroz, S., El-Ganiny, A. M., Sanders, D. A., and Kaminskyj, S. G. (2011). Roles of the Aspergillus nidulans UDP-galactofuranose transporter, UgtA in hyphal morphogenesis, cell wall architecture, conidiation, and drug sensitivity. *Fungal Genetics and Biology*, 48(9):896–903.

Aguilar, G. B., Pedersen, C., and Thordal-Christensen, H. (2016). Identification of eight effector candidate genes involved in early aggressiveness of the barley powdery mildew fungus. *Plant Pathology*, 65:953–958.

Ahmed, A. A., Pedersen, C., and Thordal-Christensen, H. (2016). The barley powdery mildew effector candidates CSEP0081 and CSEP0254 promote fungal infection success. *PloS ONE*, 11(6).

Ahrazem, O., Prieto, A., San-Blas, G., Leal, J. A., Jiménez-Barbero, J., and Bernabé, M. (2003). Structural differences between the alkali-extracted water-soluble cell wall polysaccharides from mycelial and yeast phases of the pathogenic dimorphic fungus Paracoccidioides brasiliensis. *Glycobiology*, 13(11):743–747.

Akcapinar, G. B. and Kappel, L. (2015). Molecular diversity of LysM carbohydrate-binding motifs in fungi. *Current Genetics*, 61(2):103–113.

Akhkha, A. (2009). Barley powerdery mildew (Blumeria graminis f. sp. hordei) interaction, resitance and tolerance. *The Egyptian Society of Experimental Biology*, 5:1–20.

Amnuaykanjanasin, A. and Epstein, L. (2003). A class V chitin synthase gene, ChsA is essential for conidial and hyphal wall strength in the fungus Colletotrichum graminicola (Glomerella graminicola). *Fungal Genetics and Biology*, 38(3):272–285.

Amselem, J., Cuomo, C. A., van Kan, J. A. L., Viaud, M., Benito, E. P., Couloux, A., Coutinho, P. M., de Vries, R. P., Dyer, P. S., Fillinger, S., Fournier, E., Gout, L., Hahn, M., Kohn, L., Lapalu, N., Plummer, K. M., Pradier, J.-M., Quévillon, E., Sharon, A., Simon, A., ten Have, A., Tudzynski, B., Tudzynski, P., Wincker, P., Andrew, M., Anthouard, V., Beever, R. E., Beffa, R., Benoit, I., Bouzid, O., Brault, B., Chen, Z., Choquer, M., Collémare, J., Cotton, P., Danchin, E. G., da Silva, C., Gautier, A., Giraud, C., Giraud, T., Gonzalez, C., Grossetete, S., Güldener, U., Henrissat, B., Howlett, B. J., Kodira, C., Kretschmer, M., Lappartient, A., Leroch, M., Levis, C., Mauceli, E., Neuvéglise, C., Oeser, B., Pearson, M., Poulain, J., Poussereau, N., Quesneville, H., Rascle, C., Schumacher, J., Séqurens, B., Sexton, A., Silva, E., Sirven, C., Soanes, D. M., Talbot, N. J., Templeton, M., Yandava, C., Yarden, O., Zeng, Q., Rollins, J. A., Lebrun, M.-H., and Dickman, M. (2011). Genomic analysis of the necrotrophic fungal pathogens Sclerotinia sclerotiorum and Botrytis cinerea. *PLoS Genetics*, 7(8).

Bartnicki-García, S. (2006). Chitosomes: Past, present and future. *FEMS Yeast Research*, 6(7):957–965.

Bäumler, S., Felsenstein, F. G., and Schawarz, G. (2003). CAPS and DHPLC analysis of a single nucleotide polymorphism in the cytochrome b gene conferring resistance to strobilurins in field isolates of Blumeria graminis f. sp. hordei. *Journal of Phytopathology*, 151(3):149–152.

Beauvais, A., Bruneau, J. M., Mol, P. C., Buitrago, M. J., Legrand, R., and Latgé, J. P. (2001). Glucan synthase complex of Aspergillus fumigatus. *Journal of Bacteriology*, 183(7):2273–2279.

Beauvais, A., Fontaine, T., Aimanianda, V., and Latgé, J.-P. (2014). Aspergillus cell wall and biofilm. *Mycopathogia*, 178:371–377.

Bindschedler, L. V., Burgis, T. A., Mills, D. J. S., Ho, J. T. C., Framer, R., and Spanu, P. D. (2009). In planta protemics and proteogenomics of the biotrophic barley fungal pathogen Blumeria graminis f. sp. hordei. *Molecular and Cellular Proteomics*, 8(10):2368–2381.

Borkovich, K. A., Alex, L. A., Yarden, O., Freitag, M., Turner, G. E., Read, N. D., Seiler, S., Bell-Pedersen, D., Paietta, J., Plesofsky, N., Plamann, M., Goodrich-Tanrikulu, M., Schulte, U., Mannhaupt, G., Nargang, F. E., Radford, A., Selitrennikoff, C., Galagan, J. E., Dunlap, J. C., Loros, J. J., Catcheside, D., Inoue, H., Aramayo, R., Polymenis, M., Selker, E. U., Sachs, M. S., Marzluf, G. A., Paulsen, I., , Davis, R., Ebbole, D. J., Zelter, A., Kalkman, E. R., Bowring, F., Yeadon, J., Ishii, C., Suzuki, K., Sakai, W., and Pratt, R. (2004). Lessons from the genome analysis of Neurospora crassa. *Microbiology and Molecular Biology Reviews*, 68(1):1–108.

Both, M., Csukai, M., Stumpf, M. P. H., and Spanu, P. D. (2005a). Gene expression prolfiles of Blumeria graminis indicate dynamic changes to primary metabolism

during development of an obligate biotrophic pathogen. *The Plant Cell*, 17(7):2107–2122.

Both, M., Eckert, S. E., Csukai, M., Müller, E., Dimopoulos, G., and Spanu, P. D. (2005b). Transcript profiles of Blumeria graminis development during infection reveal a cluster of genes that are potential virulence determinants. *Molecular Plant Microbe Interactions*, 18(2):125–133.

Bowen, A., Chen-Wu, J., Momany, M., Young, R., Szaniszlo, P., and Robbins, P. (1992). Classification of fungal chitin synthases. *PNAS*, 89(2):519–23.

Brown, C., Leijon, F., and Bulone, V. (2012). Radiometric and spectrophotometric in vitro assays of glycosyltransferases involved in plant cell wall carbohydrate biosynthesis. *Nature Protocols*, 7(9):1634–1650.

Brown, J. K. M. and Hovmøller, M. S. (2002). Aerial dispersal of pathogens on the global and continental scales and its impact on plant disease. *Science*, 297(5581):537–541.

Bulawa, C. E. (1992). CSD2, CSD3, and CSD4, genes required for chitin synthesis in Saccharomyces cerevisiae: The CSD2 gene product is related to chitin synthases and to developmentally regulated proteins in Rhizobium species and Xenopus laevis. *Molecular and Cellular Biology*, 12(4):1764–1776.

Bulone, V., Chanzy, H., Gay, L., Girard, V., and Févre, M. (1992). Characterization of chitin and chitin synthase from the cellulosic cell wall fungus Saprolegnia monoïca. *Experimental Mycology*, 16(1):8–21.

Burton, R. A., Gidley, M. J., and Fincher, G. B. (2010). Heterogeneity in the chemistry, structure and function of plant cell walls. *Nature Chemical Biology*, 6(10):724–732.

Bushnell, W. R., Mendgen, K., and Liu, Z. (1987). Accumulation of potentiometric and other dyes in haustoria of Erysiphe graminis in living host cell. *Physiological and Molecular Plant Pathology*, 31(2):237–250.

Carotti, C., Ragni, E., Palomares, O., Fontaine, T., Tedeschi, G., Rodríguez, R., Latgé, J.-P., Vai, M., and Popolo, L. (2004). Characterization of recombinant forms of the yeast Gas1 protein and identification of residues essential for glucanosyltransferase activity and folding. *European Journal of Biochemistry*, 271(18):3635–3645.

Carpita, N. C. and Shea, E. M. (1988). Linkage structure of carbohydrates by gas chromatography-mass spectrometry (GC-MS) of partially methylated alditol acetates. In Biermann, C. J. and McGinnis, G. D., editors, *Analysis of Carbohydrates by GLC and MS*, chapter 9, pages 157–216. CRC Press.

Carver, T. L. W. and Ingerson, S. M. (1987). Responses of Erysiphe graminis germlings to contact with artificial and host surfaces. *Physiological and Molecular Plant Pathology*, 30(3):359–372.

Carver, T. L. W. and Thomas, B. J. (1990). Normal germling development by Erysiphe graminis on cereal leaves freed of epicuticular wax. *Plant Pathology*, 39:367–375.

Castro, N. d. S., de Castro, K. P., Orlandi, I., Feitosa, L. d. S., Rosa e Silva, L. K., Vainstein, M. H., Nair, B. S., Vai, M., and de Almeida Soares, C. M. (2009). Characterization and functional analysis of the β-1,3-glucanosyltransferase 3 of the human pathogenic fungus Paracoccidioides brasiliensis. *FEMS Yeast Research*, 9(1):103–114.

Chaffin, W. L., López-Ribot, J. L., Casanova, M., Gozalbo, D., and Martínez, J. P. (1998). Cell wall and secreted proteins of Candida albicans: Identification, function, and expression. *Microbiology and Molecular Biology Reviews*, 62(1):130–180.

Chaure, P., Gurr, S. J., and Spanu, P. D. (2000). Stable transformation of Erysiphe graminis an obligate biotrophic pathogen of barley. *Nature Biotechnology*, 18(2):205–207.

Chigira, Y., Abe, K., Gomi, K., and Nakajima, T. (2002). chsZ, a gene for a novel class of chitin synthase from Aspergillus oryzae. *Current Genetics*, 41(4):261–267.

Chin, K. M., Chavaillaz, D., Kaesbohrer, M., Staub, T., and Felsenstein, F. G. (2001). Characterizing resistance risk of Erysiphe graminis f.sp. tritici to strobilurins. *Crop Protection*, 20(2):87–96.

Chiou, C. C., Mavrogiorgos, N., Tillem, E., Hector, R., and Walsh, T. J. (2001). Synergy, pharmacodynamics, and time-sequenced ultrastructural changes of the interaction between nikkomycin Z and the echinocandin FK463 against Aspergillus fumigatus. *Antimicrobial Agents and Chemotherapy*, 45(12):3310–3321.

Choquer, M., Boccara, M., Gonçalves, I. R., Soulié, M. C., and Vidal-Cros, A. (2004). Survey of the Botrytis cinerea chitin synthase multigenic family through the analysis of six euascomycetes genomes. *European Journal of Biochemistry*, 271(11):2153–2164.

Chowdhury, J., Henderson, M., Schweizer, P., Burton, R. A., Fincher, G. B., and Little, A. (2014). Differential accumulation of callose, arabinoxylan and cellulose in nonpenetrated versus penetrated papillae on leaves of barley infected with Blumeria graminis f. sp. hordei. *New Phytologist*, 204(3):650–660.

Christiansen, S. K., Knudsen, S., and Giese, H. (1995). Biolistic transformation of the obligate plant pathogenic fungus, Erysiphe graminis f.sp. hordei. *Current Genetics*, 29(1):100–102.

Cid, V. C., Durán, A., Del Rey, F., Snyder, M. P., Nombela, C., and Sánchez, M. (1995). Molecular basis of cell integrity and morphogenesis in Saccharomyces cerevisiae. *Microbiological Reviews*, 59(3):345–386.

Ciucanu, I. and Kerek, F. (1984). A simple and rapid method for the permethylation of carbohydrates. *Carbohydrate Research*, 131(2):209–217.

Cooper, B., Garret, W. M., and Campbell, K. B. (2006). Shotgun identification of proteins from uredospores of the bean rust Uromyces appendiculatus. *Proteomics*, 6:2477–2484.

Cooper, B., Neelam, A., Campbell, K. B., Lee, J., Liu, G., Garrett, W. M., Scheffler, B., and Tucker, M. L. (2007). Protein accumulation in the germinating Uromyces appendiculatus uredospore. *Molecular Plant Microbe Interactions*, 20(7):857–866.

Coronado, J. E., Mneimneh, S., Epstein, S. L., Qiu, W.-G., and Lipke, P. N. (2007). Conserved processes and lineage-specific proteins in fungal cell wall evolution. *Eukaryotic Cell*, 6(12):2269–2277.

Costa, C., Dias, P. J., Sá-Correia, I., and Teixeira, M. C. (2014). MFS multidrug transporters in pathogenic fungi: Do they have real clinical impact? *Frontiers in Physiology*, 5(197).

Cutler, P., editor (2004). *Protein Purification Protocols*, volume 244 of *Methods in Molecular Biology*. Humana Press.

de Groot, P. W. J., Ram, A. F., and Klis, F. M. (2005). Features and functions of covalently linked proteins in fungal cell walls. *Fungal Genetics and Biology*, 42(8):657–675.

de Groot, P. W. J., Ruiz, C., Vázquez de Aldana, C. R., Dueñas, E., Cid, V. J., Del Rey, F., Rodríquez-Peña, J. M., Pérez, P., Andel, A., Caubín, J., Arroyo, J., García, J. C., Gil, C., Molina, M., García, L. J., Nombela, C., and Klis, F. M. (2001). A genomic approach for the identification and classification of genes involved in cell wall formation and its regulation in Saccharomyces cerevisiae. *Comparative and Functional Genomics*, 2(3):124–142.

de Jonge, R., van Esse, H. P., Kombrink, A., Shinya, T., Desaki, Y., Bours, R., van der Krol, S., Shibuya, N., Joosten, M. H. A. J., and Thomma, B. P. H. J. (2010). Conserved fungal LysM effector Ecp6 prevents chitin-triggered immunity in plants. *Science*, 329(5994):953–955.

de Medina-Redondo, M., Arnaíz-Pita, Y., Clavaud, C., Fontaine, T., del Rey, F., Latgé, J.-P., and de Aldana, C. R. V. (2010). β(1,3)-glucanosyl-transferase activity is essential for cell wall integrity and viability of Schizosaccharomyces pombe. *PLoS ONE*, 5(11).

de Sousa Lima, P., Bailão, E. F. L. C., Silva, M. G., Castro, N. d. S., Nair, B. S., Orlandi, I., Vai, M., and de Almeida Soares, C. M. (2012). Characterization of the Paracoccidioides β-1,3-glucanosyltransferase family. *FEMS Yeast Research*, 12(6):685–702.

de Witt, P. J. G. M., van der Burgt, A., Ökmen, B., Stergiopoulos, I., Abd-Elsalam, K. A., Aerts, A. L., Bahkali, A. H., Beenen, H. G., Chettri, P., Cox, M. P., Datema, E., de Vries, R. P., Dhillon, B., Ganley, A. R., Griffiths, S. A., Guo, Y., Hamelin, R. C., Henrissat, B., Kabir, M. S., Jashni, M. K., Kema, G., Klaubauf, S., Lapidus, A., Levasseur, A., Lindquist, E., Mehrabi, R., Ohm, R. A., Owen, T. J., Salamov, A., Schwelm, A., Schijlen, E., Sun, H., van den Burg, H. A., van Ham, R. C. H. J., Zhang, S., Goodwin, S. B., Grigoriev, I. V., Collemare, J., and Bradshaw, R. E. (2012). The genomes of the fungal plant pathogens Cladosporium fulvum and Dothistroma septosporum reveal adaptation to different hosts and lifestyles but also signatures of common ancestry. *Walters*, 8(11).

Dean, R., van Kan, J. A. L., Pretorius, Z. A., Hammond-Kosack, K. E., Di Pietro, A., Spanu, P. D., Rudd, J. J., Dickman, M., Kahmann, R., Ellis, J., and Foster, G. D. (2012). The top 10 fungal pathogens in molecular plant plantathology. *Molecular Plant Pathology*, 13(4):414–430.

Denning, D. W. (2003). Echinocandin antifungal drugs. *Lancet*, 362(9390):1142–1151.

Depree, J., Emerson, G. W., and Sullivan, P. A. (1993). The cell wall of the oleaginous yeast Trichosporon cutaneum. *Journal of General Microbiology*, 139(9):2123–2133.

Din, A. B. and Yarden, O. (1994). The Neurospora crassa chs-2 gene encodes a non-essential chitin synthase. *Microbiology*, 140:2189–2197.

Douglas, C. M. (2001). Fungal β(1,3)-D-glucan synthesis. *Medical Mycology*, 39(Suppl 1):55–66.

Drew, D., Newstead, S., Sonoda, Y., Kim, H., von Heijne, G., and Iwata, S. (2008). GFP-based optimization scheme for the overexpression and purification of eukaryotic membrane proteins in Saccharomyces cerevisiae. *Nature Protocols*, 3(5):784–798.

Drgonová, J., Drgon, T., Tanaka, K., Kollár, R., Chen, G.-C., Ford, R. A., Chan, C. S., Takai, Y., and Cabib, E. (1996). Rho1p, a yeast protein at the interface between cell polarization and morphogenesis. *Science*, 272(5259):277–279.

Duplessis, S., Cuomo, C. A., Lin, Y.-C., Aerts, A., Isserant, E., Veneault-Fourrey, C., Joly, D. L., Hacquard, S., Amselem, J., Cantarel, B. L., Chiu, R., Coutinho, P. M., Feau, N., Field, M., Frey, P., Gelhaye, E., Goldberg, J., Grabherr, M. G., Kodira, C. D., Kohler, A., Kües, U., Lindquist, E. A., Lucas, S. M., Mago, R., Mauceli, E., Morin, E., Murat, C., Pangilinan, J. L., Park, R., Pearson, M., Quesneville, H., Rouhier, N., Sakthikumar, S., Salamov, A. A., Schmutz, J., Selles, B., Shapiro, H.,

Tanguay, P., Tuskan, G. A., Henrissat, B., van de Peer, Y., Rouzé, P., Ellis, J. G., Dodds, P. N., Schein, J. E., Zhong, S., Hamelin, R. C., Grigoriev, I. V., Szabo, L. J., and Martin, F. (2011). Obligate biotrophy features unraveled by the genomic analysis of rust fungi. *PNAS*, 108(22):9166–9171.

Durán, A. and Cabib, E. (1978). Solubilization and partial purification of yeast chitin synthetase: Confirmation of the zymogenic nature of the enzyme. *Journal of Biological Chemistry*, 253(12):4419–4425.

Durán, A. and Nombela, C. (2004). Fungal cell wall biogenesis: Building a dynamic interface with the environment. *Microbiology*, 150(10):3099–3103.

Ecker, M., Deutzmann, R., Lehle, L., Mrsa, V., and Tanner, W. (2006). Pir proteins of Saccharomyces cerevisiae are attached to β-1,3-glucan by a new protein-carbohydrate linkage. *The Journal of Biological Chemistry*, 281(17):11523–11529.

Edwards, H. H. (2002). Development of primary germ tubes by conidia of Blumeria graminis f.sp. hordei on leaf epidermal cells of Hordeum vulgare. *Canadian Journal of Botany*, 80(10):1121–1125.

El-Ganiny, A. M., Sanders, D. A. R., and Kaminskyj, S. G. W. (2008). Aspergillus nidulans UDP-galactopyranose mutase, encoded by ugmA pays key roles in colony growth, hyphal morphogenesis and conidiation. *Fungal Genetics and Biology*, 45(12):1533–1542.

El Gueddari, N. E., Rauchhaus, U., Moerschbacher, B. M., and Deising, H. B. (2002). Developmentally regulated conversion of surface-exposed chitin to chitosan in cell walls of plant pathogenic fungi. *New Phytologist*, 156(1):103–112.

Erwig, L. P. and Gow, N. A. R. (2016). Interactions of fungal pathogens with phagocytes. *Nature Reviews Microbiology*, 14(3):163–176.

Eslami, H., Khorramizadeh, M. R., Pourmand, M. R., Moazeni, M., and Rezaie, S. (2014). Down-regulation of sidB gene by use of RNA interference in Aspergillus nidulans. *Iranian Biomedical Journal*, 18(1):55–59.

Fajardo-Somera, R. A., Jöhnk, B., Bayram, O., Valerius, O., Braus, G. H., and Riquelme, M. (2015). Dissecting the function of the different chitin synthases in vegetative growth and sexual development in Neurospora crassa. *Fungal Genetics and Biology*, 75:30–45.

Ferrari, S., Savatin, D. V., Sicilia, F., Gramegna, G., Cervone, F., and de Lorenzo, G. (2013). Oligogalacturonides: Plant damage-associated molecular patterns and regulators of growth and development. *Frontiers in Plant Science*, 4(49).

Firon, A., Beauvais, A., Latgé, J. P., Couvé, E., Grosjean-Cournoyer, M. C., and d'Enfert, C. (2002). Characterization of essential genes by parasexual genetics in the human fungal pathogen Aspergillus fumigatus: Impact of genomic

rearrangements associated with electroporation of DNA. *Genetics*, 161(3):1077–1087.

Fontaine, T., Simenel, C., Dubreucq, G., Adam, O., Delepierre, M., Lemonine, J., Vorgias, C. E., Diaquin, M., and Latgé, J.-P. (2000). Molecular organisation of the alkali-insoluble fraction of Aspergillus fumigatus cell wall. *Journgal of Biological Chemistry*, 275(36):27594–27607.

Francis, S. A., Dewey, F. M., and Gurr, S. J. (1996). The role of cutinase in germling development and infection by Erysiphe graminis f. sp. hordei. *Physiological and Molecular Plant Pathology*, 49(3):201–211.

Free, S. J. (2013). Fungal cell wall organization and biosynthesis. *Advances in Genetics*, 81:33–82.

Fujikawa, T., Kuga, Y., Yano, S., Yoshimi, A., Tachiki, T., Abe, K., and Nishimura, M. (2009). Dynamics of cell wall components of Magnaporthe grisea during infectious structure development. *Molecular Microbiology*, 73(4):553–570.

Fujikawa, T., Sakaguchi, A., Nishizawa, Y., Kouzai, Y., Minami, E., Yano, S., Koga, H., Meshi, T., and Nishimura, M. (2012). Surface α-1,3-glucan facilitates fungal stealth infection by interfering with innate immunity in plants. *PLoS Pathogens*, 8(8).

Gantner, B. N., Simmons, R. M., and Underhill, D. M. (2005). Dectin-1 mediates macrophage recognition of Candida albicans yeast but not filaments. *EMBO Journal*, 24(6):1277–1286.

Gastebois, A., Fontaine, T., Latgé, J.-P., and Mouyna, I. (2010). β(1-3)glucanosyltransferase Gel4p is essential for Aspergillus fumigatus. *Eukaryotic Cell*, 9(8):1294–1298.

Geoghegan, I. A. and Gurr, S. J. (2016). Chitosan mediates germling adhesion in Magnaporthe oryzae and is required for surface sensing and germling morphogenesis. *PLoS Pathogens*, 12(6).

Gilbert, S. R., Cools, H. J., Fraaije, B. A., Bailey, A. M., and Lucas, J. A. (2009). Impact of proquinazid on appressorial development of the barley powdery mildew fungus Blumeria graminis f.sp hordei. *Pesticide Biochemistry and Physiology*, 94(2-3):127–132.

Glawe, D. A. (2008). The powdery mildews: A review of the world's most familiar (yet poorly known) plant pathogens. *Annual Review of Phytopathology*, 46(1):27–51.

Gniwotta, F., Vogg, G., Gartmann, V., Carver, T. L., Riederer, M., and Jetter, R. (2005). What do microbes encounter at the plant surface? Chemical composition of pea leaf cuticular waxes. *Plant Physiology*, 129(1).

Godfrey, D., Zhang, Z., Saalbach, G., and Thordal-Christensen, H. (2009). A proteomics study of barley powdery mildew haustoria. *Proteomics*, 9:3222–3232.

Gonçalves, I. R., Brouillet, S., Soulié, M. C., Gribaldo, S., Sirven, C., Charron, N., Boccara, M., and Choquer, M. (2016). Genome-wide analyses of chitin synthases identify horizontal gene transfers towards bacteria and allow a robust and unifying classification into fungi. *BMC Evolutionary Biology*, 16(1).

Gow, N. A. R., Latgé, J.-P., and Munro, C. A. (2017). The fungal cell wall: Structure, biosynthesis and function. *Microbiology Spectrum*, 5(3).

Gow, N. A. R., van de Veerdonk, F. L., Brown, A. J. P., and Netea, M. G. (2011). Candida albicans morphogenesis and host defence: Discriminating invasion from colonization. *Nature Reviews Microbiology*, 10(2):112–122.

Hacquard, S., Kracher, B., Maekawa, T., Vernaldi, S., Schulze-Lefert, P., and Ver Loren van Themaat, E. (2013). Mosaic genome structure of the barley powdery mildew pathogen and conservation of transcriptional programs in divergent hosts. *PNAS*, 110(24).

Hadwiger, L. A. (2013). Multiple effects of chitosan on plant systems: Solid science or hype. *Plant Science*, 208:42–49.

Hansjakob, A., Bischof, S., Bringmann, G., Riederer, M., and Hildebrandt, U. (2010). Very-long-chain aldehydes promote in vitro prepenetration processes of Blumeria graminis in a dose- and chain length-dependent manner. *New Phytologist*, 188(4):1039–1054.

Hansjakob, A., Riederer, M., and Hildebrandt, U. (2011). Wax matters: Absence of very-long-chain aldehydes from the leaf cuticular wax of the glossy11 mutant of maize compromises the prepenetration processes of Blumeria graminis. *Plant Pathology*, 60(6):1151–1161.

Hansjakob, A., Riederer, M., and Hildebrandt, U. (2012). Appressorium morphogenesis and cell cycle progression are linked in the grass powdery mildew fungus Blumeria graminis. *Fungal Biology*, 116(8):890–901.

Hartland, R. P., Fotaine, T., Debeaupuis, J.-P., Simenel, C., Delepierre, M., and Latgé, J.-P. (1996). A novel β-(1-3)-glucanosyltransferase from the cell wall of Aspergillus fumigatus. *The Journal of Biological Chemistry*, 271(43):2683–26849.

Hector, R. F. (1993). Compounds active against cell walls of medically important fungi. *Clinical Microbiology Reviews*, 6(1):1–21.

Hirano, S., Ohe, Y., and Ono, H. (1976). Selective N-acylation of chitosan. *Carbohydrate Research*, 47:315–320.

Hollomon, D. W., Wheeler, I., Dixon, K., Longhurst, C., and Skylakakis, G. (1997). Defining the resistance risk of the new powdery mildew fungicide quinoxyfen. *Pesticide Science*, 51(3):347–351.

Ibeas, J. I., Yun, D. J., Damsz, B., Narasimhan, M. L., Uesono, Y., Ribas, J. C., Lee, H., Hasegawa, P. M., Bressan, R. A., and Pardo, J. M. (2001). Resistance to the plant PR-5 protein osmotin in the model fungus Saccharomyces cerevisiae is mediated by the regulatory effects of SSD1 on cell wall composition. *The Plant Journal*, 25(3):271–280.

Ing, B. (1990). An introduction to british powdery mildews - 5. *Mycologist*, 4:24–27.

Inoue, S. B., Qadota, H., Arisawa, M., Watanabe, T., and Ohya, Y. (1999). Prenylation of Rho1p is required for activation of yeast 1,3-β-glucan synthase. *Journal of Biological Chemistry*, 274(53):38119–38124.

Ishihara, S., Hirata, A., Nogami, S., Beauvais, A., Latgé, J. P., and Ohya, Y. (2007). Homologous subunits of 1,3-β-glucan synthase are important for spore wall assembly in Saccharomyces cerevisiae. *Eukaryotic Cell*, 6(2):143–156.

Jetter, R., Kunst, L., and Samuels, A. L. (2007). Composition of plant cuticular waxes. In Riederer, M. and Müller, C., editors, *Annual Plant Reviews Volume 23: Biology of the Plant Cuticle*, chapter 4, pages 145–181. Wiley-Blackwell.

Jetter, R., Schäffer, S., and Riederer, M. (2000). Leaf cuticular waxes are arranged in chemically and mechanically distinct layers: Evidence from Prunus laurocerasus L. *Plant Cell and Environment*, 23(2):619–628.

Kämper, J., Kahmann, R., Bölker, M., Ma, L.-J., Brefort, T., Saville, B. J., Banuett, F., Kronstad, J. W., Gold, S. E., Müller, O., Perlin, M. H., Wösten, H. A. B., de Vries, R., Ruiz-Herrera, J., Reynaga-Peña, C. G., Snetselaar, K., McCann, M., Pérez-Martín, J., Feldbrügge, M., Basse, C. W., Steinger, G., Ibeas, J. I., Holloman, W., Guzman, P., Farman, M., Stajich, J. E., Sentandre, R., González-Prieto, J. M., Kennell, J. C., Molina, L., Schirawski, J., Mendoza-Mendoza, A., Greilinger, D., Münch, K., Rössel, N., Scherer, M., Vraneš, M., Ladendorf, O., Vincon, V., Fuchs, U., Sandrock, B., Meng, S., Ho, E. C. H., Cahill, M. J., Boyce, K. J., Klose, J., Klostermann, S. J., Deestra, H. J., Ortiz-Castellanos, L., Li, W., Sanchez-Alonso, P., Schreier, P. H., Häuser-Hahn, I., Vaupel, M., Koopmann, E., Friedrich, G., Voss, h., Schlüter, T., Margolis, J., Platt, D., Swimmer, C., Gnirke, A., Chen, F., Vysotskaia, V., Manhaupt, G., Güldener, U., Münsterkötter, M., Kaase, D., Oesterheld, M., Hans-Werner, M., Mauceli, E. W., DeCaprio, D., Wade, C. M., Butler, J., Young, S., Jaffe, D. B., Calco, S., Nusbaum, C., Galagan, J., and Birren, B. W. (2006). Insights from the genome of the biotrophic fungal plant pathogen Ustilago maydis. *Nature*, 444(7115):97–101.

Kang, X., Kirui, A., Muszyński, A., Widanage, M. C. D., Chen, A., Azadi, P., Wang, P., Mentink-Vigier, F., and Wang, T. (2018). Molecular architecture of fungal cell walls revealed by solid-state NMR. *Nature Communications*, 9(1).

Kathiravan, M. K., Salake, A. B., Chothe, A. S., Dudhe, P. B., Watode, R. P., Mukta, M. S., and Gadhwe, S. (2012). The biology and chemistry of antifungal agents: A review. *Bioorganic and Medicinal Chemistry*, 20(19):5678–5698.

Kawahara, H., Matsuda, Y., Sakaguchi, T., Arai, N., and Koide, Y. (2016). Antifreeze activity of xylomannan from the mycelium and fruit body of Flammulina velutipes. *Biocontrol Science*, 21(3):153–159.

Keller, A., Nesvizhskii, A. I., Kolker, E., and Aebersold, R. (2002). Empirical statistical model to estimate the accuracy of peptide identifications made by MS/MS and database search. *Analytical Chemistry*, 74(20):5383–5392.

Kelly, R., Register, E., Hsu, M.-J., Kurtz, M., and Nielsen, J. (1996). Isolation of a gene involved in 1,3-β-glucan synthesis in Aspergillus nidulans and purification of the corresponding protein. *Journal of Bacteriology*, 178(15):4381–4391.

Kessner, D., Chambers, M., Burke, R., Agus, D., and Mallick, P. (2008). ProteoWizard: Open source software for rapid proteomics tools development. *Bioinformatics*, 24(21):2534–2536.

Kim, I. J., Nam, K. H., Yun, E. J., Kim, S., Youn, H. J., Lee, H. J., Choi, I.-G., and Kim, K. H. (2015). Optimization of synergism of a recombinant auxiliary activity 9 from Chaetomium globosum with cellulase in cellulose hydrolysis. *Applied Microbiology and Biotechnology*, 99(20):9537–8547.

Kim, J.-B. and Carpita, N. C. (1992). Changes in esterification of the uronic acid groups of cell wall polysaccharides during elongation of maize coleoptiles. *Plant Physiology*, 98(2):646–653.

Kim, Y.-T., Kim, E.-H., Cheong, C., Williams, D. L., Kim, C.-W., and Lim, S.-T. (2000). Structural characterization of β-(1$\rightarrow$ 3;1$\rightarrow$ 6)-linked glucans using NMR spectroscopy. *Carbohydrate Research*, 328(3):331–341.

Klis, F. M., Boorsma, A., and de Groot, P. W. J. (2006). Cell wall construction in Saccharomyces cerevisiae. *Yeast*, 23(3):185–202.

Klis, F. M., Mol, P., Hellingwerf, K., and Brul, S. (2002). Dynamics of cell wall structure in Saccharomyces cerevisiae. *FEMS Microbiology Reviews*, 26(3):239–256.

Klis, F. M., Ram, A. F. J., and de Groot, P. W. J. (2007). A molecular and genomic view of the fungal cell wall. In Howard, R. J. and Gow, N. A. R., editors, *The Mycota*, chapter 4, pages 97–120. Springer-Verlag Berlin Heidelberg.

Kobayashi, I., Tanaka, C., Yamaoka, N., and Kunoh, H. (1991). Morphogenesis of Erysiphe graminis conidia on artificial membranes. *Transactions of the Mycological Society of Japan*, 32(2):187–198.

Kock, C., Dufrône, Y. F., and Heinisch, J. J. (2015). Up against the wall: Is yeast cell wall integrity ensured by mechanosensing in plasma membrane microdomains. *Applied and Environmental Microbiology*, 81(3):806–811.

Kollár, R., Petráková, E., Ashwell, G., Robbins, P. W., and Cabib, E. (1995). Architecture of the yeast cell wall the linkage between chitin and $\beta(1\rightarrow6)$-glucan. *Journal of Biological Chemistry*, 270(3):1170–1178.

Kollár, R., Renhold, B. B., Petráková, E., Yeh, H. J. C., Ashwell, G., Drgonová, J., Kapteyn, J. C., Klis, F. M., and Cabib, E. (1997). Architecture of the yeast cell wall $\beta(1\rightarrow6)$-glucan interconnects mannoprotein $\beta(1\rightarrow3)$-glucan, and chitin. *Journal of Biological Chemistry*, 272(28):17762–17775.

Kopecká, M., Phaff, H. J., and Fleet, G. H. (1974). Demonstration of a fibrillar component in the cell wall of the yeast Saccharomyces cervisiae and its chemical nature. *The Journal of Cell Biology*, 62:66–76.

Kováčová, K., Degani, G., Stratilová, E., Farkaš, V., and Popolo, L. (2015). Catalytic properties of Phr family members of cell wall glucan remodeling enzymes: Implications for the adaptation of Candida albicans to ambient pH. *FEMS Yeast Research*, 15(2):1–13.

Kuroki, M., Okauchi, K., Yoshida, S., Ohno, Y., Murata, S., Nakajima, Y., Nozaka, A., Tanaka, N., Nakajima, M., Taguchi, H., Saitoh, K. I., Teraoka, T., Narukawa, M., and Kamakura, T. (2017). Chitin-deacetylase activity induces appressorium differentiation in the rice blast fungus Magnaporthe oryzae. *Scientific Reports*, 7(1).

Latgé, J.-P. (2007). The cell wall: A carbohydrate armour for the fungal cell. *Molecular Microbiology*, 66(2):279–290.

Latgé, J.-P. and Calderone, R. (2006). The fungal cell wall. In Esser, K., Kües, U., and Fischer, R., editors, *The Mycota*, chapter 5, pages 73–104. Springer-Verlag Berlin Heidelberg.

Latgé, J.-P., Mouyna, I., Tekaia, F., Beauvais, A., Debeaupuis, J. P., and Nierman, W. (2005). Specific molecular features in the organization and biosynthesis of the cell wall of Aspergillus fumigatus. *Medical Mycology Supplement*, 43(Suppl 1):S15–S22.

Lenardon, M. D., Whitton, R. K., Munro, C. A., Marshall, D., and Gow, N. A. R. (2007). Individual chitin synthase enzymes synthesize microfibrils of differing structure at specific locations in the Candida albicans cell wall. *Molecular Microbiology*, 66(5):1164–1173.

Lending, C. R., Leal-Morales, C. A., Flores-Martinez, A., Bracker, C. E., and Bartnicki-Garcia, S. (1991). Purification and characterization of 16 S chitin synthetase particles from cell walls of Mucor rouxii. *Experimental Mycology*, 15(1):11–25.

Lesage, G. and Bussey, H. (2006). Cell wall assembly in Saccharomyces cerevisiae. *Microbiology and Molecular Biology Reviews*, 70(2):317–343.

Levasseur, A., Drula, E., Lombard, V., Coutinho, P. M., and Henrissat, B. (2013). Expansion of the enzymatic repertoire of the CAZy database to integrate auxiliary redox enzymes. *Biotechnology for Biofuels*, 6(41).

Levin, D. E. (2011). Regulation of cell wall biogenesis in Saccharomyces cerevisiae: The cell wall integrity signaling pathway. *Genetics*, 189(4):1145–1175.

Liu, P. and Stajich, J. E. (2015). Characterization of the carbohydrate binding module 18 gene family in the amphibian pathogen Batrachochytrium dendrobatidis. *Fungal Genetics and Biology*, 77:31–39.

Liu, Y., Beyer, A., and Aebersold, R. (2016). On the dependency of cellular protein levels on mRNA abundance. *Cell*, 165(3):535–550.

Loginov, D. and Šebela, M. (2016). Proteomics of survival structures of fungal pathogens. *New Biotechnology*, 33(5):655–665.

Lowman, D. W., Greene, R. R., Bearden, D. W., Kruppa, M. D., Pottier, M., Monteiro, M. A., Soldatov, D. V., Ensley, H. E., Cheng, S.-C., Netea, M. G., and Williams, D. L. (2014). Novel structural features in Candida albicans hyphal glucan provide a basis for differential innate immune recognition of hyphae versus yeast. *The Journal of Biological Chemistry*, 289(6):3432–3443.

Lowman, D. W. and Williams, D. L. (2001). A proton nuclear magnetic resonance method for the quantitative analysis on a dry weight basis of (1$\rightarrow$ 3)-β-D-glucans in a complex, solvent-wet matrix. *Journal of Agricultural and Food Chemistry*, 49(9):4188–4191.

Lucas, J. A., Hawkins, N. J., and Fraaije, B. A. (2015). The evolution of fungicide resistance. In Sariaslani, S. and Gadd, G. M., editors, *Advances in Applied Microbiology*, chapter 2, pages 29–92. Academic Press.

Luo, Z., Li, Y. J., Mousa, J., Bruner, S. D., Zhang, Y., Pei, Y., and Keyhani, N. O. (2015). Bbmsn2 acts as a pH-dependent negative regulator of secondary metabolite production in the entomopathogenic fungus Beauveria bassiana. *Environmental Microbiology*, 17:1189–1202.

Maddi, A. and Free, S. J. (2010). α-1,6-mannosylation of N-linked oligosaccharide present on cell wall proteins is required for their incorporation into the cell wall in the filamentous fungus Neurospora crassa. *Eukaryotic Cell*, 9(11):1766–1775.

Maier, T., Güell, M., and Serrano, L. (2009). Correlation of mRNA and protein in complex biological samples. *FEBS Letters*, 583(24):3966–3973.

Malm, E. K., Srivastava, V., Sundqvist, G., and Bulone, V. (2014). APP: An automated proteomics pipeline for the analysis of mass spectrometry data based on multiple open access tools. *BMC Bioinformatics*, 15(441).

Mandel, M. A., Galgiani, J. N., Kroken, S., and Orbach, M. J. (2006). Coccidioides posadasii contains single chitin synthase genes corresponding to classes I to VII. *Fungal Genetics and Biology*, 43(11):775–788.

Mazur, P., Morin, N., Baginsky, W., El-Sherbeini, M., Clemas, J. A., Nielsen, J. B., and Foor, F. (1995). Differential expression and function of two homologous subunits of yeast 1,3-β-D-glucan synthase. *Molecular and Cellular Biology*, 15(10):5671–5681.

Mélida, H., Sain, D., Stajich, J. E., and Bulone, V. (2015). Deciphering the uniqueness of mucoromycotina cell walls by combining biochemical and phylogenomic approaches. *Environmental Microbiology*, 17(5):1649–1662.

Mélida, H., Sandoval-Sierra, J. V., Diéguez-Uribeondo, J., and Bulone, V. (2013). Analyses of extracellular carbohydrates in oomycetes unveil the existence of three different cell wall types. *Eukaryotic Cell*, 12(2):194–203.

Mellado, E., Aufauvre-Brown, A., Gow, N. A. R., and Holden, D. W. (1996a). The Aspergillus fumigatus ChsC and ChsG genes encode class III chitin synthases with different functions. *Molecular Microbiology*, 20(3):667–679.

Mellado, E., Aufauvre-Brown, A., Specht, C. A., Robbins, P. W., and Holden, D. W. (1995). A multigene family related to chitin synthase genes of yeast in the opportunistic pathogen Aspergillus fumigatus. *Molecular and General Genetics*, 246(3):353–359.

Mellado, E., Dubreucq, G., Mol, P., Sarfati, J., Paris, S., Diaquin, M., Holden, D. W., Rodriguez-Tudela, J. L., and Latgé, J. P. (2003). Cell wall biogenesis in a double chitin synthase mutant (ChsG-/ChsE-) of Aspergillus fumigatus. *Fungal Genetics and Biology*, 38(1):98–109.

Mellado, E., Specht, C. A., Robbins, P. W., and Holden, D. W. (1996b). Cloning and characterization of chsD, a chitin synthase-like gene of Aspergillus fumigatus. *FEMS Microbiology Letters*, 143(1):69–76.

Mello, B. L. and Polikarpov, I. (2014). Family 1 carbohydrate binding-modules enhance saccharification rates. *AMB Express*, 4(36).

Mendoza-Mendoza, A., Berndt, P., Djamei, A., Weise, C., Linne, U., Marahiel, M., Vraneš, M., Kämper, J., and Kahmann, R. (2009). Physical-chemical plant-derived signals induce differentiation in Ustilago maydis. *Molecular Microbiology*, 71(4):895–911.

Merzendorfer, H. (2013). Chitin synthesis inhibitors: Old molecules and new developments. *Insect Science*, 20(2):121–138.

Micali, C. O., Neumann, U., Grunewald, D., Panstruga, R., and O'Connell, R. (2011). Biogenesis of a specialized plant-fungal interface during host cell internalization of Golovinomyces orontii haustoria. *Cellular Microbiology*, 13(2):210–226.

Montenegro-Montero, A., Goity, A., and Larrondo, L. F. (2015). The bZIP transcription factor HAC-1 is involved in the unfolded protein response and is necessary for growth on cellulose in Neurospora crassa. *PLoS One*, 10(7).

Motoyama, T., Nobuko, K., Horiuchi, H., Ohta, A., and Takagi, M. (1994). Isolation of a chitin synthase gene (chsC) of Aspergillus nidulans. *Bioscience Biotechnology Biochemistry*, 58(12):2254–2257.

Moukadiri, I. and Zueco, J. (2001). Evidence for the attachment of Hsp150/Pir2 to the cell wall of Saccharomyces cerevisiae through disulfide bridges. *FEMS Yeast Research*, 1(3):241–245.

Mousavi, B., Hedayati, M. T., Teimoori-Toolabi, L., Guillot, J., Alizadeh, A., and Badali, H. (2015). cyp51A gene silencing using RNA interference in azole-resistant Aspergillus fumigatus. *Mycoses*, 58(12):699–706.

Mouyna, I., Fontaine, T., Vai, M., Monod, M., Fonzi, W. A., Diaquin, M., Popolo, L., Hartland, R. P., and Latgé, J.-P. (2000). Glycosylphosphatidylinositol-anchored glucanosyltransferases play an active role in the biosynthesis of the fungal cell wall. *The Journal of Biological Chemistry*, 275(20):14882–14889.

Mouyna, I., Hartland, R. P., Fontaine, T., Diaquin, M., Simenel, C., Delepierre, M., Henrissat, B., and Latgé, J. P. (1998). A 1,3-β-glucanosyltransferase isolated from the cell wall of Aspergillus fumigatus is a homologue of the yeast Bgl2p. *Microbiology*, 144:3171–3180.

Mouyna, I., Morelle, W., Vai, M., Monod, M., Léchenne, B., Fontaine, T., Beauvais, A., Sarfati, J., Prévost, M. C., Henry, C., and Latgé, J.-P. (2005). Deletion of GEL2 encoding for a β(1-3)glucanosyltransferase affects morphogenesis and virulence in Aspergillus fumigatus. *Molecular Microbiology*, 56(6):1675–1688.

Munro, C. A. and Gow, N. A. R. (2001). Chitin synthesis in human pathogenic fungi. *Medical Mycology*, 19(Suppl 1):41–52.

Munro, C. A., Schofield, D. A., Gooday, G. W., and Gow, N. A. R. (1998). Regulation of chitin synthesis during dimorphic growth of Candida albicans. *Microbiology*, 144:391–401.

Munro, C. A., Selvaggini, S., de Bruijn, I., Walker, L., Lenardon, M. D., Gerseen, B., Milne, S., Brown, A. J. P., and Gow, N. A. R. (2007). The PCK, HOG and Ca2+ signalling pathway co-ordinately regulates chitin syntesis in Candida albicans. *Molecular Microbiology*, 63(5):1399–1413.

Munro, C. A., Winter, K., Buchan, A., Henry, K., Becker, J. M., Brown, A. J. P., Bulawa, C. E., and Gow, N. A. R. (2001). Chs1 of Candida albicans is an essential chitin synthase required for synthesis of the septum and for cell integrity. *Molecular Microbiology*, 39(5):1414–1426.

Murray, G. M. and Brennan, J. P. (2009). The current and potential costs from diseases of barley in australia. Technical report, GRDC.

Murray, G. M. and Brennan, J. P. (2010). Estimating disease losses to the Australian barley industry. *Australian Plant Pathology*, 39(1):85–96.

Muszewska, A., Pilsyk, S., Perlińska-Lenart, U., and Kruszewska, J. S. (2018). Diversity of cell wall related proteins in human pathogenic fungi. *Journal of Fungi*, 4(6).

Nagahashi, S., Sudoh, M., Ono, N., Sawada, R., Yamaguchi, E., Uchida, Y., Mio, T., Takagi, M., Arisawa, M., and Yamada-Okabe, H. (1995). Characterization of chitin synthase 2 of Saccharomyces cerevisiae: Implication of two highly conserved domains as possible catalytic sites. *Journal of Biological Chemistry*, 270(23):13961–13967.

Netea, M. G., Brown, G. D., Kullberg, B. J., and Gow, N. A. R. (2008). An integrated model of the recognition of Candida albicans by the innate immune system. *Nature Reviews Microbiology*, 6(1):67–78.

Niño-Vega, G., Carrero, L., and San-Blas, G. (2004). Isolation of the CHS4 gene of Paracoccidioides brasiliensis and its accommodation in a new class of chitin synthases. *Medical Mycology*, 42(1):51–57.

Noir, S., Colby, T., Harzen, A., Schmidt, J., and Panstruga, R. (2009). A proteomic analysis of powdery mildew (Blumeria graminis f.sp. hordei) conidiospores. *Molecular Plant Pathogens*, 10(2):223–236.

Novodvorska, M., Stratford, M., Blythe, M. J., Wilson, R., Beniston, R. G., and Archer, D. B. (2016). Metabolic activity in dormant conidia of Aspergillus niger and developmental changes during conidial outgrowth. *Fungal Genetics and Biology*, 94:23–31.

Nowara, D., Gay, A., Lacomme, C., Shaw, J., Ridout, C., Douchkov, D., Hensel, G., Kumlehn, J., and Schweizer, P. (2010). HIGS: Host-induced gene silencing in the obligate biotrophic fungal pathogen Blumeria graminis. *The Plant Cell*, 22(9):3130–3141.

Oliveira-Garcia, E. and Deising, H. B. (2013). Infection structure-specific expression of β-1,3-glucan synthase is essential for pathogenicity of Colletotrichum graminicola and evasion of β-glucan-triggered immunity in maize. *The Plant Cell*, 25(6):2356–2378.

Oliveira-Garcia, E. and Deising, H. B. (2016). Attenuation of PAMP-triggered immunity in maize requires down-regulation of the key β-1,6-glucan synthesis genes KRE5 and KRE6 in biotrophic hyphae of Colletotrichum graminicola. *The Plant Journal*, 87(4):355–375.

Orlean, P. (2012). Architecture and biosynthesis of the Saccharomyces cerevisiae cell wall. *Genetics*, 192(3):775–818.

Osumi, M. (1998). The ultrastructure of yeast: Cell wall structure and formation. *Micron*, 29(2-3):207–233.

O'Meara, T. R. and Alspaugh, J. A. (2012). The Cryptococcus neoformans capsule: A sword and a shield. *Clinical Microbiology Reviews*, 25(3):387–408.

Park, J.-N., Lee, D.-J., Kwon, O., Oh, D.-B., Bahn, Y.-S., and Kang, H. A. (2012). Unraveling unique structure and biosynthesis pathway of N-linked glycans in human fungal pathogen Cryptococcus neoformans by glycomics analysis. *Journal of Biological Chemistry*, 287(23):19501–19515.

Pedersen, C., van Themaat, E. V. L., McGuffin, L. J., Abbott, J. C., Burgis, T. A., Barton, G., Bindschedler, L. V., Lu, X., Maekawa, T., Weßling, R., Cramer, R., Thordal-Christensen, H., Panstruga, R., and Spanu, P. D. (2012). Structure and evolution of barley powdery mildew effector candidates. *BMC Genomics*, 13(694).

Pereira, M., Felipe, M. S. S., Brígido, M. M., Soares, C. M. A., and Azevedo, M. O. (2000). Molecular cloning and characterization of a glucan synthase gene from the human pathogenic fungus Paracoccidioides brasiliensis. *Yeast*, 16(5):451–462.

Pettolino, F., Sasaki, I., Turbic, A., Wilson, S. M., Bacic, A., Hrmova, M., and Fincher, G. B. (2009). Hyphal cell walls from the plant pathogen Rhynchosporium secalis contain (1,3/1,6)-β-D-glucans, galacto- and rhamnomannans, (1,3;1,4)-β-D-glucans and chitin. *FEBS Journal*, 276(14):3698–3709.

Pettolino, F. A., Walsh, C., Fincher, G. B., and Bacic, A. (2012). Determining the polysaccharide composition of plant cell walls. *Nature Protocols*, 7(9):1590–1607.

Pliego, C., Nowara, D., Bonciani, G., Gheorghe, D. M., Xu, R., Surana, P., Whigham, E., Nettleton, D., Bogdanove, A. J., Wise, R. P., Schweizer, P., Bindschedler, L. V., and Spanu, P. D. (2013). Host-induced gene silencing in barley powdery mildew reveals a class of ribonuclease-like effectors. *Molecular Plant Microbe Interactions*, 26(6):633–642.

Pryce-Jones, E., Carver, T., and Gurr, S. J. (1999). The roles of cellulase enzymes and mechanical force in host penetration by Erysiphe graminis f.sp. hordei. *Physiological and Molecular Plant Pathology*, 55(3):175–1582.

Raffaele, S. and Kamoun, S. (2012). Genome evolution in filamentous plant pathogens: Why bigger can be better. *Nature Reviews Microbiology*, 10(6):417–430.

Raffaele, S., Leger, A., and Roby, D. (2009). Very long chain fatty acid and lipid signaling in the response of plants to pathogens. *Plant Signaling and Behavior*, 4(2):94–99.

Rappleye, C. A., Eissenberg, L. G., and Goldman, W. E. (2007). Histoplasma capsulatum α-(1,3)-glucan blocks innate immune recognition by the β-glucan receptor. *PNAS*, 104(4):1366–1370.

Reid, I. D. and Bartnicki-Garcia, S. (1976). Cell-wall composition and structure of yeast cells and conjugation tubes of Tremella mesenterica. *Journal of General Microbiology*, 96(1):35–50.

Reis, E. M., Basso, D. F., and Zanatta, M. (2013). Loss of sensitivity of Blumeria graminis f. sp. tritici to triadimenol applied as seed treatment. *Tropical Plant Pathology*, 38(1):55–57.

Riquelme, M. (2013). Tip growth in filamentous fungi: A road trip to the apex. *Annual Review of Microbiology*, 67:587–609.

Roberts, D. R., Mims, C. W., and Fuller, M. S. (1996). Ultrastructure of the ungerminated conidium of Blumeria graminis f. sp. hordei. *Canadian Journal of Botany*, 74(2):231–237.

Rogg, L. E., Fortwendel, J. R., Juvvadi, P. R., Lilley, A., and Steinbach, W. J. (2011). The chitin synthase genes ChsA and ChsC are not required for cell wall stress responses in the human pathogen Aspergillus fumigatus. *Biochemical and Biophysical Research Communications*, 411(3):549–554.

Rogg, L. E., Fortwendel, J. R., Juvvadi, P. R., and Steinbach, W. J. (2012). Regulation of expression, activity and localization of fungal chitin synthases. *Medical Mycology*, 50(1):2–17.

Roncero, C. (2002). The genetic complexity of chitin synthesis in fungi. *Current Genetics*, 41(6):367–378.

Rosano, G. L. and Ceccarelli, E. A. (2014). Recombinant protein expression in Escherichia coli: Advances and challenges. *Frontiers in Microbiology*, 5(172).

Ruiz-Herrera, J., editor (1992). *Fungal Cell Wall: Structure, Synthesis and Assembly*. CRC Press.

Ruiz-Herrera, J., Elorza, M. V., Valentín, E., and Sentandreu, R. (2006). Molecular organization of the cell wall of Candida albicans and its relation to pathogenicity. *FEMS Yeast Research*, 6(1):14–29.

Ruiz-Herrera, J., Leon, C. G., Carabez-Trejo, A., and Reyes-Salinas, E. (1996). Structure and chemical composition of the cell walls from the haploid yeast and mycelial forms of Ustilago maydis. *Fungal Genetics and Biology*, 20(2):133–142.

Ruiz-Herrera, J., Lopez-Remero, E., and Bartnicki-Garcia, S. (1997). Properties of chitin synthetase in isolated chitosomes from yeast cells of Mucor rouxii. *The Journal of Biological Chemistry*, 252(10):3338–3343.

Ruiz-Herrera, J. and Ortiz-Castellanos, L. (2010). Analysis of the phylogenetic relationships and evolution of the cell walls from yeasts and fungi. *FEMS Yeast Research*, 10(3):225–243.

Ruiz-Herrera, J., Sentandreu, R., and Martinez, J. (1992). Chitin biosynthesis in fungi. In Arora, D. K., Mukerji, K. G., and Elander, R. P., editors, *Handbook of Applied Mycology*, volume 4, pages 281–312. Marcel Dekker.

Russell, P. E. (2005). A century of fungicide evolution. *The Journal of Agricultural Science*, 143(1):11–25.

Salgado-Lugo, H., Sánchez-Arreguín, A., and Ruiz-Herrera, J. (2016). Heterologous expression of an active chitin synthase from Rhizopus oryzae. *Fungal Genetics and Biology*, 97:10–17.

Samalova, M., Mélida, H., Vilaplana, F., Bulone, V., Soanes, D. M., Talbot, N. J., and Gurr, S. J. (2016). The β-1,3-glucanosyltransferases (Gels) affect the structure of the rice blast fungal cell wall during appressorium-mediated plant infection. *Cellular Microbiology*, 19(3).

Samar, D., Kieler, J. B., and Klutts, J. S. (2015). Identification and deletion of Tft1, a predicted glycosyltransferase necessary for cell wall β-1,3;1,4-glucan synthesis in Aspergillus fumigatus. *Plos One*, 10(2).

Sánchez-León, E., Bowman, B., Seidel, C., Fischer, R., Novick, P., and M., R. (2015). The rab gtpase ypt-1 associates with golgi cisternae and spitzenkörper microvesicles in neurospora crassa. *Molecular Microbiology*, 95(3):472–490.

Sánchez-León, E., Verdín, J., Freitag, M., Roberson, R. W., Bartnicki-Garcia, S., and Riquelme, M. (2011). Traffic of chitin synthase 1 (chs-1) to the spitzenkörper and developing septa in hyphae of Neurospora crassa: Actin dependence and evidence of distinct microvesicle populations. *Eukaryotic Cell*, 10(5):683–695.

Schmalhorst, P. S., Krappmann, S., Vervecken, W., Rohde, M., Müller, M., Braus, G. H., Contreras, R., Braun, A., Bakker, H., and Routier, F. H. (2008). Contribution of galactofuranose to the virulence of the opportunistic pathogen Aspergillus fumigatus. *Eukaryotic Cell*, 7(8):1268–1277.

Schoonbeek, H.-j., Raaijmakers, J. M., and de Waard, M. A. (2002). Fungal ABC transporters and microbial interactions in natural environments. *Molecular Plant Microbe Interactions*, 15(11):1165–1172.

Schuster, M., Martin-Urdiroz, M., Higuchi, Y., Hacker, C., Kilaru, S., Gurr, S. J., and Steinberg, G. (2016). Co-delivery of cell-wall-forming enzymes in the same vesicle for coordinated fungal cell wall formation. *Nature Microbiology*, 1(16149).

Sietsma, J. and Wessels, J. (2006). Apical wall biogenesis. In Esser, K., Kües, U., and Fischer, R., editors, *The Mycota*, chapter 4, pages 53–72. Springer-Verlag Berlin Heidelberg.

Silverman, S. J., Sburlati, A., Slater, M. L., and Cabib, E. (1988). Chitin synthase 2 is essential for septum formation and cell division in Saccharomyces cerevisiae. *PNAS*, 85(13):4735–4739.

Soulié, M. C., Perino, C., Piffeteau, A., Choquer, M., Malfatti, P., Cimerman, A., Kunz, C., Boccara, M., and Vidal-Cros, A. (2006). Botrytis cinerea virulence is drastically reduced after disruption of chitin synthase class III gene (Bcchs3a). *Cellular Microbiology*, 8(8):1310–1321.

Spanu, P. D., Abbot, J. C., Amselem, J., Burgis, T. A., Soanes, D. M., Stüber, K., van Themaat, E. V. L., Brown, J. K. M., Butcher, S. A., Gurr, S. J., Lebrun, M.-H., Ridout, C. J., Schulze-Lefert, P., Talbot, N. J., Ahmadinejad, N., Ametz, C., Barton, G. R., Benjdia, M., Bidzinski, P., Bindschedler, L. V., Both, M., Brewer, M. T., Cadle-Davidson, L., Cadle-Davidson, M. M., Collemare, J., Cramer, R., Frenkel, O., Godfrey, D., Harriman, J., Hoede, C., King, B. C., Klages, S., Kleemann, J., Knoll, D., Koti, P. S., Kreplak, J., López-Ruiz, F. J., Lu, X., Maekawa, T., Mahanil, S., Micali, C., Milgroom, M. G., Montana, G., Noir, S., O'Connel, R. J., Oberhaensli, S., Parlange, F., Pendersen, C., Quesneville, H., Reinhardt, R., Rott, M., Sacristán, S., Schmidt, S. M., Schön, M., Skaminoti, P., Sommer, H., Stephens, A., Takahra, H., Thordal-Christensen, H., Vigouroux, M., Weßling, R., Wicker, T., and Pastrunga, R. (2010). Genome expansion and gene loss in powdery mildew fungi reveal tradeoffs in extreme parasitism. *Science*, 330(6010):1543–1546.

Specht, C. A., Liu, Y., Robbins, P. W., Bulawa, C. E., Iartchouk, N., Winter, K. R., Riggle, P. J., Rhodes, J. C., Dodge, C. L., Culp, D. W., and Borgia, P. T. (1996). The chsD and chsE genes of Aspergillus nidulans and their roles in chitin synthesis. *Fungal Genetics and Biology*, 20(2):153–167.

Srivastava, V., Malm, E., Sundqvist, G., and Bulone, V. (2013). Quantitative proteomics reveals that plasma membrane microdomains from poplar cell suspension cultures are enriched in markers of signal transduction, molecular transport, and callose biosynthesis. *Molecular and Cellular Proteomics*, 12(12):3874–3885.

Srivastava, V., Rezinciuc, S., and Bulone, V. (2018). Quantitative proteomic analysis of four developmental stages of Saprolegnia parasitica. *Frontiers in Microbiology*, 8(2658).

Stevens, D. A. (2000). Drug interaction studies of a glucan synthase inhibitor (LY 303366) and a chitin synthase inhibitor (nikkomycin Z) for inhibition and killing of fungal pathogens. *Antimicrobial Agents and Chemotherapy*, 44(9):2547–2548.

Sweet, D. P., Shapiro, R. H., and Albersheim, P. (1975). Quantitative analysis by various G.L.C. response-factor theories for partially methylated and partially ethylated alditol acetates. *Carbohydrate Research*, 40(2):217–225.

Takeshita, N., Ohta, A., and Horiuchi, H. (2005). CsmA, a class V chitin synthase with a myosin motor-like domain, is localized through direct interaction with the actin cytoskeleton in Aspergillus nidulans. *Molecular Biology of the Cell*, 16(4):1961–1970.

Tanaka, S., Yamada, K., Yabumoto, K., Fujii, S., Huser, A., Tsuji, G., Koga, H., Dohi, K., Mori, M., Shiraishi, T., O'Connell, R., and Kubo, Y. (2007). Saccharomyces cerevisiae SSD1 orthologues are essential for host infection by the ascomycete plant pathogens Colletotrichum lagenarium and Magnaporthe grisea. *Molecular Microbiology*, 64(5):1332–1349.

Thind, T. S., editor (2012). *Fungicide Resistance in Crop Protection: Risk and Management*. CABI.

Thompson, J. R., Douglas, C. M., Li, W., Jue, C. K., Pramanik, B., Yuan, X., Rude, T. H., Toffaletti, D. L., Perfect, J. R., and Kurtz, M. (1999). A glucan synthase FKS1 homolog in Cryptococcus neoformans is single copy and encodes an essential function. *Journal of Bacteriology*, 181(2):444–453.

Tian, L., Yu, J., Wang, Y., and Tian, C. (2017). The C_2H_2 transcription factor VdMsn2 controls hyphal growth, microsclerotia formation, and virulence of Verticillium dahliae. *Fungal Biology*, 121(12):1001–1010.

Toh-e, A., Yasunagat, S., Nisogit, H., Tanakas, K., Oguchi, T., and Matsui, Y. (1993). Three yeast genes, PIR1, PIR2 and PIR3, containing internal tandom repeats, are related to each other, and PIR1 and PIR2 are required for tolerance to heat shock. *Yeast*, 9(5):481–494.

Tomazett, P. K., Félix, C. R., Lenzi, H. L., de Paula Faria, F., de Almeida Soares, C. M., and Pereira, M. (2010). 1,3-β-glucan synthase of Paracoccidioides brasiliensis: Recombinant protein, expression and cytolocalization in the yeast and mycelium phases. *Fungal Biology*, 114(10):809–816.

Tsuba, M., Katagiri, C., Takeuchi, Y., and Yamaoka, N. (2002). Chemical factors of the leaf surface involved in the morphogenesis of Blumeria graminis. *Physiological and Molecular Plant Pathology*, 60(2):51–57.

Tucker, M. A., Lopez-Ruiz, F., Jayasena, K., and Oliver, R. P. (2015). Origin of fungicide-resistant barley powdery mildew in Western Australia: Lessons to be

learned. In Ishii, H. and Hollomon, D. W., editors, *Fungicide Resistance in Plant Pathogens*, chapter 20, pages 329–340. Springer Japan, 1st edition.

Tzelepis, G. D., Melin, P., Jensen, D. F., Stenlid, J., and Karlsson, M. (2012). Functional analysis of glycoside hydrolase family 18 and 20 genes in Neurospora crassa. *PLoS Pathogens*, 49(9):717–730.

Uchida, Y., Shimmi, O., Sudoh, M., Arisawa, M., and Yamada-Okabe, H. (1996). Characterization of chitin synthase 2 of Saccharomyces cerevisiae II: Both full size and processed enzymes are active for chitin synthesis. *Journal of Biochemistry*, 119(4):659–666.

Utermark, J. and Karlovsky, P. (2006). Quantification of green fluorescent protein fluorescence using real-time PCR thermal cycler. *Biotechniques*, 41(2):150, 152, 154.

van den Burg, H. A., Harrison, S. J., Joosten, M. H. A. J., Vervoort, J., and de Witt, P. J. G. M. (2006). Cladosporium fulvum Avr4 protects fungal cell walls against hydrolysis by plant chitinases accumulating during infection. *Molecular Plant Microbe Interactions*, 19(12):1420–1430.

Walker, L. A., Gow, N. A. R., and Munro, C. A. (2010). Fungal echinocandin resistance. *Fungal Genetics and Biology*, 47(2):117–126.

Walker, L. A., Gow, N. A. R., and Munro, C. A. (2013). Elevated chitin content reduces the susceptibility of Candida species to caspofungin. *Antimicrobial Agents and Chemotherapy*, 57(1):146–154.

Walker, L. A., Munro, C. A., de Bruijn, I., Lenardon, M. D., McKinnon, A., and Gow, N. A. R. (2008). Stimulation of chitin synthesis rescues Candida albicans from echinocandins. *PLoS Pathogens*, 4(4).

Walls, D. and Loughran, S., editors (2017). *Protein Chromatography - Methods and Protocols*, volume 1485 of *Methods in Molecular Biology*. Humana Press.

Walters, K. R., Serianni, A. S., Voituron, Y., Sformo, T., Barnes, B. M., and Duman, J. G. (2011). A thermal hysteresis-producing xylomannan glycolipid antifreeze associated with cold tolerance is found in diverse taxa. *Journal of Comparative Physiology B*, 181(5):631–640.

Wang, Q., Liu, H., and Szaniszlo, P. J. (2002). Compensatory expression of five chitin synthase genes, a response to stress stimuli, in Wangiella (Exophiala) dermatitidis, a melanized fungal pathogen of humans. *Microbiology*, 148(9):2811–2817.

Wiederhold, N. P. (2009). Paradoxical echinocandin activity: A limited in vitro phenomenon? *Medical Mycology*, 47(Suppl 1):S369–S375.

Win, J., Chaparro-Garcia, A., Belhaj, K., Saunders, D. G., Yoshida, K., Dong, S., Schornack, S., Zipfel, C., Robatzek, S., Hogenhout, S. A., and Kamoun, S. (2012).

Effector biology of plant-associated organisms: Concepts and perspectives. *Cold Spring Harbor Symposia on Quantitative Biology*, 77:235–47.

Wolfe, M. S. (1984). Trying to understand and control powdery mildew. *Plant Pathology*, 33(4):451–466.

Wolfe, M. S. and Mcdermott, J. M. (1994). Population genetics of plant pathogen interactions: The examlpe of the Erysiphe graminis-Hordeum vulgare pathosystem. *Annual Review of Phytopathology*, 32:89–113.

Wyand, R. A. and Brown, J. K. M. (2003). Genetic and forma specialis diversity in Blumeria graminis of cereals and its implications for host-pathogen co-evolution. *Molecular Plant Pathology*, 4(3):187–198.

Xoconostle-Cázaresa, B., Specht, C. A., Robbins, P. W., Liub, Y., Leóna, C., and Ruiz-Herrera, J. (1997). Umchs5, a gene coding for a class IV chitin synthase in Ustilago maydis. *Fungal Genetics and Biology*, 22(3):199–208.

Yamaoka, N., Matsumoto, I., and Nishiguchi, M. (2006). The role of primary germ tubes (pgt) in the life cycle of Blumeria graminis: The stopping of pgt elongation is necessary for the triggering of appressorial germ tube (agt) emergence. *Physiological and Molecular Plant Pathology*, 69:153–159.

Yang, S. L. and Ellingboe, A. (1972). Cuticle layer as a determining factor for the formation of mature appressoria of Erysiphe graminis on wheat and barley. *Phytopathology*, 62:708–714.

Yeats, T. H. and Rose, J. K. C. (2013). The formation and function of plant cuticles. *Plant Physiology*, 163:5–20.

Yin, Q. Y., de Groot, P. W. J., Dekker, H. L., de Jong, L., Klis, F. M., and de Koster, C. G. (2005). Comprehensive proteomic analysis of Saccharomyces cerevisiae cell walls: Identification of proteins covalently attached via glycosylphosphatidylinositol remnants or mild alkali-sensitive linkages. *Journal of Biological Chemistry*, 280(21):20894–20901.

Zabka, V., Stangl, M., Bringmann, G., Vogg, G., Riederer, M., and Hildebrandt, U. (2008). Host surface properties affect prepenetration processes in the barley powdery mildew fungus. *New Phytologist*, 177(1):251–263.

Zeng, F.-S., Menardo, F., Xue, M.-F., Zhang, X.-J., Gong, S.-J., Yang, L.-J., Shi, W.-Q., and Yu, D.-Z. (2017). Transcriptome analyses shed new insights into primary metabolism and regulation of Blumeria graminis f. sp. tritici during conidiation. *Frontiers in Plant Science*, 8:2107–2122.

Zhang, H., Zhao, Q., Guo, X., Guo, M., Qi, Z., Tang, W., Dong, Y., Ye, W., Zheng, X., Wang, P., and Zhang, Z. (2014). Pleiotropic function of the putative zinc-finger

protein MoMsn2 in Magnaporthe oryzae. *Molecular Plant Microbe Interactions*, 27(5):446–460.

Zhang, W.-J., Pedersen, C., Kwaaitaal, M., Gregersen, P. L., Mørch, S. M., Hanisch, S., Kristensen, A., Fuglsang, A. T., Collinge, D. B., and Thordal-Christensen, H. (2012). Interaction of barley powdery mildew effector candidate CSEP0055 with the defence protein PR17c. *Molecular Plant Pathology*, 13(9):1110–1119.

Zhang, Y. Z., Chen, Q., Liu, C. H., Liu, Y. B., Yi, P., Niu, K. X., Wang, Y. Q., Wang, A. Q., Yu, H. Y., Pu, Z. E., Jiang, Q. T., Wei, Y. M., Qi, P. F., and Zheng, Y. L. (2016). Chitin synthase gene Fgchs8 affects virulence and fungal cell wall sensitivity to environmental stress in Fusarium graminearum. *Fungal Biology*, 120(5):764–774.

Zhang, Z., Hall, A., Perfect, E., and Gurr, S. J. (2000). Differential expression of two Blumeria graminis chitin synthase genes. *Molecular Plant Pathology*, 1(2):125–138.

Zhang, Z., Henderson, C., Perfect, E., Carver, T. L. W., Thomas, B. J., Skamnioti, P., and Gurr, S. J. (2005). Of genes and genomes, needles and haystacks : Blumeria graminis and functionality. *Molecular Plant Pathology*, 6(5):561–575.

Zhao, W., Li, C., Liang, J., and Sun, S. (2014). The Aspergillus fumigatus β-1,3-glucanosyltransferase Gel7 plays a compensatory role in maintaining cell wall integrity under stress conditions. *Glycobiology*, 24(5):418–427.

Zhao, Z., Liu, H., Wang, C., and Xu, J.-R. (2013). Comparative analysis of fungal genomes reveals different plant cell wall degrading capacity in fungi. *BMC Genomics*, 14(274).

Zlotnik, H., Fernandez, M. P., Bowers, B., and Cabib, E. (1984). Saccharomyces cerevisiae mannoproteins form an external cell wall layer that determines wall porosity. *Fungal Genetics and Biology*, 159(3):1018–1026.